The Dissertation Committee for David Gerard Wahman Certifies that this is the approved version of the following dissertation:

COMETABOLISM OF TRIHALOMETHANES BY NITRIFYING BIOFILTERS UNDER DRINKING WATER TREATMENT PLANT CONDITIONS

Committee:

Gerald E. Speitel Jr., Supervisor

Lynn E. Katz

Desmond F. Lawler

Mary Jo Kirisits

George Georgiou

COMETABOLISM OF TRIHALOMETHANES BY NITRIFYING BIOFILTERS UNDER DRINKING WATER TREATMENT PLANT CONDITIONS

by

David Gerard Wahman, B.S.; M.S.E.

Dissertation

Presented to the Faculty of the Graduate School of

The University of Texas at Austin

in Partial Fulfillment

of the Requirements

for the Degree of

Doctor of Philosophy

The University of Texas at Austin

December 2006

Dedication

To my wife, Lauren, for her love and support. You are my best friend.

Acknowledgements

I would like to thank my wife Lauren, the love of my life, for her perpetual patience and support, keeping "Team Wahman" moving towards our life goals. Thank you to my family, for their support over the years and knowing when to let me find my own way. Sometimes, the best support is to say nothing at all.

I am grateful for funding provided by the American Water Works Association Research Foundation, Texas Advanced Technology Research Program, and the United States Environmental Protection Agency STAR Fellowship.

I would also like to thank Dr. Gerald E. Speitel Jr. for providing the example of what I will aspire to become in this field. In addition, I would like to thank the rest of my committee members for their support in this endeavor. Finally, I thank my colleagues for their discussions, friendship, and support as we walked down this road together.

COMETABOLISM OF TRIHALOMETHANES BY NITRIFYING BIOFILTERS UNDER DRINKING WATER TREATMENT PLANT CONDITIONS

Publication No._____

David Gerard Wahman, Ph.D.

The University of Texas at Austin, 2006

Supervisor: Gerald E. Speitel Jr.

This research studied the feasibility of THM cometabolism in laboratory-scale biofilters under conditions that reflect drinking water treatment practice. Initially, batch kinetic studies were conducted to determine whether nitrifying bacteria could reliably cometabolize all four THMs at a sufficient rate to make the process attractive to utilities. The kinetic experiments showed that nitrifier communities likely to be seen in drinking water treatment facilities can degrade THMs at a sufficient rate by themselves, without seeding a pure culture. These results also indicated that temperature sensitivity and product toxicity could be concerns if THM cometabolism by nitrifying bacteria was implemented as a treatment option in treatment facilities. In particular, as bromine substitution increases, both THM degradation kinetics and product toxicity increase.

A series of laboratory-scale biofilter experiments was conducted to investigate the feasibility of THM cometabolism in the envisioned process configuration. The operating conditions of the mixed culture biofilters scaled to typical full-scale rapid filtration

operating conditions seen in drinking water treatment practice. Overall, the biofilter experiments suggest that, for a 2 mg N/L $TOTNH_3$ (the sum of ammonia-nitrogen and ammonium-nitrogen) removal, total THM removals might initially approach 32-38% (25-31 μg/L total THMs). This initial removal might decline to 11-12% (9-10 μg/L total THMs) over time as bacteria are selected from THM product toxicity. Even if this decreased performance occurs, the 11-12% removal is potentially attractive in drinking water treatment practice. The allowable influent monochloramine concentration resides between 1 mg/L to 2.5 mg/L as Cl_2, with the use of 1 mg/L as Cl_2 being conservative.

A simple kinetic model for THM cometabolism was incorporated into AQUASIM to describe biofilter performance under conditions where by-product toxicity is not a concern. Overall, total THM removal of 9 to 54% was projected in the full-scale simulations, which illustrates the potential of THM cometabolism to have a significant impact on treated water quality for utilities where their water quality will likely see a benefit from the proposed process. Even though these removals are modest, drinking water treatment plants might only require removals in this range to maintain compliance with existing and future regulations.

Table of Contents

List of Tables

List of Figures

Chapter 1: Introduction

1.1. PROBLEM STATEMENT

During drinking water disinfection, natural organic matter (NOM) reacts with the disinfectant to produce disinfection by-products (DBPs), such as haloacetic acids (HAAs) and four THMs; trichloromethane (TCM) or chloroform, bromodichloromethane (BDCM), dibromochloromethane (DBCM), tribromomethane (TBM) or bromoform. Chlorine disinfection remains quite popular in the U.S. (Connell et al. 2000a; Connell et al. 2000b), although many utilities now use combinations of chlorine and chloramines to avoid excessive THM and HAA formation. A typical chloramine treatment scheme consists of an initial period of chlorination to help achieve disinfection goals followed by quenching with ammonia at some point in the treatment train to meet DBP goals through the lower DBP formation rates associated with chloramines. Significant formation of THMs and HAAs can occur within treatment plants even during relatively short periods of chlorination (Singer et al. 1999b; Symons et al. 1982). Therefore, approaches for minimizing DBP formation or for removing DBPs within treatment plants are potentially of much practical value.

Evidence of HAA biodegradation in drinking water environments continues to mount (Baribeau et al. 2000; McRae et al. 2004; Singer et al. 1999a; Williams et al. 1997; Williams et al. 1998; Xie and Zhou 2000; Xie and Zhou 2002). HAA biodegradation is not at all surprising, as the ability of mono- and dichloroacetic acid to support microbial growth is well documented in the microbiology and hazardous waste literature (Janssen et al. 1985; Motosugi and Soda 1983).

Of course, THMs and HAAs tend to form together, so biological DBP removal processes must be able to deal with both classes of DBPs to be of practical value in

regulatory compliance. Unfortunately, THM biodegradation is a much more difficult proposition than HAA biodegradation. No evidence indicates that THMs can support microbial growth. Considerable evidence is available, however, for cometabolism of TCM by bacteria growing on other chemicals, including ammonia (Alvarez-Cohen and McCarty 1991b; Aziz et al. 1999; Ely et al. 1997). Cometabolism can be defined as the fortuitous biodegradation of a target chemical (i.e., the cometabolite - THMs) through reactions catalyzed by one or more non-specific microbial enzymes (Dalton and Stirling 1982). Because of the greater difficulty in biodegrading THMs, the development of a THM biotreatment process is the limiting factor in implementing biological treatment for DBP control.

1.2. OBJECTIVES AND APPROACH

The overall objective of this research was to study the feasibility of THM cometabolism in laboratory-scale biofilters under conditions that reflected water treatment plant practice. The specific research objectives were to:

1. Extend the previous work on TCM cometabolism kinetics to the other three regulated THMs for the pure culture organism *Nitrosomonas europaea* and compare these findings with those obtained from selected mixed culture nitrifiers.
2. Demonstrate THM cometabolism in continuous-flow biofilters.
3. Quantify the abundance and spatial distribution of nitrifiers among other microorganisms in the biofilters, thereby improving our ability to interpret process performance data.
4. Create a steady-state mathematical model of the process and propose a strategy for design and operation based on experimental observations and modeling.

To meet the above objectives, three main research tasks were undertaken as outlined below.

Task 1 involved batch kinetic studies to determine cometabolism kinetics for the pure culture organism, *N. europaea*, providing information to the key question as to whether nitrifying bacteria can reliably cometabolize all four THMs at a sufficient rate to make the process attractive to utilities that practice (or want to practice) prechlorination, in particular, utilities practicing a combination of chlorination and chloramination.

Task 2 demonstrated THM cometabolism performance in the envisioned process configuration, continuous-flow biofilters. In addition, operational issues were also studied, including THM product toxicity, nutrient limitations, and monochloramine inhibition of ammonia and THM degradation. Finally, molecular analysis of the developed biofilm was undertaken to provide additional information to interpret process performance.

Task 3 developed a steady-state mathematical model of the process. Apparent steady-state data from the biofilter experiments and supporting batch experiments were used to estimate kinetic parameters. Subsequently, the model was verified against other experimental biofilter data. Finally, the model was used to simulate full-scale filter performance under different filter surface loading rates and THM speciation seen in practice.

1.3. ORIGINALITY

This research studies the feasibility of trihalomethane (THM) cometabolism in laboratory-scale biofilters under conditions that reflect water treatment plant practice. This research is unique in that almost no work has been done on biological control mechanisms for THMs. By extending findings from aquifer remediation and hazardous waste treatment research to drinking water treatment, a new biological treatment process

was evaluated based on THM cometabolism by bacteria growing on ammonia in laboratory-scale biofilters.

Chapter 2: Literature Review

2.1. TRIHALOMETHANES

2.1.1. Usage and Properties

Trihalomethanes (THMs) include the chemicals trichloromethane (TCM) also referred to as chloroform, bromodichloromethane (BDCM), dibromochloromethane (DBCM), and tribromomethane (TBM) also referred to as bromoform. The chemical structures of the THMs are presented in Figure 2.1. THMs are volatile and only slightly water soluble as Table 2.1 shows.

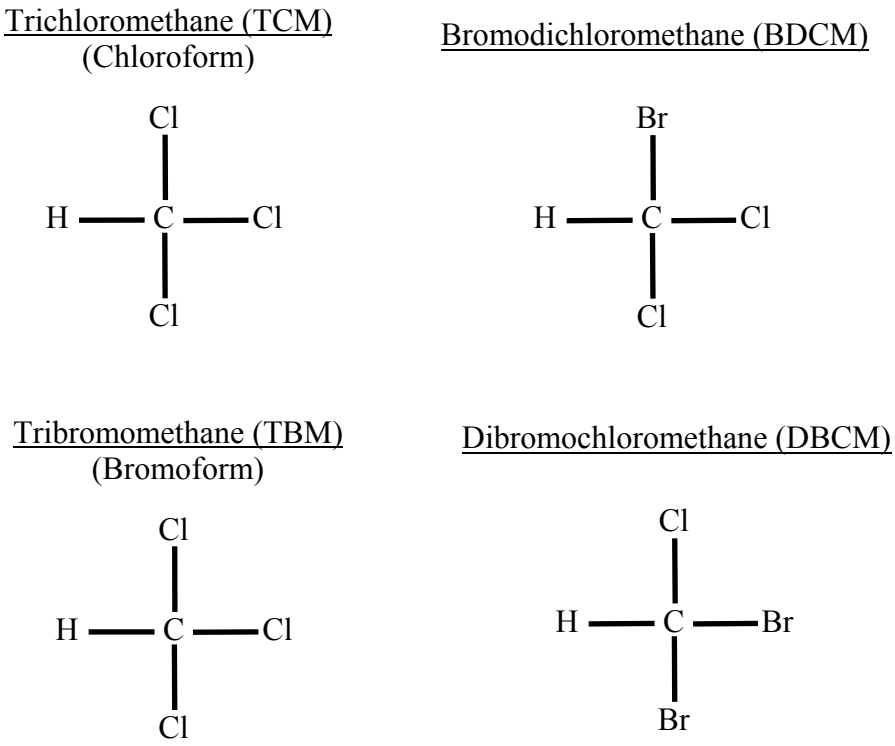

Figure 2.1 Trihalomethane chemical structures

Table 2.1 Trihalomethane chemical properties

Chemical	Molecular Weight (g/mole)	Density (g/mL)	Melting Point (°C)	Boiling Point (°C)	Solubility (mg/L)	Vapor Pressure (mm Hg)
TCM[a]	119.4	1.48	-63.3	61.4	8,450	188
BDCM[a]	163.8	1.97	-57.1	90.0	4,616	49.6
DBCM[b]	208.3	2.44	-20	120	4,000	76
TBM[a]	252.8	2.89	8.3	149.6	3,110	5.43

[a](Schwarzenbach et al. 2003) – Except for density (20°C), all data given for 25°C

[b](Montgomery and Welkom 1990) – Except for density (25°C), all data given for 20°C

2.1.2. Formation in Drinking Water

Disinfection by-products (DBPs) are formed during drinking water disinfection. DBPs are a class of chemicals of which THMs are a more specific category. The general formula for DBP formation is described by the following equation (Krasner 1999):

$$\text{Disinfectant} + \text{Precursor} \rightarrow \text{DBPs}$$

Table 2.2 details typical disinfectants used, precursor materials, and the resulting major DBPs formed during drinking water disinfection. Out of this list of major DBPs, THMs and HAAs consistently are found in the greatest number and highest concentrations when chlorinating drinking water, with THMs and HAAs representing approximately 20% and 13% of the halogenated organic matter after disinfection,

respectively (Clark et al. 2001; Krasner 1999; Letterman and American Water Works Association. 1999).

Table 2.2 Disinfection by-products formation component summary

Disinfectants	Precursors	Major DBPs
▪ Chlorine ▪ Chloramines ▪ Ozone ▪ Chlorine Dioxide	▪ Natural organic matter (NOM) ▪ Algae ▪ Bromide	▪ Trihalomethanes (THMs) ▪ Haloacetic acids (HAAs) ▪ Haloacetonitriles ▪ Haloketones ▪ Chloral hydrate ▪ Chloropicrin ▪ Cyanogen halides ▪ Oxyhalides ▪ Aldehydes ▪ Aldoketoacids ▪ Carboxylic acids ▪ Maleic Acids

Source: (Singer 1999)

2.1.3. Potential Health Affects

All four THMs have been classified as having a carcinogenic potential by the United States Environmental Protection Agency (USEPA). Table 2.3 provides a summary of the USEPA classification system for chemicals based on carcinogenic potential and related information on the THMs' classification in this scheme, their potential health affects, and sources in drinking water.

Table 2.3 Trihalomethane health affects summary

Contaminant	Group	10^{-6} Cancer Risk	Potential Health Affects	Sources of Drinking Water Contamination
TCM	B2	6 μg/L	Cancer, liver, kidney, reproductive effects	Chlorination and chloramination DBP
BDCM	B2	0.6 μg/L	Cancer, liver, kidney, reproductive effects	Chlorination and chloramination DBP
DBCM	C	Not Determined	Nervous system, liver, kidney, reproductive effects	Chlorination and chloramination DBP
TBM	B2	4 μg/L	Cancer, nervous system, liver, kidney effects	Ozonation, chlorination, and chloramination DBP

EPA Scheme for Categorizing Chemicals According to Carcinogenic Potential

Group	Classification	Definition
B2	Probable human carcinogen	Limited evidence in epidemiologic studies and/or sufficient evidence from animal studies
C	Possible human carcinogen	Limited evidence from animal studies and inadequate or no data in humans

Source: (Clark et al. 2001; Zavaleta et al. 1999)

2.1.4. Regulations

Total THMs (TTHMs), the sum of the four THMs, is regulated under the Stage 1 and Stage 2 Disinfectants/Disinfection By-products Rule (D/DBPR). A summary of the USEPA regulations concerning THMs is presented in Table 2.4, detailing the maximum contaminant level goals (MCLGs) for each THM and maximum contaminant level (MCL) for TTHMs (USEPA 1998; USEPA 2006). The envisioned THM treatment process studied in this research would provide utilities with another option to comply with these regulations by reducing the TTHM concentrations in their finished drinking waters.

Table 2.4 Trihalomethane regulation summary

THM	MCLG (mg/L)	MCL (mg/L)
TCM	0.07	-
BDCM	Zero	-
DBCM	0.06	-
TBM	Zero	-
TTHM	-	0.08

2.1.5. Current Drinking Water Treatment Options

Much effort over the past two decades has gone into approaches for minimizing DBP formation through modification of disinfection practices and removal of precursor materials (Singer 1999), while comparatively little effort has been expended on approaches for removing the DBPs formed in treatment plants before sending finished

water into distribution systems. The current research seeks to evaluate the feasibility of a treatment process to remove THMs once formed, adding an additional option to the current practices used for DBPs. The current practices used for DBPs are summarized as follows (Owen 1999; Pontius 2003; Randtke 1999):

- Alternative disinfectants – Utilization of disinfectants other than chlorine and/or in combination with chlorine. The other disinfectants include chloramines, chlorine dioxide, ozone, and ultraviolet light.
- Precursor removal – Removal of the precursor materials that lead to DBP formation.
    - Enhanced coagulation – The coagulation process is used to remove DBP precursor compounds such as NOM. In general, the process becomes more effective at precursor removal as coagulant dose increases and pH decreases, but the actual conditions of operation are site-specific.
    - Enhanced softening – The softening process is used to remove DBP precursor compounds such as NOM.
    - Granular activated carbon (GAC) adsorption – GAC is used to adsorb precursor material, and its effectiveness is directly related to the adsorbability of the precursor material in the water.
    - Membrane separation – This is accomplished through nanofiltration (NF) and reverse osmosis (RO). The processes operate at high pressures, 80 to 250 psi (550 to 1,700 kPa), and can remove 95 to 99 percent of precursor material.

2.2. NITRIFYING BACTERIA

In general, nitrifying bacteria carry out the biological oxidation of ammonia (NH_3) to nitrate (NO_3^-). This occurs in a two-step process. The first step is the oxidation of ammonia to nitrite (NO_2^-) and is carried out by ammonia oxidizing bacteria (AOB). The second step is the oxidation of nitrite to nitrate and is carried out by nitrite oxidizing bacteria (NOB) (Prosser 1986). This research focused on the use of AOB as explained in the following sections.

2.2.1. Ammonia Oxidizing Bacteria

AOB are gram-negative bacteria that utilize ammonia as their sole source of energy and inorganic carbon as their main carbon source. The oxidation of ammonia is an aerobic process carried out optimally between pH 7.5-8.0 and temperatures between 25-30°C. AOB have low growth rates and yields because of the small energy gain from the oxidation of ammonia and large energy investment needed to reduce inorganic carbon, resulting in generation times varying from eight hours to several days (Prosser 1986; Prosser 1989).

2.2.2. Model Nitrifier *Nitrosomonas europaea* (ATCC 19718)

The most studied bacterium of the AOB is the pure culture *Nitrosomonas europaea*; therefore, it was used in this research to provide a basis of comparison to other research. *N. europaea* is a gram-negative bacterium in the β-subdivision of the Proteobacteria. The oxidation of ammonia to nitrite provides it with all of its required reductant for energy and biosynthesis, and it uses inorganic carbon for all of its required carbon for growth. As a result, it is classified as an obligate chemolithoautotrophic bacteria (Arp et al. 2002). Its complete genome has been sequenced and its pathway for ammonia degradation has been well studied (Chain et al. 2003). As a result of the recent

sequencing of its genome, research has shown that *N. europaea* can grow on the organic carbon sources of fructose and pyruvate, possibly indicating that its classification should be changed from an obligate chemolithoautotrophic to facultative chemolithoorganotroph (Hommes et al. 2003).

Molecular Biology and Biochemistry

Figure 2.2 depicts the central metabolic pathway of *N. europaea*. For the oxidation of ammonia to nitrite, *N. europaea* uses two enzymes in two reaction steps. The first reaction converts ammonia to hydroxylamine (NH_2OH) and is catalyzed by the membrane-bound enzyme ammonia monooxygenase (AMO). The second step converts hydroxylamine to nitrite and is catalyzed by the periplasmic-residing enzyme hydroxylamine oxidoreductase (HAO) (Arp et al. 2002). Because of its metabolic pathway, *N. europaea* is typically cultivated on an inorganic medium as that used by Ely (1996).

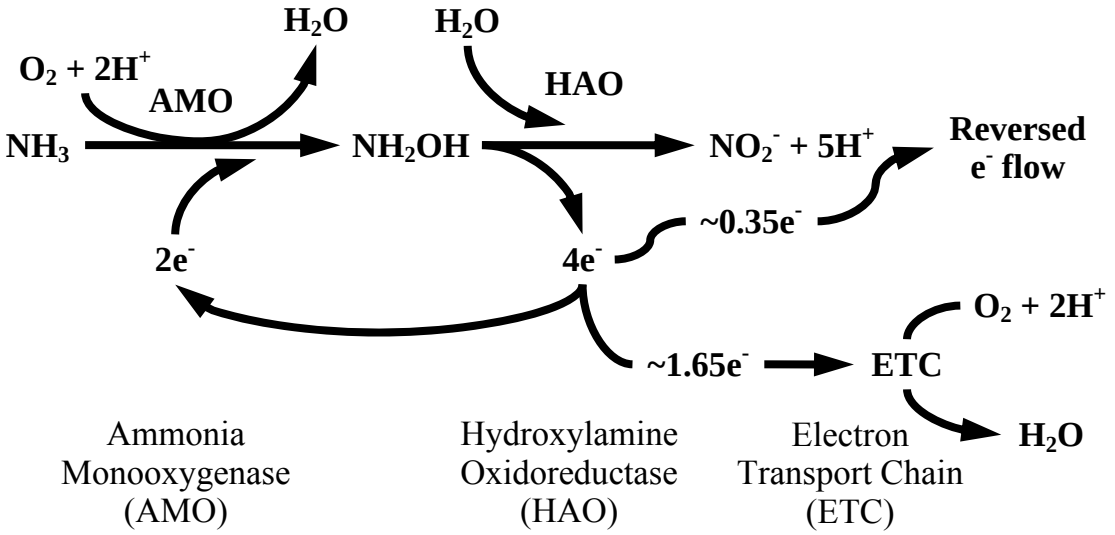

Source: (Adapted from Stein 1998)

Figure 2.2 Central metabolism of *N. europaea*

Ammonia Monooxygenase

AMO requires oxygen, electrons, and ammonia. Ammonia is the only source of reductant for *N. europaea* through the subsequent oxidation of hydroxylamine as shown in Figure 2.2. Two of the four electrons resulting from hydroxylamine oxidation are cycled back to AMO, while the other two electrons are used for other cellular processes, with an average of 1.65 electrons passing to the terminal oxidase for ATP generation and 0.35 passing to NAD^+ to form NADH for biosynthesis (Arp et al. 2002; Whittaker et al. 2000). In addition to serving as the substrate for AMO, ammonia is believed to be a signal for gene expression, inducing a global transcription response in *N. europaea* (Arp et al. 2002).

AMO is a non-specific enzyme as is evident by the extensive list of substrates presented in Table 2.5 for the AMO enzyme of *N. europaea*. AMO's non-specificity was used in this research for THM cometabolism. The active site for AMO is believed to be hydrophobic as all substrates and competitive inhibitors are non-polar (Hooper et al. 1997). As a result, ammonia (NH_3) and not ammonium (NH_4^+) is the true substrate for AMO (Suzuki et al. 1974). It has been proposed that a second active site exists on AMO at which noncompetitive inhibitors can bind and oxidation can occur at either active site. In this model, AMO would contain at least two substrate binding sites, an oxygen binding site, and a site for electron donation to AMO (Keener and Arp 1993; Keener et al. 1998).

Iron and Copper

The importance of iron to *N. europaea* is evidenced by the 20 genes contained in its genome for iron siderophore receptors and their regulators, and in addition, 14% of the active transport proteins are for iron (Chain et al. 2003). Interestingly, no genes for the synthesis of siderophores were recognized. From this, it was deduced that *N. europaea* acquires iron at the expense of other bacteria that produce siderophores (Chain et al.

2003). AMO is believed to contain copper and iron based on the evidence summarized in Table 2.6. Even with this evidence, the metal content of AMO is speculative until AMO is extensively purified with activity.

Table 2.5 Substrates of ammonia monooxygenase for *N. europaea*

	General	
Ammonia	Methane[d, p, r]	Methanol[o, p]
Carbon Monoxide[j, p, q]	Dimethyl Ether[c]	Ethylene Oxide[s]
	Alkanes and Alkenes	
n-Alkanes to C_8[b]	1-Alkenes to C_5[b]	cis- and trans-2-Butene[b]
Cyclohexane[a]	Ethylene[s]	
	Sulfur Compounds	
Methylsulfide[e]	Methylphenylsulfide[e]	Ethylsulfide[e]
Allylmethylsulfide[e]	Tetrahydrothiophene[e]	Allylsulfide[e]
Thiophene[e]		
	Halogenated Alkanes	
Fluoromethane[c]	Chloroethane[h]	1,1,2-Trichloroethane[k]
Chloromethane[h]	Bromoethane[h, g, t]	1,1,2,2-Tetrachloroethane[i]
Bromoethene[t]	Iodoethane[h]	Chloropropane[h]
Dichloromethane[k]	1,1-Dichloroethane[i]	1,2-Dichloropropane[g]
Dibromomethane[k]	1,2-Dichloroethane[i]	1,2,3-Trichloropropane[k]
Trichloromethane[k]	1,2-Dibromoethane[k]	1,2-Dibromo-3-chloropropane[g]
Fluoroethane[h]	1,1,1-Trichloroethane[k]	Chlorobutane[h]
	Halogenated Alkenes	
Chloroethylene[k]	Trichloroethylene[k,v]	2,3-Dichloropropene[m]
gem-Dichloroethylene[k]	Tribromoethylene[k]	cis-1,3-Dibromopropene[m]
cis-Dichloroethylene[k]	3-Iodopropene[m]	trans-1,3-Dibromopropene[m]
trans-Dichloroethylene[k]	cis-1,3-Dichloropropene[m]	1,1,3-Trichloropropene[m]
cis-Dibromoethylene[k]	trans-1,3-Dichloropropene[m]	
	Aromatics	
Benzene[f, u]	Bromobenzene[f]	ortho-Cresol[f]
Toluene[f]	Iodobenzene[f]	2,5-Dimethylphenol[f]
para-Xylene[f]	1,2-Dichlorobenzene[f]	Acetophenone[f]
Ethylbenzene[f]	Phenol[f]	Aniline[f]
Styrene[f]	Anisole[n]	Nitrobenzene[f]
Naphthalene[n, x]	para-Methylbenzyl Alcohol[f]	Benzonitrile[n]
Fluorobenzene[n]	Phenethyl Alcohol[f]	Nitrapyrin[l, w]
Chlorobenzene[f]	sec-Phenethyl Alcohol[f]	2-Methyl Napthalene[x]
Acenaphthalene[x]	Acenaphthene[x]	

[a](Knowles 1980); [b](Hyman et al. 1988); [c](Hyman et al. 1994); [d](Jones and Morita 1983b); [e](Juliette et al. 1993); [f](Keener and Arp 1994); [g](Rasche et al. 1990b); [h](Rasche et al. 1990a); [i](Rasche et al. 1991); [j](Tsang and Suzuki 1982); [k](Vannelli et al. 1990); [l](Vannelli and Hooper 1992); [m](Vannelli 1994); [n](Vannelli and Hooper 1995); [o](Voysey and Wood 1987); [p](Suzuki et al. 1976); [q](Jones and Morita 1983a); [r](Hyman and Wood 1983); [s](Hyman and Wood 1984b); [t](Hyman and Wood 1984a); [u](Hyman et al. 1985); [v](Arciero et al. 1989); [w](Vannelli and Hooper 1993); [x](Chang et al. 2002)

Source: (Adapted from Hooper et al. 1997)

Because AMO has not been extensively purified with activity, particulate Methane Monooxygenase (pMMO) is used to derive information about AMO as it is genetically, catalytically, and structurally similar (Arp and Stein 2003). Recently, the crystal structure of pMMO at a resolution of 2.8 Å for *Methylococcus capsulatus* (Bath) was determined (Lieberman and Rosenzweig 2005a; Lieberman and Rosenzweig 2005b). The pMMO crystal structure contained three metal centers, two being occupied by copper with the third being occupied by zinc. The authors believe the zinc center is from the zinc acetate in their crystallization solution that displaced the biologically relevant metal. Based on the surrounding residues at the zinc site, it might contain iron or copper (Lieberman and Rosenzweig 2005a; Lieberman and Rosenzweig 2005b). Because of the apparent importance of iron and copper to AMO, these metals might become limiting during implementation of the proposed process in this research.

Table 2.6 Evidence for iron and copper in ammonia monooxygenase

Metal	Evidence
Copper	1. Inhibition by copper chelators. 2. Cell extracts activated by copper. 3. Analogy with pMMO that contains copper.
Iron	1. Electron paramagnetic resonance (EPR) spectroscopy.

Source: (Arp and Stein 2003; Zahn et al. 1996)

2.2.3. Cometabolism

Cometabolism can be defined as the fortuitous biodegradation of a target chemical (i.e., the cometabolite) through reactions catalyzed by one or more non-specific microbial enzymes (Dalton and Stirling 1982). Bacteria rarely derive carbon, energy, or any other benefit from cometabolism. As such, bacteria must have true carbon and energy sources available to sustain biological activity. Typically, the growth substrate induces production of the non-specific enzyme that catalyzes both metabolism of the growth substrate and cometabolism of the cometabolite. Much research has been performed over the past 15 years on the cometabolism of halogenated aliphatic chemicals (Alvarez-Cohen and Speitel 2001). In particular, a vast body of research exists on the cometabolism of trichloroethylene (TCE), which for a long time has been the "model" halogenated chemical in cometabolism studies. Various non-specific oxygenase enzymes produced by bacteria growing aerobically on methane, propane, butane, toluene, phenol, and ammonia have been used to cometabolize halogenated chemicals. From the viewpoint of drinking water treatment applications, ammonia appears to be the only readily viable growth substrate. The use of the other growth substrates obviously involves the addition of organic chemicals during treatment, which has various technical disadvantages and major problems with respect to utility and perhaps consumer acceptance.

With respect to THM cometabolism, chloroform was the only chemical that has been studied prior to this research. Both methane and ammonia-degraders (i.e., nitrifiers) can cometabolize chloroform (Alvarez-Cohen and Speitel 2001; Aziz et al. 1999; Ely 1996). In some methane degraders, the methane monooxygenase that catalyzes the oxidation of methane to methanol is non-specific and can catalyze the addition of oxygen to chloroform (and presumably the other THMs) producing trichloromethanol. The

metabolic pathways for methane and chloroform degradation are shown in Figure 2.3 and Figure 2.4, respectively, to demonstrate the similarities in the degradation of the two chemicals. In Figure 2.3, PQQH2 and YH2 are electron carriers. Chloroform can be viewed as structurally similar to methane, while trichloromethanol is structurally similar to methanol. Methanol is further metabolized by the organisms to provide energy and carbon for cell growth. Trichloromethanol is not further oxidized by the organism because the next enzyme in the metabolic pathway is very specific. Fortunately, trichloromethanol is chemically unstable and degrades to inorganic products without the need for further microbial catalysis of the reaction. In a similar way, the first enzyme in the metabolic pathway for ammonia degradation, AMO, is non-specific in some nitrifiers, thereby catalyzing the oxidation of both ammonia to hydroxylamine and chloroform to trichloromethanol.

Most of the cometabolism research with nitrifiers has been done with the soil bacteria, *N. europaea*, which has been used as an example of the ubiquitous soil- and water-dwelling nitrifying bacteria. Vannelli et al. (1990) showed that this organism could cometabolize various halogenated methanes, ethanes, and ethenes including chloroform, dichloromethane, and dibromomethane. THMs, other than chloroform, were not studied. Chloroform cometabolism by *N. europaea* was subsequently confirmed by Rasche et al. (1991) and Ely (1996), who also conducted detailed kinetic experiments. Melin et al. (1996) and Ginestet et al. (2001) showed that a mixed culture of nitrifiers from a marine sediment and activated sludge, respectively, could cometabolize chloroform, thereby providing some evidence that non-specific AMO enzymes might be widely distributed in the environment. Wide distribution of non-specific AMO enzymes would be advantageous for easy implementation of the proposed THM cometabolism process.

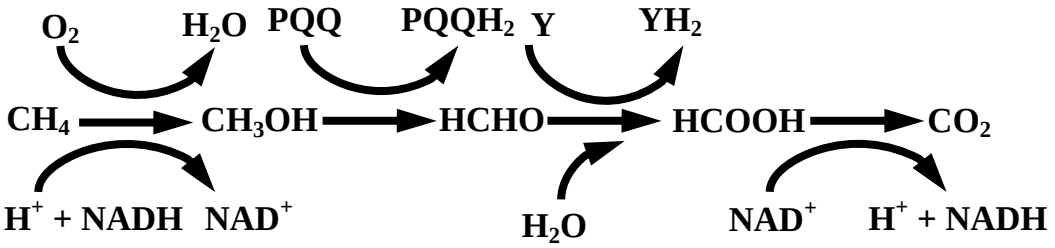

Source: (Adapted from Anthony 1982; Large 1983)

Figure 2.3 Metabolic pathway for biodegradation of methane

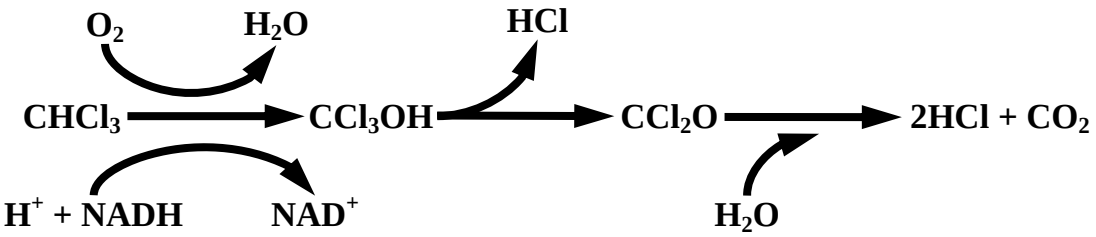

Source: (Adapted from Davidson et al. 1982)

Figure 2.4 Possible pathway for the cometabolism of chloroform (TCM)

The intermediate products of cometabolism can be toxic to the bacteria carrying out the reaction. With some exceptions, the cometabolism products of chlorinated aliphatics are transient, so they do not accumulate appreciably. Rather, they exert toxicity either while being formed or immediately after formation because they are unstable and highly reactive (Arp et al. 2001). Product toxicity associated with the cometabolism of chlorinated aliphatics is most often described by a transformation capacity (T_c) term. T_c represents the maximum mass of cometabolite that can be

degraded per unit mass cells, or, in other words, the mass of cometabolite degradation required to completely inactivate the cells (Alvarez-Cohen and McCarty 1991a). The magnitude of T_c is a function of both the bacteria and the cometabolite participating in the reaction. T_c values for chloroform seem to be at an intermediate level relative to other chemicals (Alvarez-Cohen and Speitel 2001; Aziz et al. 1999). It is important to note that product toxicity has been observed most often at relatively high cometabolite concentrations in comparison to those expected in drinking water treatment. Some work (Segar 1994) indicates that product toxicity is of little consequence at the concentrations expected in drinking water treatment.

Cometabolism of THMs with nitrifiers is expected to be harmful to nitrifiers in one of three ways as illustrated in Figure 2.5:

- Formation of toxic intermediates
- Reductant (electron) depletion
- Competition with ammonia monooxygenase (AMO).

As mentioned previously, the intermediates of cometabolism can be toxic. The first step in this process is the hydroxylation of chloroform, $CHCl_3$, by AMO to trichloromethanol, CCl_3OH. Trichloromethanol is unstable and releases hydrochloric acid to form phosgene, CCl_2O. Phosgene is also unstable and reacts with water to form hydrochloric acid, HCl, and carbon dioxide, CO_2. Pohl et al. (1977) proposed the mechanism shown in Figure 2.6 for the oxidative dechlorination of chloroform by liver microsomes of rats. As shown in Figure 2.6, the unstable phosgene can bind with macromolecules as well as degrade to carbon dioxide. Based on this mechanism, phosgene could attack the bacteria cell directly, increasing toxicity to the cell with increasing degradation of chloroform.

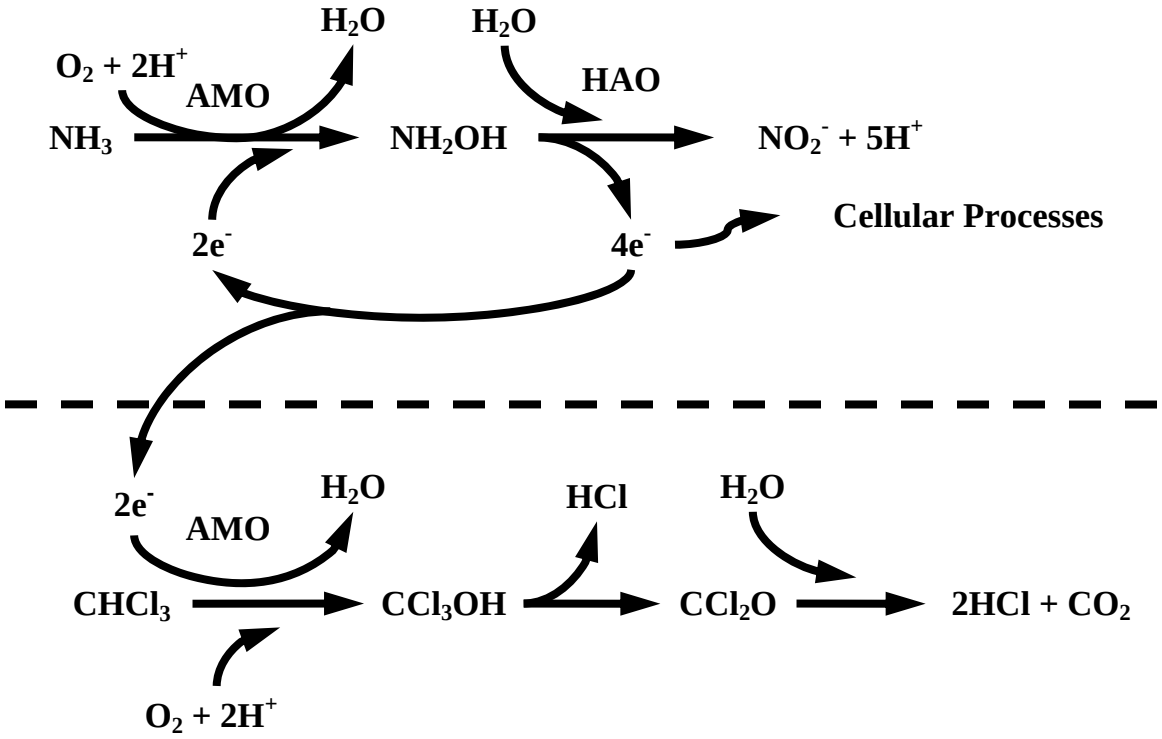

Figure 2.5 Proposed metabolic pathway for nitrifier cometabolism of chloroform

Two other possible results of cometabolism on nitrifiers are detailed in Figure 2.5, the first step in both ammonia and chloroform degradation uses AMO. Because of this, competition could exist for the enzyme. In addition, as mentioned previously, two electrons are recycled from the subsequent degradation of hydroxylamine from ammonia. Chloroform cometabolism would require these same two electrons, and its further degradation would not result in the production of electrons to recycle back for its further degradation. As a result, cometabolism could result in depletion of the reductant (i.e., electrons) in nitrifiers and would require the presence of ammonia to provide a source of reductant for its sustained degradation.

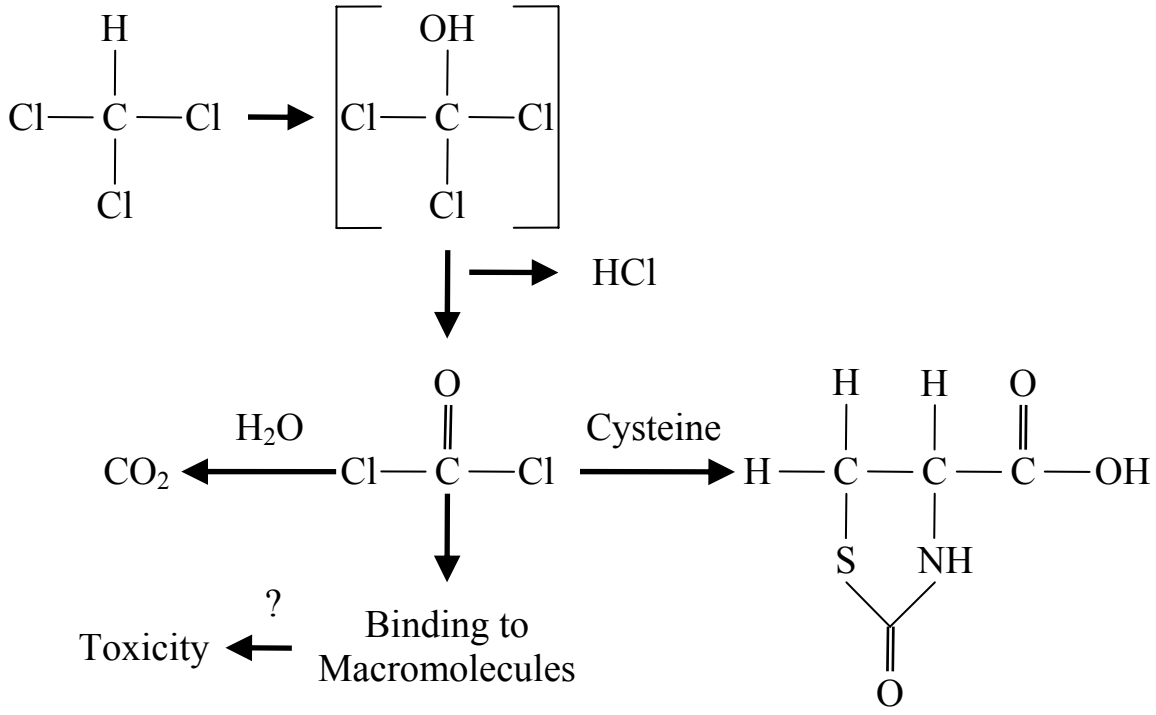

Source: (Adapted from Pohl et al. 1977)

Figure 2.6 Proposed trichloromethane mechanism

2.3. MICROBIAL KINETICS

Degradation kinetics are an important issue in determining the practicality of any cometabolism treatment process. The kinetic model for ammonia degradation and four models appropriate for THM cometabolism are summarized in Table 2.7 along with their major assumptions (Alvarez-Cohen and Speitel 2001; Arcangeli and Arvin 1997; Criddle 1993). The four models presented for THM cometabolism were evaluated and ultimately one model, the reductant model, was selected to represent THM cometabolism based on fitting of experimental results to the models. A detailed derivation of each individual rate equation is provided in Appendix A.

Table 2.7 THM and ammonia kinetic model equation summary

Chemical	Model Name	Fitting Parameters	Rate Equations and Assumption(s)
Ammonia	Saturation Kinetics	3	$r_{TOTNH_3} = -\frac{k_{TOTNH_3} XS_{TOTNH_3} \alpha_1}{K_{s_{NH_3-N}} + S_{TOTNH_3} \alpha_1}$ 1. THMs do not compete with ammonia.
THM	First-Order	2	$r_{THM} = -k_{1THM} XS_{THM}$ 1. Ammonia does not compete with THMs. 2. THMs do not compete with ammonia. 3. THMs do not compete with each other. 4. One limiting reactant (THM).
THM	Competition	2	$r_{THM} = -\frac{k_{1THM} XS_{THM}}{1 + \frac{S_{TOTNH_3} \alpha_1}{K_{s_{NH_3-N}}}}$ 1. Ammonia competes with THMs. 2. THMs do not compete with ammonia. 3. THMs do not compete with each other. 4. One limiting reactant (THM).
THM	Reductant	2	$r_{THM} = -\frac{k_{1THM} XS_{THM}}{1 + \frac{K_{s_{NH_3-N}}}{S_{TOTNH_3} \alpha_1}}$ 1. Ammonia does not compete with THMs. 2. THMs do not compete with ammonia. 3. THMs do not compete with each other. 4. Two limiting reactants (THM and Reductant).
THM	Combined	2	$r_{THM} = -\frac{k_{1THM} XS_{THM}}{\left(1 + \frac{S_{TOTNH_3} \alpha_1}{K_{s_{NH_3-N}}}\right)\left(\frac{K_{s_{NH_3-N}}}{S_{TOTNH_3} \alpha_1} + 1\right)}$ 1. Ammonia competes with THMs. 2. THMs do not compete with ammonia. 3. THMs do not compete with each other. 4. Two limiting reactants (THM and Reductant).

α_1 = NH_3-N fraction of $TOTNH_3$ (pH dependent)
$k_{1_{THM}}$ = THM rate constant (L/mg TSS–day)
$K_{s_{NH_3\text{-}N}}$ = ammonia half-saturation constant (mg NH_3-N/L)
k_{TOTNH_3} = ammonia maximum specific rate of degradation (mg $TOTNH_3$/mg TSS–Day)
r_{TOTNH_3} = rate of $TOTNH_3$ degradation (mg $TOTNH_3$/L-Day)
r_{THM} = rate of THM degradation (mg THM/L-Day)
S_{THM} = THM concentration (mg/L THM)
S_{TOTNH_3} = $TOTNH_3$ concentration (mg/L $TOTNH_3$)
$TOTNH_3$ = total ammonia-nitrogen = [NH_3-N] + [NH_4^+-N] (mg N/L)
X = Biomass concentration (mg/L TSS)

2.3.1. Ammonia Speciation

Because ammonia (NH_3) and not ammonium (NH_4^+) is the substrate for AMO, accounting for ammonia is required to determine degradation kinetics for any model that incorporates ammonia concentration. During experiments, the total ammonia-nitrogen ($TOTNH_3$) was measured; therefore, acid-base chemistry was used to convert from $TOTNH_3$ to ammonia. The following relationship exists for the ratio of ammonia to $TOTNH_3$, correcting K_a for temperature ($K_{a,T}$), incorporating an ionic strength correction (s) based on the Davies equation, and using the medium's pH (Emerson et al. 1975; Messer et al. 1984; Soderberg and Meade 1991):

$$NH_4^+ \overset{K_{a,T}}{\Leftrightarrow} NH_3 + H^+$$

$$\alpha_1 = \frac{1}{1+10^{(pK_{a,T}-pH-s)}} = \frac{[NH_3]}{[TOTNH_3]}$$

$$pK_{a,T} = -\log K_{a,T} = 0.09018 + \frac{2729.92}{T+273.16}$$

$$pH = -\log\{H^+\}$$

$$s = \log_{10}\gamma_{NH_4^+} = -A\left(z_{NH_4^+}\right)^2\left[\frac{I^{1/2}}{1+I^{1/2}} - 0.2I\right]$$

$$A = 1.82483\times10^6\left[E(T+273.16)\right]^{-1.5}$$

$$E = 87.74 - 0.4008\,T + 9.398\times10^{-4}\,T^2 - 1.41\times10^{-6}\,T^3$$

$$I = \frac{1}{2}\sum c_i z^2$$

where α_1 = NH_3-N fraction of $TOTNH_3$

$K_{a,T}$ = Temperature corrected equilibrium constant (Valid for 0ºC < T < 50ºC)

T = Temperature in ºC

s = Activity correction term (Valid for I < 0.5 M)

$\gamma_{NH_4^+}$ = Activity coefficient for ammonium ion

$z_{NH_4^+}$ = Ionic charge of NH_4^+ = 1

A = Coefficient depending on dielectric constant at temperature T

E = Dielectric constant

I = Ionic strength of medium

c_i = Concentration in terms of molarity (M) of species i in medium

z_i = Ionic charge of species i in medium

2.3.2. Available Kinetic Information

As noted previously, TCE kinetics are frequently used as the standard against which other cometabolic chemical degradation rates are judged. The most rapid TCE kinetics are provided by a methane-degrading bacteria, *Methylosinus trichosporium* OB3b (Alvarez-Cohen and Speitel 2001). Much of the chloroform cometabolism research also has been performed with this organism (Aziz et al. 1999; Chang and Alvarez-Cohen 1996; Speitel et al. 1993; Vlieg et al. 1997). Detailed kinetic data for nitrifiers are available only for *N. europaea* (Ely 1996). Table 2.8 provides a summary of kinetic coefficients based on the pseudo-first order rate constants, k_1, the easiest basis for comparison. Chloroform cometabolism is somewhat slower than TCE cometabolism for both *M. trichosporium* OB3b and *N. europaea*. In addition, the kinetics for both chlorinated chemicals are somewhat slower for *N. europaea* than for *M. trichosporium* OB3b. For all four cases, however, the rate constants would be considered quite large for cometabolism kinetic coefficients (Alvarez-Cohen and Speitel 2001). For example, treatment process feasibility has been demonstrated for cometabolic degradation reactors operating at rate constants of 0.03 to 0.1 L/mg-day (Segar et al. 1995).

Table 2.8 also shows that the nitrification kinetic coefficients for *N. europaea* are similar to typical kinetic parameters encountered with mixed cultures of nitrifying bacteria, as would be seen in practical applications. An important issue highlighted in Table 2.8 is the relatively low half saturation coefficient for ammonia (0.5 to 1 mg/L (36 to 71 μM) versus chloroform (32 mg/L (268 μM)). This difference in K_s values indicates that the enzyme has a greater affinity for ammonia than chloroform, implying that enzyme competition can be a significant consideration. If the ammonia concentration is too large, the chloroform cometabolism rate could decrease precipitously. If competition occurs, the cometabolism rate would steadily decrease with increasing ammonia concentration. Thus, addition of too much ammonia would be counterproductive to THM cometabolism. Enzyme competition might not be a major concern in biofilters, however, at the anticipated influent ammonia concentration of 1 to 4 mg N/L, especially considering that this represents the maximum ammonia concentration present. As water moves through the biofilter and ammonia diffuses into the biofilm, the ammonia concentration will decrease through biodegradation thereby also decreasing the extent of enzyme competition. Ammonia addition could also lead to excessive dissolved oxygen consumption in the biofilter and/or violation of the MCL of 10 mg N/L for nitrate-nitrogen and 1 mg N/L for nitrite-nitrogen, which are products of ammonia metabolism. These concerns must be considered during process design.

In comparing how THM degradation rates might be expected to vary between THMs, there are two studies that have competing implications. To evaluate possible implications of these studies, it is first useful to note that that $k_{1_{THM}}$ is a simplification appropriate to low THM concentrations (i.e., $k_{1_{THM}} \approx k_{THM}/K_{s_{THM}}$) as detailed in Appendix A.

Table 2.8 Microbial kinetics coefficients for TCE, chloroform, and ammonia

Organism	Chemical	k_{TOTNH_3} (mg/mg-day)	K_s (mg/L)	k_1 (L/mg-day)	Source
M. trichosporium OB3b	TCE	21	11	1.9	a
M. trichosporium OB3b	Chloroform	3.1	3.1	1.0	a
N. europaea	TCE	1.6	1.6	1.0	b
N. europaea	Chloroform	10	32	0.32	b
N. europaea	Ammonia	8.8	0.54	-	b
Nitrifying Mixed Culture	Ammonia	2.3	1.0	-	c

Sources: a. (Aziz et al. 1999); b.(Ely 1996); c. (Rittmann and McCarty 2001)

In the first study, a proposed active site model for AMO (Keener and Arp 1993) predicts that THMs bind at a hydrophobic site, where NH_3 also binds. Because bromine is more nucleophilic (less electrophilic) than chlorine, the hydrogen on the THM could reduce its partial charge and become relatively more hydrophobic as bromine-substitution increases. Thus, bromine substitution would make THMs more attractive to AMO's active site, which implies that $K_{s_{THM}}$ decreases (and $k_{1_{THM}}$ increases) as bromine-substitution increases. On the other hand, a second study by Rasche et al. (1990a) studied oxidation of monohalogenated ethanes by *N. europaea* and found that the maximum rate of oxidation (k_{THM}) decreased from chloroethane to bromoethane. These findings suggest that k_{THM} might decrease (along with $k_{1_{THM}}$) with increasing THM bromine substitution.

The current research was designed to delineate whether the relative nucleophilicity of bromine compared to chlorine dominates over possible differences in

the maximum rates for the low THM concentrations (less than 100 μg/L for a given THM) used in this research. The relative importance of these two competing factors will determine the ultimate effect on $k_{1_{THM}}$.

2.4. LABORATORY BIOFILTER SCALING TO FULL-SCALE BIOFILTERS

To design laboratory biofilters representative of full-scale biofilters, the scaling procedure proposed by Manem and Rittmann (1990) was used. In this procedure, three similitude criteria are used: (1) biofilm surface concentration, (2) biofilm shear loss-rate, and (3) mass balance. When these three criteria are met, the laboratory and full-scale biofilters will have the same flux into the biofilm, accumulation of biofilm, and mass balance on the substrate. In their research, Manem and Rittmann (1990) determined that the laboratory and full-scale systems could not meet all three criteria with the same influent substrate concentration. Because of this, this research reports a range of full-scale biofilters that correspond to the laboratory biofilters, depending on whether biofilm shear loss or external mass transport is chosen for scaling.

2.5. CHLORAMINE CHEMISTRY

Chloramine chemistry has been studied extensively over the past several decades. In the presence of ammonia or ammonium ion, hypochlorous acid, HOCl, and hypochlorite ion, OCl^-, (collectively referred to as free chlorine) react in a stepwise manner to form chloramines as depicted in the following simplified reaction sequence (Bauer and Snoeyink 1973):

$$NH_3 + HOCl = NH_2Cl + H_2O \text{ or } NH_4^+ + HOCl = NH_2Cl + H_2O + H^+$$
$$NH_2Cl + HOCl = NHCl_2 + H_2O$$
$$NHCl_2 + HOCl = NCl_3 + H_2O$$

The reaction products (monochloramine (NH_2Cl), dichloramine ($NHCl_2$), and nitrogen trichloride or trichloramine (NCl_3)) contribute to the total (or combined) chlorine residual.

Chloramine speciation depends primarily on the solution pH and the chlorine to nitrogen (Cl_2:N) ratio. The formation of dichloramine and nitrogen trichloride in drinking water is undesirable because these compounds impart a disagreeable taste at concentrations above 0.8 and 0.2 mg/L-Cl_2, respectively (Wolfe et al. 1984). In general, monochloramine is dominant at pH values greater than 7, dichloramine becomes dominant between pH 4.5 to 5.0, and below pH 4, nitrogen trichloride is the dominant species (Pressley et al. 1972).

At sufficiently high chlorine doses, ammonia is completely oxidized to nitrate and nitrogen gas. This breakpoint dose denotes the amount of chlorine that must be added to a water before a stable free residual can be obtained. Stoichiometrically, ammonia oxidation by monochloramine to nitrogen gas requires a Cl_2:N mass ratio of 7.6:1. However, in practice a Cl_2:N dose as high as 15:1 might be needed to achieve breakpoint due to demands exerted by reduced inorganic and organic species (Letterman and American Water Works Association. 1999). Because breakpoint chlorination should be avoided during chloramination, utilities typically use Cl_2:N doses ranging from 3 to 5 on a mass basis (USEPA 1999).

Chloramines are inherently unstable, and auto-decompose by a complex set of reactions that result in the oxidation of ammonia and the reduction of active chlorine (Vikesland et al. 2001). In the absence of NOM, monochloramine decomposition yields equal amounts of ammonia and nitrogen gas which together account for approximately 90% of the nitrogen mass balance. Vikesland et al. (1998) postulated that NOM acts as a reductant in these systems yielding increased ammonia and nitrate production and

decreased nitrogen gas production. Further, they concluded that adding excess ammonia after monochloramine formation, increasing pH, and decreasing NOM concentration enhanced monochloramine stability.

Monochloramine autodecomposition has been shown to be catalyzed by phosphate, sulfate, carbonate, and possibly silicate (Valentine and Jafvert 1988). Both nitrate and bromide can exert a significant monochloramine demand at levels at or above 0.5 mg/L. In addition, the presence of Fe(II) can also enhance monochloramine decomposition, especially at lower pH values (Vikesland and Valentine 2002a; Vikesland and Valentine 2002b).

Studies have also shown that lower Cl_2:N ratios and higher pH (over the range of 6.6 to 8.3) yield more stable disinfectant residual. The overall rate of chloramine loss for the neutral pH range is primarily limited by the rate of dichloramine formation. Once dichloramine forms, it decomposes via a series of rapid redox reactions that yield ammonia, chloride, and nitrogen gas (Jafvert and Valentine 1992).

2.6. BIOFILM MODELING

AQUASIM is a computer program developed by the Swiss Federal Institute for Environmental Science and Technology (EAWAG) for the identification and simulation of aquatic systems (Reichert 1994). The biofilm reactor model included in this program is a one-dimensional mixed-culture biofilm model based on the work of Wanner and Reichert (Reichert and Wanner 1997; Wanner and Reichert 1996). The necessary biofilm equations are inherently nonlinear, and AQUASIM allows these equations to be solved numerically (Reichert 1998b). Wanner and Morgenroth (2004) provide an overview of biofilm modeling with AQUASIM. Specifically, this model has the following features applicable to the current research:

- Ability to model multiple substrates (i.e., ammonia and THMs simultaneously).
- Ability to consider substrate interactions within the biofilm (i.e., competition and reductant supply considerations).
- Ability to perform model simulations and sensitivity analysis of variables and parameter estimates for a given model using measured data.

2.7. MOLECULAR BIOFILM INVESTIGATION

Molecular techniques can be used to further identify and characterize microbial populations in biological treatment processes by providing additional information. Rittmann (2002) makes the following statement concerning the use of molecular methods in biological treatment processes:

> There are two underlying themes on the effective use of molecular biology to improve biological treatment processes: (1) molecular methods can provide high-level information not attainable by traditional methods and (2) molecular methods are important complements of traditional and quantitative analyses, but they are not substitutes.

The molecular methods utilized in this research were undertaken to supplement and gain a better understanding of biofilter performance. One molecular method allowing quantitative determinations of bacteria present is real-time polymerase chain reaction (PCR). Mackay (2004) provides a review of real-time PCR and its applications. Real-time PCR has been adapted to enumerate AOB in soil and chloraminated drinking water systems (Okano et al. 2004; Regan et al. 2004). Regan et al. (2004) developed a method to differentiate *Nitrosomonas oligotropha*, non-*oligotropha* species of

Nitrosomonas, and *Nitrosopira* AOB. This method was used in the current research to investigate the biofilter biofilm population.

2.8. SUMMARY

From the background material provided in this chapter, it was evident that many factors might influence THM cometabolism with nitrifying bacteria and that little was known about the proposed process other than TCM cometabolism could be accomplished by nitrifying bacteria. This research sought to address some of these knowledge gaps and evaluate the proposed process. In particular, this research addressed whether the three other regulated THMs (BDCM, DBCM, and TBM) could be cometabolized by nitrifying bacteria. It extended this work with selection of the appropriate kinetic model for the process, allowing an initial determination to be made on process feasibility based on the process kinetics. In addition, the importance of product toxicity associated with THM cometabolism was evaluated.

The research then continued to investigate the process in its envisioned arrangement (i.e., continuous flow biofilters) while studying the effects of seed cultures, source water, nutrients, monochloramine, and individual THM concentrations and speciations. Ultimately, the data collected during the research was implemented into a model of THM cometabolism in biofilters to evaluate the process feasibility under conditions that reflect water treatment plant practice.

Chapter 3: Materials and Methods

3.1. WATER COLLECTION AND STORAGE

Lake Austin water was obtained from the raw water line of drinking water treatment facilities in Austin, Texas prior to any treatment. Water was subsequently stored in a 4ºC temperature controlled room in LDPE and HDPE storage tanks until its use. Lake Austin water is a typical central U.S. surface water with an alkaline pH (8.26-8.43), moderate alkalinity (169-190 mg/L as $CaCO_3$), and dissolved organic carbon (3.4-4.6 mg/L as C) (Roalson et al. 2003).

3.2. CHEMICALS

Trihalomethanes (THMs) were the primary contaminants of interest for cometabolism studies. The four species of THMs, including trichloromethane or chloroform (TCM), bromodichloromethane (BDCM), dibromochloromethane (DBCM), and tribromomethane or bromoform (TBM), were purchased individually from Chem Services, Inc. as neat solutions. The THM solutions were diluted with acetone to make a stock standard solution of approximately 100 g/L for each THM. These stock standards were stored in 2-mL crimp-sealed glass gas chromatograph vials in a -80°C freezer. Typical manufacturer reported characteristics of each of the THM neat solutions are given in Table 3.1.

The nutrient solution used in the biological experiments was composed of several different chemicals to encourage biomass growth and were developed based on the work of Ely (1996) with nitrifying bacteria. Table 3.2 details *N. europaea*'s growth medium. Chlorine was obtained in 4-6% sodium hypochlorite (NaOCl) stock solutions. Each chemical used was ACS certified.

Table 3.1 Trihalomethane neat solution characteristics

Pure Compound	Storage	Density (g/mL)	Purity (%)
TCM	Cool, Dry	1.492	99.0%
BDCM	Cool, Dry	1.980	99.0%
DBCM	Refrigeration	2.451	98.5%
TBM	Cool, Dry	2.89	98.4%

Table 3.2 *N. europaea* growth media composition

Chemical	Final Media Concentration (mM)
$(NH_4)_2SO_4$	25
KH_2PO_4	43
$MgSO_4$	0.73
$CaCl_2$	0.20
$FeSO_4$	0.010
EDTA	0.017
$CuSO_4$	0.007
NaH_2PO_4	4.4
Na_2CO_3	0.04% (wt/vol)

3.3. ANTHRACITE

Virgin anthracite was obtained from the Davis Water Treatment Plant in Austin, Texas. The appropriate mesh size (30 x 40) was obtained by grinding the anthracite in a blender and sieving with the appropriately sized sieves. To remove the fines from the

ground anthracite, it was first washed on the sieves with distilled-deionized (DDI) water. Further washing was achieved by placing the ground anthracite in a glass beaker with an approximate volume ratio of 9 parts Millipore water and 1 part anthracite where the mixture was stirred and allowed to settle before decanting the water. This process was repeated approximately 30 times or until the decanted water was clear.

3.4. CITY OF LAREDO GRANULAR ACTIVATED CARBON (F400)

In-use Filtrasorb 400 (F400) was obtained from the granular media filters at the City of Laredo drinking water treatment plant. The F400 media was hand ground with a mortar and pestle and sieved to obtain a 30 x 40 mesh size media. The fines were removed as per anthracite media.

3.5. BACTERIAL CULTURES

The pure culture was obtained from the American Type Culture Collection (ATCC), *Nitrosomonas europaea* (ATCC 19718), and cultivated according to their recommendations. Three different mixed-culture sources were also used for biofilter experiments: Lake Austin, Rio Grande, and University of Wisconsin (Wahman et al. 2006). The sample from Lake Austin was taken directly from Lake Austin in Austin, Texas, the Rio Grande sample was collected from the influent line of a drinking water treatment facility in Laredo, Texas, and the University of Wisconsin mixed culture was provided by Dr. Noguera and was an enriched culture of nitrifiers from several distribution systems in California and Wisconsin. This nitrifier community was dominated by *Nitrosomonas oligotropha* representatives and is referred to in this dissertation as *Nitrosomonas oligotropha*.

3.6. BIODEGRADATION KINETICS EXPERIMENTS

3.6.1. Nitrifier Growth Methods

N. europaea was grown in a series of autoclaved 1-L brown glass bottles with foam plugs on 500 mL of the media described in Table 3.2. An inoculum of approximately 10% (by volume) was used when transferring cultures between bottles. After inoculation, the bottles were placed on a rotary shaker at room temperature (22-24°C) for approximately one week, then placed in a 4°C refrigerator, and subsequently transferred to fresh media within six weeks. To check for contamination during each bottle transfer, a portion of each bottle transferred was used to make plates on R2A agar. These plates were incubated for three weeks at 30°C and inspected for any visible cultures. If colonies were detected, the bottle was discarded.

To culture a larger mass for kinetic experiments, *N. europaea* was grown axenically in a Bioflow 3000 fermentor with a 2.5-L working volume (New Brunswick Scientific, NJ) operating in batch mode, using the same nutrient solution and growth conditions as described previously by Ely (1996), except that the temperature was maintained at 30°C. The fermentor was inoculated from bottle cultures and covered in aluminum foil to prevent inactivation of the culture by light (Hooper and Terry 1974; Shears and Wood 1985). The pH was controlled by the automatic addition of 5% (by weight) sodium carbonate (Na_2CO_3) to maintain the pH at 7.8, and the dissolved oxygen was automatically maintained in the range of 2.0 to 4.0 mg/L by adjusting the agitation and/or by adding air into the fermentor.

3.6.2. Batch Kinetic Analysis

Organisms were harvested from the batch reactor by centrifugation three days after inoculation, washed, centrifuged again, and resuspended in fresh buffer medium (8

mM phosphate and 10 mM carbonate, pH 8) for kinetic studies. The fresh buffer media was aerated with pure oxygen to increase the dissolved oxygen concentration to levels that would not be fully consumed by ammonia degradation during the experiment. To verify that no adverse effects occurred from the elevated dissolved oxygen concentrations, baseline experiments for ammonia degradation were conducted before commencing with the batch experiments at the higher oxygen levels and are presented in Appendix D. Comparing these experiments with those conducted at the higher dissolved oxygen concentration, kinetic parameters were similar. In addition, work by Uemoto et al. (2000) suggests that longer duration exposure to high dissolved oxygen concentrations (>12 hours at greater than 30% O_2 for suspended cultures) than present in these experiments (60 to 80 minutes) would be needed to see any adverse effects.

The approach of Aziz et al. (1999) was used in this research. Briefly, batch kinetic assays were carried out head-space-free in 250-mL or 500-mL, glass, gas-tight syringes. Each syringe contained a small Teflon-coated stir bar so that the contents were well-mixed using a magnetic stirring plate and wrapped in aluminum foil to prevent inactivation from light. The chemicals to be studied were injected through the nose of the syringe to start an experiment. Samples for measuring chemical concentrations, cell concentrations, pH, and DO were collected over time by depressing the syringe plunger and ejecting the samples into a smaller gas-tight syringe. Thus, head-space-free conditions were maintained throughout the experiment, thereby virtually eliminating the loss of chemicals through volatilization. In addition, control experiments under abiotic conditions showed no loss of THMs from the syringe and are presented in Appendix D.

The kinetic experiments were run rapidly (60 to 80 minutes) to avoid significant changes in the metabolic state of the organisms during the experiments. Five batch kinetic experiments were performed at room temperature (22-23°C). Nominally, the

starting individual THM concentrations were 100 μg/L each with either 4 (Experiment 3) or 8 (Experiments 1, 2, 4, and 5) mg N/L $TOTNH_3$ present initially. From these experiments, ammonia kinetic and THM cometabolism kinetic parameters were determined. Bicinchoninic acid (BCA) protein analysis was performed with bovine serum albumin standards to determine the protein content of the *N. europaea* culture to compare with Ely (1996).

During certain biofilter operating periods, biofilter backwash water was collected and used in batch kinetic tests. Experimental methods were identical to those used for determining kinetics for *N. europaea* and were based on the approach of Aziz et al. (1999) and were described previously.

3.6.3. Determination of Kinetic Parameters

For ammonia kinetics, Monod kinetic coefficients were estimated by nonlinear regression analysis using the Solver routine in Excel. The model was formulated to account for the fact that $TOTNH_3$ was measured experimentally, while NH_3 is the only form that attaches to the active site of AMO (Suzuki et al. 1974); therefore, pH was inherently included in the model to convert from measured $TOTNH_3$ to NH_3-N through the use of a common acid/base parameter, α_1, using measured pH values. A fourth-order Runge-Kutta numerical approximation of the Monod equation was fit to the data by minimizing the normalized residual sum of squares (NRSS) between the predicted and experimental values. The normalization was achieved by dividing the residual sum of squares by the experimental value squared, resulting in a dimensionless sum of squares error (Aziz et al. 1999). For THMs, four different kinetics models were initially evaluated. For each of these four models, the same fitting method was performed as for the ammonia kinetics, and if required, the ammonia kinetic parameters determined in this research were used in the THM parameter determination without adjustment. As a result,

the only adjustable parameters for the THM kinetics models were the THM rate constant and the initial concentration of each THM. A derivation of the kinetic models and their major assumptions are provided in Appendix A.

The nonlinear regression analysis yielded estimates of THM rate constant ($k_{1_{THM}}$), ammonia maximum specific rate of degradation (k_{TOTNH_3}), and ammonia half-saturation constant ($K_{s_{NH_3\text{-}N}}$), as well as the initial concentrations (S_0) for ammonia and each THM. Further statistical analyses permitted estimates of the approximate 95% joint confidence limit (CL) for each parameter (Robinson 1985; Smith et al. 1997; Smith et al. 1998). A summary of the technique used to determine kinetic coefficients and joint 95% confidence intervals is provided in Appendix B.

For the batch kinetic experiments, transformation capacity was ignored in estimating the kinetic parameters because of the small amount of transformation capacity utilized in these experiments (12 to 26% with an average of 19%). The validity of this assumption was confirmed by analyzing all the data from Experiment 2, which started at 8 mg/L $TOTNH_3$, and a subset of the data at concentrations of 4 mg/L $TOTNH_3$ and below, which corresponded to a point where significant THM transformation had occurred. In addition, 4 mg/L matched the starting concentration of Experiment 3, which was conducted with the same batch of organisms as in Experiment 2. The ammonia kinetic parameters were essentially the same for all three analyses, indicating that by-product toxicity can be ignored in kinetic experiments that consume a small fraction of the transformation capacity.

3.6.4. Transformation Capacity Experiments

Transformation capacity (T_c) represents the maximum mass of cometabolite that can be degraded per unit mass cells, or, in other words, the mass of cometabolite degradation required to completely inactivate the cells (Alvarez-Cohen and McCarty

1991a). Product toxicity was established and transformation capacities were calculated in experiments run in a similar manner to the experiments performed for batch kinetic experiments. In these experiments, however, the organisms were exposed to a higher concentration of THMs for a longer period. The experiments were also conducted with increased initial ammonia and dissolved oxygen concentrations to compensate for the increased experiment duration. The completion of the experiment was defined as the point when the nitrifiers ceased to degrade ammonia with excess ammonia and dissolved oxygen present. This criterion ensured that the cells were inactivated because of product toxicity and not because of some other limiting reactant.

3.6.5. Temperature Controlled Experiments

A low temperature experiment was conducted to determine the effect of temperature on the kinetics. This experiment was undertaken by running two batch kinetics experiments simultaneously, one at room temperature (22°C) and one in a temperature-controlled (14ºC) room. Samples were taken from the syringe in 10-mL volumes and measured with an alcohol thermometer before beginning the experiment to ensure that the temperature of the media was equal to the temperature in the room. The bacteria were kept at 14°C for approximately 30 minutes before the start of the experiment. The nitrifiers used in the simultaneous experiments were taken from the same batch reactor and biomass, ammonia, and THM initial concentrations for each experiment were equivalent so that temperature was the only variable in the experiment.

3.6.6. ^{14}C-Radiolabeled Chloroform

Batch experiments were conducted with ^{14}C-radiolabeled chloroform to determine the resulting products from TCM cometabolism with *N. europaea*. The procedures were identical to the batch kinetic experiments performed to determine kinetic parameters,

with the only change being that only one THM was present, TCM, and a portion of the TCM was ^{14}C-radiolabeled. This allowed determination of the fraction of converted ^{14}C that accumulated as either CO_2, biomass, or nonpurgeable products.

^{14}C-radioactivity was measured on a Beckman LS 5000 TD liquid scintillation counter (LSC). Quench correction was by H-number technique using the instrument's internal cesium-137 source. ScintiVerse II (Fisher Scientific) was used as the scintillation cocktail (SC). For analysis, four 5-mL samples were taken and analyzed for different components as summarized:

1. Total – Sample added directly to 10 mL of SC and analyzed on the LSC.
2. Filtered – Sample filtered through a 0.45-µm Osmonics cellulose nitrate filter and rinsed with 15 mL of 50% ethanol after filtration. The filter placed into 10 mL of SC and analyzed on the LSC.
3. Acid – Sample added directly to 50 µL 6N HCl to acidity to pH ~1.5. Sample was then purged with N_2 gas at 65 mL/min for 6 min. 10 mL of SC was then added to sample before analysis on the LSC.
4. Base – Sample added directly to 300 µL of Carbosorb to adjust pH to ~10.5. Sample was then purge with N_2 gas at 65 mL/min for 6 min. 10 mL of SC was then added to sample before analysis on the LSC.

From these four LSC samples, the proportions of ^{14}C present in different fractions were determined as summarized in Table 3.3.

Table 3.3 ^{14}C sample component calculation summary

^{14}C Component Location	Component Calculation
CO_2	Base minus Acid
TCM	Total minus Base
Biomass	Filtered
Nonpurgeable Products	Acid minus Filtered

3.6.7. Endogenous Decay

A batch experiment was conducted with *N. europaea* to determine the endogenous decay coefficient for use in biofilter modeling efforts. Bacteria were prepared in a similar manner to the batch kinetic tests except that no THMs or $TOTNH_3$ were present in the gas-tight syringe. Total suspended solids (TSS) samples were taken over a period of 30 days. A first order decay model was used to fit the TSS data by nonlinear regression analysis by minimizing the residual sum of squares between predicted and experimental values.

3.7. BIOFILTER EXPERIMENTS

3.7.1. Primary Column Setup

The primary column setup (Figure 3.1) consisted of a 0.2-µm-filtered DDI water feed supplemented with nutrients (i.e., calcium, magnesium, copper, and iron) based on batch *N. europaea* growth and a carbonate/phosphate buffer to simulate natural waters (approximately 200 mg/L as $CaCO_3$). Table 3.4 details the nutrient water column feed makeup. When required, THMs were added via a syringe pump, and oxygen was added to the feed water, raising the biofilter influent dissolved oxygen (DO) to non-limiting levels (approximately 16-20 mg/L). The biofilters were packed wet and were seeded

during the packing process. Before initiating flow, the biofilters were operated in batch mode for approximately one hour to promote nitrifier attachment to the media.

Experiments were conducted with three to four parallel trains (A, B, C, and D) with each train consisting of either one or two biofilters in series. Sampling points were at the first biofilter's influent (sample location 0), between the two biofilters in a train corresponding to the first biofilter's effluent and second biofilter's influent (sample location 1), and at the second biofilter's effluent (sample location 2). For some experiments, the feed water was changed from DDI to Lake Austin water. As required when feeding Lake Austin water, the system was modified to form chloramines or add micronutrients such as iron and copper.

Table 3.4 Mixing chamber water composition

Species	Concentration (M)	Concentration (mg/L)
Ca^{2+}	2.0×10^{-6}	0.080
Cl^{-}	4.0×10^{-6}	0.14
Cu^{2+}	6.5×10^{-9}	0.00041
Total Fe	10.0×10^{-8}	0.0056
K^{+}	6.9×10^{-5}	2.7
Mg^{2+}	7.0×10^{-6}	0.17
Na^{+}	4.2×10^{-3}	96
PO_4^{3-} as P	3.4×10^{-5}	1.1
SO_4^{2-}	7.1×10^{-6}	0.68
EDTA	1.7×10^{-7}	0.049
CO_3^{2-}	4.2×10^{-3}	250

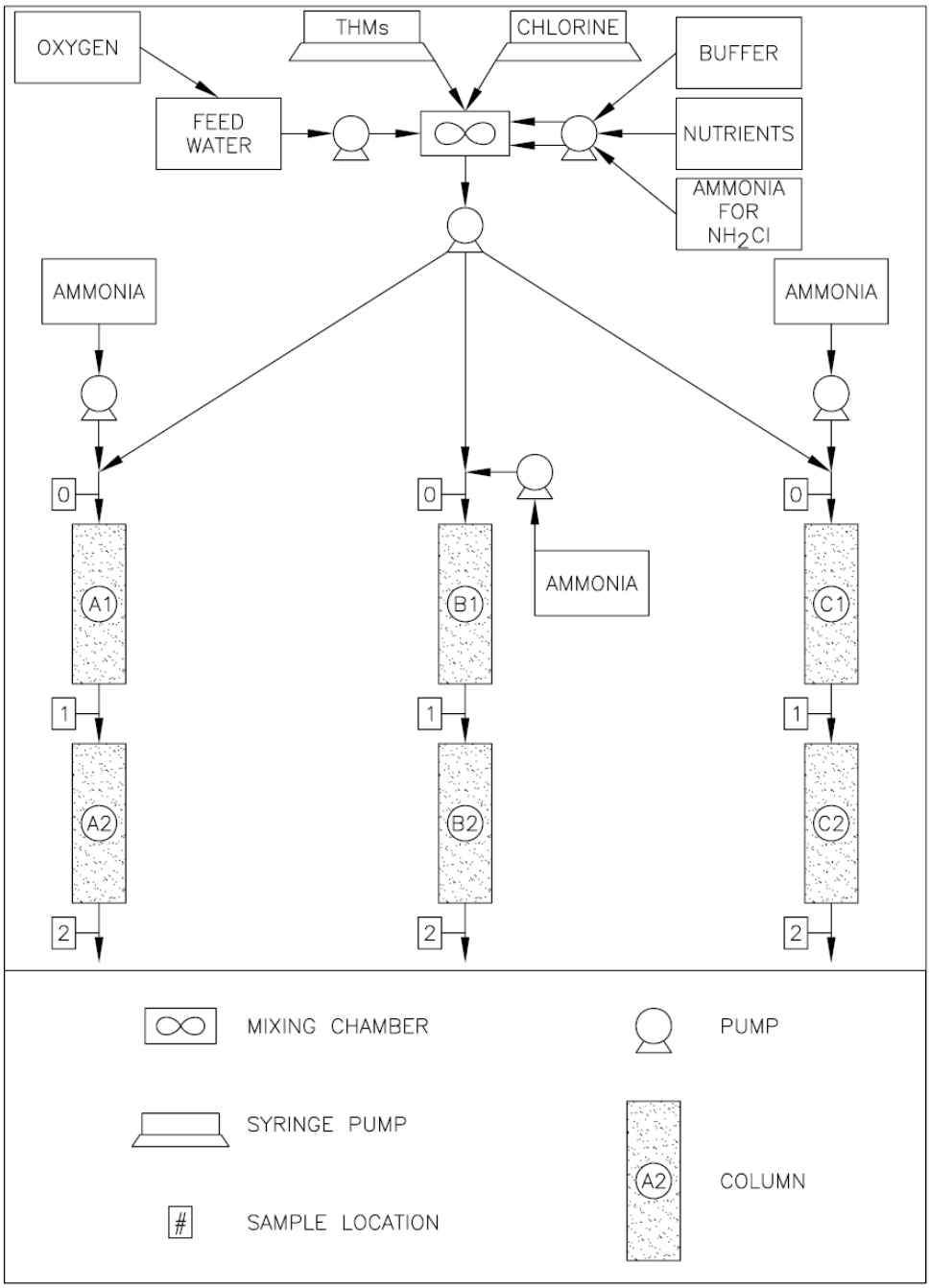

Figure 3.1 Biofilter system schematic

3.7.2. Secondary Column Setup

A secondary column setup was constructed to allow initial seeding of the columns with nitrifiers before transfer to the primary columns. The purpose of the secondary column setup was to allow a second column set to be started up so that when they were transferred to the primary column setup data could be taken with a much shorter startup time.

Briefly, the system consisted of a single feed water tank with the composition as described in Table 3.4 except that no THMs were present and the influent contained a nominal $TOTNH_3$ concentration of 4 mg N/L to all three column trains. A peristaltic pump was used to pull the feed water through a 0.2-μm filter and deliver a flow of 0.3 mL/min (2-hour EBCT) to each train. Effluent samples were collected to monitor the columns. When experiments were conducted on this setup, THMs were introduced into the influent through a syringe pump.

When the feed water was changed to Lake Austin water, the setup of the secondary columns was changed to separate the ammonia feed so that it was not degraded in the feed tank because of the long detention times in the feed tank.

3.8. WATER TYPE CHARACTERIZATION

To determine the practical efficacy of the proposed THM cometabolism process, settled water THM speciation and concentration must be considered to estimate possible removal efficiency. To this end, a search of the Information Collection Rule (ICR) database (Science Applications International Corporation 2001) was conducted for all plants that use chlorine and chloramines or chloramines alone as their disinfectant; 575 samples of finished water were isolated from the database from 119 utilities using chloramines. The THM speciation was broken down into three broad water types (Table

3.5) based on the degree of bromine substitution represented by the bromine incorporation ratio (η) defined in Equation 3.1.

$$\eta = \frac{[\text{BDCM}] + 2[\text{DBCM}] + 3[\text{TBM}]}{[\text{TTHM}]} \quad (3.1)$$

where η = Bromine incorporation ratio (dimensionless)

[BDCM], [DBCM], [TBM], [TTHM] = Respective THM molar concentration (M)

The three water types based on η ranges and the resulting average THM masses present are summarized in Table 3.5. Because not all utilities using chloramines would be candidates for this process, the search was further refined to utilities with finished water total THM concentrations likely to receive a benefit from the proposed process (60 to 150 μg/L). In this subquery, 88 samples from 50 different utilities were isolated (Table 3.5). Simulations of the full-scale filters were conducted with all three water types for each full-scale filter.

Table 3.5 ICR water characterization summary

ICR Water Type	Number of Samples	% of Total	THM Mean (μg/L)				
			TCM	BDCM	DBCM	TBM	Total
All Samples							
1	427	74	25	9	3	0	39
2	121	21	10	15	14	4	42
3	27	5	2	6	13	13	33
Total	575	100	21	10	6	2	39
Samples ranging from 60 μg/L < Total THM < 150 μg/L							
1	62	70	52	19	7	1	79
2	23	26	18	26	25	6	75
3	3	3	7	21	36	18	82
Total	88	100	41	21	13	3	78

THM ICR Water Type Explanation		
ICR Water Type	η range	Individual THM Mass Comparison
1	$0.0 \leq \eta \leq 0.8$	TCM > BDCM > DBCM > TBM
2	$0.8 < \eta < 1.5$	(BDCM + DBCM) > (TCM + TBM) and TCM > TBM
3	$1.5 \leq \eta \leq 3.0$	(BDCM + DBCM) > (TCM + TBM) and TBM > TCM

3.9. BIOFILTER TRACER TEST

To model the biofilter hydraulics, a tracer test was conducted to determine the number of equal sized continuous flow stirred tank reactors (CFSTRs) in series needed to model the plug flow conditions present in the experimental biofilters. A 220-mM cupric

sulfate heptahydrate ($CuSO_4 \cdot 5H_2O$) solution was used as the tracer. Absence of adsorption of the tracer onto anthracite was confirmed by placing anthracite and the tracer into a beaker, mixing for 30 minutes, and comparing initial and final tracer absorbance readings. Tracer absorbance linearity was confirmed at 810 nm by preparing a standard curve shown as Figure 3.2.

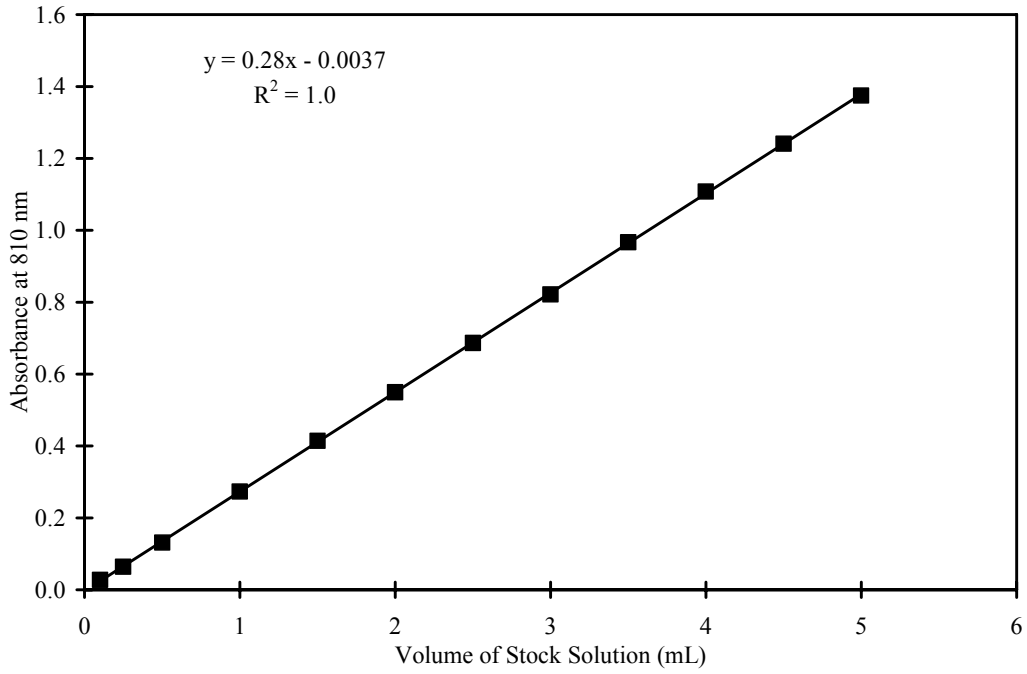

Figure 3.2 Tracer standard curve

For the test, an anthracite column was packed in an identical manner as to those run for the biofilter experiments, except that bacteria were not introduced into the column. Figure 3.3 details the experimental setup for the tracer test. Briefly, a peristaltic pump was connected to two feed tanks (DDI water and tracer) pumping to the anthracite column. The influent to the column was manually changed between DDI and tracer

water feed as appropriate for the tracer test. To initiate the test, the influent to the column was switched from DDI to tracer water with continuous composite samples collected every five seconds for a period of three minutes (36 samples total). The process was repeated for the step down by switching the feed from the tracer back to DDI water and collecting samples again for another three minutes. Flow rates were determined for both feed conditions. The column porosity was also determined based on the change in water volume when a known volume of anthracite was added to a graduated cylinder containing a known volume of water.

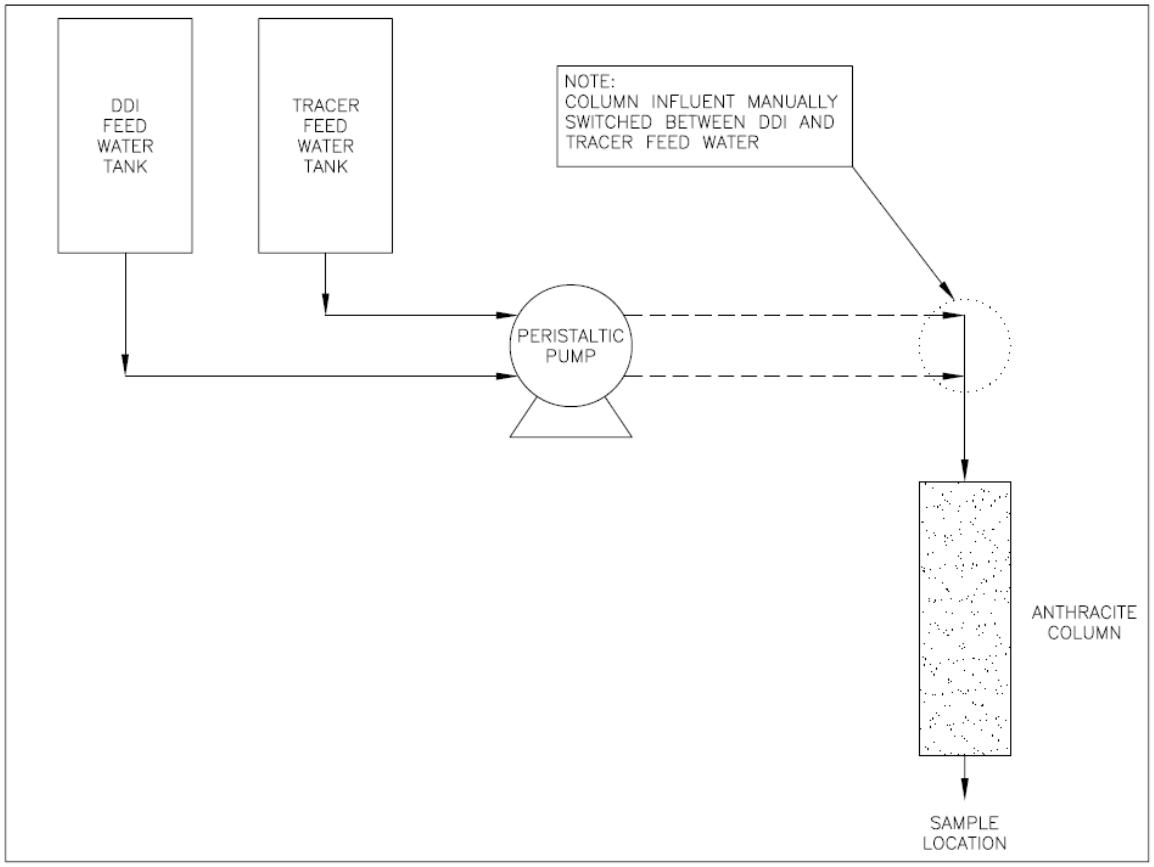

Figure 3.3 Tracer test schematic

For tracer analysis, 200 µL of each sample was placed into one well of a 96-well tissue culture plate and measured at 810 nm on a BIO-TEK Synergy™ HT spectrophotometer multi-detection micro-plate reader with KC4 v3.3 software. Normalized influent tracer concentrations were used to generate F and E-curves, and the number of CFSTRs in series required to model the measured hydraulics was determined as detailed by Lawler and Benjamin (forthcoming).

3.10. MOLECULAR TECHNIQUES

3.10.1. DNA Extraction

DNA was extracted from anthracite biofilter samples using the MO BIO UltraClean™ soil DNA isolation kit according to the manufacturer's instructions modified so that exact quantities are transferred to quantify the DNA extracted per gram of anthracite.

After extraction, 5 µL of DNA with 1 µL 6x loading buffer was loaded on a 1% agarose gel in 1x Tris base, acetic acid, and EDTA (TAE) buffer. The gel was run on a BIO-RAD Mini-Sub Cell GT powered by a BIO-RAD PowerPac Basic at 100 Volts (constant voltage) for 60 minutes with a New England BioLabs®, Inc., 2-Log DNA Ladder as reference. After running, the gel was stained by placing it in a solution of 0.5 µg ethidium bromide (EtBr) per mL of 1x TAE buffer and mixed gently on a shaker table for 20 minutes. Subsequently, the gel was imaged on a Kodak Gel Logic 100 Imaging System.

Quality (absorbance at 260 nm divided by absorbance at 280 nm) and concentration (absorbance at 260 nm) of DNA was quantified on a NanoDrop ND-1000 spectrophotometer. Extracted DNA was stored frozen at -20°C for further use.

3.10.2. Real Time Polymerase Chain Reaction

The method of Regan et al. (2004) was used to conduct real time polymerase chain reaction analysis of DNA to determine AOB quantities from the DNA extracted biofilter samples. Table 3.6 details the primers used to amplify the *amoA* gene and the dual-labeled probes used to detect the amplicons. The probes allowed detection of three classes of AOB: *Nitrosospira*, *Nitrosomonas oligotropha*, and non-*oligotropha Nitrosomonas* species.

Table 3.6 Real time PCR primers and probes

Type	Name	Target	Sequence (5'-3')
Forward Primer	amoA-1F	*amoA* gene	GGG GTT TCT ACT GGT GGT
Reverse Primer	amoA-2R	*amoA* gene	CCC CTC KGS AAA GCC TTC TTC
TaqMan Probe	amoA-Ns1	*Nitrosospira amoA* gene	CCG ACS CAC CTG CCG CTG G
TaqMan Probe	amoA-Nm3	*Nitrosomonas amoA* gene	TGT CGA TGG CTG AYT ACA TGG G
TaqMan Probe	amoA-Nm4	*Nitrosomonas oligotropha amoA* gene	ATC ATG TTG CTG ACC GGT AAC TGG C

Source: (Adapted from Regan et al. 2004)

Table 3.7 and Table 3.8 summarize the PCR mixture and thermal profile, respectively. After an initial denaturation step, the thermal profile was repeated for 50 cycles with amplifications performed on an Applied Biosystems 7900 HT Sequence Detector. Standard curves for each of the three probes were generated using serial dilutions of pGEM®-T vectors with the appropriate *amoA* insert and plotting the respective Ct value for each standard's copy number. Linear regression for the standard curve was conducted with the SDS 2.2.1 software (Applied Biosystems 2004). Samples were analyzed in duplicate, and standards were analyzed in triplicate.

Table 3.7 PCR mixture composition

Component	Volume Added (μL)	Final Concentration
Bio-Rad iQ Supermix (2x)	12.5	1x
DNA	5	Varies
Forward Primer	1	200 nM
Reverse Primer	1	200 nM
TaqMan Probe	0.5	100 nM
Bovine Serum Albumin	2.5	0.1 mg/mL
Water	2.5	
Total Mixture	25	

Source: (Adapted from Regan et al. 2004)

Sample results were converted to AOB mass extracted per starting mass of dry anthracite for comparison with model results by using the assumptions that the *Nitrosopira* genomes contain three copies of *amoA*, *Nitrosomonas* genomes contain two

copies of *amoA*, a constant DNA extraction efficiency, a typical cell is 3% by weight DNA, and a typical AOB genome size of 2.8 million base pairs as determined for *N. europaea* (Chain et al. 2003; Madigan et al. 2000; Regan et al. 2004).

Table 3.8 PCR thermal profile

PCR Step	Temperature (°C)	Time (seconds)	Number of Cycles
Initial Denaturation	95	30	1
Denaturation	95	40	50
Annealing	58	60	50
Extension	72	45	50

Source: (Adapted from Regan et al. 2004)

3.11. ANALYTICAL METHODS

3.11.1. Trihalomethanes

THM concentrations were measured using USEPA Method 551.1 with some modifications (USEPA 1995). The concentrations of individual THM species were analyzed on a Hewlett Packard 5890A gas chromatograph equipped with a liquid autosampler. A J&W DB-5 column was used with constant pressure and splitless injection. The initial oven temperature was 32°C and was held for the first 3.5 minutes. After this initial phase, the temperature was increased at a rate of 20°C/minute to a temperature of 72°C and the oven remained at this temperature for another 3.5 minutes. The total time for an analysis was 9 minutes. THM concentrations for transformation capacity calculations were determined using the same gas chromatograph, but with a slightly modified method due to the higher concentrations of THMs required for this type

of experiment. The initial temperature was still 32°C but, for these experiments, remained at this initial phase for 9 minutes. The oven temperature was increased to 40°C at a rate of 20°C/minute and remained at this temperature for 3 minutes. The oven temperature was increased again at the same rate to 72°C and stayed at this temperature for 4 minutes resulting in a total injection time of 20 minutes.

If THM samples were analyzed upon completion of an experiment, the THM samples were placed into 40-mL screw top vials with Teflon lined septa, and 50 µl of 6 N HCl was added to the vials to inactivate any biomass in a sample. These vials were then inverted and stored until the end of the sampling period, which was usually less than two hours. The samples were analyzed by USEPA Method 551.1 using pentane as the extraction fluid and a sodium sulfate salt to drive the THMs from the sample into the extraction fluid. 1,1,1-trichloroethane, TCA, was used as the internal standard (IS) in the pentane for all experiments (0.53 mg TCA/L of pentane). If the THM samples were not analyzed immediately, a sample preservative was added to the samples with subsequent sample storage at 4°C for up to two weeks as described in USEPA Method 551.1.

The pentane with IS was stored at 4°C between experiments before being injected into the open top of the 40-mL sample vial by a Hamilton gas-tight 5-mL syringe. A 3-mL volume of the pentane with IS was added to the sample for an extraction ratio of 1:10. After the addition of pentane with IS, extraction salt was added to the sample at an inclined position to prevent the salt from gathering at the bottom of the vial. The samples were then placed on a horizontal shaker for 30 minutes. Shaking, along with the salt addition, forced the THMs into the pentane layer at the top of the vials. This layer was removed from the vial with a disposable Pasteur pipette and placed in a 2-mL gas chromatograph vial with a rubber lined metal cover, using GC vial inserts as required if sample volume was low. The cover was then sealed with a crimping tool to prevent the

THMs from volatilizing. These samples were suitable for storage at -80°C up to two weeks before being analyzed as specified in USEPA Method 551.1. All standards were measured in triplicate and all samples were measured in duplicate. For quality control purposes, a blank and duplicate sample was placed every 20 vials and a standard calibration check was run every 10 samples. The method detection limit (MDL) for each THM was 0.2 μg/L.

3.11.2. Ammonia

Spectrophotometry

An Agilent 8453 UV-visible spectrophotometer was used to measure ammonia according to HACH colorimetric method 10023 (Salicylate Method), using HACH Low Range (LR) Test 'N Tube Nitrogen-Ammonia AmVer Reagent sets for 0.02 to 2.5 mg/L NH_3-N. Standard curves were prepared according the method description and run periodically to ensure reproducibility and adequate instrument function. High purity Millipore water was used for blanks. If a sample's expected ammonia concentration was greater than the highest concentration used to prepare the standard curve (approximately 3 mg/L ammonia-nitrogen), the sample was diluted as required (approximately 25-50%) with buffer water (pH 8.0) consisting of sodium carbonate and potassium phosphate monobasic.

Ion Selective Electrode

An ion selective electrode probe, Thermo Orion 9512, connected to an Orion Model 920A pH/ISE electrode meter was also used to measure ammonia. Before each set of samples, a three-point calibration was performed with ammonia-nitrogen standard concentrations of 0.1, 1.0, and 5.0 mg/L as N. To analyze a sample, an Orion ammonia pH adjusting ISA solution was added to the sample in a defined ratio (2 mL ISA to 100

mL sample). A magnetic stir bar was placed in the sample, and then the sample was placed on a magnetic stir plate were the probe was inserted for measurement.

3.11.3. Bacterial Cell Mass

Spectrophotometry

The concentration of biomass in nitrifier cultures was measured on an Agilent 8453 UV-visible spectroscopy system at a wavelength of 600 nm. A sample containing Millipore water was used as a blank and standard curves for determining biomass concentration were prepared by preparing dilutions of bacteria in the same buffer water used in the batch kinetic experiments. Standard curves were prepared for the pure culture of *N. europaea* (Figure 3.4) by measuring total suspended solids (TSS) and correlating this with absorbance readings at 600 nm. TSS measurements were also taken periodically to determine biomass concentrations used in experiments to check the validity of the standard curves.

Total Suspended Solids

Total suspended solids, TSS, was measured to determine the biomass for biodegradation kinetic experiments to provide a check against the biomass concentrations obtained from absorbance readings. The solids were measured with the buffer solution/biomass mixture remaining after kinetics experiments were completed, and the volume of solution usually ranged from 50 to 100 mL. This volume was vacuum filtered through a Whatman cellulose nitrate 0.2-μm filter according to Standard Methods (APHA et al. 1998).

Protein Analysis

The Pierce BCA (Bicinchonic Acid) Protein Assay was used to measure protein to correlate TSS with protein for comparison to previous data from Ely (1996). A protein

standard curve from 0-250 mg/L was prepared using BSA (Bovine Serum Albumin). Samples and standards were prepared per the manufacturer's instructions (Pierce Document Number 1296, Enhanced Protocol) and measured on an Agilent 8453 UV-visible spectrophotometer at 562 nm.

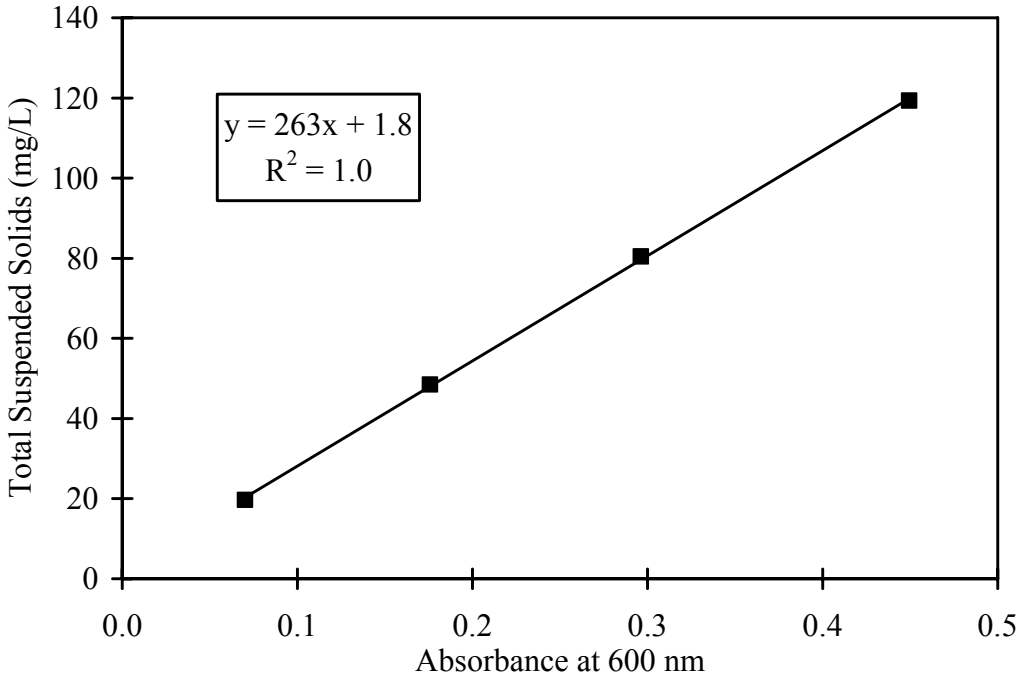

Figure 3.4 *N. europaea* biomass determination standard curve

3.11.4. Total Organic Carbon

Dissolved organic carbon (DOC), a surrogate parameter frequently used to quantify natural organic matter (NOM) concentrations in water, was measured using an Apollo 9000 Combustion TOC analyzer with autosampler (Tekmar-Dohrmann). Water samples taken after filtration (0.2-µm Polycap 75 AS filter, Whatman Inc., Clifton NJ), were collected in 50-mL acid-washed vials and preserved for up to one month by addition

of a few drops of concentrated phosphoric acid and stored at 4°C until measurement. Organic carbon standards were prepared in distilled water at concentrations between 1 and 5 mg/L using potassium hydrogen phthalate ($C_8H_5KO_4$). Standards were measured at the beginning and end of each run to calibrate and ensure stability of the TOC analyzer. A detailed description of the sample and standard preparation procedure that was followed in this research can be found in Gerwe (2003).

3.11.5. Chlorine

Chlorine solutions were obtained by diluting 4-6% sodium hypochlorite (NaOCl) stock solutions with Millipore water as needed. Stock NaOCl solutions were standardized periodically by diluting samples 1:10,000 with Millipore water and titrating with 0.01 N sodium thiosulfate by the procedure given in Standard Methods 4500-Cl B. Iodometric Method 1 (APHA et al. 1998).

3.11.6. Monochloramine

Monochloramine was measured on an Agilent 8453 UV-visible spectrophotometer at 655 nm, according to HACH method 10171 (0.04 to 4.5 mg/L-Cl_2). If a sample's expected concentration was greater than the standard curve, it was diluted accordingly.

3.11.7. Nitrite and Nitrate

Spectrophotometry was also used to measure the nitrite and nitrate concentrations on an Agilent 8453 UV-visible, according to HACH colorimetric method 5807 (Diazotization Method) and 10023 (Chromotropic Acid Method), respectively. Nitrite analysis was conducted using HACH powder pillows for 0.002 to 0.3 mg/L NO_2-N. Nitrate analysis was conducted using HACH Test 'N Tube Reagent sets for 0.2 to 30

mg/L NO_3^--N. If a sample's expected concentration was outside the range of the standard curve, it was diluted accordingly.

3.11.8. Dissolved Oxygen and pH

Dissolved oxygen was measured with a YSI 5905 oxygen probe on a YSI Model 54ARC dissolved oxygen meter calibrated per the manufacturer's recommendations. pH was measured using an Orion 81-56 ROSS™ epoxy body combination pH electrode with bulb guard on an Orion Model 920A pH/ISE meter calibrated with pH standards of 4, 7, and 10.

Chapter 4: Batch Kinetic Studies

Batch kinetic studies were conducted to extend the previous work on TCM cometabolism kinetics to the other three regulated THMs (BDCM, DBCM, and TBM), providing a basis for assessing the feasibility of the proposed treatment process. The key question was whether nitrifying bacteria can reliably cometabolize all four THMs at a sufficient rate to make the process attractive to utilities that practice (or want to practice) prechlorination, in particular, utilities practicing a combination of chlorination and chloramination. Information was developed on TCM, BDCM, DBCM, and TBM cometabolism kinetics, as well as the toxicity of their intermediate by-products. *N. europaea* was chosen as a starting point for this evaluation to build on the large body of literature on this organism and to provide a pure-culture baseline for evaluating the performance of the mixed cultures (Wahman et al. 2006) that are likely to dominate in practice. The key results of these experiments are presented in this chapter with additional experimental data provided in Appendix D.

4.1. PURE CULTURE

4.1.1. Model Selection and Kinetic Parameter Determination

Table 4.1 summarizes the conditions for each experiment performed with the pure culture of *N. europaea*. Four models were evaluated for describing the kinetics of THM cometabolism; they differed based on the assumptions made (Table 4.2) about the presence or absence of competition between ammonia and THMs and whether reductant (NH_3) was viewed as a second limiting reactant.

Table 4.1 *N. europaea* batch kinetic test summary nominal conditions

Exp.	Time (min.)	TSS (mg/L)	$TOTNH_3$ (mg/L)	TCM (µg/L)	BDCM (µg/L)	DBCM (µg/L)	TBM (µg/L)
1	60	58	8	100	100	100	100
2	80	77	8	100	100	100	100
3	60	81	4	100	100	100	100
4	70	99	8	100	100	100	100
5 (22°C)	70	108	8	100	100	100	100
14°C	140	103	8	100	100	100	100

A representative figure detailing the fit for each kinetic model to the data from Experiment 1 follows, using TCM as a representative THM (Figure 4.1 through Figure 4.5). Based on analysis of the four THM degradation models, the reductant model, as described by Arcangeli and Arvin (1997), was chosen as it best represented the experimental data by visual inspection and normalized residual sum of squares (NRSS) analysis. As an example of the NRSS comparison, Table 4.3 provides the NRSS comparison for Experiment 3.

The absence of competition among the THMs is in accordance with the previous work of Aziz et al. (1999) in which no competition was observed between cometabolites at low concentrations (< ~5 mg/L). The absence of competition between THMs is not a direct conclusion of this research, but rather is inferred from the modeling results. No competition was observed between $TOTNH_3$ and the THMs at the $TOTNH_3$ concentrations tested (<8 mg/L as N) as evidenced by the better fit of the reductant model in comparison to the competition model.

Table 4.2 Summary of ammonia and THM kinetic models evaluated in batch kinetic experiments

Chemical	Model name	Fitting parameters	Batch reactor mathematical form and assumption(s)	Figure
Ammonia	Saturation Kinetics	3	$\frac{dS_{TOTNH_3}}{dt} = -\frac{k_{TOTNH_3} X S_{TOTNH_3} \alpha_1}{K_{s_{NH_3-N}} + S_{TOTNH_3} \alpha_1}$ 1. THMs do not compete with ammonia.	Figure 4.1
THM	First-Order	2	$\frac{dS_{THM}}{dt} = -k_{1THM} X S_{THM}$ 1. Ammonia does not compete with THMs. 2. THMs do not compete with ammonia. 3. THMs do not compete with each other. 4. One limiting reactant (THM).	Figure 4.2
THM	Competition	2	$\frac{dS_{THM}}{dt} = -\frac{k_{1THM} X S_{THM}}{1 + \frac{S_{TOTNH_3} \alpha_1}{K_{s_{NH_3-N}}}}$ 1. Ammonia competes with THMs. 2. THMs do not compete with ammonia. 3. THMs do not compete with each other. 4. One limiting reactant (THM).	Figure 4.3
THM	Reductant	2	$\frac{dS_{THM}}{dt} = -\frac{k_{1THM} X S_{THM}}{1 + \frac{K_{s_{NH_3-N}}}{S_{TOTNH_3} \alpha_1}}$ 1. Ammonia does not compete with THMs. 2. THMs do not compete with ammonia. 3. THMs do not compete with each other. 4. Two limiting reactants (THM and Reductant).	Figure 4.4
THM	Combined	2	$\frac{dS_{THM}}{dt} = -\frac{k_{1THM} X S_{THM}}{\left(1 + \frac{S_{TOTNH_3} \alpha_1}{K_{s_{NH_3-N}}}\right)\left(\frac{K_{s_{NH_3-N}}}{S_{TOTNH_3} \alpha_1} + 1\right)}$ 1. Ammonia competes with THMs. 2. THMs do not compete with ammonia. 3. THMs do not compete with each other. 4. Two limiting reactants (THM and Reductant).	Figure 4.5

α_1 = NH_3-N fraction of $TOTNH_3$ (pH dependent)
$k_{1_{THM}}$ = THM rate constant (L/mg TSS–day)
$K_{s_{NH_3\text{-}N}}$ = ammonia half-saturation constant (mg NH_3-N/L)
k_{TOTNH_3} = ammonia maximum specific rate of degradation (mg $TOTNH_3$/mg TSS–Day)
S_{THM} = THM concentration (mg THM/L)
S_{TOTNH_3} = $TOTNH_3$ concentration (mg $TOTNH_3$/L)
$TOTNH_3$ = total ammonia-nitrogen = [NH_3-N] + [NH_4^+-N] (mg N/L)
X = Biomass concentration (mg/L TSS)

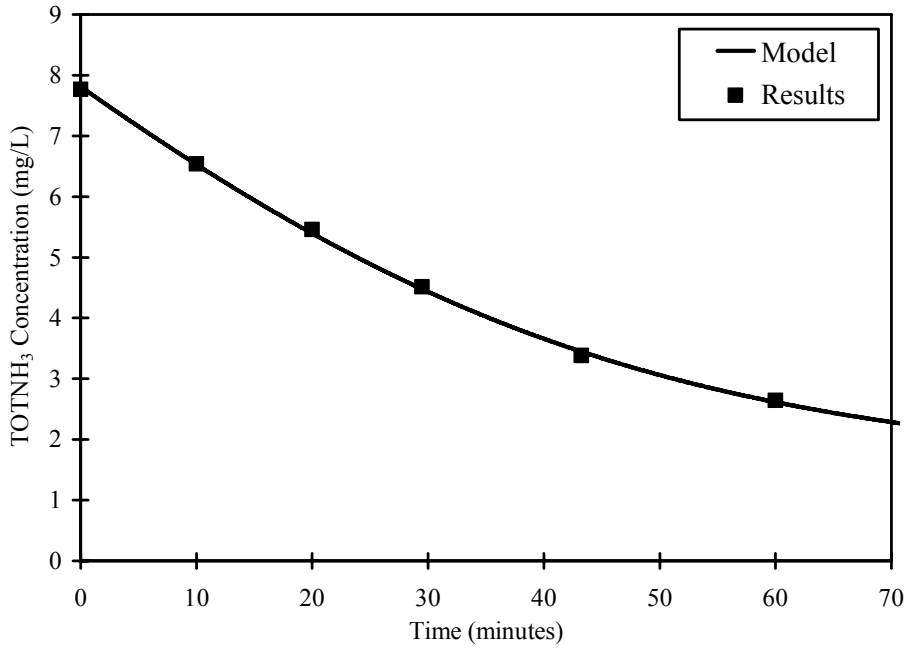

Figure 4.1 Typical batch kinetic experiment showing an ammonia saturation kinetic model fit to $TOTNH_3$ experimental data for Experiment 1

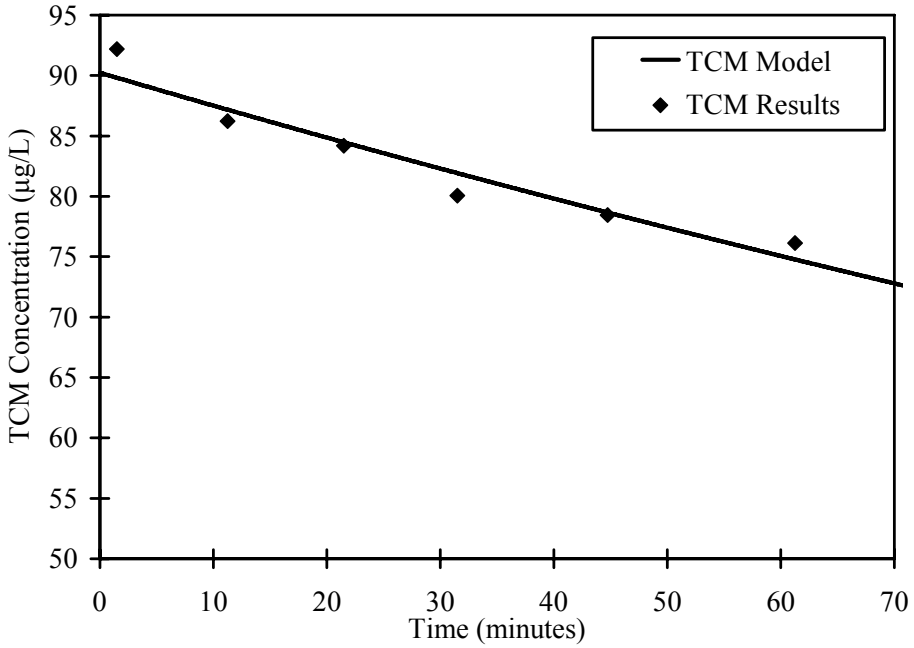

Figure 4.2 Typical batch kinetic experiment showing a THM first-order kinetic model fit to TCM experimental data for Experiment 1

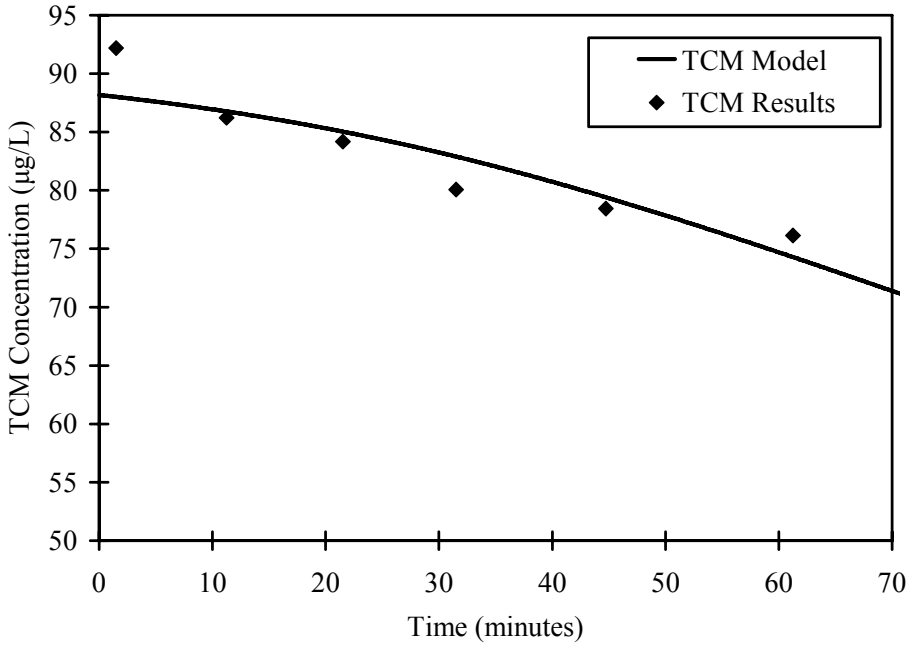

Figure 4.3 Typical batch kinetic experiment showing a THM competition kinetic model fit to TCM experimental data for Experiment 1

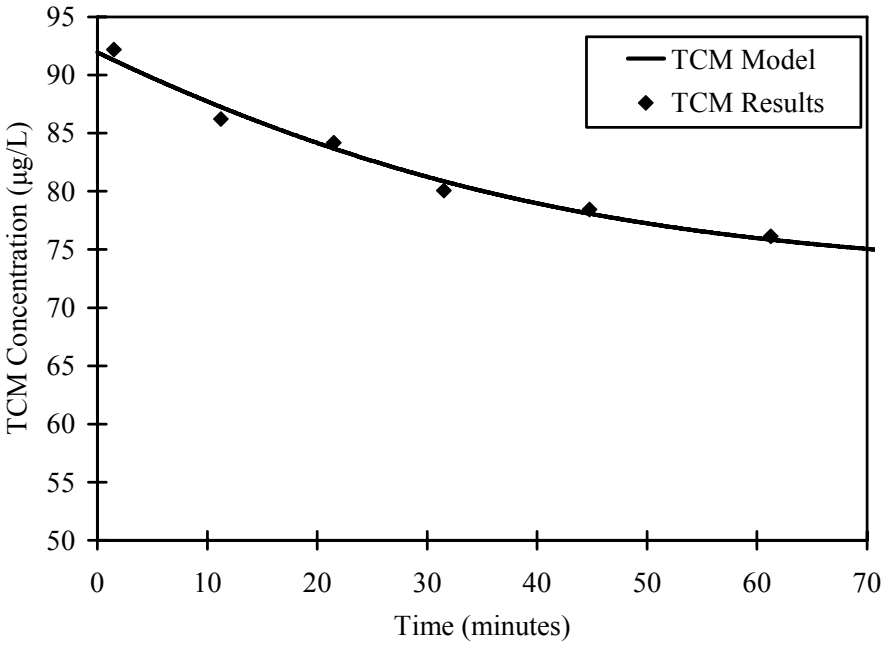

Figure 4.4 Typical batch kinetic experiment showing a THM reductant kinetic model fit to TCM experimental data for Experiment 1

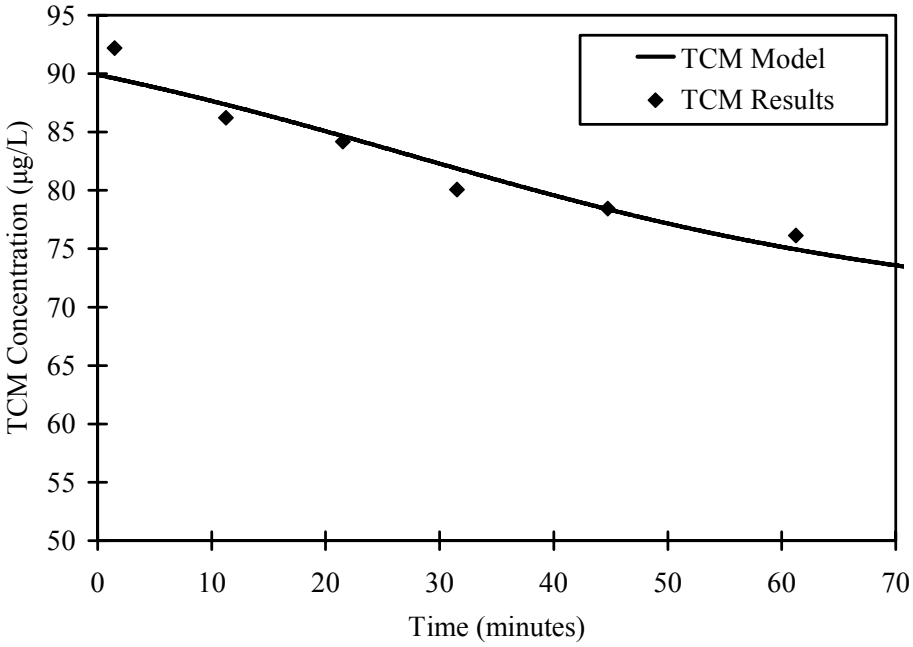

Figure 4.5 Typical batch kinetic experiment showing a THM combined kinetic model fit to TCM experimental data for Experiment 1

Table 4.3 Experiment 3 NRSS comparison between THM kinetic models evaluated for batch kinetic experiments

Model	NRSS value (10^3)			
	TCM	BDCM	DBCM	TBM
First order	1.3	1.9	4.1	8.0
Competition	4.1	7.5	15	26
Combined	1.4	1.7	3.6	7.3
Reductant	0.20	0.10	1.0	2.3

Figure 4.6 details experimental and model results for Experiment 1 for all four THMs and $TOTNH_3$, using the reductant model for THM kinetic parameter determination. The fit of the data shown in Figure 4.6 is typical of all experiments. A

summary of the ammonia and THM kinetic parameters determined from the experiments is presented in Table 4.4 and Table 4.5, respectively. The Monod half-saturation coefficient for ammonia ranged from 0.088 to 0.27 mg/L NH_3-N, and the maximum specific substrate utilization rate ranged from 1.9 to 4.3 mg $TOTNH_3$/mg TSS-day, which are typical kinetic coefficients for nitrifiers (Ely 1996; Rittmann and McCarty 2001).

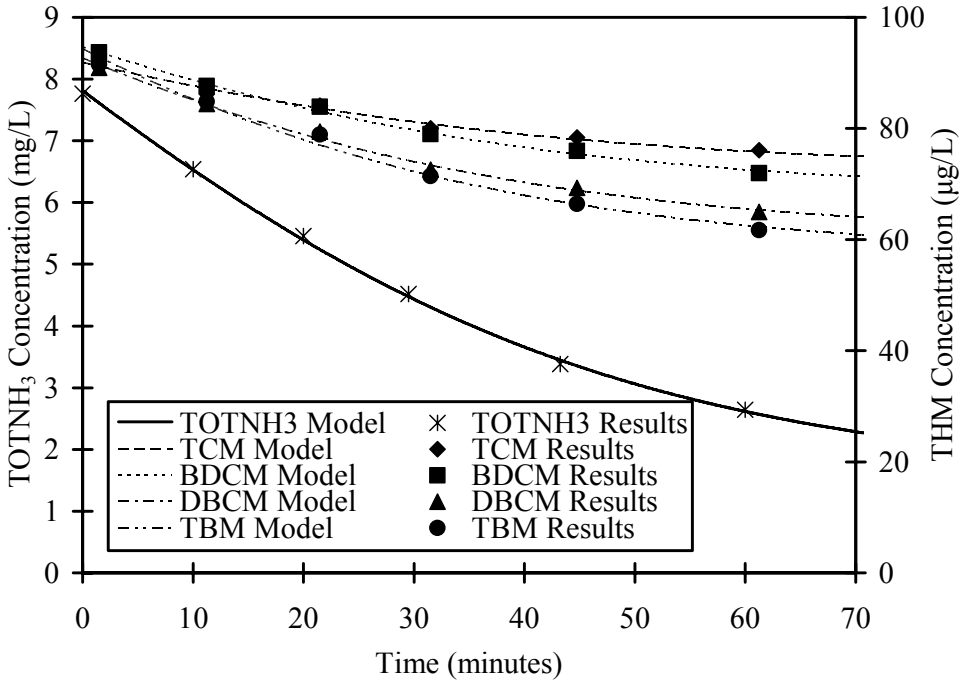

Figure 4.6 Typical batch kinetic experiment showing a reductant model kinetic model fit to $TOTNH_3$ and THM experimental data for Experiment 1

The THM rate constants ranged from 0.050 to 0.16 L/mg TSS-day for TCM, 0.081 to 0.22 L/mg TSS-day for BDCM, 0.11 to 0.28 L/mg TSS-day for DBCM, and 0.14 to 0.34 L/mg TSS-day for TBM. Based on the work of Segar et al. (1995), treatment process feasibility has been demonstrated for cometabolic degradation reactors operating with rate constants of 0.03 to 0.1 L/mg-day. The values determined for the THMs meet

this requirement. In addition, these rate constants fall in the middle of the range reported for the breadth of halogenated aliphatic chemicals and bacteria that have been tested (Alvarez-Cohen and Speitel 2001). Taking this in total, the THM rate constants are typical and at a level that suggests practical feasibility for process implementation.

A protein content of 0.4 mg albumin protein per mg TSS was determined and was used to convert Ely's (1996) kinetic coefficients to the units shown in Table 4.4 and Table 4.5. Although the TCM rate constants were less than those reported by Ely (1996), the THM degradation rates ($k_{1_{THM}}$) varied in proportion to the ammonia degradation rate (k_{TOTNH_3}), as shown in Table 4.5, and the ratios for TCM compare well with that determined from Ely (1996). The similar ratio among experiments for each THM suggests that the differences in observed rate constants in Table 4.5 might have resulted from differing enzyme levels or activity among the different batches of organisms.

Table 4.4 95% joint CL summary for ammonia kinetic parameters ($K_{s_{NH_3\text{-}N}}$ and k_{TOTNH_3}) determined during batch kinetic experiments

Experiment	$K_{s_{NH_3\text{-}N}}$ (mg NH_3-N/L)			k_{TOTNH_3} (mg $TOTNH_3$/mg TSS-day)		
	Lower 95%	Mean	Upper 95%	Lower 95%	Mean	Upper 95%
1	0.016	0.27	0.53	2.4	4.3	6.1
2	0.073	0.088	0.10	2.1	2.2	2.3
3	0.082	0.10	0.11	2.2	2.4	2.6
4	0.15	0.24	0.34	2.8	3.6	4.5
5	0.00	0.089	0.18	1.3	1.9	2.5
Average		0.16			2.9	
Ely (1996)					6.7	

Table 4.5 THM kinetic parameter summary and THM:$TOTNH_3$ kinetic coefficient ratios from batch kinetic experiments

Experiment	$k_{1_{THM}}$ (L/mg TSS-d)				$k_{1_{THM}}/k_{TOTNH_3}$ (L/mg $TOTNH_3$)			
	$k_{1_{TCM}}$	$k_{1_{BDCM}}$	$k_{1_{DBCM}}$	$k_{1_{TBM}}$	TCM	BDCM	DBCM	TBM
1	0.16	0.22	0.28	0.34	0.036	0.051	0.066	0.078
2	0.081	0.12	0.16	0.19	0.037	0.054	0.073	0.086
3	0.092	0.14	0.19	0.24	0.039	0.057	0.081	0.10
4	0.13	0.20	0.26	*N/D	0.035	0.055	0.072	N/D[a]
5	0.050	0.081	0.11	0.14	0.027	0.043	0.059	0.072
Average	0.10	0.15	0.20	0.23	0.035	0.052	0.070	0.084
Ely (1996)	0.25				0.038			

[a]N/D – Not Determined

4.1.2. Estimation of Confidence Limits for the Kinetic Coefficients

The estimation of 95% joint confidence limits (CLs) for kinetic coefficients was determined by the method described previously. A detailed description of this method is provided in Appendix B. Typical 95% joint CLs are shown in Figure 4.7 for the ammonia kinetic parameters and in Figure 4.8 for the THM kinetic parameters. The data shown are typical of all experiments. The kinetic parameters fit to the saturation kinetics model for ammonia were the initial $TOTNH_3$ concentration (S_0), the maximum specific degradation rate (k_{TOTNH_3}), and the half-saturation constant ($K_{s_{NH_3\text{-}N}}$), whereas for the reductant model for THMs they were initial THM concentration (S_0) and the pseudo first-order rate constant ($k_{1_{THM}}$).

For ammonia kinetic parameter determination, three parameters were fit, resulting in a three dimensional space for the 95% joint CL. To present these data in the two-

dimensional form shown in Figure 4.7, S_0 was fixed. The resulting two-dimensional ellipsoid area contains the 95% joint CL for k_{TOTNH_3} and $K_{s_{NH_3\text{-}N}}$ at this fixed value of S_0. The 95% joint CL was evaluated at three extreme values of S_0, the mean value of S_0, the mean value of S_0 plus two standard deviations, and the mean value of S_0 minus two standard deviations. This results in three ellipsoids as shown in Figure 4.7. The actual 95% joint CL for the ammonia kinetic parameters, k_{TOTNH_3} and $K_{s_{NH_3\text{-}N}}$, for all values of S_0 is the bounding area encompassing all three ellipsoids. For THM kinetic parameters, only two parameters were fit, resulting in a two-dimensional 95% joint CL.

Table 4.4 summarizes the analysis of the ammonia kinetic parameters for all the experiments with the corresponding 95% joint CLs. This analysis was also completed for the THM kinetic parameters with Figure 4.9 summarizing these results. The 95% joint CL analysis shows that the rate constants for both ammonia and THM degradation were similar across experiments.

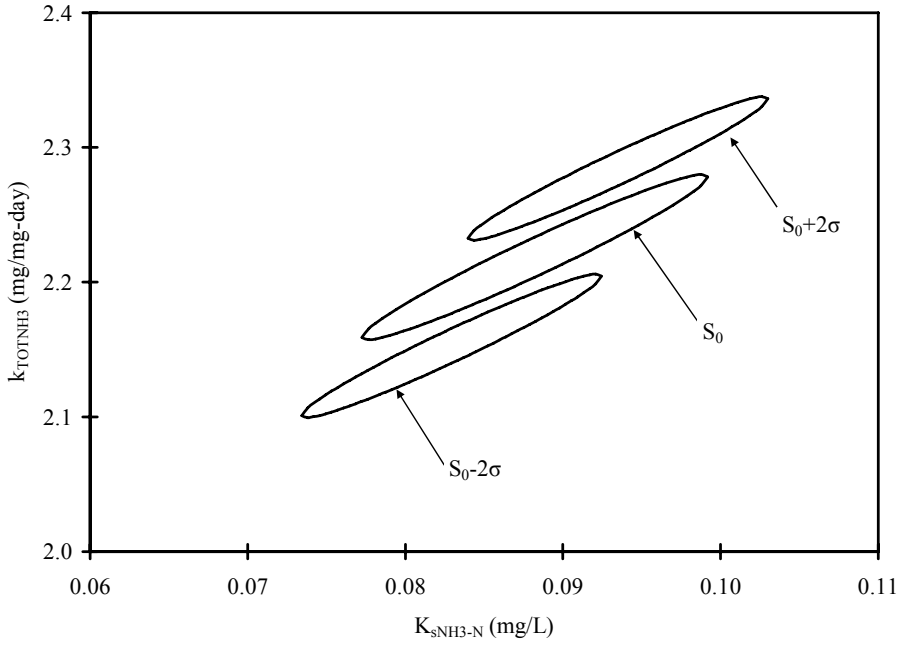

Figure 4.7 Typical batch kinetic experiment 95% joint confidence limits for ammonia kinetics using Experiment 2 as an example

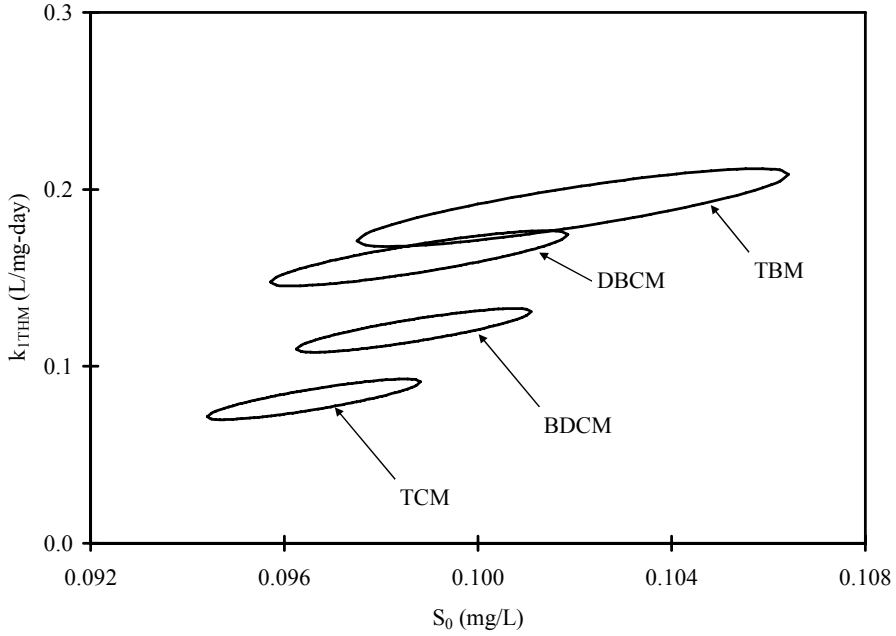

Figure 4.8 Typical batch kinetic experiment 95% joint confidence limits for THM kinetics using Experiment 2 as an example

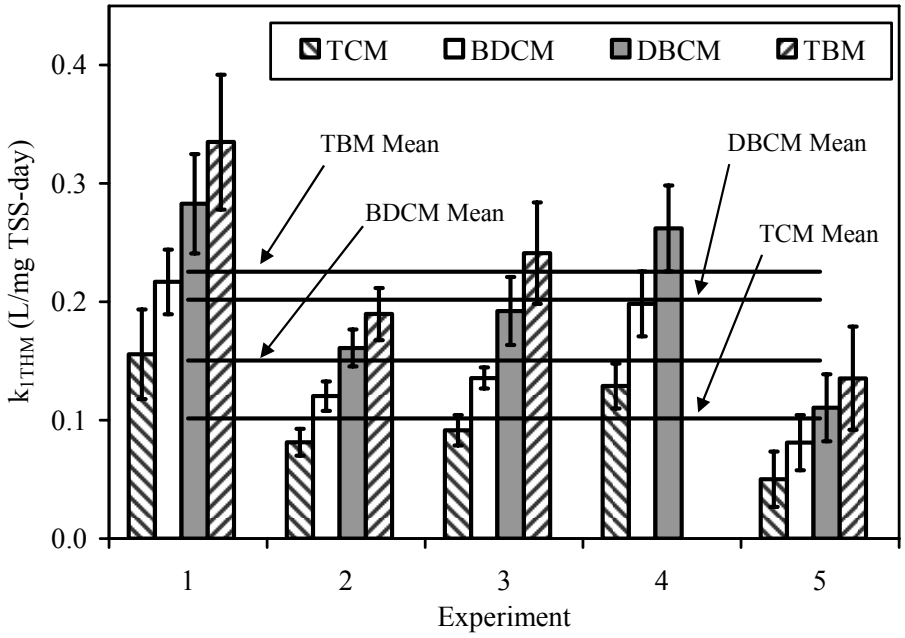

Figure 4.9 THM kinetics 95% joint confidence limits experiment summary for batch kinetic experiments with *N. europaea*

Table 4.5 also indicates that, as THM species became more bromine-substituted, the magnitude of the rate constants increased. For each experiment, Tukey's method of multiple comparisons (Berthouex and Brown 2002) was used to determine whether the observable trend in THM rate constants was statistically significant. Looking at THM degradation in each of the five experiments, only Experiment 5 for a comparison of TBM to DBCM was not significantly different at the 95% significance level. All other comparisons within an experiment for THM degradation rates were statistically different from each other at the 95% significance level, verifying a trend of increasing THM rate constants with THM bromine-substitution.

To evaluate possible reasons for this trend in $k_{1_{THM}}$, it is first useful to note that that $k_{1_{THM}}$ is a simplification appropriate to low THM concentrations (i.e., $k_{1_{THM}} \approx k_{THM}/K_{s_{THM}}$). A proposed active site model for AMO (Keener and Arp 1993) predicts that THMs bind at a hydrophobic site, at which NH_3 also binds. Because bromine is more nucleophilic (less electrophilic) than chlorine, the hydrogen on the THM could reduce its partial charge and become relatively more hydrophobic as bromine-substitution increases. Thus, bromine substitution would make THMs more attractive to AMO's active site, which implies that $K_{s_{THM}}$ decreases (and $k_{1_{THM}}$ increases) as bromine-substitution increases. On the other hand, Rasche et al. (1990a) studied oxidation of monohalogenated ethanes by *N. europaea* and found that the maximum rate of oxidation decreased from chloroethane to bromoethane. These findings suggest that k_{THM} might decrease (and $k_{1_{THM}}$ decreases) with increasing THM bromine substitution. Nevertheless, at the low concentrations of this research, the relative nucleophilicity of bromine compared to chlorine clearly dominated over possible differences in the maximum rates, resulting in the observed trend in $k_{1_{THM}}$ values.

4.1.3. Significance of $k_{1_{THM}}/k_{TOTNH_3}$ Ratio

To gain further insight into the parameter $k_{1_{THM}}/k_{TOTNH_3}$, a closed form equation can be obtained for a batch reactor system, as detailed in Appendix A, and is shown as Equation 4.1.

$$\frac{S_{THM}(t)}{S_{THM}(0)} = e^{-\Delta TOTNH_3 \frac{k_{1THM}}{k_{TOTNH_3}}} \quad (4.1)$$

Because this equation is also the form for a plug flow reactor with hydraulic residence time, t, it can be used as a first approximation to the expected performance of the envisioned process in a drinking water biofilter. Based on Equation 4.1, the THM normalized effluent concentration ($\frac{S_{THM}(t)}{S_{THM}(0)}$), and therefore THM fractional removal, will be (1) independent of the influent THM and $TOTNH_3$ concentrations and (2) for a given $TOTNH_3$ removal, dependent on the THM rate constant ($k_{1_{THM}}$). Thus, Equation 4.1 can be used to approximate the maximum expected removal of each THM species as a function of total-ammonia removal ($\Delta TOTNH_3$). $\Delta TOTNH_3$ in Equation 4.1 is a function of time. Using Equation 4.1 and average values of the kinetic coefficients from Table 4.4 and Table 4.5, initial performance predictions were made based on likely maximum $TOTNH_3$ removal and ICR water types. The results of this analysis are summarized in Table 4.6 with removals ranging from 4-23%, depending on the conditions.

Table 4.6 Initial THM removal performance predictions based on *N. europaea* kinetic parameters and ICR water types

$\Delta TOTNH_3$ (mg N/L)	THM Percent Removal						
	TCM	BDCM	DBCM	TBM	Total THMs for ICR Water Type		
					1	2	3
1	3.4	5.1	6.8	8.1	4.2	5.5	6.3
2	6.7	9.9	13	16	8.2	11	12
4	13	19	24	29	16	20	23

4.1.4. Temperature Effects

An experiment was completed to examine the effect of reducing the temperature of the medium on degradation kinetics and resulting predicted THM removals. From a single batch of *N. europaea*, similar experiments were conducted with the only variance being that one experiment was conducted at room temperature, 22°C, and the other was conducted in a constant temperature room at 14°C. The ammonia degradation curves for both experiments are shown as Figure 4.10. Because all parameters of the experiment were the same except temperature, the effect of a lesser temperature is clearly illustrated by the slower removal at 14°C. The same impact of temperature can be seen when looking at THM degradation curves for both experiments. For example, Figure 4.11 displays the TBM degradation curve for both experiments. The other THMs showed similar degradation curves, degrading faster at the greater temperature.

Kinetic parameters and 95% joint CLs were determined for both experiments. The results are shown comparatively in Figure 4.12 and Figure 4.13 for ammonia and THM kinetic parameters, respectively, and a summary comparison is presented in Table 4.7.

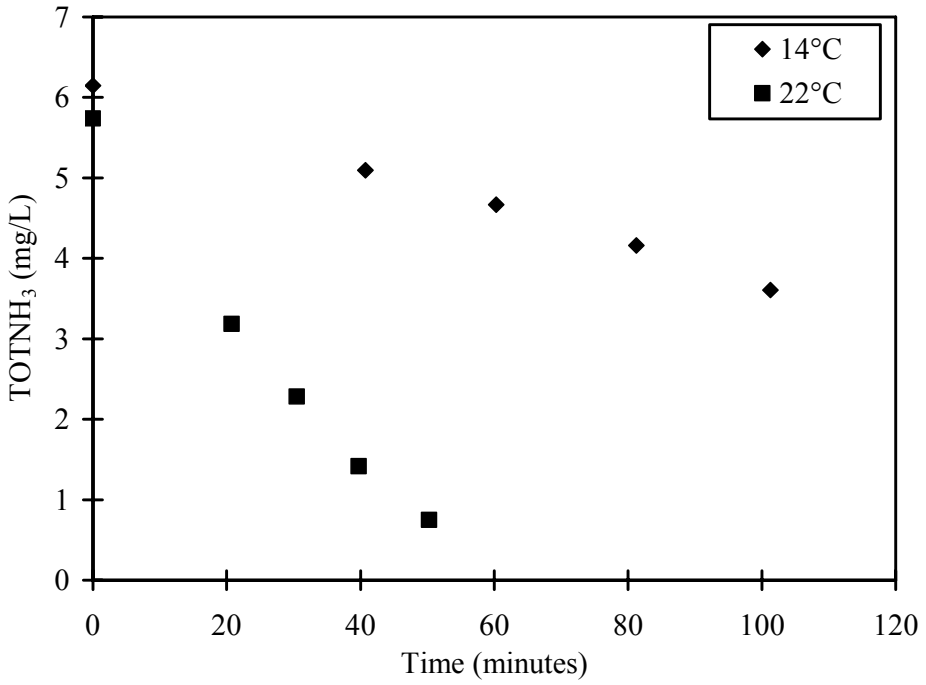

Figure 4.10 *N. europaea* $TOTNH_3$ degradation in temperature experiments

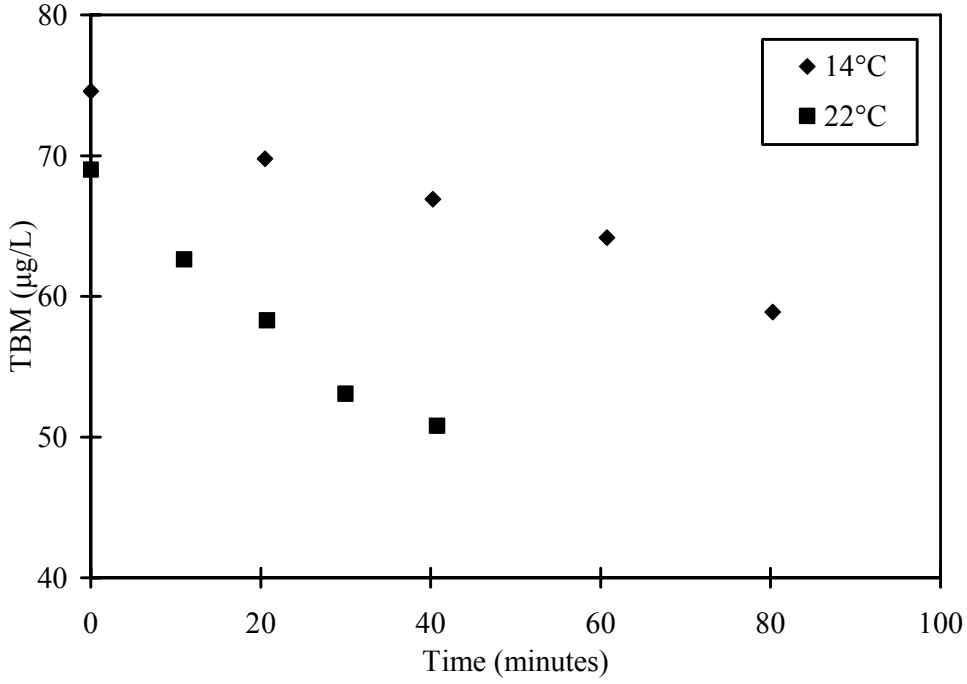

Figure 4.11 *N. europaea* TBM degradation in temperature experiments

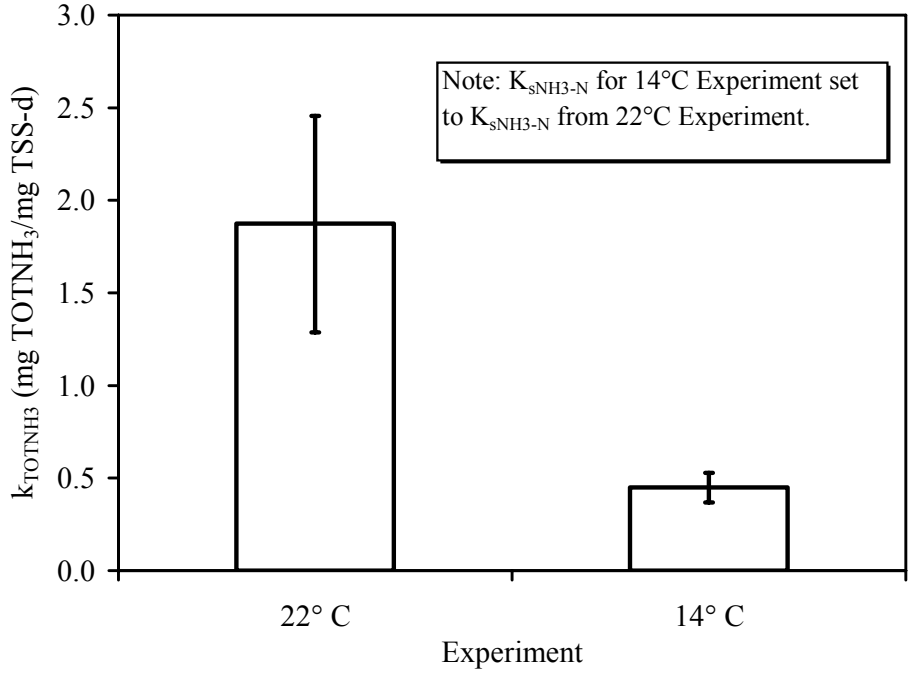

Figure 4.12 *N. europaea* ammonia kinetics comparison for temperature experiment

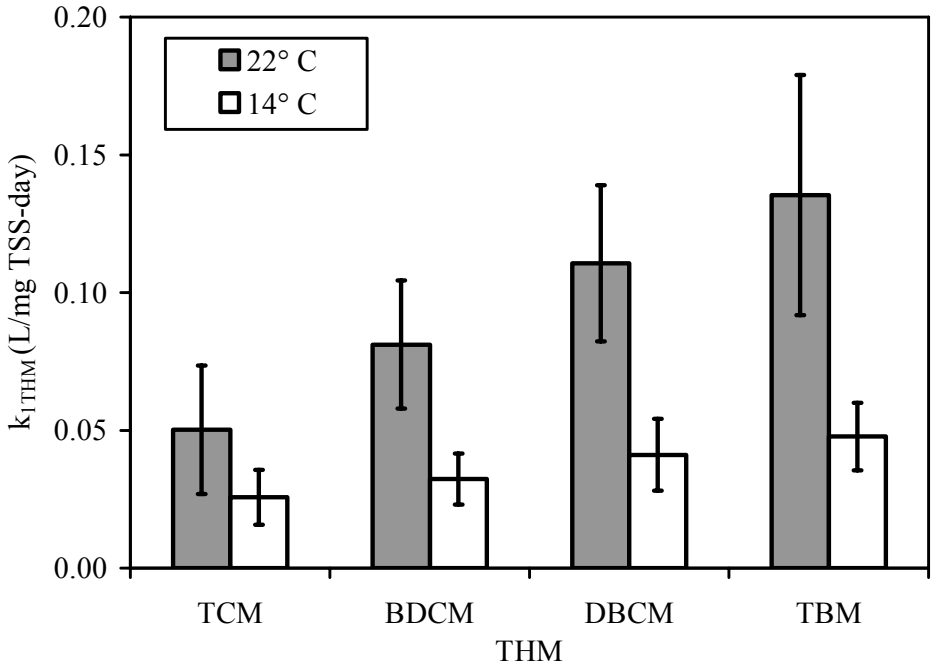

Figure 4.13 *N. europaea* THM kinetics comparison for temperature experiment

Table 4.7 Comparison of temperature effects on kinetic parameters between room temperature kinetic experiment (22°C) and reduced temperature kinetic experiment (14°C)

Parameter	k_{TOTNH_3} (mg/mg-day)	$k_{1_{THM}}$ (L/mg-day)			
		TCM	BDCM	DBCM	TBM
14°C	0.45	0.026	0.032	0.041	0.048
22°C	1.9	0.050	0.081	0.11	0.14
% of 22°C	24	51	40	37	35
Activation energy (kJ/mol)	130	59	81	87	92
Predicted 10°C	0.21	0.018	0.020	0.025	0.028
Predicted 30°C	7.3	0.094	0.19	0.28	0.36

The THM rate constants at 14°C ranged from 35% to 50% of their values at 22°C, and the impact of decreased temperature increased with an increasing degree of THM bromine substitution. The Monod maximum specific substrate utilization rate was affected to an even greater extent than the THM kinetic coefficients and was only 24% of its value at 22°C. Because the 14°C experiment did not progress to an adequately low $TOTNH_3$ concentration, the $K_{s_{NH_3\text{-}N}}$ could not be determined from the experimental data; therefore, the $K_{s_{NH_3\text{-}N}}$ was fixed to the value determined from the 22°C experiment in the data analysis. Overall, the temperature effect on the THM cometabolism rate was less than on the nitrification rate, but was nevertheless significant.

The calculated activation energies varied from 59 kJ/mol for TCM to 92 kJ/mol for TBM (Table 4.7). The reason for the observable trend in activation energies, increasing with THM bromine-substitution, is not obvious. The activation energy for the $TOTNH_3$ maximum specific substrate utilization rate was calculated as 130 kJ/mol. This

value is greater than, but similar to, reported values by Wong-Chong and Loehr (1975) for ammonia-oxidation (67 to 90 kJ/mol). When comparing THM and $TOTNH_3$ activation energies, it seems reasonable that those for the THMs should be less than that for the $TOTNH_3$ maximum specific substrate utilization rate. Relative to its primary substrate, an enzyme should not be as efficient in catalyzing the reaction of a cometabolite; therefore, only chemicals with activation energies less than that of the primary substrate should be amenable to cometabolism.

Using the calculated activation energies (Table 4.7), the THM rate constants maintain the trend of increasing with increasing bromine-substitution over the range of expected applicable temperatures in practice (approximately 10 to 30°C) as shown in Table 4.7, but this trend decreases with decreasing temperature. Another observation with respect to changes in temperature is the relative rates of ammonia and THM kinetics. Based on the calculated rates constants at 10 and 30°C, the ratio used in Equation 4.1 ($k_{1_{THM}}/k_{TOTNH_3}$) increases with decreasing temperature. This implies that if the same $TOTNH_3$ removal can be achieved as temperature decreases, the resulting THM removal will increase at lesser temperatures. Table 4.8 summarizes this effect in a similar manner as was done in Table 4.6. The more practical aspect of this trend is that ammonia removal will likely decrease at lower temperatures. To maintain the same THM removal as at the higher temperature, a lower ammonia removal will be required. For example and looking at Table 4.8, similar THM removals are predicted at 10°C with a $TOTNH_3$ removal of 1 mg N/L as at 22°C and 30°C with $TOTNH_3$ removals of 2 and 4 mg N/L, respectively.

Table 4.8 Total THM percent removal based on ICR water type and temperature

$\Delta TOTNH_3$ (mg N/L)	Total THM Percent Removal for Temperature and ICR Water Types								
	10°C			22°C			30°C		
	1	2	3	1	2	3	1	2	3
1	8.7	9.7	10	3.4	4.6	5.4	1.9	2.9	3.5
2	17	18	20	6.6	8.9	10	3.7	5.7	6.9
4	30	33	36	13	17	20	7.3	11	13

4.1.5. Transformation Capacity

Product toxicity associated with the cometabolism of chlorinated aliphatic compounds is most often described by a transformation capacity (T_c) term. T_c represents the maximum mass of cometabolite that can be degraded per unit mass of cells, or, in other words, the mass of cometabolite degradation required to completely inactivate the cells (Alvarez-Cohen and McCarty 1991a). Mathematically, T_c is defined as follows:

$$T_c = \frac{S_{I_{THM}} - S_{F_{THM}}}{X} \qquad (4.2)$$

where T_c = Transformation capacity (μg THM/mg TSS or nmole THM/mg TSS)

$S_{I_{THM}}$ = Initial THM concentration (μg/L THM or nM THM)

$S_{F_{THM}}$ = Final THM concentration (μg/L THM or nM THM)

X = Initial biomass concentration (mg/L TSS)

For a T_c experiment to reach completion, ammonia degradation must stop with excess $TOTNH_3$ and oxygen present, assuring that the cells have been inactivated by the

degradation of the THMs and not from some other limiting reactant. Experiments with high concentrations of individual THMs and several experiments with all four THMs present were conducted with various initial THM and cell concentrations in arriving at an experimental design that would meet these requirements. Figure 4.14 through Figure 4.17 show the degradation curves for experiments meeting the requirements for each of the four THMs when run separately. Figure 4.18 shows an experiment run with all four THMs simultaneously to examine the combined toxicity of the four THMs and to determine if this combined toxicity could be predicted from the T_c values.

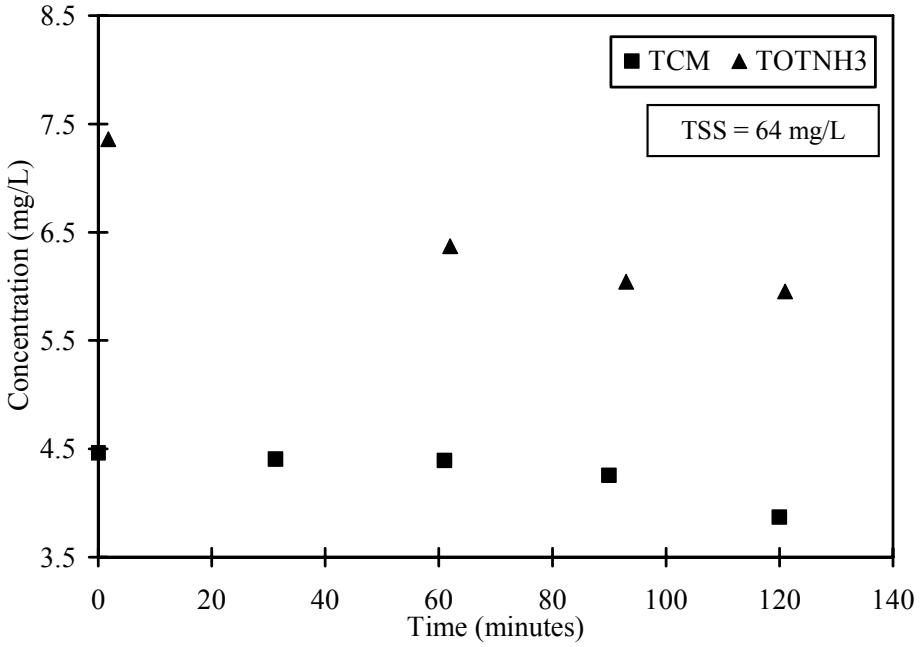

Figure 4.14 *N. europaea* TCM transformation capacity experiment TCM and $TOTNH_3$ concentrations

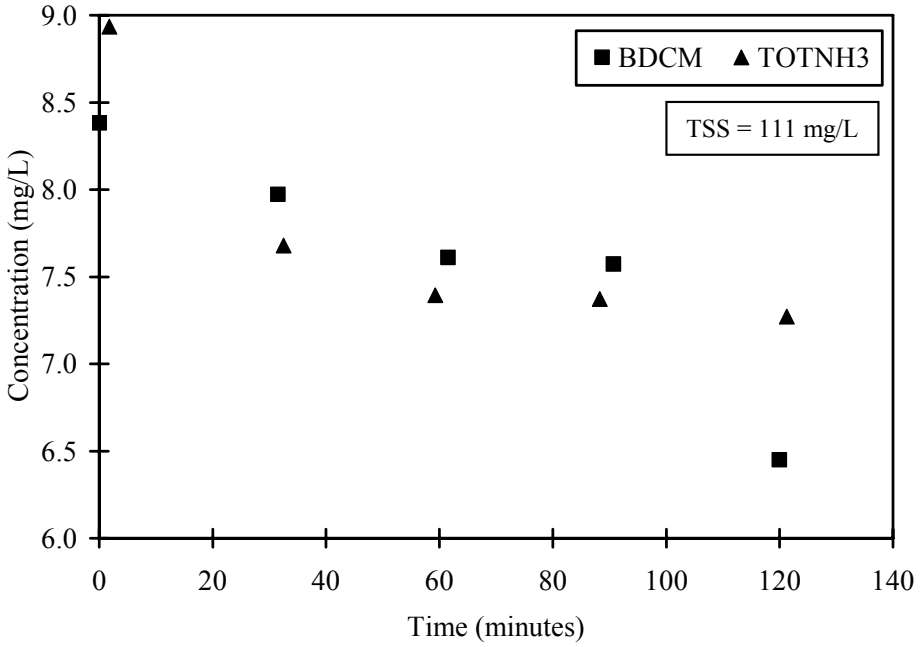

Figure 4.15 *N. europaea* BDCM transformation capacity experiment BDCM and $TOTNH_3$ concentrations

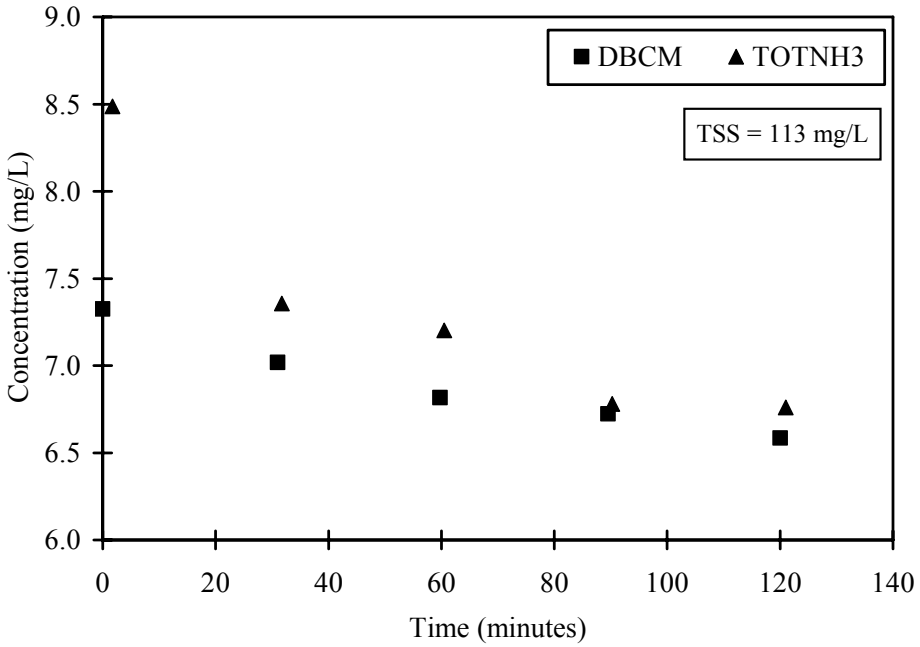

Figure 4.16 *N. europaea* DBCM transformation capacity experiment DBCM and $TOTNH_3$ concentrations

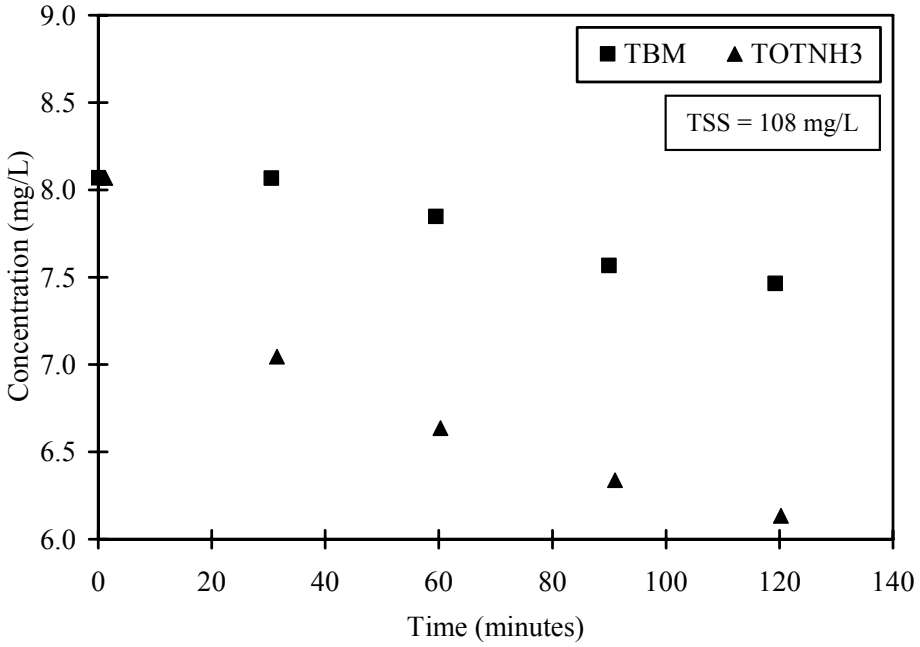

Figure 4.17 *N. europaea* TBM transformation capacity experiment TBM and $TOTNH_3$ concentrations

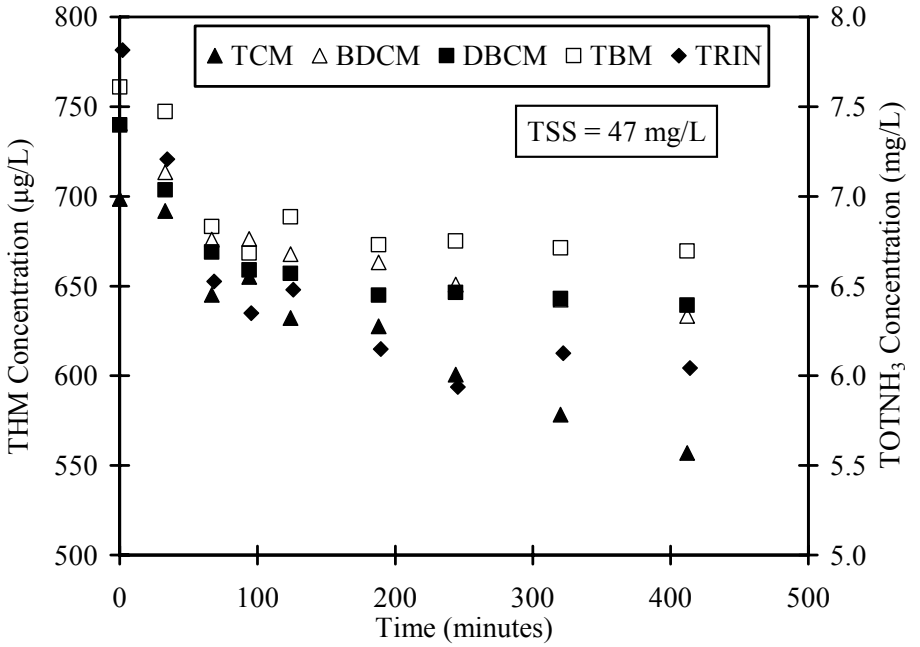

Figure 4.18 *N. europaea* combined THM transformation capacity experiment THM and $TOTNH_3$ concentrations

As shown in Figure 4.18, ammonia, DBCM, and TBM degradation ceased at approximately 200 minutes, but TCM and possibly BDCM degradation continued beyond this point. The possible continuation of TCM and BDCM degradation after ammonia degradation ceased was also seen in the individual TCM and BDCM experiments (Figure 4.14 and Figure 4.15, respectively). Nevertheless, the organisms were considered inactivated, for all T_c experiments, at the point at which ammonia degradation ceased, as the bacteria were no longer able to degrade their energy source. Keener and Arp (1993) have proposed a two-site model for AMO that might account for continued degradation of TCM and BDCM once ammonia degradation ceased.

Table 4.9 details each THM's T_c on both a mass and molar basis and compares the experiments with individual THMs to that with all four present simultaneously. In considering the mixture, it was assumed that each THM contributed to the overall toxicity in proportion to the mass of the THM degraded and its relative toxicity. Thus, the mass of each THM degraded was normalized by the total mass of each THM that would have been required to inactivate the cells had that THM been present individually. In this way, the percentage of T_c realized in the mixture for each THM was calculated. These percentages were then summed for all four THMs to arrive at the overall percentage of the T_c that was utilized, with a value of 100% indicating a perfect match between the assumed contributions to toxicity and the results observed. The calculated percentage was 103%, which verified the approach for estimating the combined effect of product toxicity in mixtures.

The results of the T_c experiments in this research are compared to values measured by others in Table 4.10. The T_c determined for TCM compared well but was slightly less than the literature value for TCM, which had a relatively low toxicity compared to the other chemicals. BDCM, DBCM, and TBM, however, showed toxicity

comparable with 1,1-DCE, a chemical with high product toxicity. Reported TCM T_c values for *M. trichosporium* OB3b ranged from 830-840 nmol/mg, indicating that, compared to other cultures, TCM degradation is highly toxic to *N. europaea* (Alvarez-Cohen and Speitel 2001). The relative differences in T_c values among the THMs indicates that both the relative speciation of THMs and their individual concentrations will be important in determining the probable toxicity associated with their degradation.

Table 4.9 *N. europaea* transformation capacity comparison

THM	MW[d]	T_c from Individual THM Experiments		THM Mixture Experiment (TSS = 47 mg/L)		
		T_c (μg/mg)	T_c (nmol/mg)	Calculated Individual ΔTHM (μg/L)[a]	Measured Δ THM (μg/L)[b]	% T_c Used[c]
TCM	119.5	9.2	77	430	71	16
BDCM	164.0	7.3	45	340	78	23
DBCM	208.5	6.5	31	310	95	31
TBM	253.0	5.6	22	260	88	33
					Total % T_c Used =	103

[a]Calculated Individual Δ THM = Concentration of THM required to inactive the cells if present individually (T_c times the initial TSS concentration).

[b]Measured Δ THM = Actual concentration of each THM degraded in the experiment.

[c]% T_c Used = Percentage of the T_c realized in experiment with all four THMs.

[d]MW, molecular weight.

Table 4.10 *N. europaea* transformation capacity summary

Current Research		Reported Values		
Chemical	T_c (nmol/mg)	Chemical[a]	T_c (nmol/mg)	Source[b]
TCM	77	TCM	92 – 150	1
BDCM	45	TCE	61 – 99	2
DBCM	31	1,1-DCE	24 – 45	2
TBM	22	1,2-DCA	>3,500	2

[a] TCE = trichloroethylene; 1,1-DCE = 1,1-dichloroethene; 1,2-DCA = 1,2-dichloroethane

[b]Source: 1 (Ely 1996); 2 (Alvarez-Cohen and Speitel 2001)

For the batch kinetic experiments, transformation capacity was ignored in estimating the kinetic parameters because of the minimal amount of total transformation capacity utilized in these experiments (12 to 26% with an average of 19%) and the added complexity of including four T_c parameters (each with their own uncertainty) to both the ammonia and THM kinetic models. The validity of this assumption was confirmed by analyzing all the data from Experiment 2, which started at 8 mg/L $TOTNH_3$, and a subset of the data at concentrations of 4 mg/L $TOTNH_3$ and less, which corresponded to a point at which significant THM transformation had occurred. In addition, 4 mg/L matched the starting concentration of Experiment 3, which was conducted with the same batch of organisms as in Experiment 2. The ammonia kinetic parameters were essentially the same for all three analyses as shown in Table 4.11, indicating that by-product toxicity can be ignored in kinetic experiments that consume a minimal fraction of the transformation capacity.

Table 4.11 Comparison of kinetic data to assess transformation capacity in kinetic experiments

Experiment	$K_{s_{NH_3\text{-}N}}$ (mg NH_3-N/L)			k_{TOTNH_3} (mg $TOTNH_3$/mg TSS-day)		
	Lower 95%	Mean	Upper 95%	Lower 95%	Mean	Upper 95%
2 (4 mg/L)	0.068	0.089	0.11	2.0	2.2	2.4
2	0.073	0.088	0.10	2.1	2.2	2.3
3	0.082	0.10	0.11	2.2	2.4	2.6

4.1.6. ^{14}C-Radiolabeled Chloroform

A batch experiment was conducted with ^{14}C-radiolabeled chloroform to determine the resulting products from TCM cometabolism. The procedure was identical to the batch kinetic experiments performed to determine kinetic parameters with the only change being that a portion of the TCM used was ^{14}C radiolabeled. Table 4.12 provides a breakdown of the radiolabeled ^{14}C products from this experiment.

A proposed pathway for TCM cometabolism was presented previously. If this reaction proceeded as shown, the radiolabeled ^{14}C would be expected to incorporate into CO_2, but in the experiment, a significant amount of radiolabeled ^{14}C accumulated in the biomass and as nonpurgeable products. Because organism growth is assumed negligible for the timeframe of the experiment, intermediates are likely reacting with the cells.

Pohl et al. (1977) proposed the mechanism previously described in Chapter 2 for the oxidative dechlorination of chloroform by liver microsomes of rats. In this mechanism, the unstable phosgene can bind with macromolecules as well as degrade to carbon dioxide. Based on this mechanism, it is proposed that the accumulation of ^{14}C in the biomass is a result of phosgene binding with cellular material and that the accumulation of ^{14}C in the nonpurgeable products is a result of cell excretions. The

ultimate result is that no new undefined DBPs should be formed during cometabolism of TCM. Rather, a known intermediate, phosgene, is attacking the bacteria cell directly. This would also explain why the bacteria could only transform a certain mass of THMs, as given by T_c, before the cumulative effects of the toxic degradation products inactivate the cell.

Table 4.12 *N. europaea* ^{14}C transformation breakdown

Time (min.)	% of Total ^{14}C Transformed	Transformed ^{14}C Breakdown (%)		
		CO_2	Nonpurgeable Products	Biomass
0.0	0	0	0	0
31.5	20	20	30	50
61.5	26	25	34	41
92.0	26	23	33	44

4.1.7. Endogenous Decay Experiment

To provide further kinetic information for use in future biofilm modeling, an endogenous decay experiment was performed. The results from this experiment yielded an endogenous decay coefficient, k_d, of 0.022/day and a standard error of ± 0.0017. The organisms exhibited an initial period of stable biomass concentration, which was ignored in the endogenous decay analysis.

4.2. COMPARISON TO MIXED CULTURES

Batch kinetics experiments were conducted with mixed-culture nitrifiers from various sources (Henry 2004; Wahman et al. 2006) and were compared to kinetic coefficients determined for THM cometabolism with the pure culture *N. europaea*. The

following sections summarize these results to tie the pure culture performance to mixed-cultures likely encountered in practice.

4.2.1. Ammonia Degradation Kinetics

A comparison of the half saturation coefficients for each mixed-culture nitrifier and *N. europaea* is shown in Figure 4.19(A), whereas Figure 4.19(B) shows the average value of all experiments for each culture. The y-axis bars in Figure 4.19 (A) represent the 95% joint CLs of estimated kinetic coefficients for each experiment to show the true variability among mixed-culture nitrifiers and among experiments. Many, but not all, of the 95% CLs overlapped within each culture and among the different cultures, illustrating some inherent variability. Nevertheless, the average values, shown in Figure 4.19(B), encompassed a relatively narrow range.

The data for the maximum substrate utilization rate, k_{TOTNH_3}, are presented in Figure 4.20 in the same manner as the half saturation constant data. k_{TOTNH_3} varied in a similar manner as did $K_{s_{NH_3\text{-}N}}$ among cultures and among experiments within a culture. As in the instance of $K_{s_{NH_3\text{-}N}}$, k_{TOTNH_3} for *N. europaea* overlapped kinetic coefficients found for the mixed composition nitrifiers.

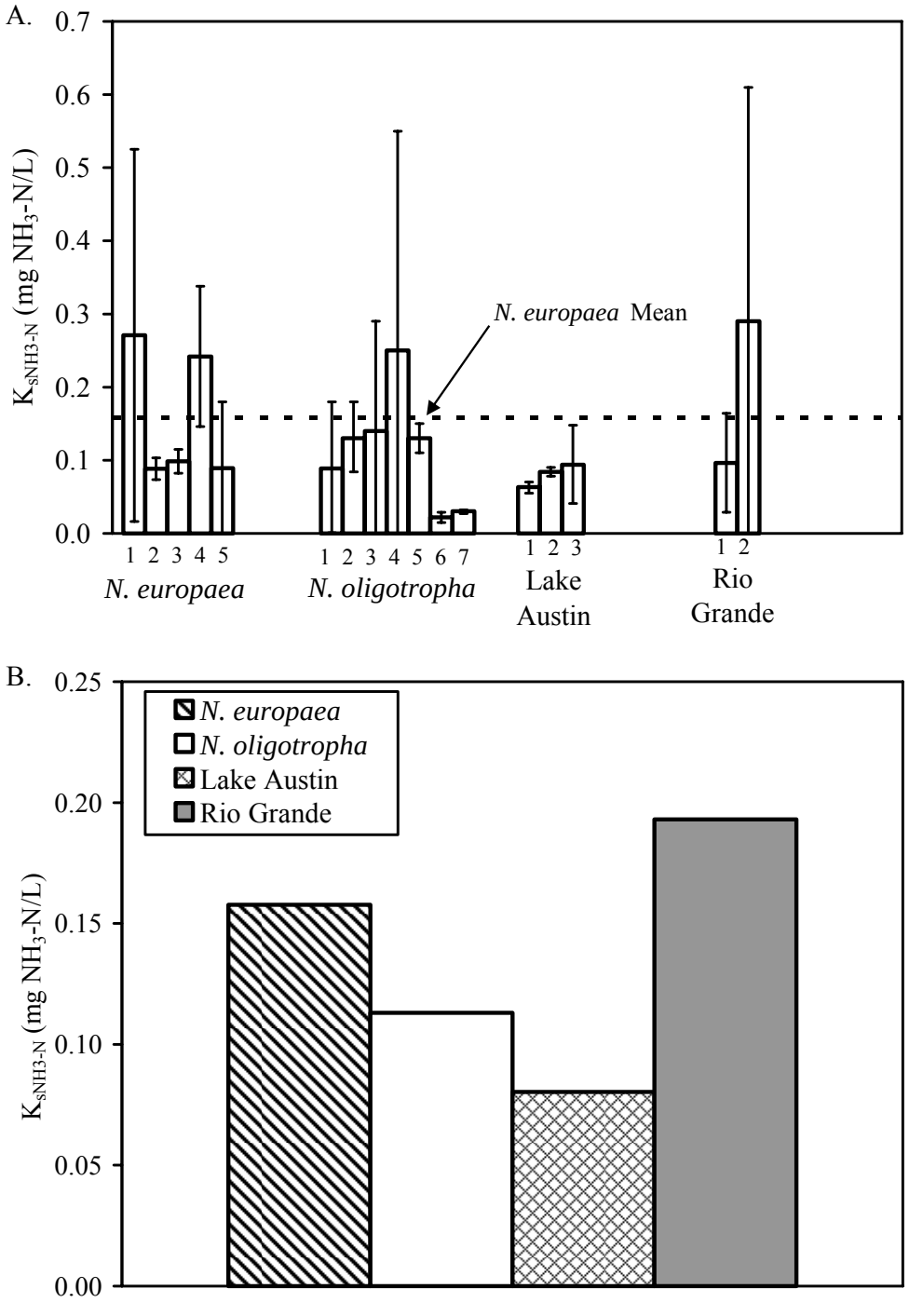

Figure 4.19 $K_{s_{NH_3-N}}$ comparison for pure and mixed cultures showing all experiments (A) and average values (B) for given cultures

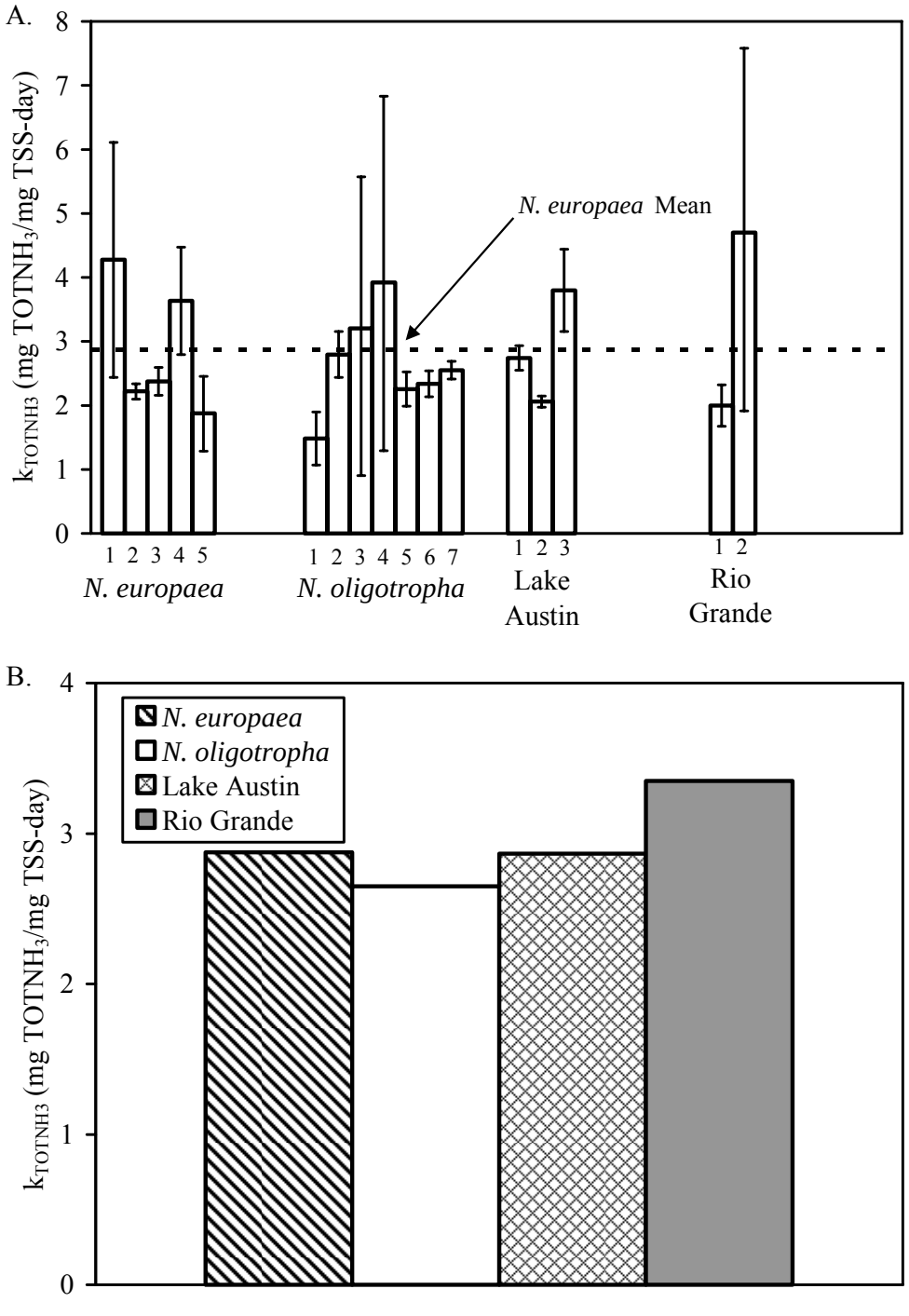

Figure 4.20 k_{TOTNH_3} comparison for pure and mixed cultures showing all experiments (A) and average values (B) for given cultures

4.2.2. THM Degradation Kinetics

In the same manner as for the ammonia kinetic parameters, Figure 4.21 details the pseudo-first-order rate constants determined for each THM experiment with each mixed-culture nitrifier and *N. europaea*. Figure 4.22 lists the average kinetic coefficients determined for each group of nitrifiers. The overlap of these data for nearly all sources of nitrifiers and species of THMs indicated that the cometabolism potential of the mixed cultures of nitrifiers were similar and that mixed cultures could cometabolize THMs as efficiently as the pure culture, *N. europaea*. Moreover, these results indicate that seeding a biofilter with a pure culture is unlikely to produce any benefit relative to the mixed cultures of nitrifiers present in source waters that would naturally grow in the biofilter.

As observed with the pure culture, THM kinetic coefficients were greater for experiments with greater ammonia degradation rates as represented by k_{TOTNH_3}. For each mixed culture, the $k_{1_{THM}}/k_{TOTNH_3}$ ratios were similar among experiments. Comparing across cultures, the average $k_{1_{THM}}/k_{TOTNH_3}$ ratios (Table 4.13) for the Rio Grande and N. oligotropha cultures were similar to those determined previously for *N. europaea*. The $k_{1_{THM}}/k_{TOTNH_3}$ ratio was lower for the Lake Austin culture, which suggests that this culture does not cometabolize THMs as efficiently as the others do; nevertheless, the THM rate constants are still suitable for practical applications.

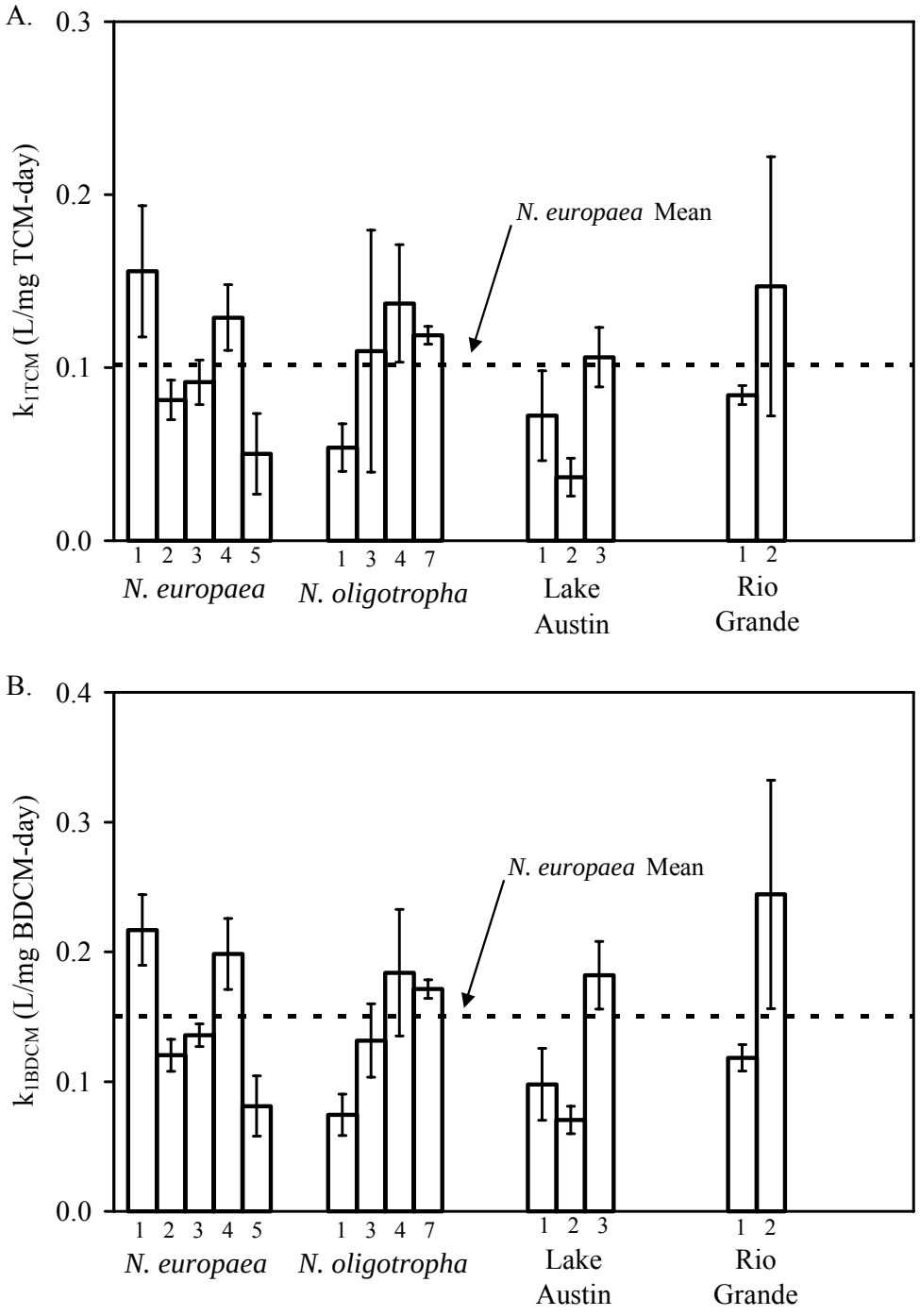
A.
0.3
0.2
0.1
0.0
k_{1TCM} (L/mg TCM-day)
N. europaea Mean
1 2 3 4 5
N. europaea
1 3 4 7
N. oligotropha
1 2 3
Lake Austin
1 2
Rio Grande
B.
0.4
0.3
0.2
0.1
0.0
k_{1BDCM} (L/mg BDCM-day)
N. europaea Mean
1 2 3 4 5
N. europaea
1 3 4 7
N. oligotropha
1 2 3
Lake Austin
1 2
Rio Grande

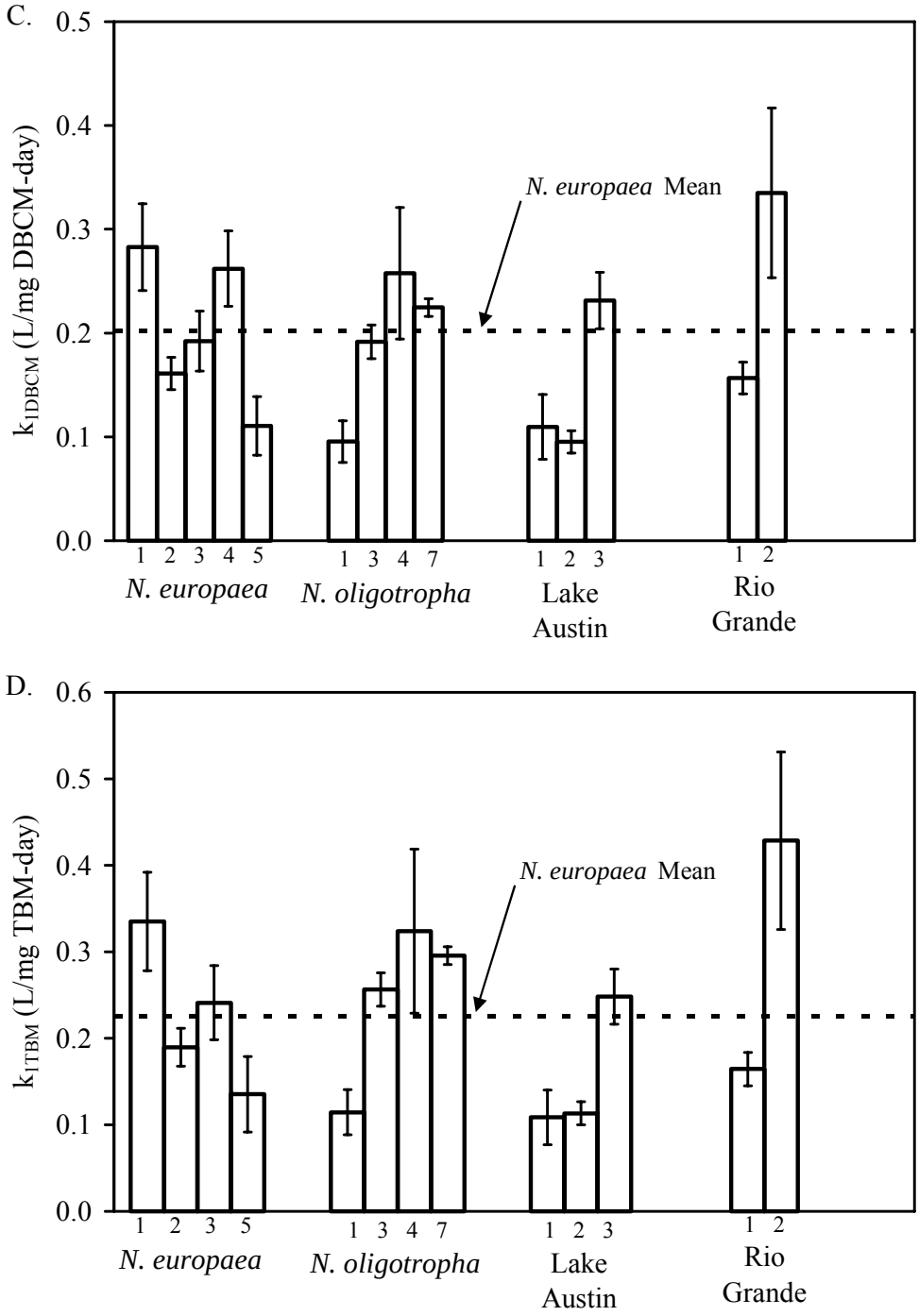

Figure 4.21 Individual experiment $k_{1_{THM}}$ comparison for pure and mixed culture nitrifiers: (A) TCM, (B) BDCM, (C) DBCM, and (D) TBM

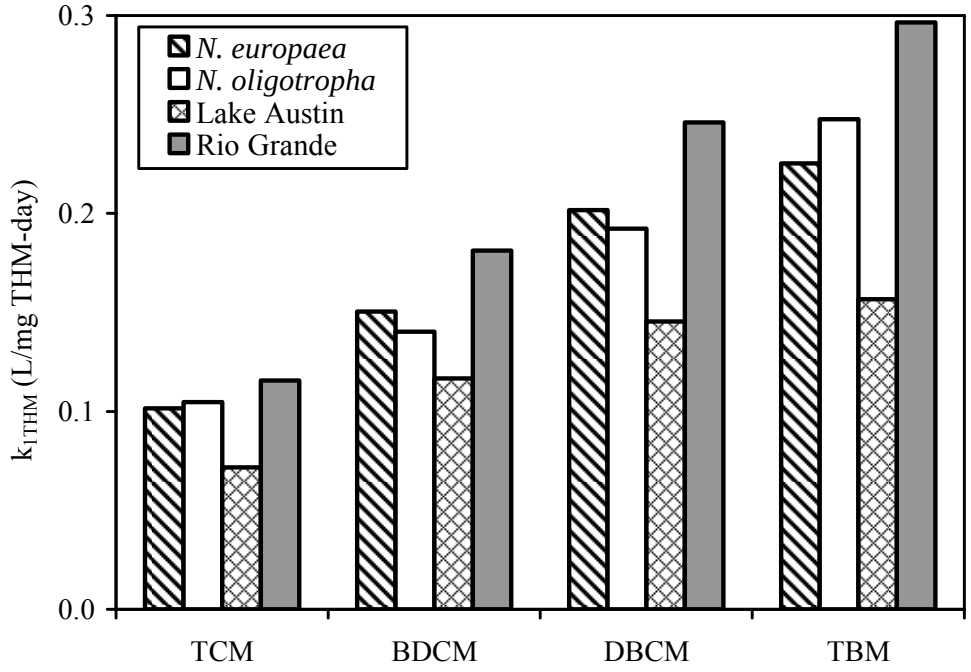

Figure 4.22 Average $k_{1_{THM}}$ comparison for pure and mixed culture nitrifiers

Table 4.13 Ratio of $k_{1_{THM}}$ to k_{TOTNH_3} comparison between mixed and pure culture nitrifiers

Nitrifier Culture	$k_{1_{THM}}/k_{TOTNH_3}$ Ratio (L/mg $TOTNH_3$)			
	TCM	BDCM	DBCM	TBM
N. europaea	0.035	0.052	0.070	0.084
N. oligotropha	0.039	0.051	0.069	0.089
Lake Austin	0.024	0.039	0.049	0.053
Rio Grande	0.037	0.056	0.075	0.087

4.2.3. Temperature Effects

Table 4.14 provides a comparison between the temperature experiment conducted with the mixed culture *N. oligotropha* and the pure culture used in this research, *N. europaea*. As seen with the pure culture, decreased temperature substantially decreased the rate of degradation for both ammonia and THMs with *N. oligotropha*. Experiments with both cultures showed two trends with decreasing temperature: (1) the THM kinetic coefficients were less affected than ammonia maximum specific degradation rate, and (2) the THM kinetic coefficients were less affected as the degree of bromine-substitution decreased. The significant effect of temperature indicates that seasonal variations in water temperature should be a consideration for implementation of this technology.

Table 4.14 Temperature effects on pure and mixed culture nitrifiers

Nitrifiers	Temperature	k_{TOTNH_3} (mg/mg-day)	$k_{1_{THM}}$ (mg/L-day)			
			TCM	BDCM	DBCM	TBM
N. europaea	14°C	0.45	0.026	0.032	0.041	0.048
	22°C	1.9	0.050	0.081	0.11	0.14
	% of 22°C	24	51	40	37	35
N. oligotropha	13ºC	0.16	0.016	0.020	0.024	0.025
	24ºC	1.1	0.037	0.061	0.080	0.094
	% of 24ºC	14	44	32	29	27

4.2.4. Transformation Capacity

Table 4.15 summarizes THM degradation for *N. oligotropha* using the previously calculated THM T_c values for *N. europaea*. The calculated percentage of 104% supported the assumption that *N. oligotropha* T_c values were similar to those of *N. europaea*.

Table 4.15 Mixed culture transformation capacity comparison

		T_c from Individual *N. europaea* THM Experiments		Combined *N. oligotropha* THM Experiment (TSS = 32 mg/L)		
THM	MW[d]	T_c (μg/mg)	T_c (nmol/mg)	Calculated Individual Δ THM (μg/L)[a]	[†]Measured Δ THM (μg/L)[b]	% T_c Used[c]
TCM	119.5	9.2	77	290	59	20
BDCM	164.0	7.3	45	230	53	22
DBCM	208.5	6.5	31	210	56	27
TBM	253.0	5.6	22	180	63	35
					Total % T_C Used =	104

[a]Calculated Individual Δ THM = Concentration of THM required to inactive the cells if present individually (T_c times the initial TSS concentration).

[b]Measured Δ THM = Actual concentration of each THM degraded in the experiment.

[c]% T_c Used = Percentage of the T_c realized in experiment with all four THMs.

[d]MW, molecular weight.

4.3. SUMMARY

Kinetic coefficients for THM degradation were successfully determined for the pure culture *N. europaea*, with the reductant model providing the best fit of the data. The implications of this model are that the removal of THMs increases at greater ammonia concentrations because the rate of THM degradation depends on both the concentration of the THM and ammonia. The reductant model also predicts no THM degradation in the absence of ammonia.

The kinetic coefficients determined for mixed-culture nitrifiers compared well to kinetic coefficients determined for the pure culture, *N. europaea*, and are typical kinetic coefficients for nitrifiers (Ely 1996; Rittmann and McCarty 2001). 95% joint CLs were determined for all kinetic coefficients, which reflected the fit of the model to the data for each experiment and cultural variability among experiments. The significant effect of temperature on kinetic coefficients was seen in experiments with decreased temperatures. These decreases in temperature led to a decrease in both ammonia and THM degradation rates compared to similar experiments performed at higher temperatures.

The kinetic experiments showed that nitrifier communities likely seen in drinking water treatment facilities could degrade THMs at a sufficient rate by themselves, without any seeding with a pure culture. These results also indicated that temperature sensitivity and product toxicity would be concerns if THM cometabolism by nitrifying bacteria was implemented as a treatment option in treatment facilities. In particular, as bromine substitution increases, both THM degradation kinetics and product toxicity increase. As a result, utilities will need to balance the attractiveness of faster kinetics with the reality of product toxicity in applying this technology to waters containing significant concentrations of bromine-substituted THMs. Furthermore, based on the THM cancer risk concentrations in Table 2.3, the health risk associated with THMs increases with

increasing THM bromine substitution. With THM degradation kinetics also increasing with bromine substitution, THM cometabolism preferentially removes THMs with the greatest health risk.

Overall, the kinetic coefficients determined for THM cometabolism by all sources of nitrifiers fall above the range of practically feasible kinetic coefficients provided by Segar et al. (1995) for biofilter cometabolism. This indicates that, according to the conditions of these studies, THM cometabolism by pure and mixed-culture nitrifying bacteria are fast enough to suggest practical feasibility in a drinking water treatment facility.

Chapter 5: Biofilter Studies

5.1. INTRODUCTION

A series of biofilter column experiments was conducted to investigate the feasibility of THM cometabolism in the envisioned process configuration. Table 5.1 displays a summary of the biofilter experiments conducted, including their configuration, operating conditions, and the full-scale filters to which these experimental filters scale. In addition to the biofilter experiments summarized in Table 5.1, an initial experiment was conducted with *N. europaea* and is also presented in this chapter.

In general, the biofilters experiments were conducted with either three (A, B, and C) or four (A, B, C, and D) parallel trains with each train consisting of one or two biofilters in series. Sampling points were at the first biofilter's influent (sample location 0), between the two biofilters in a train corresponding to the first biofilter's effluent and second biofilter's influent (sample location 1), and at the second biofilter's effluent (sample location 2). Using the biofilm scaling procedure proposed by Manem and Rittmann (1990), the experimental biofilters simulate full-scale filters as summarized in Table 5.1, depending on whether biofilm shear loss or external mass transport is chosen for scaling. The scaled operating conditions cover the range of typical values reported for rapid filtration for which filter depths range from 2-6 feet (0.6-1.8 meters) and surface loading rates (SLRs) range from 2-6 gpm/ft^2 (5-15 m/h) (MWH et al. 2005).

Table 5.1 Summary of operating conditions for biofilter experiments and their scaling to full-scale filters

Experiment	Experimental Setup[a]	Run(s)	Source Water[b]	EBCT (min.)	SLR (gpm/ft^2)	Full-Scale Filter Scaling[c] EBCT (min.)	Depth (feet)	SLR (gpm/ft^2)
Lake Austin Biofilters	A(LA/2/A)	1 & 2	NW	4.0	0.63	8.0	2.6-3.8	2.5-3.5
	B(LA/2/A)							
	C(LA/2/A)	3 & 4	LA					
Mixed Culture Biofilters 1	A(RG/2/A)	1	LA	4.0	0.63	8.0	2.6-3.8	2.5-3.5
	B(NO/2/A)	2	LA/NW	2.0	1.3	4.0	2.6-3.8	4.9-7.0
	C(RG/2/G)	3	NW					
Mixed Culture Biofilters 2	A(LA/2/A)	1 & 2	NW	1.0	1.3	2.0	1.3-1.9	4.9-7.0
	B(LA/1/A)							
	C(NO/2/A)							
	D(NO/1/A)							

[a] Biofilter train designation letter(culture/number of biofilters in series/packing media)

Culture:

LA = Lake Austin mixed culture

NO = *Nitrosomonas oligotropha* enrichment culture

RG = Rio Grande mixed culture

Packing Media:

A = 30 x 40 mess anthracite

G = 30 x 40 mess granular activated carbon

[b]Source Water:

NW = Nutrient water

LA = Lake Austin water

[c]Range based on basis of SLR scaling for full-scale filters:

(1) SLR scaling based on biofilm shear loss, or

(2) SLR scaling based on external mass transport

5.2. TRIHALOMETHANE PRODUCT TOXICITY AND RELATIONSHIP TO BIOFILTER EXPERIMENTS

Product toxicity was observed when THMs were cometabolized by nitrifiers in the batch kinetic experiments and initial biofilter experiments presented in this chapter. Therefore, a simple formula was derived to quantify the expected product toxicity of THMs fed during biofilter experiments to guide the design and interpretation of subsequent experiments. For bacteria to provide sustained degradation of THMs, the net growth rate on ammonia (based on Monod kinetics) must be greater than the inactivation rate from THM degradation. Inactivation results from the toxicity of THM degradation products and is characterized by transformation capacity (T_c). To help quantify the balance between net growth and inactivation rates, a new term, the cometabolism stability index (C_{si}), was developed. C_{si} is the ratio of the net growth rate (r_g') to the sum of the inactivation rates for the four THMs (r_i) and is shown as Equation 5.1:

$$C_{si} = \frac{r_g'}{r_i} = \frac{Yk_{TOTNH_3} - k_d\left(\frac{K_{s_{NH_3-N}} + \alpha_1 S_{TOTNH_3}}{\alpha_1 S_{TOTNH_3}}\right)}{\frac{k_{1_{TCM}} S_{TCM}}{T_{c_{TCM}}} + \frac{k_{1_{BDCM}} S_{BDCM}}{T_{c_{BDCM}}} + \frac{k_{1_{DBCM}} S_{DBCM}}{T_{c_{DBCM}}} + \frac{k_{1_{TBM}} S_{TBM}}{T_{c_{TBM}}}} \qquad (5.1)$$

where r_g' = Net rate of bacterial cell growth (mg total suspended solids (TSS)/day);

r_i = Rate of THM bacterial inactivation (mg TSS/day);

S_{TOTNH_3} = $TOTNH_3$ concentration (mg N/L);

S_{THM} = THM concentration (μg THM/L); and

other terms are defined in Table 5.2.

Equation 5.1 indicates that for stable biofilter operation C_{si} must be greater than or equal to one. All the terms in the C_{si}, except THM and $TOTNH_3$ concentrations, are bacteria specific and were previously determined from batch kinetics experiments for the pure culture, *N. europaea*. Because the mixed cultures showed kinetic values similar to *N. europaea* and individual THM transformation capacity values were determined for *N. europaea* and verified for a mixed culture, the information for *N. europaea* was used in these calculations. In this analysis, it is assumed that kinetic parameters of the batch suspended growth bacteria are representative of the biofilm attached growth bacteria.

To simplify the analysis, the influent $TOTNH_3$ and THM concentrations were used to evaluate possible product toxicity. Rigorously, these concentrations only define the C_{si} at the influent to the first biofilter in the absence of mass transfer resistances into the biofilm. The parameter values used to calculate C_{si} are summarized in Table 5.2, while Table 5.3 and Table 5.4 provide C_{si} values as a reference for combinations of THM concentration and speciation tested in the three major biofilter experiments presented in this chapter.

Table 5.2 Trihalomethane product toxicity evaluation parameters for biofilter experiments

Variable	Definition	Value[a]	Units
α_1	$[NH_3\text{-}N]/[TOTNH_3]$ at 23.5°C & pH 8.0	0.049	dimensionless
Y	Bacterial cell yield	0.33[b]	mg TSS/mg $TOTNH_3$
$K_{s_{NH_3\text{-}N}}$	Ammonia-nitrogen half-saturation coefficient	0.16	mg NH_3-N/L
k_{TOTNH_3}	$TOTNH_3$ maximum substrate utilization rate constant	2.9	mg $TOTNH_3$/mg TSS-day
k_d	Endogenous decay coefficient	0.02	1/day
$k_{1_{TCM}}$	TCM pseudo-first-order rate constant	0.10	L/mg TSS–day
$k_{1_{BDCM}}$	BDCM pseudo-first-order rate constant	0.15	L/mg TSS–day
$k_{1_{DBCM}}$	DBCM pseudo-first-order rate constant	0.20	L/mg TSS–day
$k_{1_{TBM}}$	TBM pseudo-first-order rate constant	0.23	L/mg TSS–day
$T_{c_{TCM}}$	TCM transformation capacity	9.2	µg TCM/mg TSS
$T_{c_{BDCM}}$	BDCM transformation capacity	7.3	µg BDCM/mg TSS
$T_{c_{DBCM}}$	DBCM transformation capacity	6.5	µg DBCM/mg TSS
$T_{c_{TBM}}$	TBM transformation capacity	5.6	µg TBM/mg TSS

[a]This research unless otherwise noted

[b](Rittmann and McCarty 2001) – value also assumes volatile suspended solids equals TSS in cells

Table 5.3 Cometabolism stability index (C_{si}) values for Lake Austin Biofilters

Nominal THM Concentrations (μg/L)											
Run (Period)	1(II)	1(IV)	1(V-VI)	3 (VI-X) 4 (I-IV)	2 (I)	2(II)	2(III) 3(IV)	2(IV)	2(V)	2(VI) 3(II)	2(VII)
TCM	40	20	30	40	50	75	100	0	0	100	100
BDCM	20	0	0	0	0	0	0	0	0	0	0
DBCM	20	0	0	0	0	0	0	10	25	10	25
TBM	20	0	0	0	0	0	0	0	0	0	0
Cometabolism Stability Index (C_{si})											
Train A	0.40	4.2	2.8	2.1	1.7	1.1	0.84	3.0	1.2	0.65	0.49
Train B	0.39	4.1	2.7	2.1	1.7	1.1	0.82	2.9	1.2	0.64	0.48
Train C	0.38	4.0	2.6	2.0	1.6	1.1	0.79	2.8	1.1	0.62	0.46

Table 5.4 Cometabolism stability index values for Mixed Culture Biofilters 1 and 2

Nominal THM Concentrations (μg/L)								
Run (Period)	Mixed Culture Biofilters 1					Mixed Culture Biofilters 2		
	1(II)	1(III-IV)	2 (I-II)	3 (I-II) 3 (IV)	3 (III)	1 (I-II)	2 (I)	2 (II)
TCM	75	110	110	100	100	50	0	15
BDCM	0	0	0	0	0	0	0	15
DBCM	0	0	0	25	25	25	25	15
TBM	0	0	0	0	0	0	0	15
Cometabolism Stability Index (C_{si})								
All Trains	1.1	0.76	0.75	0.49	0.48	0.69	1.2	0.59

5.3. *NITROSOMONAS EUROPAEA* BIOFILTERS FED NUTRIENT WATER

An initial biofilter experiment was conducted with *N. europaea* to provide a basis of comparison with biofilter experiments that examined less defined mixed cultures. In addition, this experiment allowed further investigation as to the attractiveness of seeding biofilters in practice with this culture. Three parallel trains were operated with each train consisting of two biofilters in series at initial empty bed contact times (EBCTs) of 2-minutes for each biofilter (4-minutes for both biofilters in series) and packed with 30x40 mesh anthracite. The experiment was initiated feeding nutrient water on the primary column setup and continued for approximately 2,500 hours. During this time, $TOTNH_3$ degradation did not occur across any of the three trains. At approximately 1,500 hours, the flow rate to the trains was decreased by 50%, increasing the EBCT for each biofilter from 2-minutes to 4-minutes (4-minutes to 8-minutes for both biofilters in series). This process change did not result in any measurable decrease in effluent $TOTNH_3$.

Because no $TOTNH_3$ degradation occurred in the primary column setup, the *N. europaea* biofilters were moved to the secondary column setup on nutrient water to see if degradation would ensue with the decreased flow rate and resulting increased EBCT, 2 hours for both biofilters in series versus 8 minutes. Because $TOTNH_3$ degradation occurred in this configuration, a short term proof of concept experiment was conducted to determine if THM cometabolism would likewise occur in the biofilters. To accomplish this, one train's feed was changed to a syringe pump, containing nutrient feed water with the addition of 17-18 μg/L of each of the four THMs and 3.5 mg N/L $TOTNH_3$.

Three EBCTs were completed before effluent sampling commenced. The results of this experiment for $TOTNH_3$ and the THMs are shown in Figure 5.1. Total THM and $TOTNH_3$ degradation was consistent over the sampling period and resulted in average reductions in $TOTNH_3$ of 0.87 mg N/L and total THMs of 18 μg/L across the biofilters.

Even though the C_{si} for this experiment was less than one (0.49), the short term nature of the experiment (approximately 11 hours) did not result in any decrease in nitrification. A further breakdown of the THMs degraded is shown in Figure 5.2.

Table 5.5 details each individual THM's degradation in terms of normalized effluent concentration (S_{THM_2}/S_{THM_0}) and calculated $k_{1_{THM}}/k_{TOTNH_3}$ ratios using the equation developed from the batch kinetic data (Equation 4.1). The general trends in the degradability of the THMs followed those of the batch kinetic experiments. As the THM bromine substitution increased, a greater THM mass was degraded.

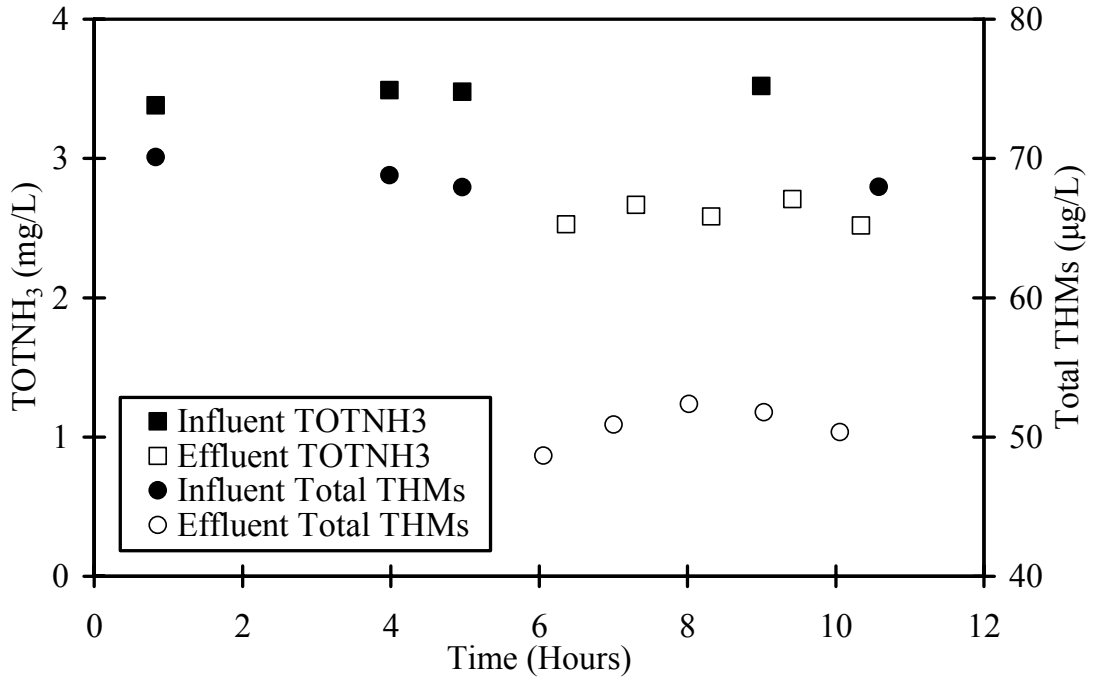

Figure 5.1 *N. europaea* biofilter experiment $TOTNH_3$ and total THM concentrations

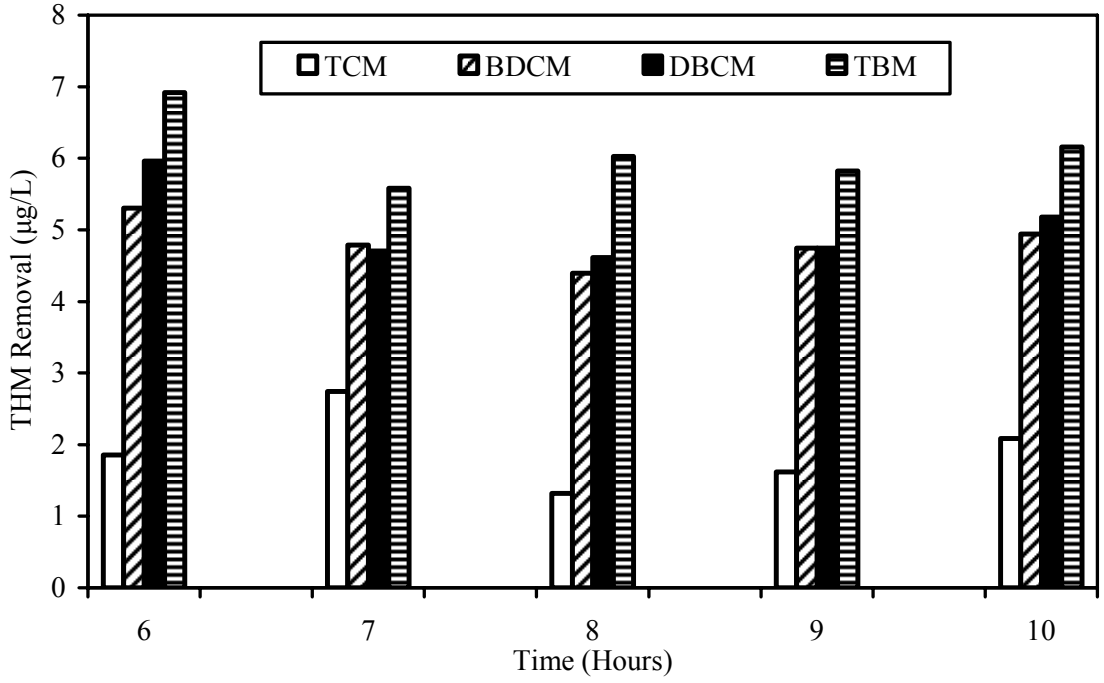

Figure 5.2 *N. europaea* biofilter experiment individual THM removal breakdown

Table 5.5 *N. europaea* biofilter experiment THM performance summary and calculated $k_{1_{THM}}/k_{TOTNH_3}$ ratios

THM	Average S_{THM_0} (µg/L)	$\frac{S_{THM\ 2}}{S_{THM\ 0}}$	$\frac{k_{1THM}}{k_{TOTNH_3}}$ (L/mg $TOTNH_3$)
TCM	17	0.89	0.14
BDCM	17	0.72	0.38
DBCM	17	0.70	0.41
TBM	18	0.66	0.48
Total	69	0.74	N/A[a]

[a]N/A = not applicable

S_{THM_0}, S_{THM_2} = Influent and effluent THM concentrations, respectively (µg/L)

This experiment demonstrated that THM cometabolism could be accomplished in a biofilter seeded with the pure culture *N. europaea*. The degradability trends of the individual THMs with respect to bromine substitution generally followed those of the batch kinetic experiments. The $k_{1_{THM}}/k_{TOTNH_3}$ ratio was greater for each THM as compared with those determined in any of the batch kinetic experiments. This possibly indicated that in biofilters, the biofilm nitrifiers are more efficient at THM degradation than suspended cultures. *N. europaea*, however, required an impractical EBCT for ammonia degradation. Insufficient affinity for attachment to surfaces is the probable cause of this difficulty because of the minimal $TOTNH_3$ degradation that occurred and the improved removal seen with subsequent biofilter experiments seeded with different cultures. As a result, it is unlikely that the use of *N. europaea* to seed biofilters in practice would be beneficial. For this biofilter experiment, THM removals ranged from 11 to 34% for the individual THMs (26% for total THMs), which are attractive removals from the viewpoint of THM cometabolism in practice. The difficulty with *N. europaea* was in establishing sufficient biomass in the biofilters. As a result, no further experiments were conducted with *N. europaea* so that the research could focus on nitrifiers with better surface attachment characteristics.

5.4. LAKE AUSTIN MIXED CULTURE BIOFILTERS FED NUTRIENT AND LAKE AUSTIN WATERS

To expand the biofilter experiments to cultures likely seen in practice, biofilters were seeded with a Lake Austin mixed culture, referred to as the Lake Austin Biofilters (LAB). Once seeded, these biofilters were operated on the secondary setup and fed nutrient water for approximately 72 days to initiate nitrification at the longer EBCTs present on the secondary setup. After the initial period on the secondary setup, these biofilters were moved to the primary setup and operated under various conditions broken

into four runs for ease of presentation. Experiments were conducted with three parallel trains (A, B, and C) each consisting of two biofilters in series. The nominal influent $TOTNH_3$ concentrations for Trains A, B, and C were different (4, 2, and 1 mg N/L, respectively) with other biofilter setup and scaling information summarized in Table 5.1. In Runs 1 and 2, the biofilters were fed nutrient water. The feed water was switched to Lake Austin water for Runs 3 and 4 with the addition of monochloramine in Run 4. To illustrate the trends seen during biofilter operation, only the data from Train A (influent 4 mg N/L $TOTNH_3$) is presented in this chapter and is representative of the trends seen in Trains B and C. Information concerning Trains B and C can be found in Appendix D.

5.4.1. Run 1

Run 1 consisted of an initial operating period to establish nitrification, explored THM product toxicity, and resolved dissolved oxygen limitations for Train A. Figure 5.3 details the $TOTNH_3$ and trichloromethane (TCM) concentrations for Train A during Run 1. Initially, only $TOTNH_3$ was added to the biofilters until nitrification was established (Period I). The initial THM addition of 40 μg/L TCM and 20 μg/L each of bromodichloromethane (BDCM), dibromochloromethane (DBCM), and tribromomethane (TBM) resulted in an immediate loss of $TOTNH_3$ degradation (Period II) as subsequently predicted from C_{si} for these THM influent concentrations (Table 5.3). The first sample after THM addition (172 hours) showed that all four THMs were degraded in all three trains as shown in Table 5.6 with this degradation leading to the decrease in $TOTNH_3$ removal because of product toxicity. Essentially no $TOTNH_3$ or THM degradation occurred after approximately 48 hours of operation during Period II.

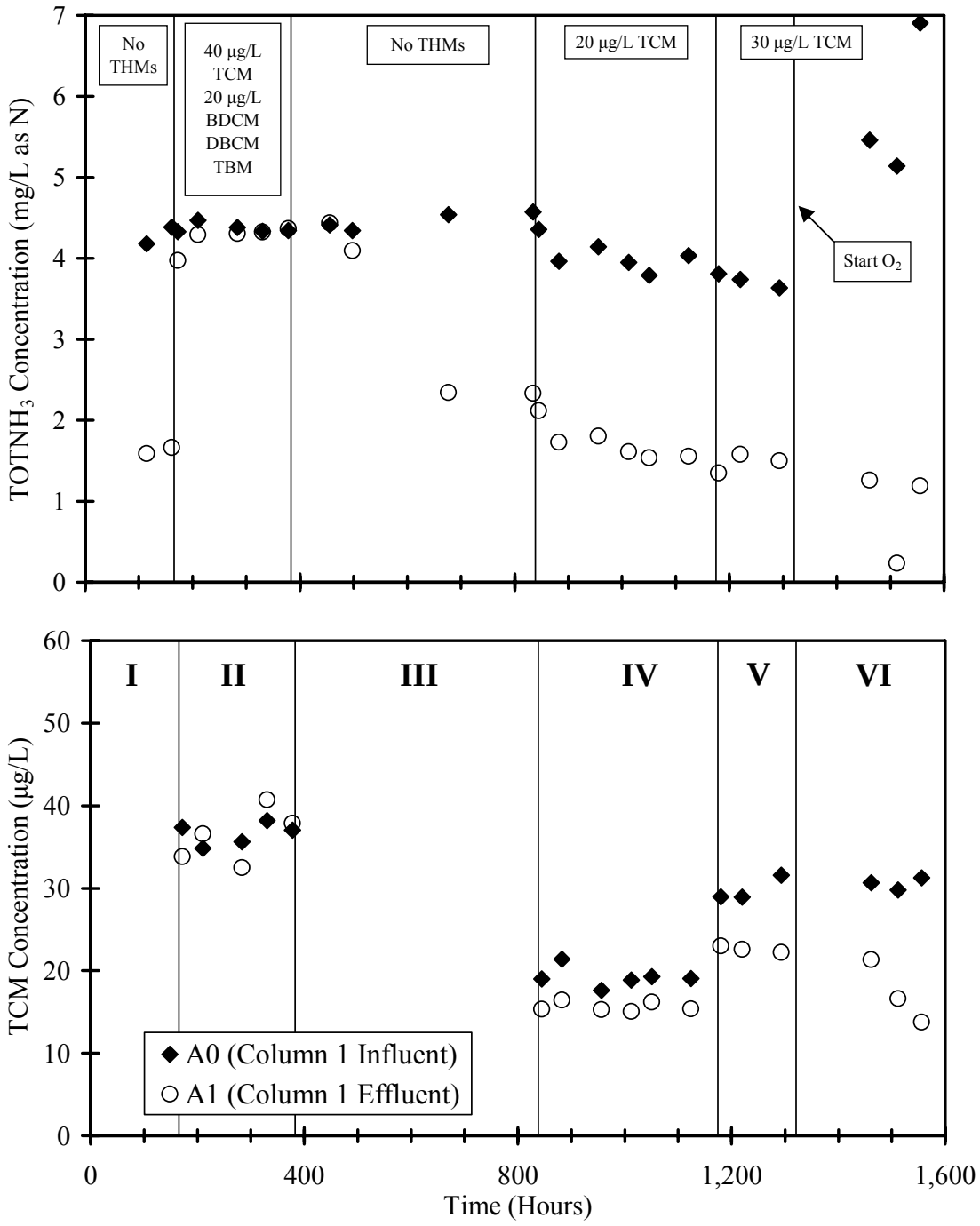

Figure 5.3 Lake Austin Biofilters Run 1 Train A $TOTNH_3$ and TCM concentrations fed nutrient water

Table 5.6 Lake Austin Biofilters Run 1 (Period II) performance at 172 hours and calculated $k_{1_{THM}}/k_{TOTNH_3}$ ratios

Train	$\Delta_{0\text{-}2}TOTNH_3$ (mg N/L)	$\frac{S_{THM_2}}{S_{THM_0}}$ $\frac{k_{1_{THM}}}{k_{TOTNH_3}}$ (L/mg $TOTNH_3$)				
		TCM	BDCM	DBCM	TBM	Total THMs
A	0.86	0.87 0.17	0.82 0.23	0.80 0.27	0.81 0.25	0.83
B	1.2	0.84 0.15	0.79 0.20	0.75 0.24	0.75 0.24	0.80
C	0.62	0.89 0.19	0.86 0.24	0.84 0.28	0.84 0.29	0.87
Average	0.89	0.87 0.17	0.83 0.22	0.80 0.26	0.80 0.26	0.83

S_{THM_0} = Influent THM concentration to first biofilter in series (μg/L)

S_{THM_2} = Effluent THM concentration from second biofilter in series (μg/L)

S_{TCM_0} = 37 μg/L; S_{BDCM_0} = 19 μg/L; S_{DBCM_0} = 18 μg/L; S_{TBM_0} = 18 μg/L; and S_{TTHM_0} = 92 μg/L

$\Delta_{0\text{-}2}TOTNH_3$ = $TOTNH_3$ removed through both biofilters in series (mg N/L)

Once the THMs were removed from the influent (Period III), all three trains recovered their previous $TOTNH_3$ degradation, as nitrification was re-established. Based on C_{si} and to avoid THM product toxicity, the influent THM concentration was set to

approximately 20 μg/L TCM after the biofilters recovered from the process upset (Period IV) with a subsequent increase to 30 μg/L TCM without (Period V) and with (Period VI) oxygen addition. TCM removal during Periods IV and V averaged 4 and 7 μg/L, respectively, for Train A. Once oxygen was added in Period VI, $TOTNH_3$ and TCM removal increased, with TCM removal reaching 15 μg/L at the end of Period VI for Train A. Oxygen addition continued throughout the remaining biofilter experiments to ensure that oxygen was not limiting in the biofilters, and it was added prior to THM addition to prevent stripping of THMs.

Referring to Table 5.3, the initial speciation and concentration of THMs fed in Run 1 resulted in a calculated value of C_{si} (0.40) that was less than one, which predicts process failure. Thus, C_{si} proved a good predictor for the loss of $TOTNH_3$ removal and the absence of THM removal under this feed condition. The subsequently decreased TCM concentrations (20 and 30 μg/L) provided a C_{si} greater than one (4.2 and 2.8, respectively) and stable biofilter operation with TCM removal. Overall for Run 1, the experimental findings were consistent with the C_{si} predictions and demonstrated sustained cometabolism of TCM in the biofilters.

5.4.2. Run 2

During Run 2 (Figure 5.4), the influent TCM concentration was increased from 50 μg/L (Period I) to a maximum nominal influent concentration of 100 μg/L (Period III). After Period III, the influent THM was changed from TCM to DBCM to provide information on a bromine-substituted THM. The influent DBCM concentration ranged from 10 to 25 μg/L (Period IV and V, respectively). Finally, both TCM and DBCM were fed simultaneously (Periods VI and VII) to provide a comparison with biofilter performance when they were fed individually.

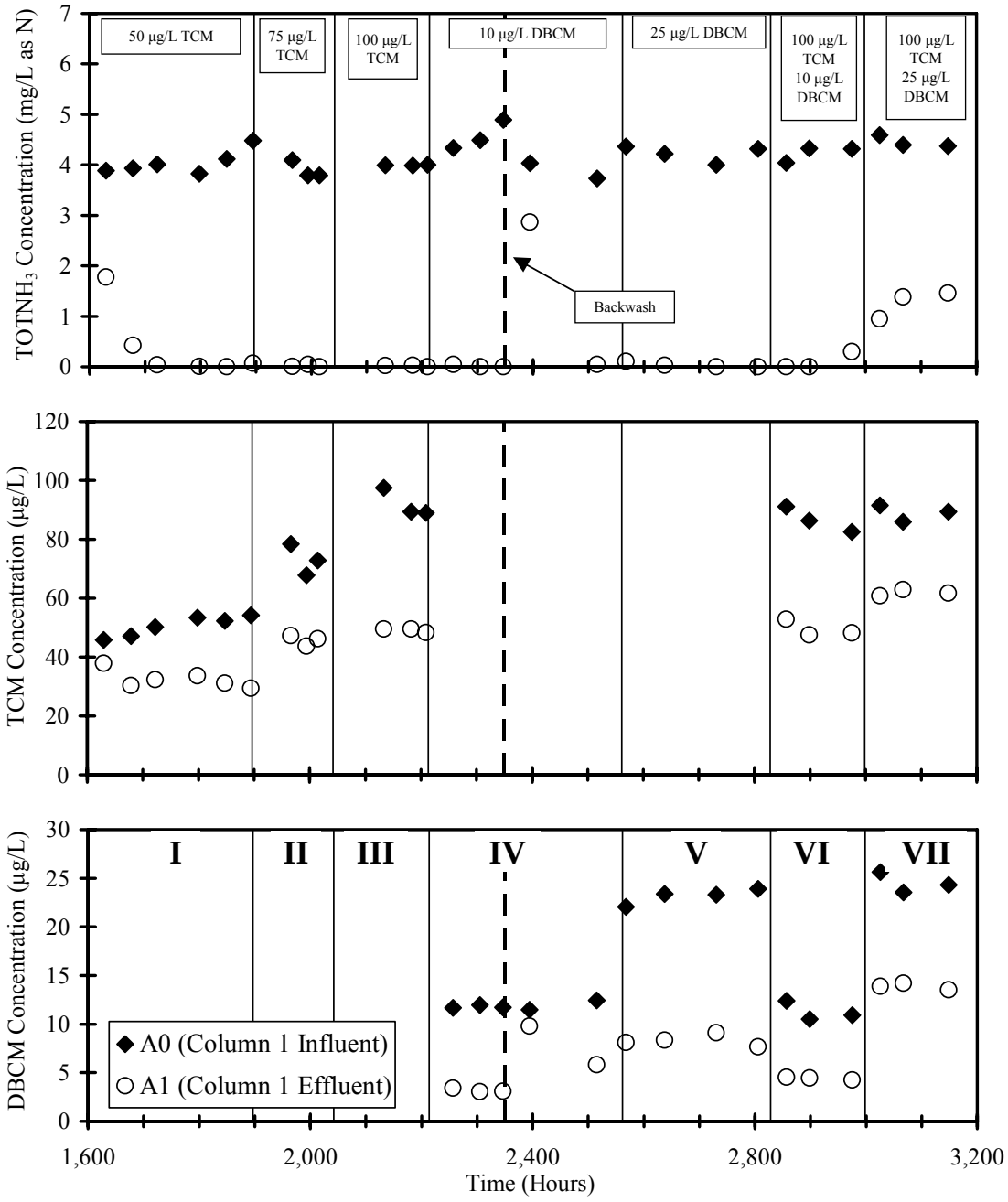

Figure 5.4 Lake Austin Biofilters Run 2 Train A $TOTNH_3$, TCM, and DBCM concentrations fed nutrient water

During Run 2, both TCM and DBCM were degraded in all three trains, with Train A achieving maximum removals of 46% and 73%, respectively. No evident THM product toxicity (based on $TOTNH_3$ removal) occurred during Run 2 except when both TCM and DBCM were fed simultaneously, and then only in Train A, as demonstrated by the increased effluent $TOTNH_3$ concentration in Figure 5.4 for Periods VI and VII. The general absence of product toxicity was expected based on the calculated C_{si} values (Table 5.3) for Period I, II, IV, and V. The C_{si} for Period III, VI, and VII during Run 2 was less than one, predicting process failure. Although these predictions proved too conservative, it is worth noting that the minimum C_{si} values prevailed during Periods VI and VII in which Train A showed a partial loss of nitrification, indicating the usefulness of the C_{si} concept. Even though the C_{si} concept did not necessarily predict performance in all instances, it provides a good framework for evaluating product toxicity. Some refinement of the parameter values in Equation 5.1 in combination with further experience in operating the process might be needed to better define the minimum feasible C_{si} value for successful operation.

Biofilter performance during Period VI was surprising in two respects: (1) based on the C_{si} values in Table 5.3, difficulties with product toxicity would have been expected for all three trains but did not occur in Trains B and C and (2) the biofilter in Train A seemed to re-stabilize at a greater $TOTNH_3$ effluent concentration, rather than proceeding to complete loss of nitrification as observed in Run 1. Nutrient limitations provide a possible explanation for these observations. The enzyme responsible for ammonia oxidation, ammonia monooxygenase (AMO), is proposed to contain iron and copper (Arp and Stein 2003). If the product toxicity associated with THM degradation results in the inactivation of AMO in a way that does not allow the recovery of the iron or copper associated with the enzyme, these nutrients could become limiting as the mass of THMs

degraded increases. Because Train A degraded the greatest mass of THMs and $TOTNH_3$, nutrient limitations could explain the observation. Likewise, nutrient limitations could explain the re-stabilization of process performance in that the process stabilized to a THM and $TOTNH_3$ degradation level that the available nutrient supply in the feed water could support. Subsequent biofilter experiments investigated this hypothesis in greater detail.

5.4.3. Run 1 and 2 Comparison

To provide a clearer picture of process performance during Runs 1 and 2, Table 5.7 summarizes average measurements, with their associated standard deviations, for Train A's different operating conditions. Because $TOTNH_3$ removal was complete after the first biofilter in series and THM removal did not occur without $TOTNH_3$ removal, only values for the first biofilter were used to calculate $TOTNH_3$ and THM concentrations. From Equation 4.1, two trends in the biofilter data are expected: (1) as $TOTNH_3$ removal ($\Delta TOTNH_3$) increases, S_{THM_n}/S_{THM_0} decreases and (2) for a given $\Delta TOTNH_3$, as the THM rate constant ($k_{1_{THM}}$) increases, S_{THM_n}/S_{THM_0} decreases. Both trends are highlighted in Table 5.7 for Train A.

In a similar fashion, Figure 5.5 shows that the two trends held for all three trains during Runs 1 and 2. In this instance, Equation 4.1 was fit to the TCM and DBCM data for all three trains to determine the $k_{1_{THM}}/k_{TOTNH_3}$ ratio and its 95% confidence limit for each THM. Because k_{TOTNH_3} should be the same for each operating condition, the greater DBCM ratio as compared with the TCM ratio implies that $k_{1_{DBCM}}$ is significantly greater than $k_{1_{TCM}}$. Therefore, the trend in degradation rates found in the batch kinetic studies continued in the biofilter experiments as the more bromine-substituted THM, DBCM, had a larger rate constant than TCM. In addition, for statistically similar $TOTNH_3$ degradation, no significant change in TCM degradation occurred whether DBCM was

present and *vice versa*. Again, this result matched observations from the batch kinetic studies that showed no enzyme competition among THMs at the concentrations typical of drinking water treatment.

Table 5.7 Lake Austin Biofilters Run 1 and 2 summary for Train A (1st biofilter in series)

Run	Period	No. of Samples	$\Delta_{0\text{-}1}TOTNH_3$ (mg N/L)	S_{TCM_0} (µg/L)	$\frac{S_{TCM_1}}{S_{TCM_0}}$	S_{DBCM_0} (µg/L)	$\frac{S_{DBCM_1}}{S_{DBCM_0}}$
1	IV	6	2.3±0.094	19±1.2	0.81±0.034		
1	V	3	2.3±0.18	30±1.5	0.76±0.049		
2	I	4	4.1±0.25	53±1.7	0.60±0.045		
2	II	3	3.9±0.18	73±5.3	0.63±0.022		
2	III	3	4.0±0.021	92±4.8	0.54±0.024		
2	IV	3	4.6±0.31			12±0.16	0.27±0.019
2	V	4	4.2±0.14			23±0.8	0.36±0.029
2	VI	3	4.1±0.17	87±4.3	0.57±0.018	11±1.0	0.39±0.029
2	VII	3	3.2±0.39	88±2.8	0.70±0.034	24±1.1	0.57±0.032

S_{TCM_0}, S_{DBCM_0} = Influent TCM and DBCM concentration to first biofilter in series (µg/L)

S_{TCM_1}, S_{DBCM_1} = Effluent TCM and DBCM concentrations from first biofilter in series (µg/L)

$\Delta_{0\text{-}1}TOTNH_3$ = $TOTNH_3$ removed through the first biofilter in series (mg N/L)

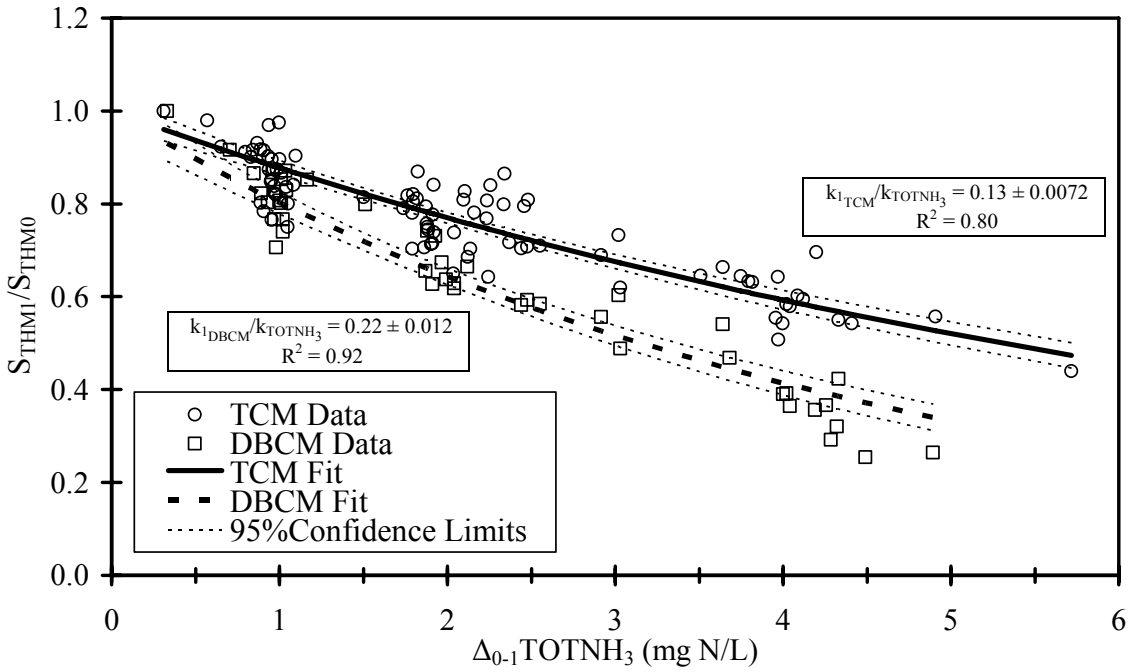

Figure 5.5 THM cometabolism performance curves and $k_{1_{THM}}/k_{TOTNH_3}$ ratio (L/mg $TOTNH_3$) determinations for Lake Austin Biofilters Runs 1 and 2 fed nutrient water

Overall, the results from Runs 1 and 2 suggest that for a $\Delta TOTNH_3$ of 2 mg N/L, TCM and DBCM removal of 25 and 35%, respectively, can be achieved; this level of performance is potentially attractive for drinking water treatment practice. These removals suggest that the biofilm bacteria in Runs 1 and 2 were more efficient at degrading THMs than those from the batch kinetics experiments. Using the batch experiment kinetic parameters, decreased TCM and DBCM removals (7 and 13%, respectively) are predicted for a $\Delta TOTNH_3$ of 2 mg N/L. As with the batch kinetic experiments, the ratio of THM cometabolism to ammonia degradation in Runs 1 and 2 was greater for the bromine-substituted THMs, but greater attention to product toxicity is required when bromine-substituted THMs are present at increasing concentrations.

5.4.4. Run 3

After completing the biofilter experiments on nutrient water, the feed water was changed to Lake Austin water to provide a more realistic test of THM cometabolism under drinking water treatment conditions. Extending the previous notation, this operating phase is noted as Run 3, which consisted of operating periods in which issues of seeming nutrient deficiency and THM product toxicity were investigated and resolved. Figure 5.6 details the $TOTNH_3$ and TCM concentrations during Run 3 for Train A. Before starting THM addition, an initial period (Period I) was provided for the trains to re-establish nitrification after backwashing. The initial THM addition of 100 μg/L TCM and 10 μg/L of DBCM resulted in a decrease in $TOTNH_3$ degradation for all three trains (Period II). As a result, THM addition was stopped, the trains were allowed to re-establish $TOTNH_3$ degradation (Period III), and only 100 μg/L TCM addition was attempted (Period IV). Again, $TOTNH_3$ degradation declined, and THM addition was stopped (Period V) until $TOTNH_3$ degradation was re-established.

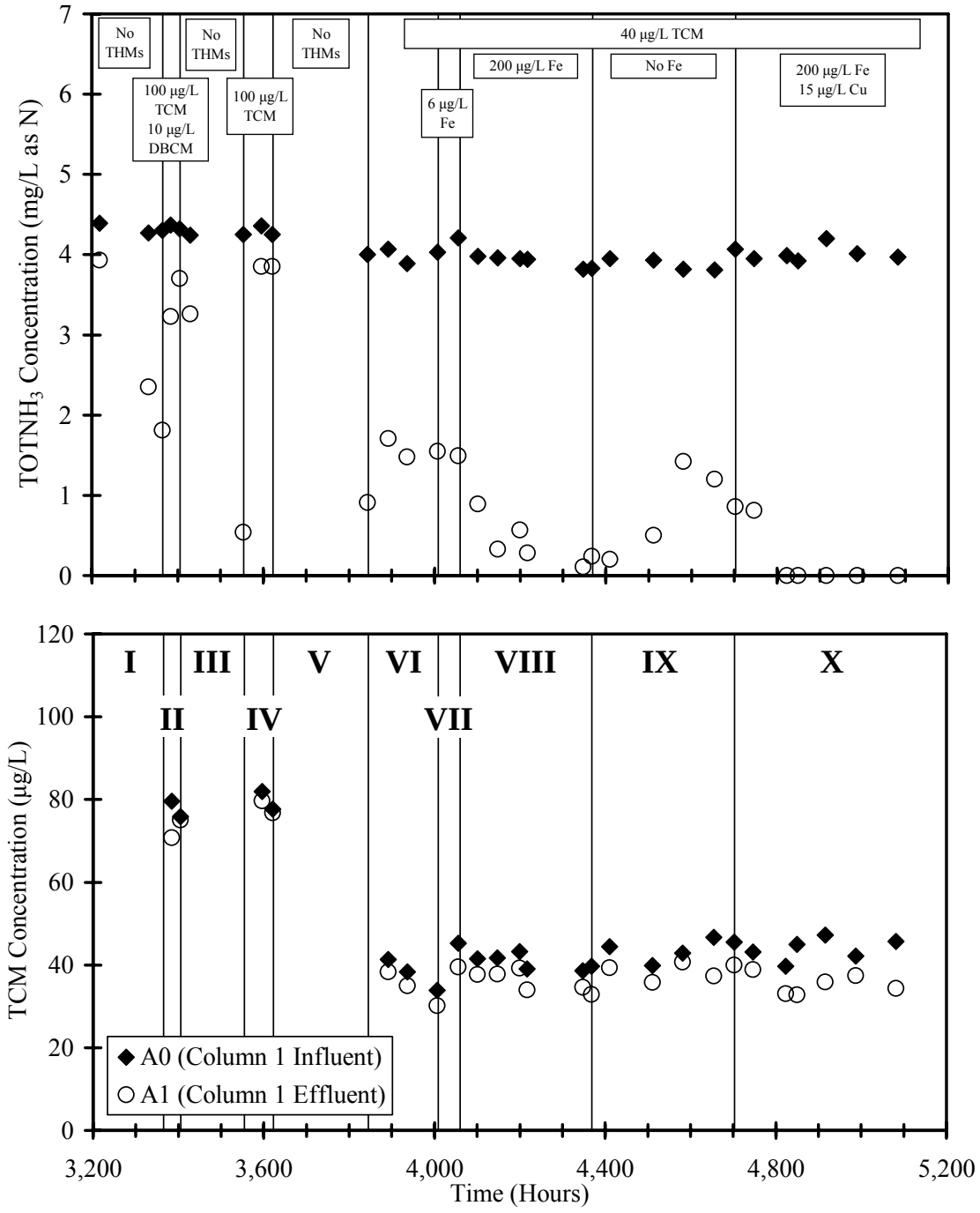

Figure 5.6 Lake Austin Biofilters Run 3 Train A $TOTNH_3$ and TCM concentrations fed Lake Austin water

Based on successful operation during Run 2 (Periods III and VI) for similar influent concentrations and $TOTNH_3$ removal (Table 5.7), it was surprising that the biofilters were proceeding to process failure (i.e., loss of nitrification) during Periods II and IV, although the C_{si} (Table 5.3) did predict problems with product toxicity for these influent THM concentrations. After recovery of $TOTNH_3$ degradation and the subsequent addition of 40 μg/L TCM (Period VI), only Train C achieved total $TOTNH_3$ removal through the first biofilter in series. This performance differed from Run 2 where, for the same TCM concentration, total $TOTNH_3$ removal occurred in the first biofilter in series for all trains. In addition, the removal of TCM was significantly less than that of the comparable operation for Run 2 for all three trains. Trains A and B seemed to stabilize at a decreased $TOTNH_3$ degradation rather than continuing to show a decline in $TOTNH_3$ degradation over time, similar to Run 2 (Period VII) for Train A. In contrast to Run 2 (Period VII), the C_{si} values during Run 3 (Period VI) were greater than one, indicating that process failure was not the cause of the decreased removals.

A hypothesis to account for the decreased $TOTNH_3$ degradation was that one or more micronutrients were limiting as compared with the nutrient water. Because the enzyme responsible for ammonia oxidation, ammonia monooxygenase (AMO), is proposed to contain iron and copper (Arp and Stein 2003) and calcium and magnesium are present at greater concentrations in Lake Austin water than nutrient water, the addition of iron and copper was investigated. To test this hypothesis, iron addition was started initially (Period VII) at the concentration used in the nutrient water (6 μg/L) and was later increased (200 μg/L) to ensure that adequate iron was available (Period VIII).

Once iron addition commenced, $TOTNH_3$ degradation improved in Trains A and B, with Train A obtaining nearly complete $TOTNH_3$ degradation through the first biofilter in series by the end of Period VIII. To provide further evidence that iron was

limiting, the iron feed was stopped (Period IX). As a result, $TOTNH_3$ degradation for Train A decreased, but no change was seen for Trains B and C. Because the previous iron addition did not result in complete $TOTNH_3$ degradation for Train A, copper addition (15 μg/L) was started as well (Period X). Upon the addition of iron and copper, all three trains completely degraded $TOTNH_3$ through the first biofilter in series, as they had when fed nutrient water, thus providing a strong indication that the hypothesis about micronutrient limitation was correct.

TCM degradation was variable during Run 3 until iron and copper addition commenced during Period X; Table 5.8 provides a summary of average measurements taken over Period X along with their associated standard deviations. As with Runs 1 and 2, once $TOTNH_3$ removal was complete, essentially no further TCM removal occurred; therefore, values for the first biofilter only were used in calculations for both $TOTNH_3$ and TCM removals. The general trends observed in Runs 1 and 2 are evident in Table 5.8. The S_{THM_n}/S_{THM_0} values for TCM again showed that increased $TOTNH_3$ degradation corresponded to increased THM degradation, as Train A had a significantly greater THM removal than Train C. Thus, the close association between $TOTNH_3$ degradation and THM cometabolism observed in the batch kinetic and previous biofilter runs held in Run 3. Comparing S_{THM_n}/S_{THM_0} values to comparable influent TCM concentrations during Run 2 (Period I, Table 5.7), shows that performance during Run 3 was significantly less for all three trains, with TCM removal only 30 to 50% of that observed during Run 2. The decreased TCM removal suggests that another condition, possibly other micronutrients, was limiting in addition to iron and copper. Another explanation for the decreased removals is that selective pressure caused by the THM product toxicity was selecting for nitrifiers that degrade THMs less efficiently (i.e., decreased $k_{1_{THM}}/k_{TOTNH_3}$ ratios).

Table 5.8 Lake Austin Biofilters Run 3 (Period X) summary (1st biofilter in series) and calculated $k_{1_{TCM}}/k_{TOTNH_3}$ ratio

Train	No. of Samples	$\Delta_{0\text{-}1}TOTNH_3$ (mg N/L)	S_{TCM_0} (µg/L)	$\frac{S_{TCM_1}}{S_{TCM_0}}$	$\frac{k_{1_{TCM}}}{k_{TOTNH_3}}$ (L/mg $TOTNH_3$)
A	5	4.0±0.11	44±3.0	0.79±0.067	0.066±0.015
B	6	2.0±0.034	44±2.7	0.89±0.070	0.074±0.026
C	6	1.0±0.032	44±2.7	0.95±0.049	0.067±0.048

S_{TCM_0} = Influent TCM concentration to first biofilter in series (µg/L)

S_{TCM_1} = Effluent TCM concentration from first biofilter in series (µg/L)

$\Delta_{0\text{-}1}TOTNH_3$ = $TOTNH_3$ removed through the first biofilter in series (mg N/L)

5.4.5. Run 4

In Run 4, the feed setup was modified to allow monochloramine (NH_2Cl) addition to the Lake Austin water feed. Figure 5.7 details the $TOTNH_3$, NH_2Cl, and TCM concentrations during Run 4 for Train A. A series of stepped increases in the influent monochloramine concentration was introduced to evaluate the effect of monochloramine on $TOTNH_3$ and TCM degradation. For the period of no monochloramine addition (Period I), Train A did not achieve complete $TOTNH_3$ removal through the first biofilter in series; therefore, analyses for all three trains were conducted based on performance through both biofilters in series. TCM degradation was not significantly different from Run 3 for each train during Period I (Table 5.8 and Table 5.9). For NH_2Cl additions of 0.5 and 1.0 mg/L as Cl_2 (Periods II and III), the $TOTNH_3$ degradation for each train was not significantly different from that in Period I.

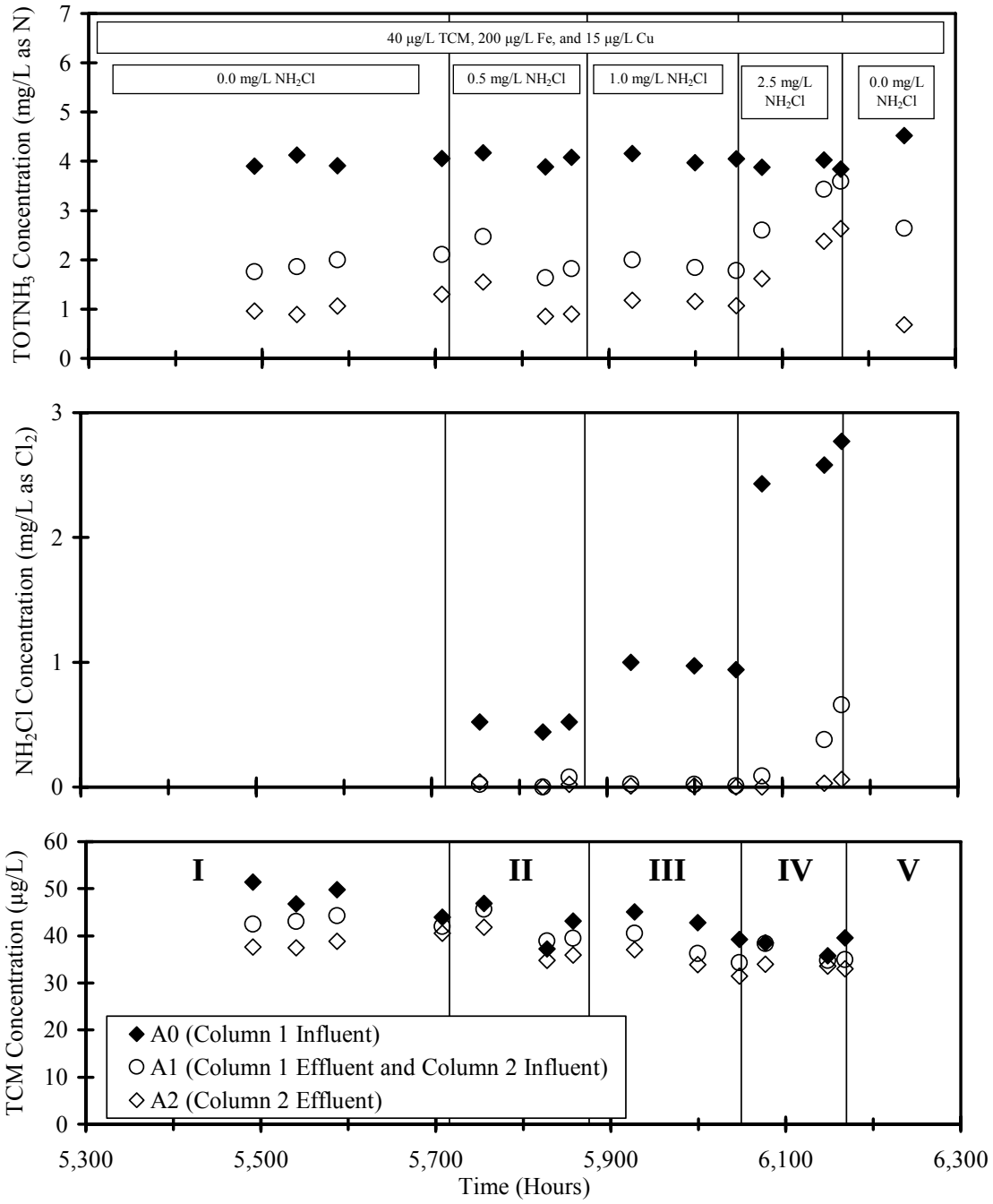

Figure 5.7 Lake Austin Biofilters Run 4 Train A $TOTNH_3$, NH_2Cl, and TCM concentrations fed Lake Austin water

Once NH_2Cl addition began at 0.5 mg/L as Cl_2 (Period II), TCM degradation decreased, but not significantly, in all three trains. During Period III, TCM degradation returned to its previous level from Period I even though the influent NH_2Cl concentration was increased to approximately 1.0 mg/L as Cl_2 (Table 5.9). Once the NH_2Cl influent was increased to 2.5 mg/L as Cl_2 (Period IV), $TOTNH_3$ degradation decreased significantly in all three trains, reaching essentially zero for Trains B and C at the end of the sampling period. The TCM degradation likewise decreased in accordance with the decrease in $TOTNH_3$ degradation. During Period IV, Train A maintained a minimal amount of $TOTNH_3$ degradation, but it steadily decreased over time. As a result, NH_2Cl addition was stopped, and one data point was taken to see if the trains showed signs of re-establishing $TOTNH_3$ degradation (Period V). Train A showed an increased $TOTNH_3$ degradation, while Trains B and C showed a minimal, yet measurable, improvement in $TOTNH_3$ degradation.

Overall, the results from Run 4 showed that monochloramine concentrations would impair stable process operation with respect to TCM or $TOTNH_3$ removal at an influent concentration somewhere between 1 and 2.5 mg/L as Cl_2. Nitrification in drinking water systems has been reported at these monochloramine concentrations (Cunliffe 1991). The precise monochloramine concentration is likely site specific and perhaps dependent on operating conditions (e.g., the allowable monochloramine concentration might increase as the influent $TOTNH_3$ concentration increases).

Table 5.9 Lake Austin Biofilters Run 4 Train A performance summary and calculated $k_{1_{TCM}}/k_{TOTNH_3}$ ratio along with the associated standard deviations

Period	No. of Samples	$TOTNH_3$ (mg N/L)		NH_2Cl (mg Cl_2/L)		TCM		
		Influent	Δ_{Total}	Influent	Δ_{Total}	S_{TCM_0} (µg/L)	$\frac{S_{TCM_2}}{S_{TCM_0}}$	$\frac{k_{1_{TCM}}}{k_{TOTNH_3}}$ [a]
I	4	4.0±0.11	2.9±0.21			48±3.3	0.81±0.081	0.073±0.033
II	3	4.0±0.14	2.9±0.29	0.49±0.046	0.47±0.031	42±4.9	0.89±0.051	0.041±0.018
III	3	4.1±0.10	2.9±0.092	0.97±0.030	0.96±0.025	42±2.9	0.81±0.015	0.074±0.082
IV	3	3.9±0.10	1.7±0.053	2.6±0.17	2.6±0.14	38±2.0	0.89±0.052	0.081±0.059

Δ_{Total} = Total change across both biofilters in series

S_{THM_0} = Influent TCM concentration to first biofilter in series (µg/L)

S_{THM_2} = Effluent TCM concentration from second biofilter in series (µg/L)

[a] L/mg $TOTNH_3$

A possible confounding factor in Run 4 was the formation of other disinfection by-products (DBPs) once monochloramine addition commenced and the likelihood that the biofilm required time to adjust to these new DBPs. The influent and effluent chromatograms for the first biofilter in Train A showed additional peaks once monochloramine addition commenced for the 2.5 mg/L as Cl_2 influent monochloramine condition (Figure 5.8 and Figure 5.9). The effluent chromatogram from this biofilter clearly showed a decrease in the number of additional peaks, indicating removal of these compounds in the biofilter (Figure 5.9). For lower influent monochloramine values (0.5 and 1 mg/L as Cl_2), the influent to the trains did not show additional peaks while the effluents from both biofilters in series for all trains showed additional peaks. Thus, DBPs seemed to have formed from the addition of monochloramine, with subsequent removal

in the biofilm. The possibility that the biofilm required time to adjust to these new DBPs offers one explanation for the experimental results seen in Run 4: (1) an initial removal of TCM in Period I, (2) the lack of TCM removal during Period II, and (3) the subsequent re-establishment of TCM removal during Period III to a similar level to Period I.

The monochloramine removal observed through the biofilters resulted from some combination of (1) the natural monochloramine demand of the Lake Austin water, (2) reaction of monochloramine with the biomass present in the biofilter, and (3) cometabolism of monochloramine in a manner similar to that for THM cometabolism (Woolschlager et al. 2001; Woolschlager 2000). The natural demand of the water would be similar for all biofilters. The reaction with biomass would be expected to increase with $TOTNH_3$ removal because a larger removal implies a larger biomass population. In a similar manner, if cometabolism of monochloramine was occurring, an increased $TOTNH_3$ removal would be expected to correspond with an increased monochloramine removal in an analogous manner to Equation 4.1 for THM cometabolism. The results for all three trains showed that an increase in $TOTNH_3$ removal corresponded with an increase in monochloramine removal; therefore, reaction of monochloramine with biomass, cometabolism of monochloramine, or both were likely occurring.

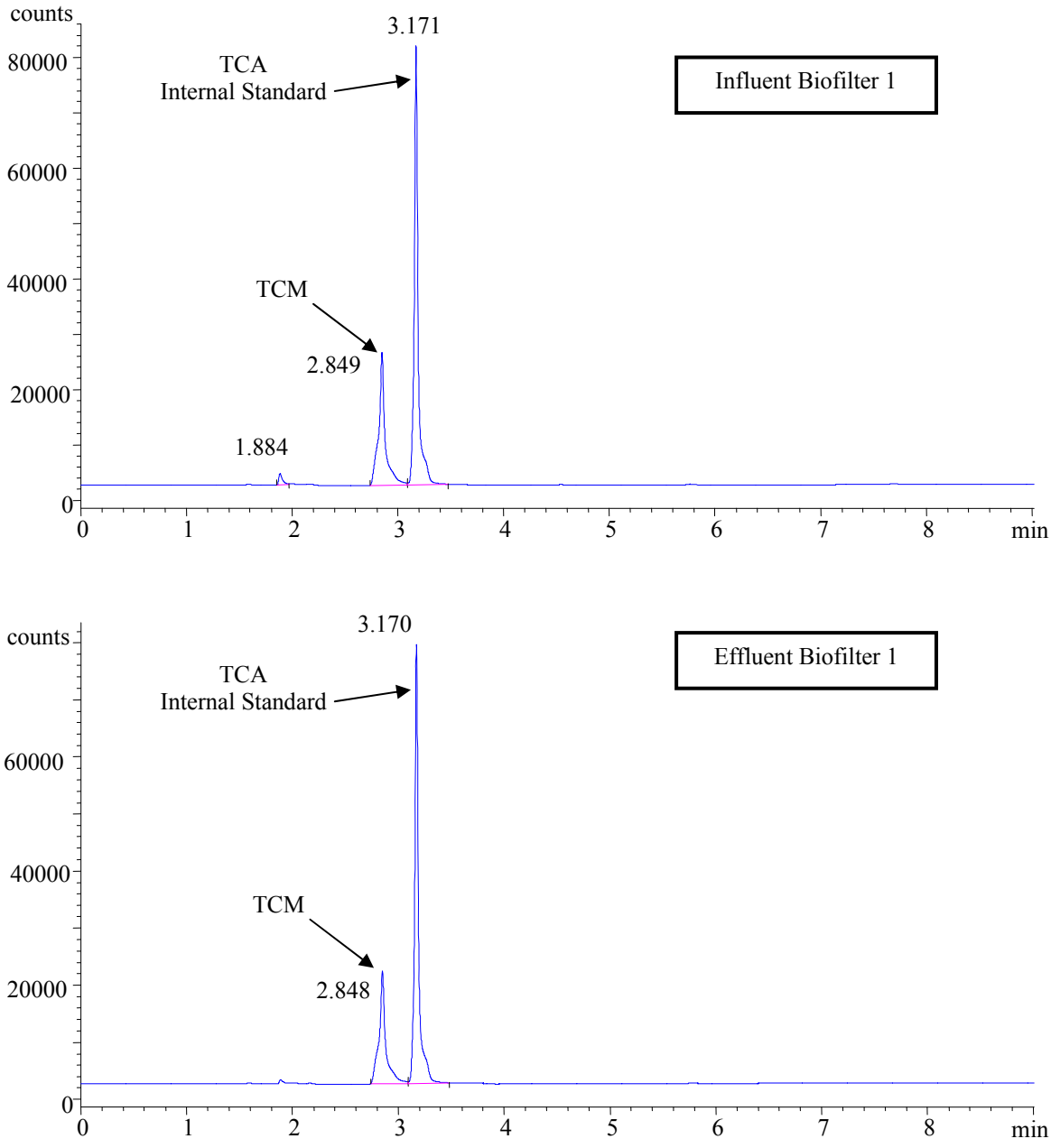

Figure 5.8 Lake Austin Biofilters Run 4 Train A biofilter 1 chromatogram (0.0 mg/L NH_2Cl at 5,491 hours)

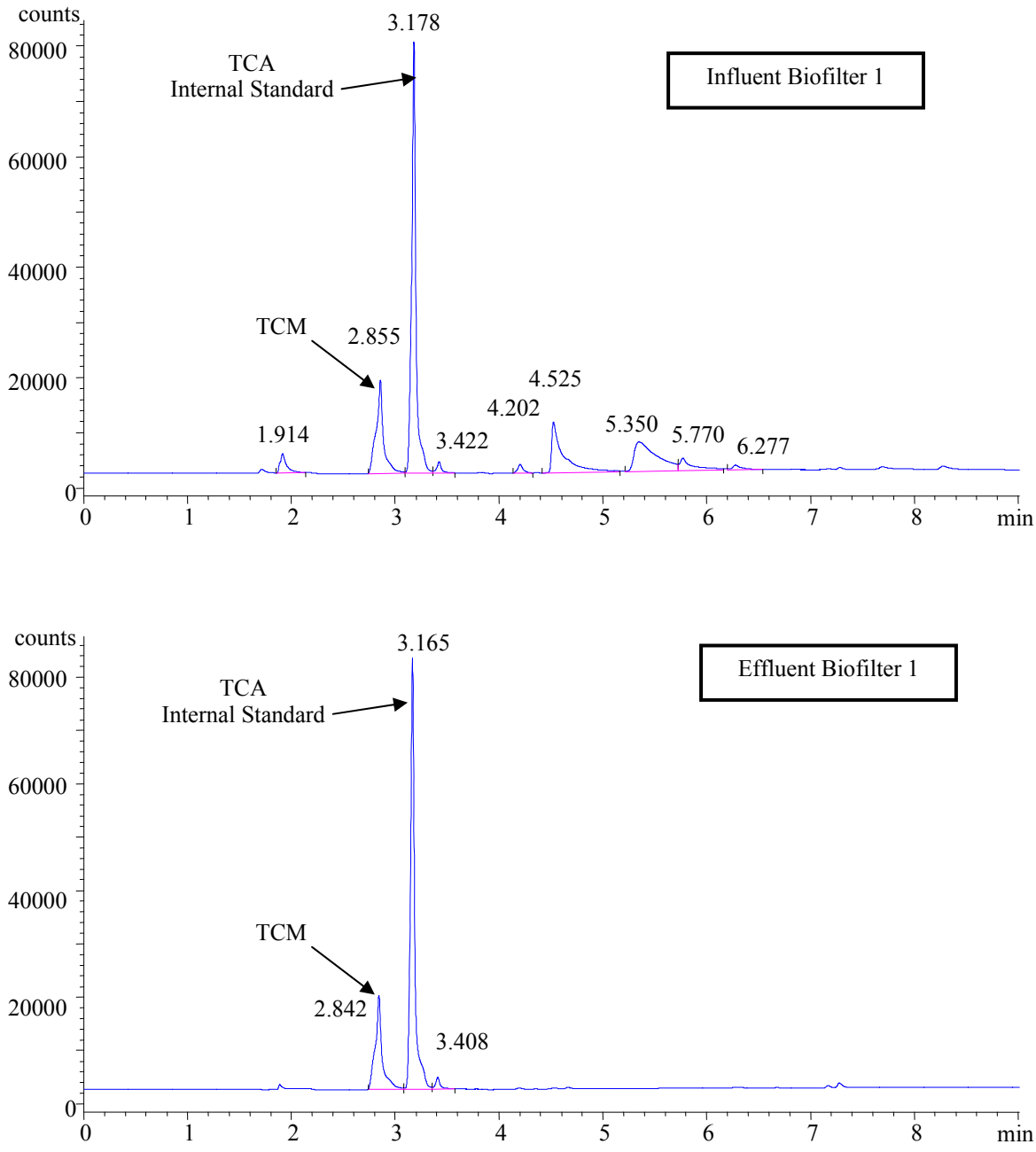

Figure 5.9 Lake Austin Biofilters Run 4 Train A biofilter 1 chromatogram (2.5 mg/L NH_2Cl at 6,148 hours)

5.4.6. Summary

THM and $TOTNH_3$ removal occurred in nitrifying biofilters seeded with a Lake Austin mixed culture. All four THMs were degraded with the THM degradation rate increasing with increasing bromine substitution. For similar $TOTNH_3$ degradation, no significant change in TCM degradation occurred whether DBCM was present and *vice versa*. This result matched observations from the batch kinetic studies that showed no enzyme competition among THMs at the concentrations typical of drinking water treatment. Increased $TOTNH_3$ degradation corresponded to increased THM degradation; thus, the close association between ammonia degradation and THM cometabolism observed in previous batch kinetic studies also held in the biofilter experiments. Overall, these experiments resulted in sustained THM removals ranging from 10 to 60% for various operating conditions.

THM speciation is important, because each THM exhibits a different product toxicity. The cometabolism stability index (C_{si}) represents a simple and useful tool for judging the likelihood of product toxicity problems in biofilter operation. Because both THM cometabolism rate constants and THM product toxicities increase with increasing THM bromine-substitution, a water's THM speciation will be an important consideration for process implementation. Even though a given water might be kinetically favored based on THM speciation, the resulting THM product toxicity might not allow stable treatment process performance.

Nutrient limitations can exist when using natural waters. To improve both $TOTNH_3$ and THM degradation, addition of both iron and copper was required with Lake Austin water. Other, unknown nutrients also might have been lacking, as overall performance was less than that observed when nutrient water was fed to the same biofilters. Another explanation for the decreased performance is that selective pressures

were selecting for nitrifiers that degrade THMs less efficiently (i.e., a decreased $k_{1_{THM}}/k_{TOTNH_3}$ ratio).

An influent monochloramine concentration of 1 mg/L as Cl_2 (or less) seems a good target for stable operation of a developed biofilm. Because monochloramine addition was initiated after biofilm development, startup considerations could not be evaluated from these data and require further investigation. During the experiment, a relatively large increase in the influent monochloramine concentration was made from approximately 1 mg/L to 2.5 mg/L as Cl_2. The influent monochloramine concentration of 2.5 mg/L as Cl_2 led to unstable operation; thus, further examination of concentrations between 1 mg/L and 2.5 mg/L as Cl_2 is needed. As a result, the actual allowable influent monochloramine concentration lies between 1 and 2.5 mg/L as Cl_2, with the use of 1 mg/L as Cl_2 being conservative. Based on the work of Fairey et al. (2004; 2006; Submitted for Review), this level of monochloramine reduction (to less than 1 mg/L as Cl_2) is achievable in GAC beds. As a result, further monochloramine research was not conducted as this research focused future efforts on addressing the reduced THM performance that occurred during Runs 3 and 4.

5.5. MIXED CULTURE BIOFILTERS 1

To extend the biofilter experiments to additional mixed cultures fed Lake Austin water, a set of three biofilters were seeded with three different mixed culture sources: (1) Rio Grande mixed culture seeded on anthracite (Train A), (2) *N. oligotropha* enrichment culture seeded on anthracite (Train B), and (3) granular activated carbon (GAC) taken from an in-service filter at the City of Laredo drinking water treatment plant (Train C). This experiment provided data to draw comparisons with the Lake Austin Biofilters from the two other mixed cultures (*N. oligotropha* enrichment and Rio Grande) studied previously in batch (Wahman et al. 2006). In addition, this experiment allowed further

exploration of the reduced performance seen when biofilters were operated with Lake Austin feed water (Lake Austin Biofilters Runs 3 and 4). The inclusion of a biofilter with GAC from the City of Laredo drinking water treatment plant provided insight into cultures likely seen in practice as this treatment plant is operated in the proposed process configuration (i.e., a plant using monochloramine for disinfection preceding a GAC filter).

Once seeded, these biofilters were operated on the secondary setup and fed nutrient water for approximately 22 days followed by Lake Austin water for 217 days while the Lake Austin Biofilters were in operation on the primary column setup. After this initial period on the secondary setup, these biofilters were moved to the primary column setup to initiate experiments. For ease of presentation, this experiment is broken into three runs and will be referred to collectively as the Mixed Culture Biofilters 1 (MCB1). In Run 1 and Run 2 (Period I), the biofilters were fed Lake Austin water. For Run 2 (Period II) and Run 3, the feed water was switched to nutrient water. Experiments were conducted with three parallel trains (A, B, and C) each consisting of two biofilters in series. The nominal influent ammonia concentration for all trains was the same for each operating condition with other biofilter setup and scaling information summarized in Table 5.1.

5.5.1. Run 1

Run 1 consisted of an initial operating period to establish nitrification (Period I), explored TCM product toxicity and recovery (Periods II and III), and attempted to address issues of decreased TCM removal by phosphorus addition (Period IV). Based on the previous work with the Lake Austin Biofilters fed Lake Austin water, iron and copper were also added during Run 1 as these were shown to improve performance on Lake

Austin water. Figure 5.10, Figure 5.11, and Figure 5.12 detail the $TOTNH_3$ and TCM concentrations for the three trains during Run 1, respectively.

During Run 1, an initial period (Period I) was provided for the biofilters to reach a seeming steady-state removal of $TOTNH_3$ without the presence of THMs. Trains A and B stabilized with an approximate 3 mg N/L $TOTNH_3$ removal through the first biofilter in series. During this same timeframe, Train C showed complete $TOTNH_3$ removal through the first biofilter in series, indicating the presence of a greater and/or more active biomass as compared with Trains A and B.

To simulate a C_{si} value close to one (1.1), an initial addition of 75 μg/L TCM (Period II) was started. This addition resulted in an immediate loss in $TOTNH_3$ removal for both Trains A and B, reducing their $TOTNH_3$ removal from 3 mg N/L to 0.7 and 0.3 mg N/L, respectively. After this sharp initial decrease in $TOTNH_3$ removal, Train A's $TOTNH_3$ removal improved and was followed by Train B at a slower rate. Contrastingly, Train C showed a minimal effluent $TOTNH_3$ concentration (0.5 mg N/L) after the initial TCM addition with subsequent samples showing complete $TOTNH_3$ removal. Train C contained GAC media; therefore, adsorption of TCM might have protected a portion of the biomass from the toxic effects of TCM cometabolism.

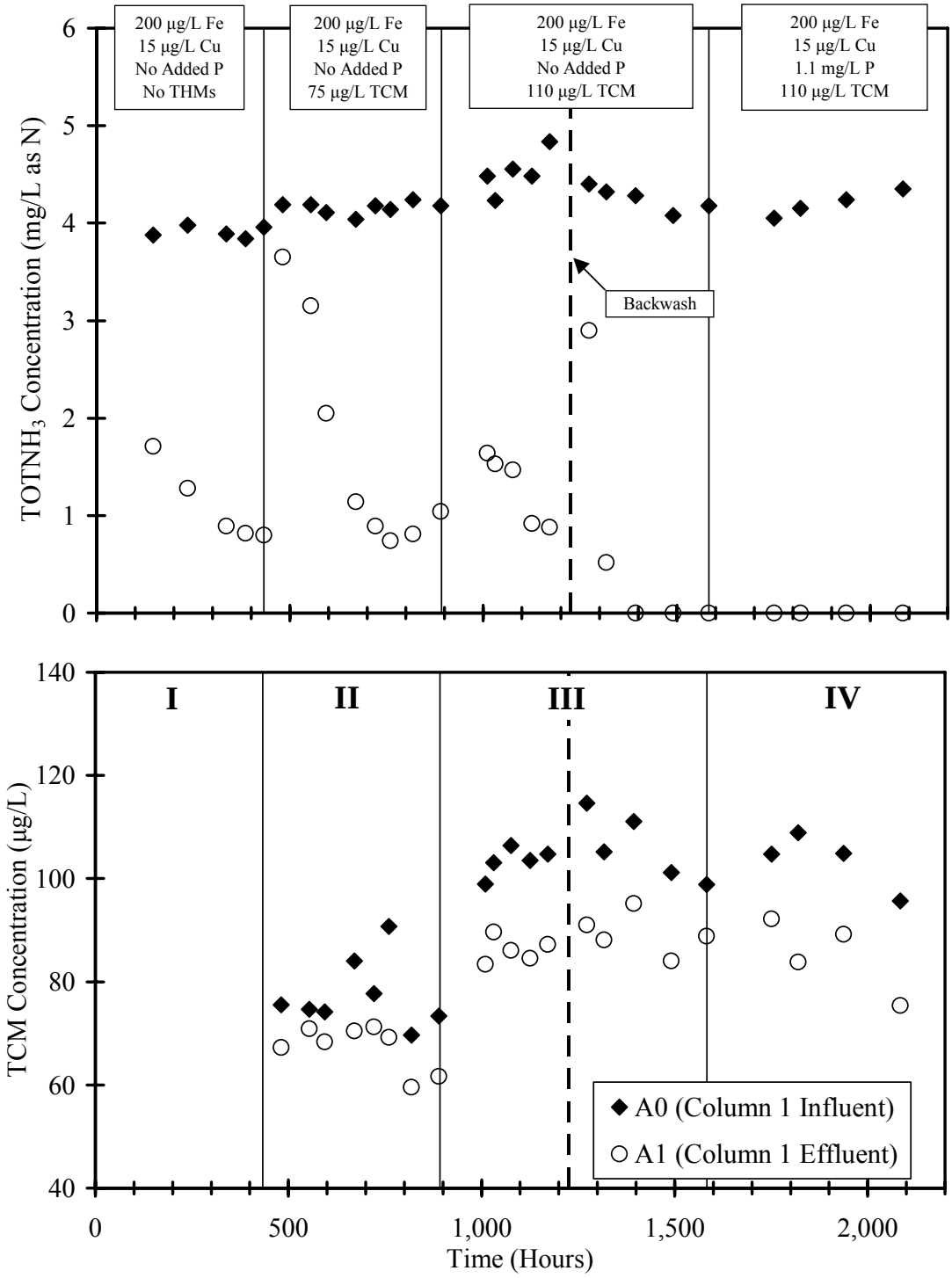

Figure 5.10 Mixed Culture Biofilters 1 Run 1 Train A (Rio Grande mixed culture) $TOTNH_3$ and TCM concentrations fed Lake Austin water

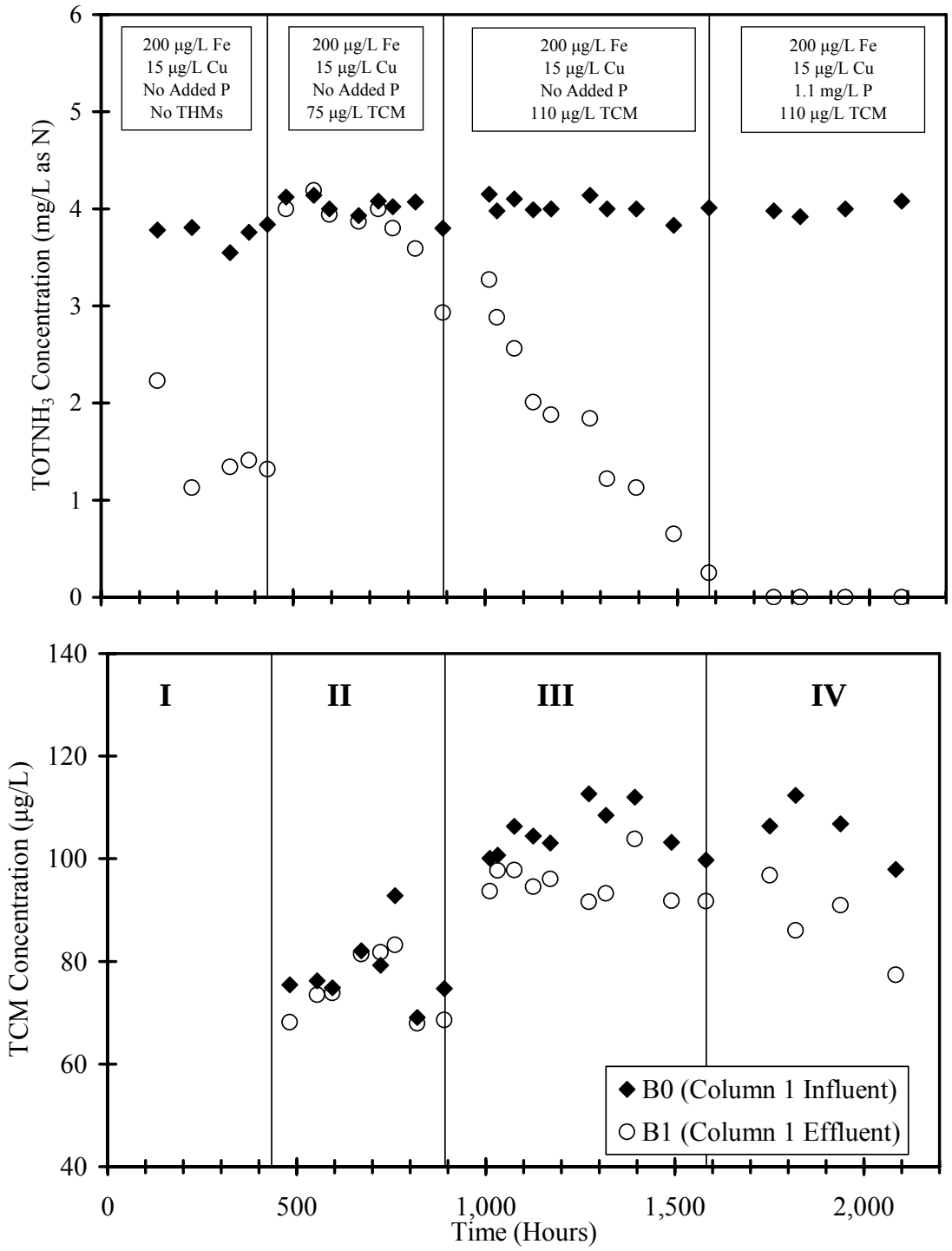

Figure 5.11 Mixed Culture Biofilters 1 Run 1 Train B (*N. oligotropha* enrichment culture) $TOTNH_3$ and TCM concentrations fed Lake Austin water

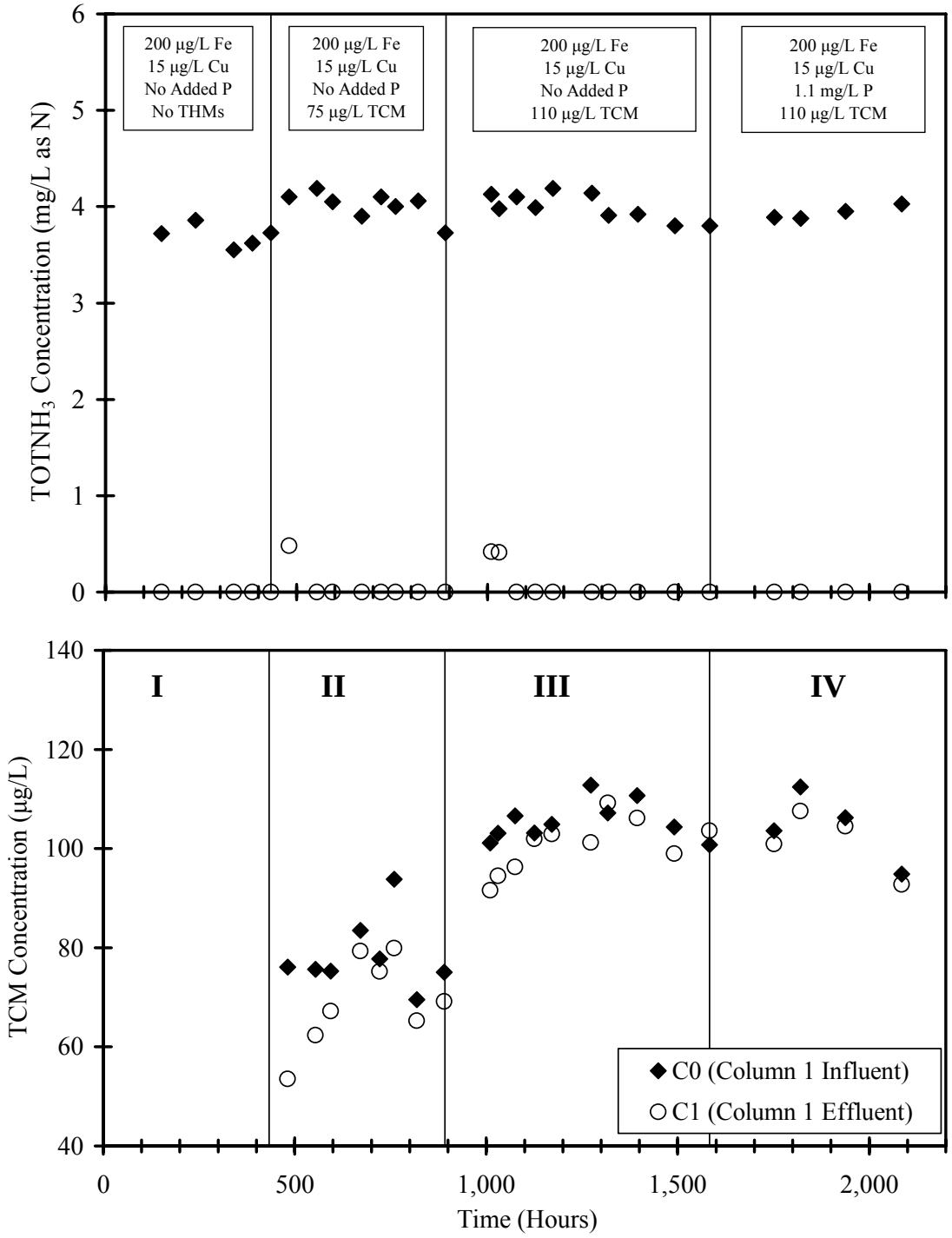

Figure 5.12 Mixed Culture Biofilters 1 Run 1 Train C (Rio Grande GAC) $TOTNH_3$ and TCM concentrations fed Lake Austin water

Because the trains showed improved $TOTNH_3$ removal after their initial decrease during Period II, the influent TCM concentration was increased to 110 µg/L (Period III) to decrease the C_{si} value (0.76) and evaluate whether recovery would continue. After showing an initial decrease in $TOTNH_3$ removal upon the increased TCM concentration, all three trains moved toward complete $TOTNH_3$ removal during Period III with only Train B having a minimal $TOTNH_3$ effluent concentration (0.25 mg N/L) at the end of Period III. Even with this $TOTNH_3$ removal in all three trains, TCM removal was variable and less than that seen with the Lake Austin Biofilters on nutrient water and similar, but less than, when fed Lake Austin water for comparable $TOTNH_3$ removals. TCM removal for Trains A and B ranged from 10-21% (10-24 µg TCM/L) and 3-19% (3-21 µg TCM/L), respectively. Train C's TCM removal declined from initial removals of 8-10% (9-10 µg TCM/L) to final removals of 0-5% (0-5 µg TCM/L) at the end of Period III. Train C's initial TCM removal was most likely a result of GAC adsorption of TCM.

Train A and B's recovery rates from TCM addition (Periods II and III) were different. Compared with Train A, Train B took approximately 800 more hours to reach complete $TOTNH_3$ removal. For Trains A and B, the recovery pattern was approximately linear with $TOTNH_3$ removal through the first biofilter in series (Figure 5.13). It is clear from this that Train B approached complete $TOTNH_3$ removal significantly more slowly (95% CL of 0.0043 ± 0.00046 mg N/L-hour) as compared with Train A (95% CL 0.012 ± 0.0040 mg N/L-hour), indicating a different response to the initial TCM addition. Train B's recovery rate was only 35% that of Train A. Based on the C_{si} concept, Train B likely possessed a biomass with either a decreased yield, k_{TOTNH_3}, or transformation capacity or an increased $k_{1_{THM}}$ or $K_{s_{NH_3\text{-}N}}$.

As a result of the decreased TCM removal seen during Periods II and III, phosphorus was added at the nutrient water feed concentration (1.1 mg P/L) to evaluate

its effect on TCM removal (Period IV). Phosphorus represents the only nutrient not studied during the Lake Austin Biofilters that was present in the nutrient water and might be limiting in the Lake Austin water. Lake Austin water's average total phosphate concentration ranged from 0.01-0.05 mg/L as P during 2004 and 2005 (City of Austin Water Utility n.d.). During Period IV, $TOTNH_3$ removal remained complete for each train. For Trains A and B, TCM removal was variable but similar to the periods without phosphorus addition, ranging from 10-25% (10-26 µg TCM/L). For Train C, the TCM removal remained minimal at 2-4% (3-5 µg TCM/L), indicating little effect from the phosphorus addition on any of the trains.

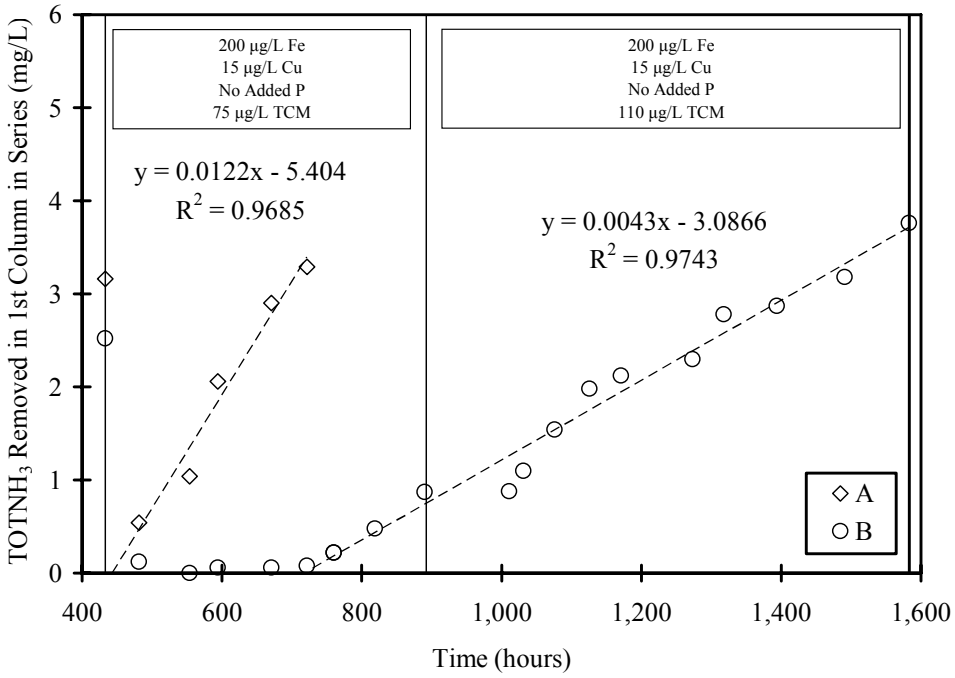

Figure 5.13 Mixed Culture Biofilters 1 Trains A (Rio Grande mixed culture) and B (*N. oligotropha* enrichment culture) recovery from initial TCM addition during Run 1

5.5.2. Run 2

For Run 2 (Figure 5.14, Figure 5.15, and Figure 5.16), the influent $TOTNH_3$ concentration was decreased from 4 to 2 mg N/L to verify that enzyme competition was not occurring because of the $TOTNH_3$ concentrations present in the biofilters. In addition, the EBCT was decreased from 4 to 2 minutes, with the goal of achieving a measurable steady-state effluent $TOTNH_3$ concentration from the first biofilter in series for mathematical modeling purposes. In an attempt to improve TCM removal during Run 2, the feed water was changed from Lake Austin (Period I) to nutrient water (Period II) as better performance with respect to TCM removal was seen with a nutrient water feed for the Lake Austin Biofilters.

During Period I, $TOTNH_3$ removal remained complete through the first biofilter in series for all three trains. Trains A and B showed a decrease in TCM removal as compared with Run 1 (Period IV) with average TCM removals decreasing from 18 to 11% and 17 to 8% for Trains A and B, respectively. This reduction in TCM removal coincided with previous results in which a decrease in $TOTNH_3$ removed (2 mg N/L versus 4 mg N/L) corresponded to a decreased THM removal. For Train C, TCM removal remained minimal, averaging 5%. The switch to nutrient water (Period II) resulted in little change in $TOTNH_3$ or TCM removal for any train. Overall, Run 2 provided evidence that the reduced TCM removal was not a result of competition with $TOTNH_3$ or source water feed and nutrient additions.

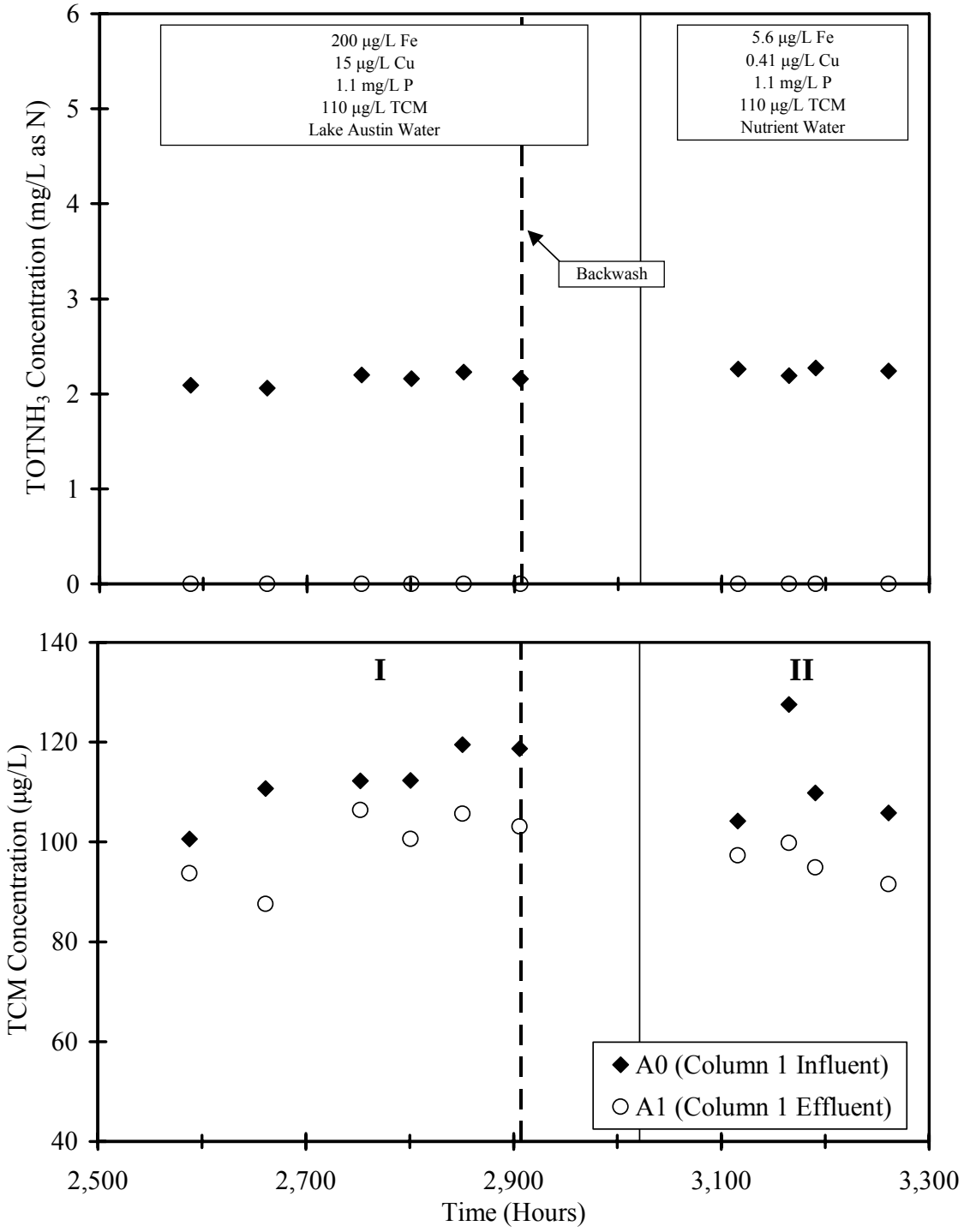

Figure 5.14 Mixed Culture Biofilters 1 Run 2 Train A (Rio Grande mixed culture) $TOTNH_3$ and TCM concentrations fed Lake Austin and nutrient waters

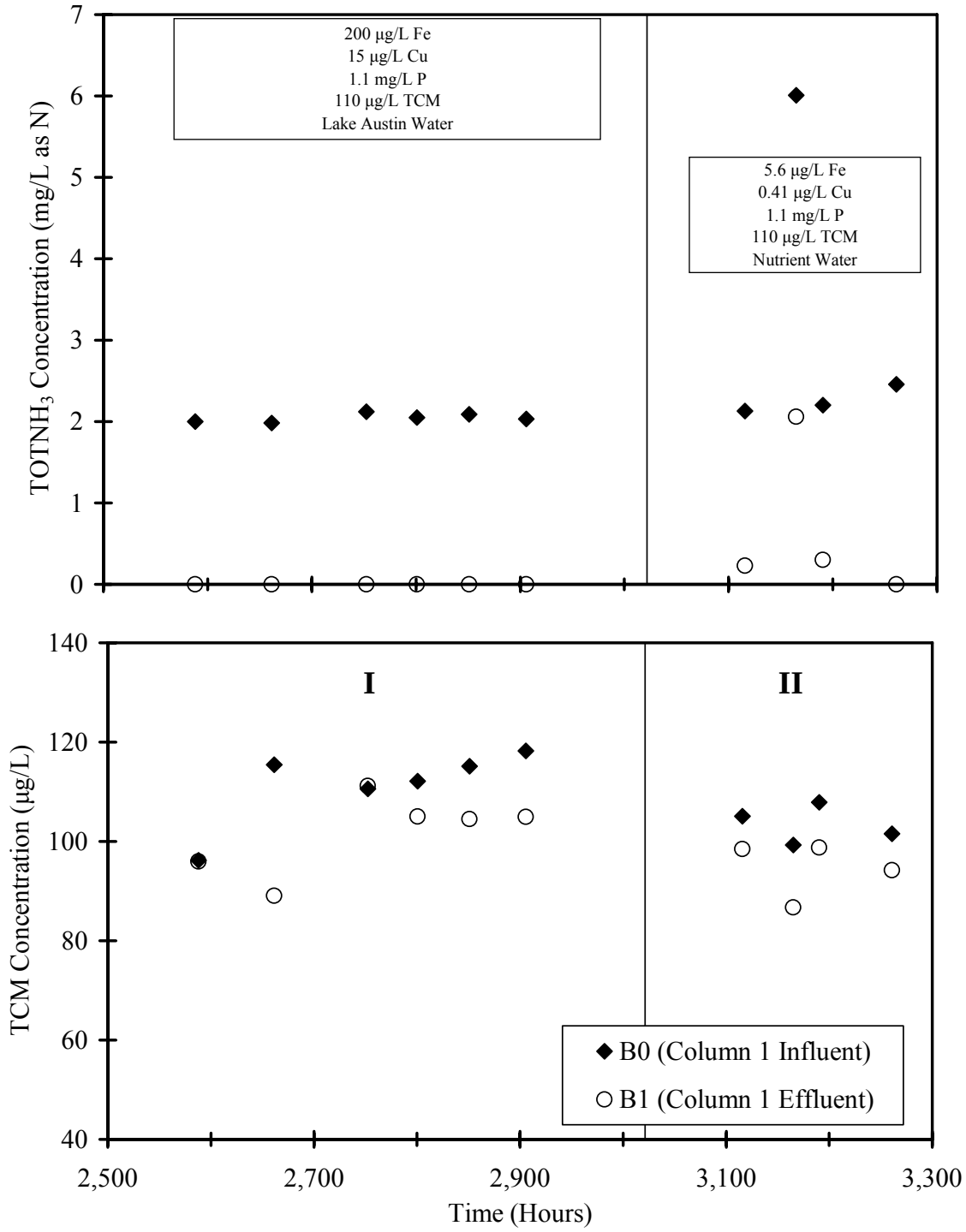

Figure 5.15 Mixed Culture Biofilters 1 Run 2 Train B (*N. oligotropha* enrichment culture) $TOTNH_3$ and TCM concentrations fed Lake Austin and nutrient waters

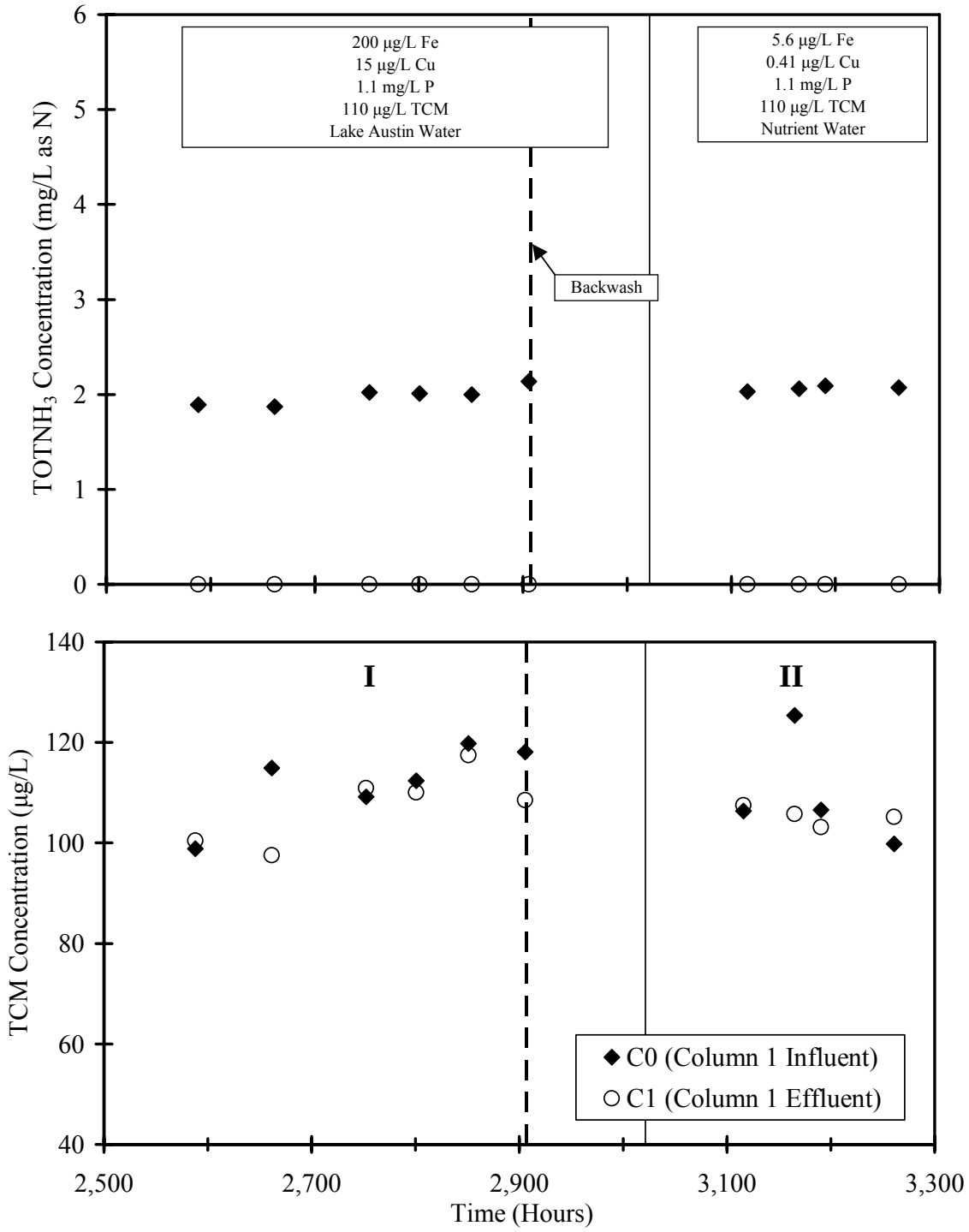

Figure 5.16 Mixed Culture Biofilters 1 Run 2 Train C (Rio Grande GAC) $TOTNH_3$ and TCM concentrations fed Lake Austin and nutrient waters

5.5.3. Run 3

To evaluate if the removal of a bromine-substituted THM would also show reduced removals similar to TCM, DBCM was added to the influent at 25 μg/L and the TCM influent was reduced to 100 μg/L to simulate the final influent conditions of the Lake Austin Biofilters fed nutrient water (LAB Run 2, Period VII). In addition, these THM feed concentrations decreased the C_{si} from Run 2 (0.76 to 0.49), evaluating whether biofilter operation continued at this decreased C_{si}. Figure 5.17, Figure 5.18, and Figure 5.19 detail the $TOTNH_3$, TCM, and DBCM concentrations for each train during Run 3, respectively.

After an initial period (Period I) of TCM and $TOTNH_3$ addition, DBCM was added to the influent (Period II). Even with the decreased C_{si}, DBCM addition did not lead to a decreased $TOTNH_3$ removal in any train as complete removal of $TOTNH_3$ was occurring after the first biofilter in series. Train A showed a substantial DBCM removal of 44-61% (9-14 μg DBCM/L) while showing a reduced TCM removal of 0-11% (0-11 μg TCM/L) compared with periods of no DBCM addition (Run 2 (Period II) and Run 3 (Period I)) in which the TCM removals ranged from 7-22% (7-28 μg TCM/L). Compared with Train A, Train B showed a decreased DBCM removal of 1-22% (0-5 μg DBCM/L) and a similar TCM removal of 0-18% (0-19 μg TCM/L) with no observable reduction in TCM removal when DBCM was added. Train C showed no TCM removal upon the addition of DBCM, and effluent TCM concentrations increased through the first biofilter in series, indicating that competitive adsorption was occurring between TCM and DBCM. During this time, Train C's DBCM removal was 39-56% (8-13 μg DBCM/L).

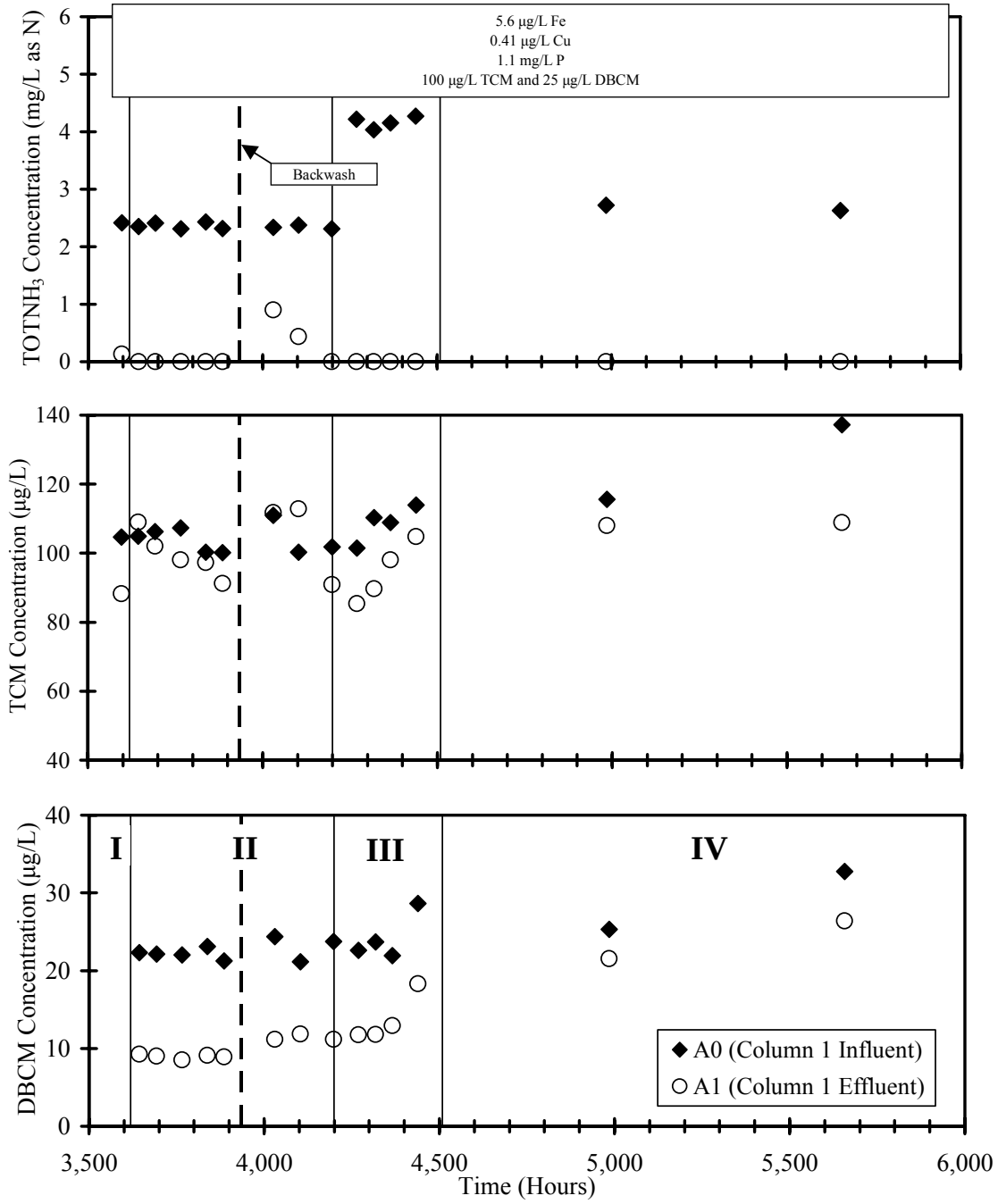

Figure 5.17 Mixed Culture Biofilters 1 Run 3 Train A (Rio Grande mixed culture) $TOTNH_3$, TCM, and DBCM concentrations fed nutrient water

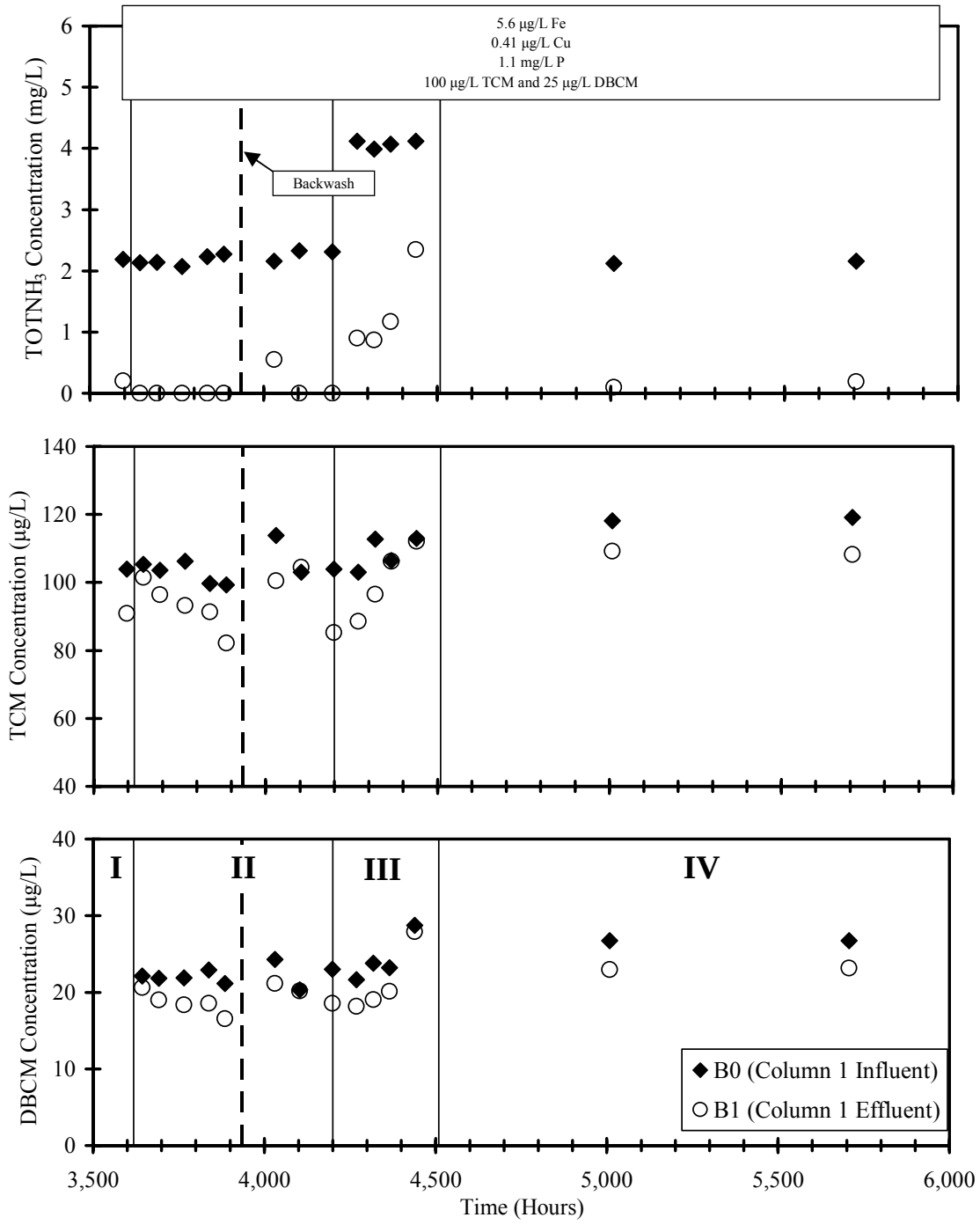

Figure 5.18 Mixed Culture Biofilters 1 Run 3 Train B (*N. oligotropha* enrichment culture) $TOTNH_3$, TCM, and DBCM concentrations fed nutrient water

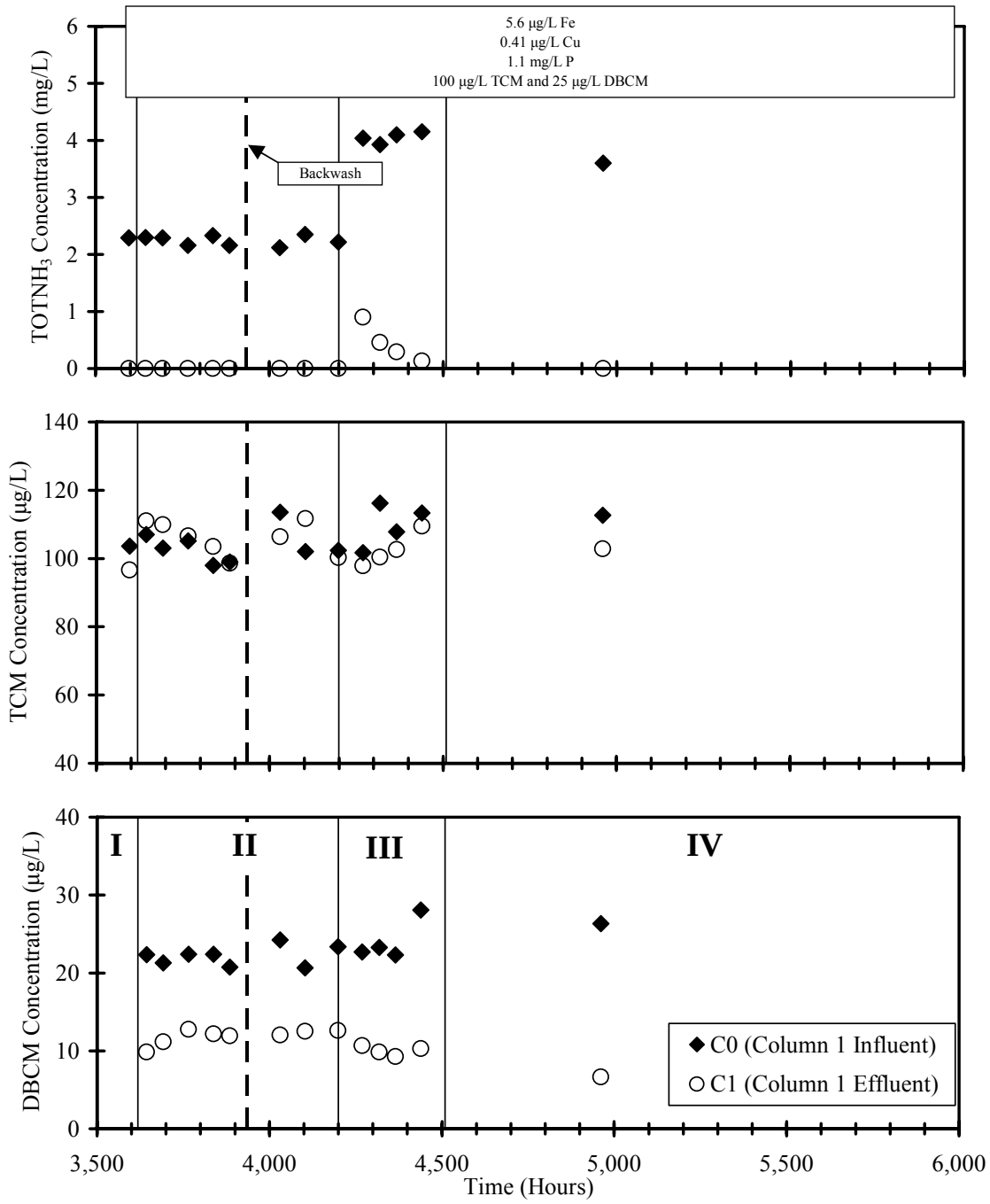

Figure 5.19 Mixed Culture Biofilters 1 Run 3 Train C (Rio Grande GAC) $TOTNH_3$, TCM, and DBCM concentrations fed nutrient water

To evaluate the effect of an increased influent $TOTNH_3$ concentration with this THM speciation, the influent $TOTNH_3$ was increased from 2 to 4 mg/L $TOTNH_3$ (Period III). The $TOTNH_3$ removal for Train A remained complete with Train C moving towards complete removal. Train B approached process failure as $TOTNH_3$ removal decreased during this period, which is predicted from the C_{si} (0.49). This provided further evidence that Train B's slower recovery during Run 1 (Periods II and III) resulted from bacteria with kinetic parameters leading to a lower C_{si} than Train A.

Because of Train B's performance, the influent was reduced to 2 mg/L $TOTNH_3$ for the remainder of Run 3 (Period IV) for all biofilters. In addition, the trains were operated to generate biomass during Period IV for backwash batch kinetic tests to determine the kinetic parameters of the biofilter biomass. During this time, samples were taken only before backwashing the biofilter for the backwash batch kinetic tests. All trains showed similar TCM removals (approximately 10%) with various DBCM removals. During Period IV, Train A's DBCM removal declined to levels similar to Train B (17 and 14%, respectively), which maintained DBCM removal. Contrastingly, Train C showed a continual improvement in DBCM removal up to 75% at the end of its operation.

5.5.4. Run Comparisons

To evaluate the performance of the Mixed Culture Biofilters 1, average values were calculated for different operating conditions in which complete $TOTNH_3$ removal occurred through the first biofilter in series. Table 5.10 summarizes these average results for each train along with their associated standard deviations.

Table 5.10 Mixed Culture Biofilters 1 performance summary (first biofilter in series)

Train	Run	Period	No. of Samples	$\Delta_{0\text{-}1}TOTNH_3$ (mg N/L)	S_{TCM_0} (µg/L)	$\frac{S_{TCM_1}}{S_{TCM_0}}$	S_{DBCM_0} (µg/L)	$\frac{S_{DBCM_1}}{S_{DBCM_0}}$
A	1	III	3	4.2±0.10	104±6.5	0.86±0.034		
	1	IV	4	4.2±0.13	104±5.6	0.82±0.052		
	2	I	6	2.1±0.064	112±6.8	0.89±0.055		
	2	II	4	2.2±0.036	112±11	0.86±0.062		
	3	II	5	2.4±0.054	104±3.4	0.95±0.038	22±0.66	0.40±0.013
	3	III	4	4.2±0.10	109±5.2	0.87±0.050	24±3.0	0.56±0.065
	3	IV	2	2.7±0.069	126±15	0.86±0.10	29±5.3	0.83±0.031
B	1	IV	4	4.0±0.066	106±5.9	0.83±0.065		
	2	I	6	2.0±0.053	111±7.9	0.92±0.085		
	3	II	7	2.2±0.10	103±2.7	0.90±0.067	22±0.95	0.86±0.076
	3[a]	IV	2	2.0±0.036	119±0.67	0.92±0.011	27±0.030	0.86±0.052
C	1	II	7	4.0±0.15	79±7.8	0.91±0.053		
	1	III	8	4.0±0.15	106±3.9	0.96±0.041		
	1	IV	4	3.9±0.069	104±7.3	0.97±0.011		
	2	I	6	2.0±0.10	112±7.6	0.95±0.060		
	2	II	4	2.1±0.025	110±11	0.95±0.074		
	3	II	8	2.2±0.088	104±4.9	0.99±0.022	22±1.3	0.54±0.051
	3[a]	III	4	3.6±0.39	110±6.4	0.94±0.048	24±2.7	0.42±0.043
	3	IV	1	3.6	113	0.91	26	0.25

[a]Complete $TOTNH_3$ removal not occurring

S_{TCM_0}, S_{DBCM_0} = Influent TCM and DBCM concentration to first biofilter in series (µg/L)

S_{TCM_1}, S_{DBCM_1} = Effluent TCM and DBCM concentrations from first biofilter in series (µg/L)

$\Delta_{0\text{-}1}TOTNH_3$ = $TOTNH_3$ removed through the first biofilter in series (mg N/L)

TCM and DBCM cometabolism was accomplished for Train A in a biofilter seeded with a mixed culture from the Rio Grande fed both Lake Austin and nutrient water. For this train, an increase in $TOTNH_3$ removal did not lead to a significant increase in TCM or DBCM removal. This result is in contrast to previous biofilter experiments in which an increase in $TOTNH_3$ removal coincided with an increase in THM removal. Excluding the period immediately after DBCM addition (Run 3, Period II), TCM removal remained relatively consistent over time (13% average), and no statistically significant difference existed in TCM removal for any operating period for Train A. TCM removal was less than similar operating periods for the Lake Austin Biofilters on nutrient water but similar to removals seen for the Lake Austin Biofilters fed Lake Austin water. Average DBCM removal significantly declined over time from an initial 60% removal to a final 17% removal, which was similar to the TCM removal for this train. The initial DBCM removal of 60% was similar to that seen for the Lake Austin Biofilters fed nutrient water under similar operating conditions, but the Lake Austin Biofilters did not show the same decrease in DBCM performance over time. This might have been a result of the extended DBCM addition for the MCB1 as opposed to the LAB.

Train B demonstrated that TCM and DBCM cometabolism was accomplished in a biofilter seeded with an *N. oligotropha* enrichment culture fed Lake Austin and nutrient water. As with Train A, TCM removal was not significantly different for any of the operating periods summarized in Table 5.10 and did not significantly decrease upon the addition of DBCM. In addition, DBCM removal started and remained at 14% which was similar to the TCM removal seen during this same period (10%) and not significantly different from Train A's final DBCM removal.

Because Train C was packed with GAC, adsorption might have occurred in the biofilter in addition to or in lieu of biological THM removal. To provide a baseline on

THM adsorption, simulated breakthrough curves for TCM and DBCM were generated from the pore surface diffusion model (PSDM) implemented into AdDesignS (Hokanson et al. 1998). A simulation was run at the operating conditions seen in the MCB1 for the first biofilter in series of Train C with TCM and DBCM additions. Adsorption isotherm parameters present in the software library were used to generate the breakthrough curves shown in Figure 5.20. TCM is predicted to completely breakthrough the biofilter at 865 and 1,249 hours for the two different influent TCM concentrations. By contrast, DBCM is predicted to show no breakthrough during the operating time of the biofilters.

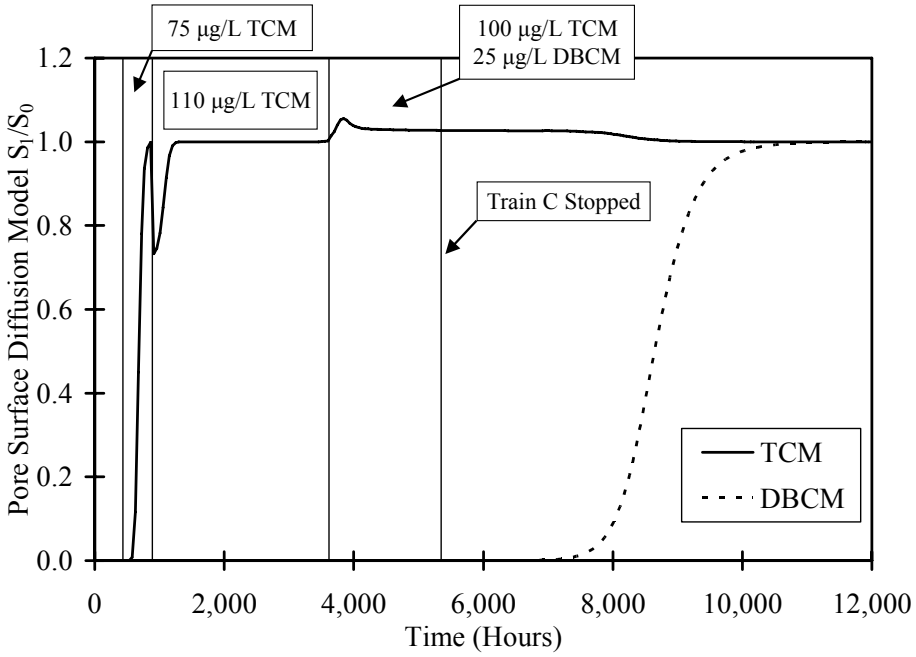

Figure 5.20 TCM and DBCM breakthrough curves for Mixed Culture Biofilters 1 Train C (Rio Grande GAC) first biofilter in series

Because the GAC from the City of Laredo would be at some point of exhaustion, the predicted breakthrough curves for TCM and DBCM might be shifted in time based on the extent of exhaustion. To address this, the TCM and DBCM breakthrough curves

were shifted in time so that the first data point for TCM and DBCM removal matched that respective point on their breakthrough curve. These adjusted breakthrough curves are shown for TCM and DBCM in Figure 5.21 overlaid with the experimental removal data for each THM.

If adsorption to GAC was only occurring in the filter, the S_1/S_0 values would be expected to increase as shown by the predicted breakthrough curves. For DBCM and after a short period of increasing S_1/S_0 values, S_1/S_0 started to decline in opposition to the proposed breakthrough curve, suggesting that the removal of DBCM was biological in nature and improving over time as $TOTNH_3$ removal improved. Furthermore, the lack of DBCM removal in the second biofilter in series in which no $TOTNH_3$ removal was occurring suggests that the removal of DBCM in the first biofilter in series was biological in nature. For TCM, the data were unclear, but because of the predicted short time to breakthrough for TCM on virgin GAC (approximately 900 hours), the GAC should have reached exhaustion early in the biofilter run, suggesting removal after 900 hours can be attributed to biological removal and not adsorption.

For TCM removal and ignoring the period in which adsorption might have occurred (i.e., the first 900 hours), TCM removal did not exceed 9% but showed a trend of improvement at the end of the operating period that coincided with an increase in DBCM removal. DBCM removal increased over time, reaching its maximum level (75%) at the end of the run. This level of removal of DBCM was greater than any previous biofilter experiment, providing evidence of improved DBCM removal with GAC versus anthracite.

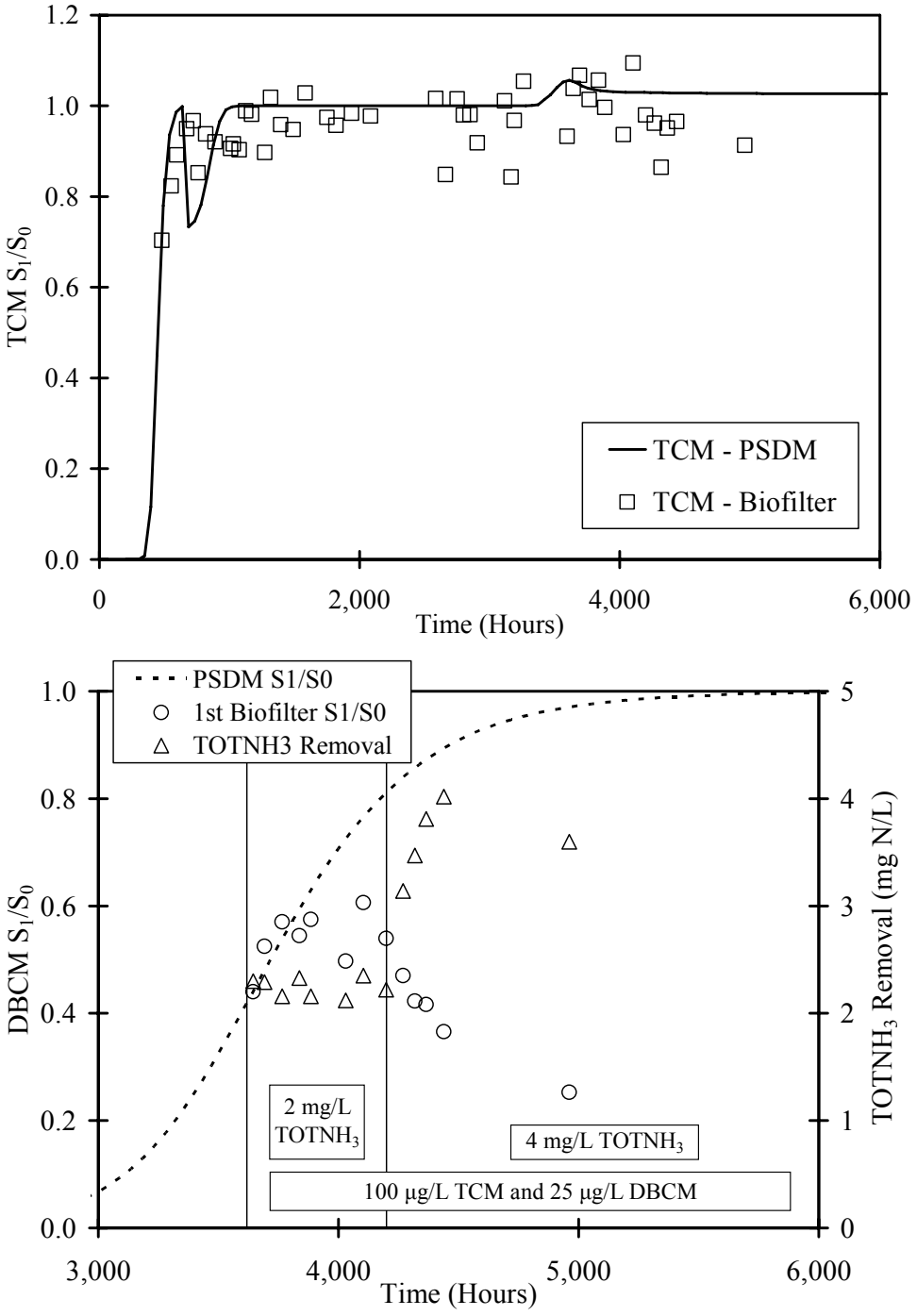

Figure 5.21 Predicted breakthrough and experimental TCM and DBCM removal for Mixed Culture Biofilters 1 Train C (Rio Grande GAC) first biofilter in series

Using the average data from Table 5.10, $k_{1_{THM}}/k_{TOTNH_3}$ ratios were determined for all three trains of the MCB1 and are shown in Table 5.11. Because of the significant changes in DBCM removal seen for Trains A and C during their operation, Table 5.11 provides two ratios for DBCM, corresponding to their initial and final removals. For this same reason, standard deviations are only provided for the TCM ratios. The kinetic rate constant ratios for Trains A and B were the same for TCM and approached each other for DBCM through time. The final DBCM ratio for Train C approached that of Train A initially with these values being larger than those seen for the LAB operating on nutrient water but similar to those calculated for the *N. europaea* biofilter experiment's bromine-substituted THMs (0.38-0.48 L/mg $TOTNH_3$).

Table 5.11 Mixed Culture Biofilters 1 average $k_{1_{THM}}/k_{TOTNH_3}$ ratio summary

Train	$\frac{k_{1_{THM}}}{k_{TOTNH_3}}$ (L/mg $TOTNH_3$)		
	TCM	DBCM Initial	DBCM Final
A	0.045±0.016	0.38	0.071
B	0.045±0.0019	0.067	0.074
C	0.017±0.0085	0.28	0.38

5.5.5. Backwash Batch Kinetic Tests

Because of the decreased biofilter TCM performance as compared with the Lake Austin Biofilters fed nutrient water, batch kinetic tests on the biofilter backwash water were performed to evaluate the ability of the bacteria present in the biofilm to cometabolize THMs. The MCB1 was maintained during this time (Run 3, Period IV)

with nominal influent concentrations of 2 mg N/L $TOTNH_3$, 100 μg/L TCM, and 25 DBCM. The first biofilter in series was backwashed at specified times and batch kinetic tests performed as described previously. Before backwashing, the biofilter was sampled to determine the performance at the time of backwashing to correlate the biofilter performance with the results of the batch kinetic tests. The biofilter performance at the time of backwashing is presented in Table 5.10 for Run 3 (Period IV).

Figure 5.22, Figure 5.23, and Figure 5.24 detail the kinetic parameters determined from these experiments along with their 95% joint CLs. Two experiments were conducted on Train A at 4,986 (A1) and 5,658 (A2) hours, one on Train B at 5,708 hours (B), and one on Train C at 4,962 hours (C). Because of the large mass of THMs removed during the experiments with Train A, the A1 batch kinetic test was analyzed in two ways to see if transformation capacity affected the results. A complete analysis was conducted of the data set as well as a subset of the data starting when the $TOTNH_3$ concentration was 3.5 mg N/L. No significant difference was seen between these two analyses, indicating that transformation capacity was not an issue. In addition, the results from the two different experiments on Train A (A1 and A2) showed similar kinetic parameters and were conducted approximately 700 hours apart, indicating the stability of the culture present in the biofilter and reproducibility of the results.

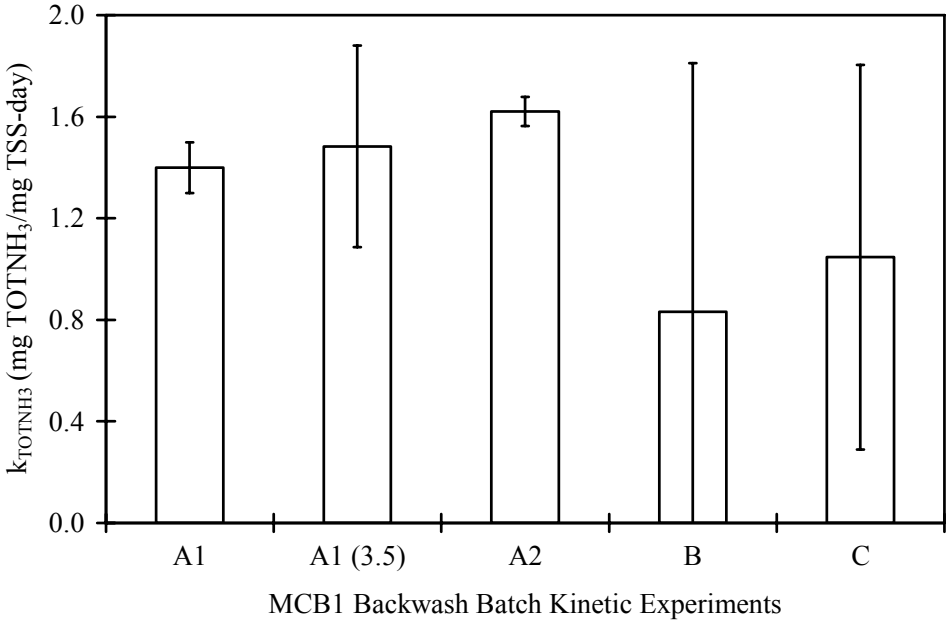

Figure 5.22 Mixed Culture Biofilters 1 backwash batch kinetic tests k_{TOTNH_3} 95% joint CL summary (A1 and A1(3.5) at 4,986; A2 at 5,658; B at 5,708; and C at 4,962 hours)

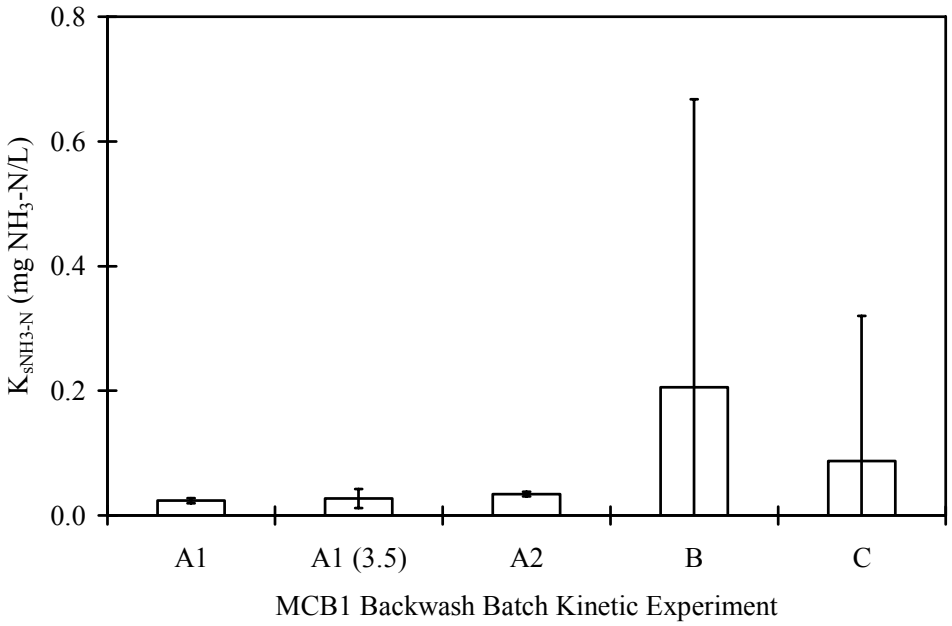

Figure 5.23 Mixed Culture Biofilters 1 backwash batch kinetic tests $K_{s_{NH_3-N}}$ 95% joint CL summary (A1 and A1(3.5) at 4,986; A2 at 5,658; B at 5,708; and C at 4,962 hours)

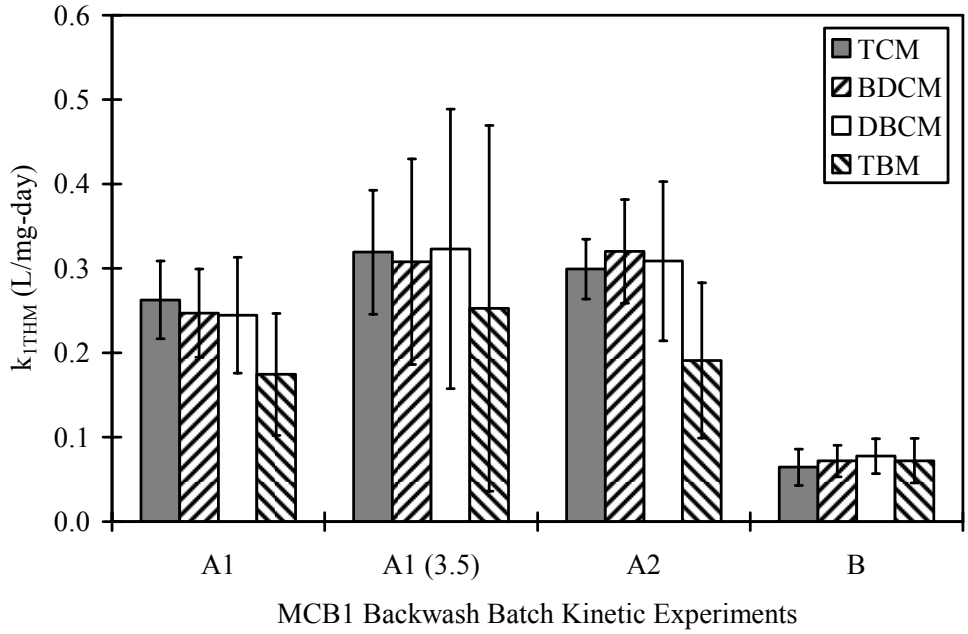

Figure 5.24 Mixed Culture Biofilters 1 backwash batch kinetic tests THM 95% joint CL summary (A1 and A1(3.5) at 4,986; A2 at 5,658; and B at 5,708 hours)

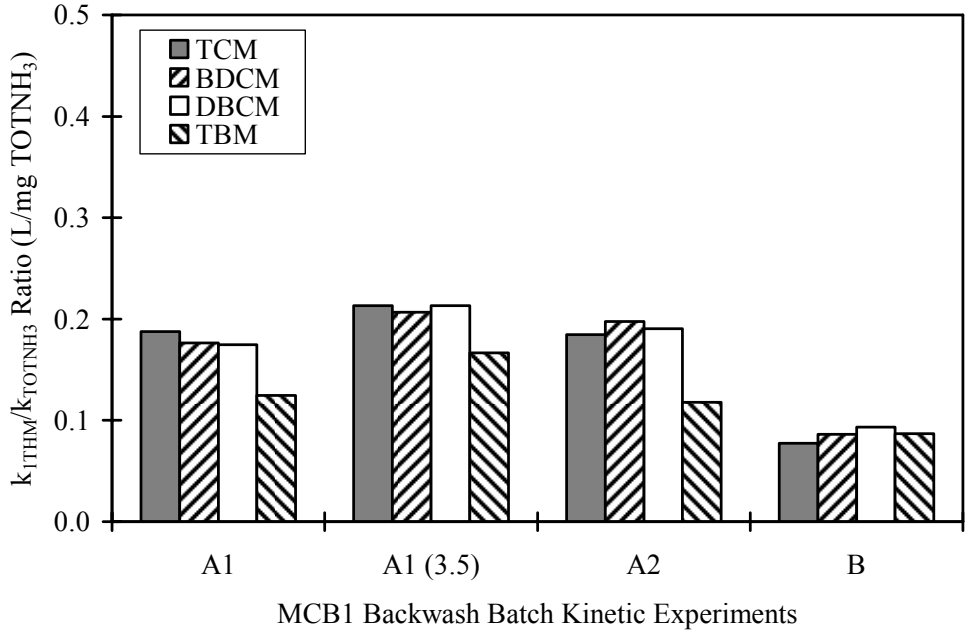

Figure 5.25 Mixed Culture Biofilters 1 backwash batch kinetic experiment coefficient ratio summary (A1 and A1(3.5) at 4,986; A2 at 5,658; and B at 5,708 hours)

For the series of backwash kinetic experiment conducted, the ammonia kinetic parameters for each biofilter showed similar results, but the THM kinetic parameters were markedly different. For Train C, no THM kinetic parameters could be determined because of interfering effects with residual GAC carried over from biofilter backwashing and the competitive adsorption seen with all four THMs present. The THM kinetic parameters for Train A were significantly greater than Train B. For both Trains A and B, the only significant difference among THMs within a given batch kinetic experiment was for A1 and A2 and then only that TBM was significantly less than the other three THMs, contrasting previous batch kinetic tests. For Trains A and B, the similar THM kinetic parameters for TCM and DBCM coincide with the similar TCM and DBCM biofilter removals at the time of the backwash tests (Figure 5.18 and Figure 5.19). Based on the backwash batch kinetic parameters and C_{si}, Train B's slower recovery during Run 1 (Periods II and III) was likely the result of a lower transformation capacity or yield as compared to Train A.

Because the biomass might be overestimated because of the inclusion of the biofilm and possible carryover of media in determining TSS, the ratios between the ammonia and THM kinetic coefficients were calculated to compare with previous batch kinetic studies on a normalized basis. A greater ratio implies that the bacteria are more efficient at THM cometabolism. The TCM ratio ($k_{1_{TCM}}/k_{TOTNH_3}$) for Train A was similar to that determined from the LAB data fit to Equation 4.1 and all the THM ratios were larger than those determined for *N. europaea* from the batch kinetic tests. Train B ratios were similar to those determined for *N. europaea* in batch.

Comparing these ratios to those presented in Table 5.11, the ratios from the backwash batch kinetic tests for Train A were 2 to 4.5 times greater than those determined from the biofilter data while those from Train B were only 1.2 to 1.7 times

greater. An increase in $k_{1_{THM}}/k_{TOTNH_3}$ calculated from the batch kinetic tests versus those from biofilter performance data is not surprising. Diffusion is not taken into account with the biofilter performance data when using Equation 4.1; therefore, decreased $k_{1_{THM}}/k_{TOTNH_3}$ values are most likely a result of biofilm and liquid layer diffusion. One explanation for the greater ratio difference with Train A as compared with Train B is that Train A was completely removing $TOTNH_3$ at the time of backwashing as opposed to Train B, which showed an effluent $TOTNH_3$ of 0.19 mg N/L. Therefore, the biomass located in the lower region of Train A might have only been partly selected for less efficient THM degraders because of THM product toxicity. The Train A backwash kinetic tests were conducted with a combination of selected, less efficient and unselected, more efficient (i.e., those seen in Runs 1 and 2 of the LAB) THM degrading bacteria located in the biofilter's upper and lower regions, respectively.

5.5.6. Summary

Taking the biofilter performance and backwash kinetic tests in total, the Mixed Culture Biofilters 1 showed varied results compared with previous batch kinetic and biofilter experiments. Based on the backwash batch kinetic experiments, these biofilters contained bacteria able to degrade all four THMs. For Train A, the backwash batch kinetic parameters predict a greater THM degradation than occurred. During biofilter operation, performance was not related to source water, nutrient addition, or influent ammonia concentration.

Selection of biofilm bacteria for less efficient THM degraders might have occurred. Upon the initial and subsequently increased TCM addition, $TOTNH_3$ removal decreased and then reestablished, indicating an adjustment by the biofilm bacteria. In addition, changes in DBCM removal seen in Train A and C over an extended period indicated a change in activity related to DBCM. Interestingly, the results from Trains A

and C trended in opposite directions with Train A decreasing in DBCM removal while Train C increased in DBCM removal. For Trains A and B, nitrifier selection might have led to bacteria that degraded each THM at similar rates between the biofilters.

5.6. MIXED CULTURE BIOFILTERS 2

To further investigate the possible causes for the decreased removals observed for the Lake Austin Biofilters fed Lake Austin water and the Mixed Culture Biofilters 1, an experiment was conducted with biofilters seeded with nitrifiers from each of these previous biofilters experiments (Lake Austin mixed and *N. oligotropha* enrichment cultures), referred to collectively as Mixed Culture Biofilters 2 (MCB2). Backwash batch kinetic tests and DNA extractions were performed on the biofilters at the end of operation to gain insights into the bacteria inhabiting the biofilms and their distributions along the length of the biofilters. These results provided additional information to better interpret biofilm performance and assist in modeling efforts of the biofilters.

Biofilters were seeded on anthracite with the Lake Austin mixed culture (Trains A and B) and the *N. oligotropha* enrichment culture (Trains C and D). Trains A and C consisted of two biofilters in series while Trains B and D consisted of one biofilter. The nominal influent ammonia concentration for all trains was the same for each operating condition with other biofilter setup and scaling information summarized in Table 5.1. Once seeded, these biofilters were operated immediately on the primary column setup and fed nutrient water to simulate conditions that produced increased removals for the Lake Austin Biofilters fed nutrient water. For ease of presentation, this experiment is broken down into two runs.

5.6.1. Run 1

After an initial startup (approximately 3,000 hours) in which nitrification was established, Run 1 investigated addition of 50 µg/L TCM and 25 µg/L DBCM without (Period I) and with (Period II) addition of iron and copper. Figure 5.26 through Figure 5.29 display the $TOTNH_3$, TCM, and DBCM concentrations of all four trains during Run 1. For Train A, Period I showed essentially no removal of $TOTNH_3$ after a backwash event at the beginning of Period I. As a result, it was reseeded with the backwash from Train B during the next backwashing event at the end of Period I. In a similar manner to Train A, Train D was showing minimal removal and was reseeded with backwash from Train C at the beginning of Period I.

During Run 1, TCM and DBCM were degraded in all trains with various percentage removals and no observable improvement with the addition of additional iron and copper (Period II). For example, Train C showed removals of TCM and DBCM ranging from 0-31% (0-19 µg TCM/L) and 4-31% (1-10 µg DBCM/L), respectively. The fluctuation in removals might be attributed to the decreased EBCT (Table 5.1) and unstable $TOTNH_3$ removals seen in these biofilters as they were operated to generate effluent $TOTNH_3$ concentrations through the first biofilter in series. The instability in the $TOTNH_3$ might have been a result of the biofilter hydraulics (i.e., short EBCT) or THM product toxicity as during Run 1 the calculated C_{si} was 0.69. Even with a C_{si} less than one, an immediate decrease in $TOTNH_3$ did not occur as was seen with the other biofilter experiments when THMs were first added to the influent. Overall, $TOTNH_3$ removals for all trains reached 2 to 3 mg N/L at the end of each period during Run 1, and all trains had effluent $TOTNH_3$ concentrations through the first biofilter in series.

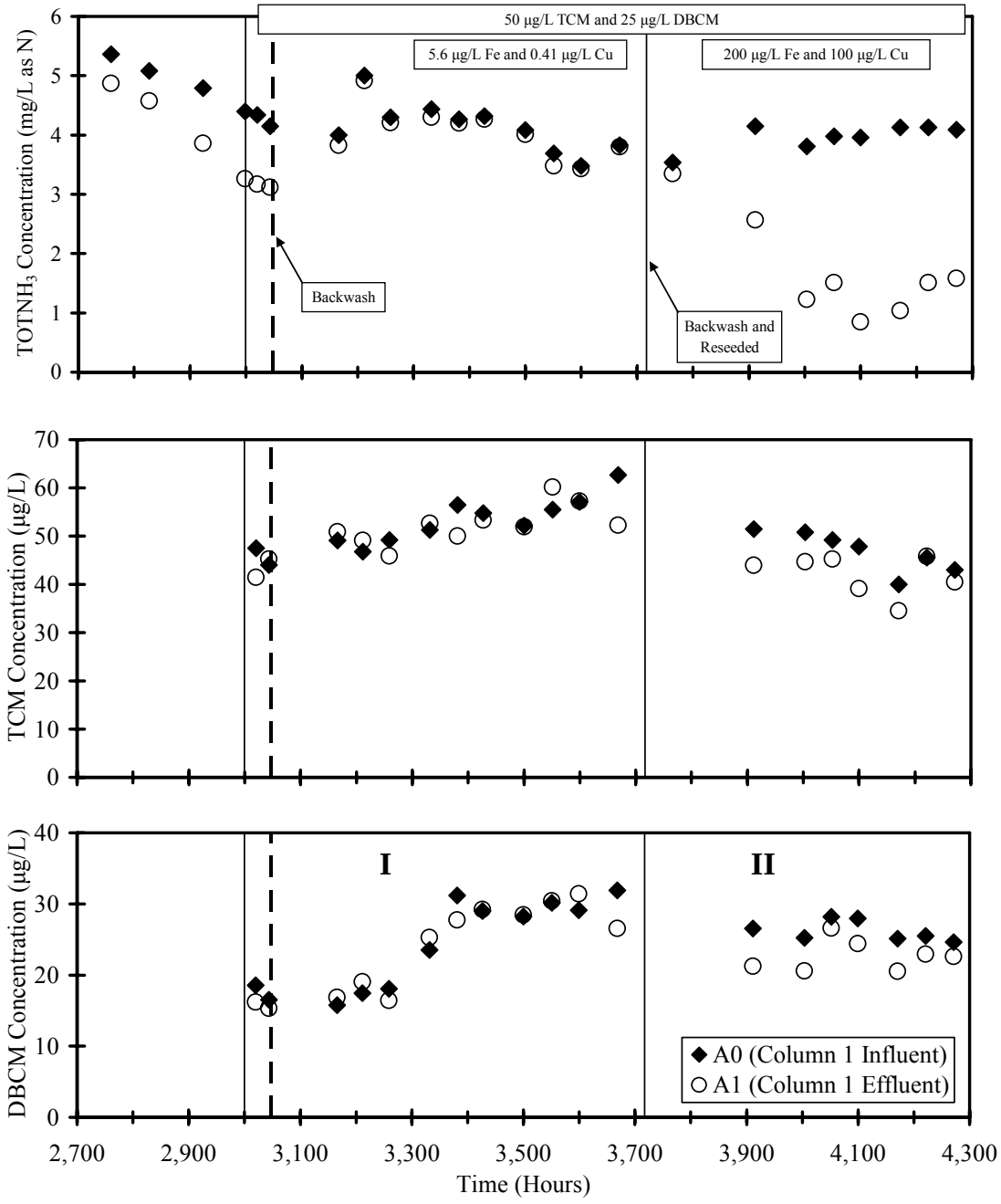

Figure 5.26 Mixed Culture Biofilters 2 Run 1 Train A (Lake Austin mixed culture) $TOTNH_3$, TCM, and DBCM concentrations fed nutrient water

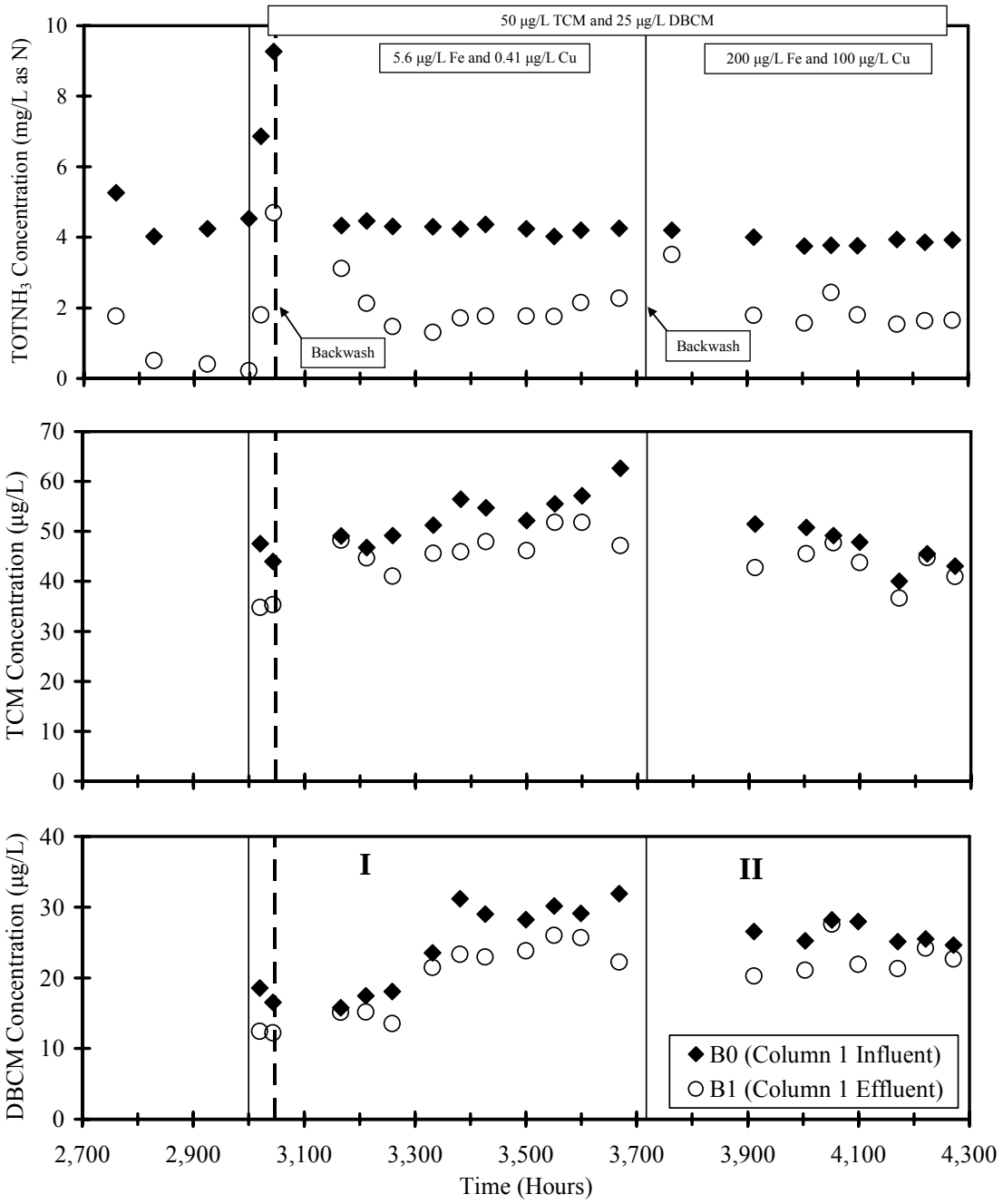

Figure 5.27 Mixed Culture Biofilters 2 Run 1 Train B (Lake Austin mixed culture) $TOTNH_3$, TCM, and DBCM concentrations fed nutrient water

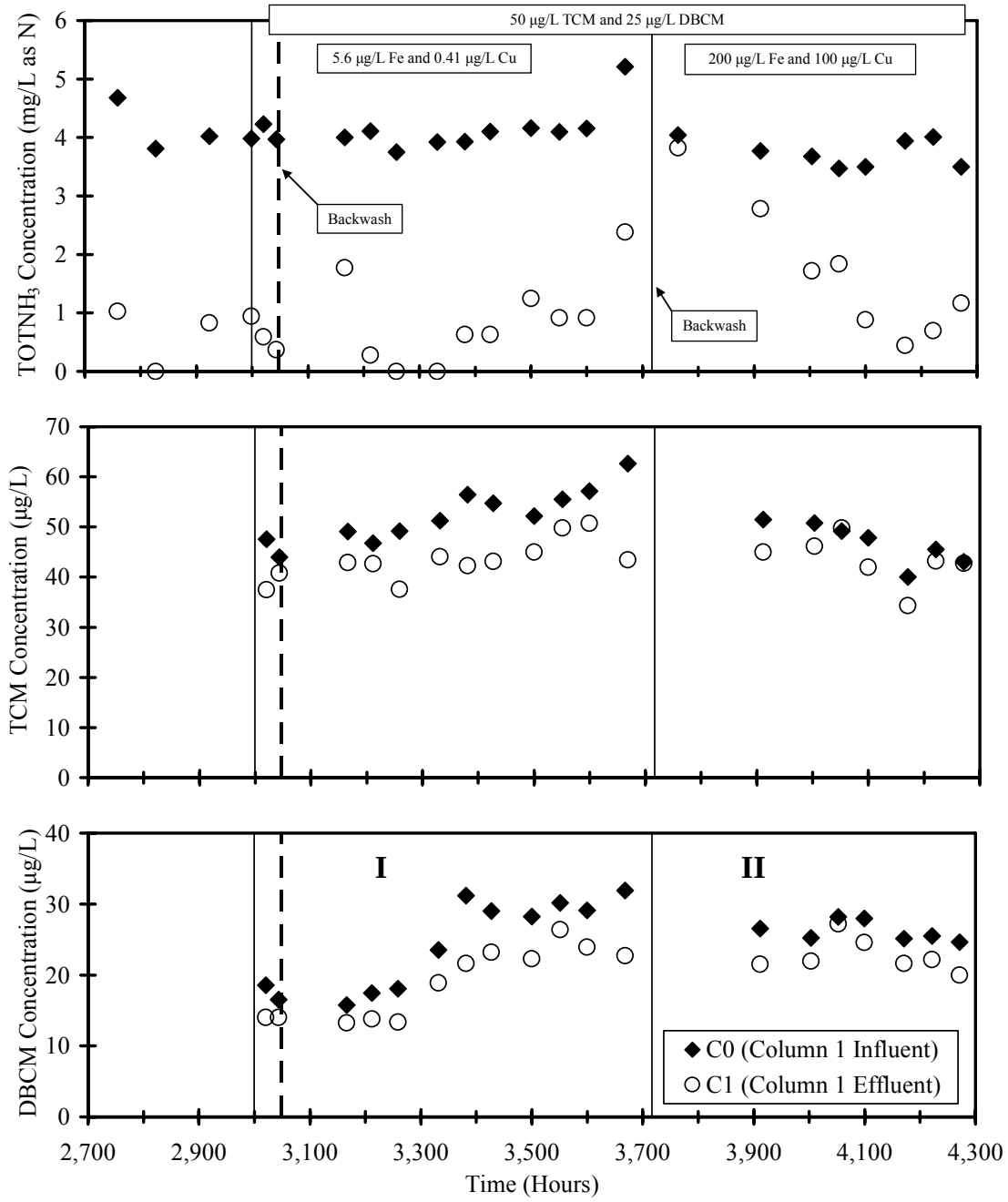

Figure 5.28 Mixed Culture Biofilters 2 Run 1 Train C (*N. oligotropha* enrichment culture) $TOTNH_3$, TCM, and DBCM concentrations fed nutrient water

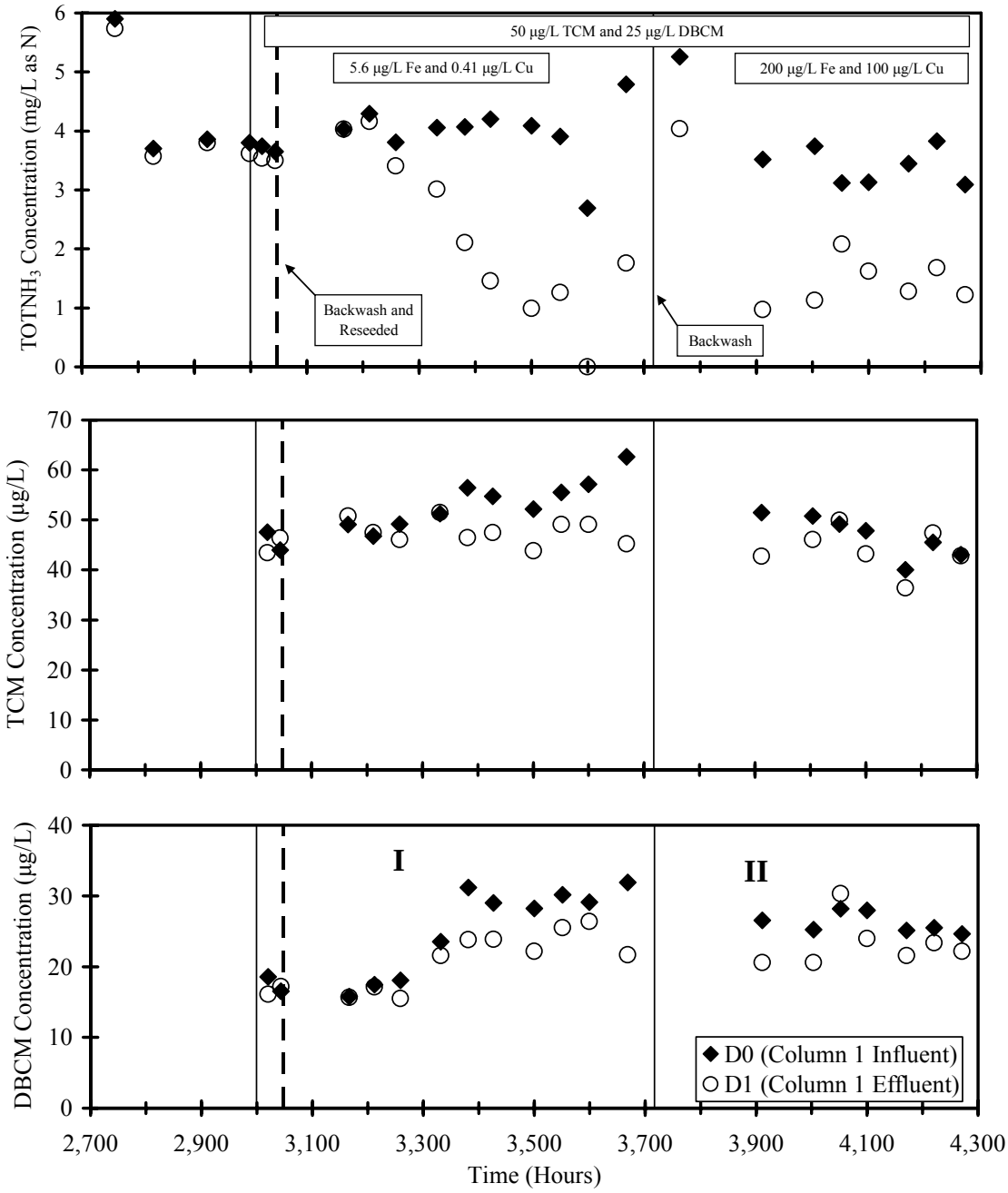

Figure 5.29 Mixed Culture Biofilters 2 Run 1 Train D (*N. oligotropha* enrichment culture) $TOTNH_3$, TCM, and DBCM concentrations fed nutrient water

5.6.2. Run 2

Run 2 investigated feeding only DBCM at 25 µg/L to increase the C_{si} value to greater than 1 (1.2) and decreasing the influent iron concentration to the baseline nutrient water concentration while maintaining the elevated copper concentration (Period I) as an elevated copper addition only had not been studied previously. At the end of Period I, the biofilters were backwashed for batch kinetic experiments. After this, the biofilters were fed all four THMs at 15 µg/L each to verify that all four THMs could be cometabolized (Period II). In addition, this allowed growing a suitable biomass to harvest for molecular analysis at the end of Run 2 that was degrading all four THMs. Figure 5.30 through Figure 5.33 summarize the performance of each train during Run 2.

For Period I, removal of DBCM in all trains was comparable to that from Run 1. Period II demonstrated that all four trains could remove all four THMs with removals for all THMs being similar and total THM removal reaching 17-24% for all trains at the end of Period II, resulting in removals of 11-16 µg/L of total THMs with $TOTNH_3$ removals of 2.9 to 3.7 mg N/L.

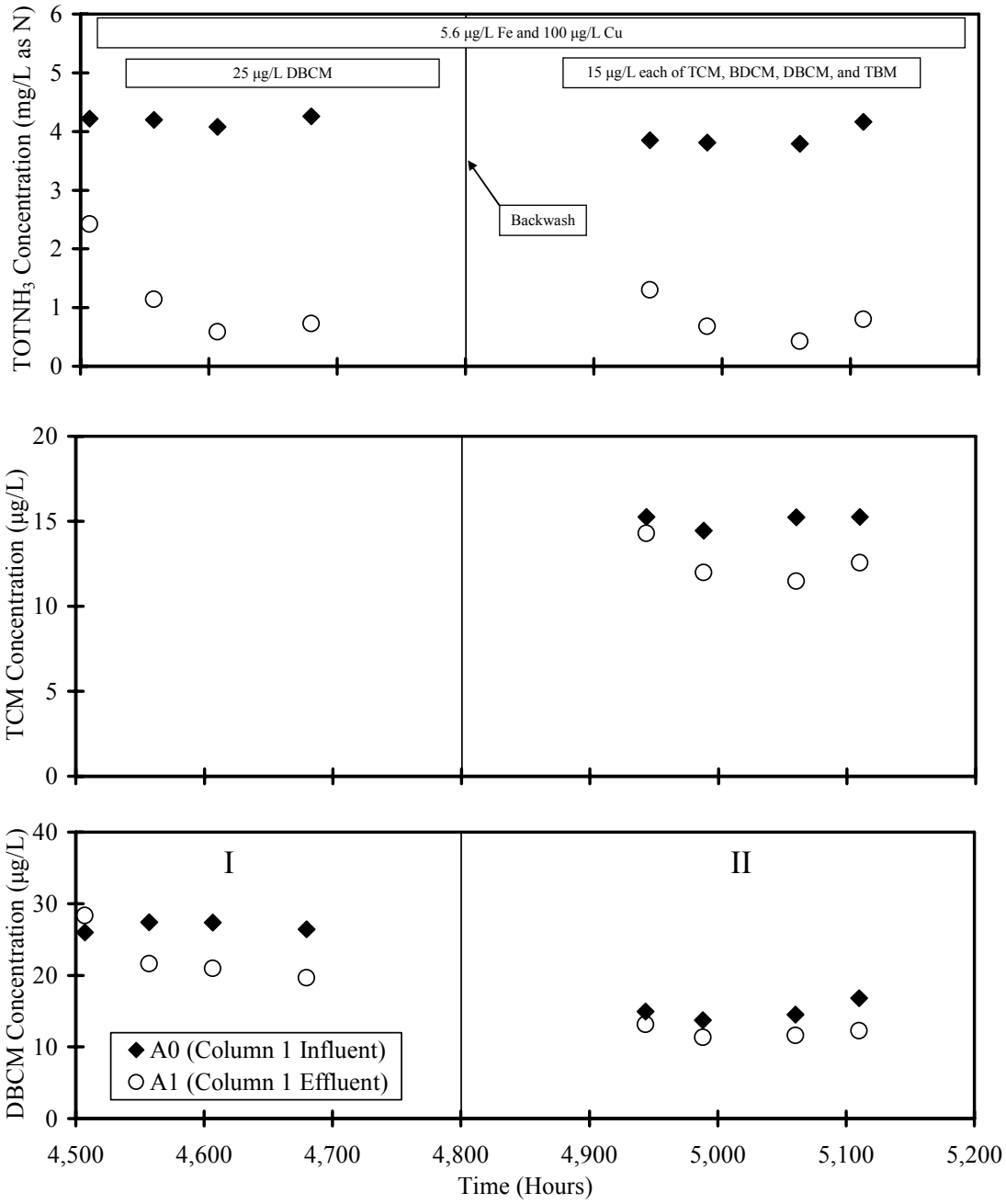

Figure 5.30 Mixed Culture Biofilters 2 Run 2 Train A (Lake Austin mixed culture) $TOTNH_3$, TCM, and DBCM concentrations fed nutrient water

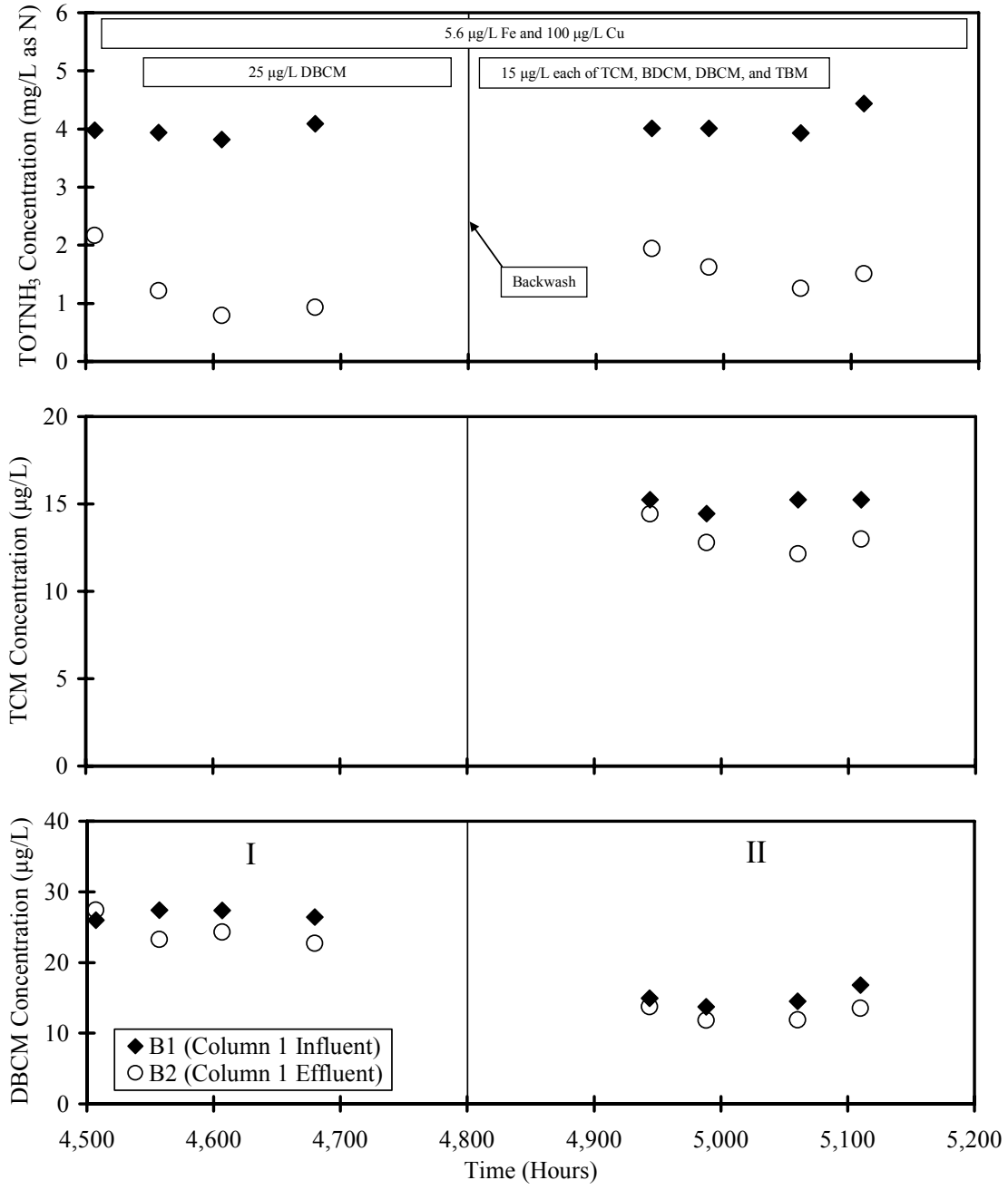

Figure 5.31 Mixed Culture Biofilters 2 Train B (Lake Austin mixed culture) $TOTNH_3$, TCM, and DBCM concentrations fed nutrient water

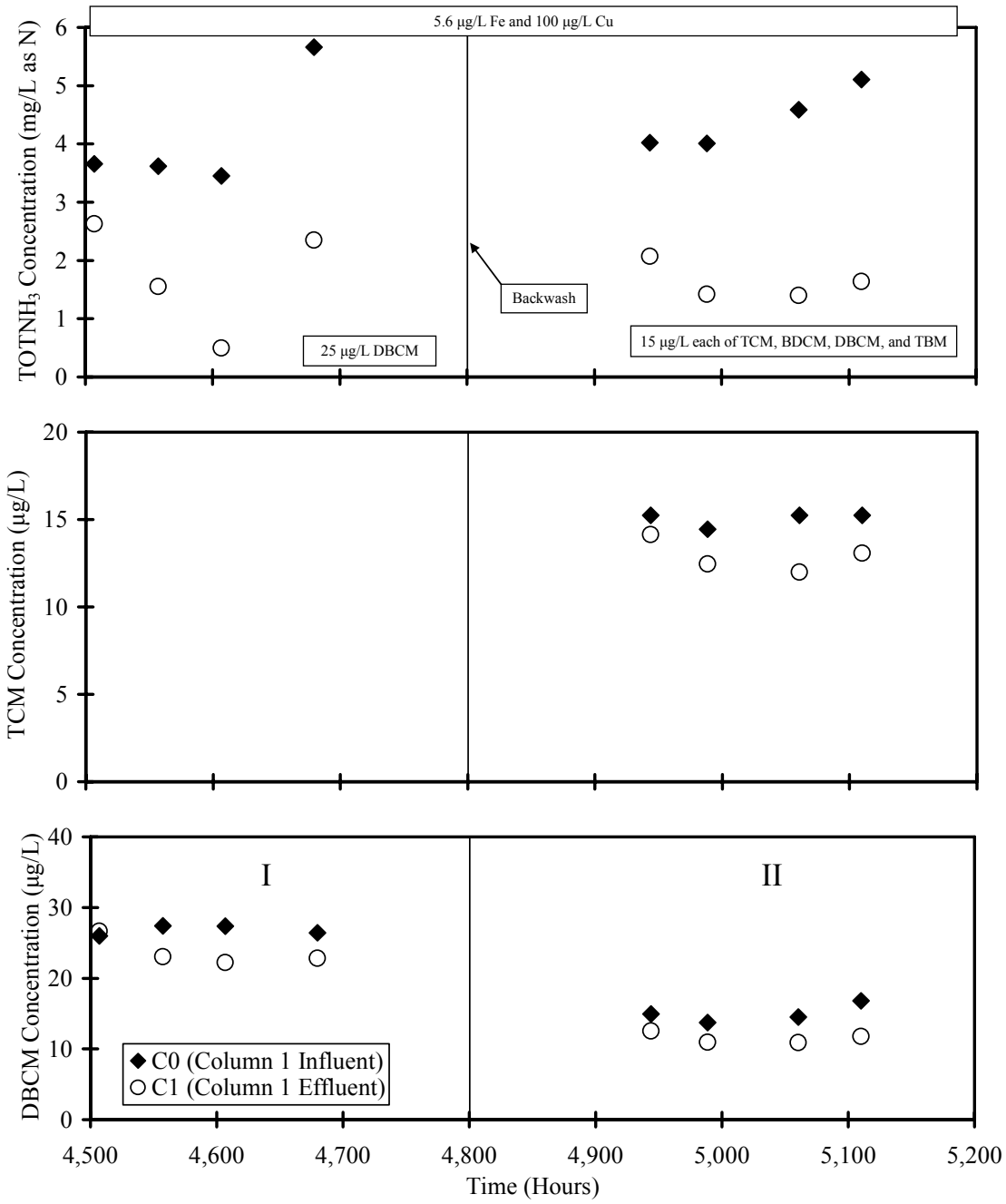

Figure 5.32 Mixed Culture Biofilters 2 Train C (*N. oligotropha* enrichment culture) $TOTNH_3$, TCM, and DBCM concentrations fed nutrient water

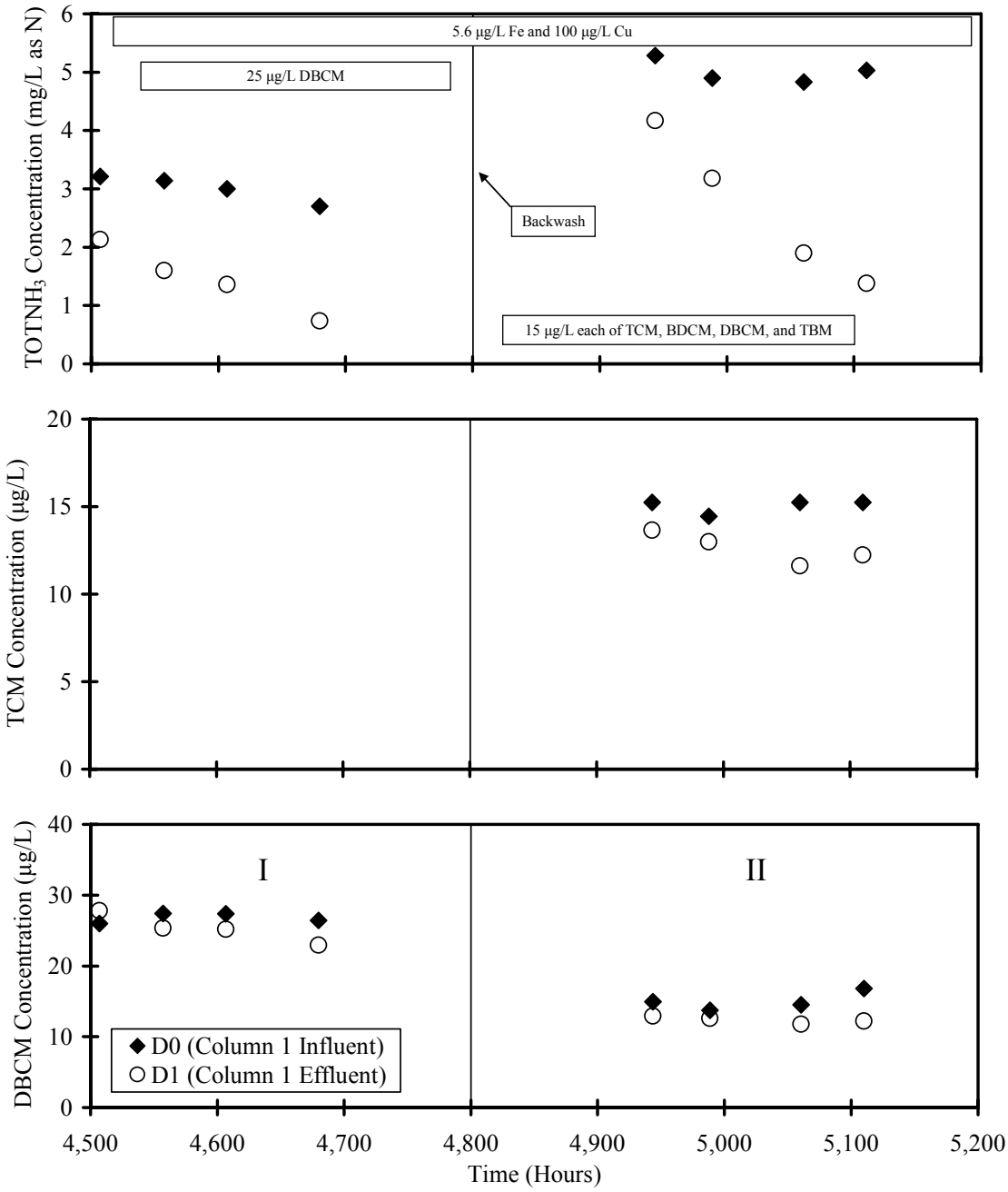

Figure 5.33 Mixed Culture Biofilters 2 Train D (*N. oligotropha* enrichment culture) $TOTNH_3$, TCM, and DBCM concentrations fed nutrient water

5.6.3. Run Comparisons

Table 5.12 provides a summary of the biofilter operation for the Mixed Culture Biofilters 2. Overall, the THM removals were variable during this experiment, with average removals ranging from 6 to 23% with no THM removals being statistically different from one another for any averaged operating period. The lack of a statistical difference might be a result of the magnitude of the standard deviations determined from the experimental data because of the varied performance seen during this biofilter experiment.

Because THM performance was not statistically different, all the operating periods in Table 5.12 were used to determine average $k_{1_{THM}}/k_{TOTNH_3}$ ratios and are shown in Table 5.13. Overall, these ratios were similar within a given culture and were averaged to compare the two cultures as shown in Table 5.13. Two different trends were seen with the two different cultures used in these biofilter experiments. The Lake Austin mixed culture trains (A and B) had greater ratios for BDCM and DBCM as compared with TCM and TBM. By comparison, the *N. oligotropha* enrichment culture trains (C and D) had greater ratios for the three bromine-substituted THMs (BDCM, DBCM, and TBM) as compared with TCM.

Table 5.12 Mixed Culture Biofilters 2 performance summary (first biofilter in series)

Train	Run	Period	No. of Samples	$\Delta_{0\text{-}1}TOTNH_3$ (mg N/L)	S_{TCM_0} / $\frac{S_{TCM_1}}{S_{TCM_0}}$	S_{BDCM_0} / $\frac{S_{BDCM_1}}{S_{BDCM_0}}$	S_{DBCM_0} / $\frac{S_{DBCM_1}}{S_{DBCM_0}}$	S_{TBM_0} / $\frac{S_{TBM_1}}{S_{TBM_0}}$
A	1	II	6	2.7±0.29	46±4.0 0.90±0.064		26±1.6 0.88±0.053	
	2	I	3	3.4±0.26			27±0.55 0.77±0.023	
	2	II	4	3.1±0.38	15±0.40 0.84±0.076	15±0.93 0.82±0.065	15±1.3 0.81±0.063	16±1.1 0.84±0.062
B	1	I	9	2.5±0.34	54±4.7 0.87±0.063		27±5.5 0.82±0.074	
	1	II	7	2.1±0.36	47±4.2 0.92±0.052		26±1.4 0.87±0.083	
	2	I	3	3.0±0.23			27±0.55 0.86±0.020	
	2	II	4	2.5±0.37	15±0.40 0.87±0.062	15±0.93 0.86±0.060	15±1.3 0.85±0.052	16±1.1 0.87±0.038
C	1	I	10	3.3±0.52	53±4.7 0.83±0.074		25±6.2 0.79±0.056	
	1	II	6	2.6±0.74	46±4.0 0.93±0.060		26±1.6 0.88±0.050	
	2	I	3	2.8±0.64			27±0.55 0.84±0.025	
	2	II	4	2.8±0.67	15±0.40 0.86±0.057	15±0.93 0.79±0.081	15±1.3 0.77±0.060	16±1.1 0.82±0.038
D	1	I	6	2.7±0.41	56±3.5 0.83±0.058		30±1.4 0.80±0.078	
	1	II	7	2.0±0.56	47±4.2 0.94±0.065		26±1.4 0.87±0.073	
	2	I	3	1.7±0.22			27±0.55 0.90±0.032	
	2	II	4	2.4±1.1	15±0.40 0.84±0.069	15±0.93 0.84±0.076	15±1.3 0.83±0.081	16±1.1 0.85±0.076

S_{THM_0} = Influent THM concentration to first biofilter in series (µg/L)

S_{THM_1} = Effluent THM concentrations from first biofilter in series (µg/L)

$\Delta_{0\text{-}1}TOTNH_3$ = $TOTNH_3$ removed through the first biofilter in series (mg N/L)

Table 5.13 Mixed Culture Biofilters 2 average $k_{1_{THM}}/k_{TOTNH_3}$ ratio summary

Train	$\frac{k_{1_{THM}}}{k_{TOTNH_3}}$ (L/mg $TOTNH_3$)			
	TCM	BDCM	DBCM	TBM
A	0.048	0.063	0.065	0.057
B	0.050	0.061	0.066	0.054
C	0.047	0.085	0.070	0.070
D	0.059	0.076	0.072	0.068
Lake Austin Average (A/B)	0.049	0.062	0.066	0.055
N. oligotropha Average (C/D)	0.053	0.080	0.071	0.069

5.6.4. Backwash Batch Kinetic Tests

As was done with the Mixed Culture Biofilters 1, the Mixed Culture Biofilters 2 were backwashed at the end of Run 2 (Period I) with the backwash water used to conduct batch tests to evaluate their kinetics. Figure 5.34, Figure 5.35, and Figure 5.36 detail the determined kinetic parameters from these experiments along with their 95% joint CLs. In addition, results from the Mixed Culture Biofilters 1 are provided for comparison purposes in these figures. One experiment was conducted for each train. Because the largest percentage of transformation capacity was utilized in Train C's experiment, it was analyzed in two ways as done previously for the Mixed Culture Biofilters 1 results. As seen before, no significant difference was seen between these two analyses, indicating that transformation capacity was not an issue. This result is surprising in that the

transformation capacity, as measured in batch experiments with cells grown in suspension, was exceeded for Trains B and C and 99% used for Train D as summarized in Table 5.14. Taken in total, the nitrifiers present in the biofilms seem to have greater transformation capacities than those grown in batch.

For the series of backwash batch kinetic experiments conducted, the ammonia kinetic parameters (Figure 5.34 and Figure 5.35) for each biofilter showed similar results within those conducted for MCB2 and compared with those previously conducted for MCB1. For the THM kinetic parameters (Figure 5.36), differing trends were present. For the cultures seeded with Lake Austin mixed culture nitrifiers, two different trends were seen. For Train A, BDCM and DBCM were statistically similar and greater than the statistically similar TCM and TBM rate constants, while for Train B, no statistical difference existed for any THM rate constant. For the biofilters seeded with the *N. oligotropha* enrichment cultures, Trains C and D showed similar trends with all the bromine-substituted THMs significantly greater than TCM, except BDCM for Train D.

As with the experiments conducted with MCB1, biomass might be overestimated because of the inclusion of the biofilm and possible carryover of media in determining TSS. The ratios between the ammonia and THM kinetic coefficients were determined to compare with previous batch kinetic studies on a normalized basis (Figure 5.37). Comparing these THM ratios to those in Table 5.13, the ratios from the backwash batch kinetic tests for all trains and for all THMs ranged from 0.98 to 1.7 times greater, which is similar to those seen with the comparison done on MCB1 Train B. In general, the trends in the ratios seen from the calculation of the $k_{1_{THM}}/k_{TOTNH_3}$ ratios between the biofilter performance data and the backwash batch kinetic tests for each culture agree.

Table 5.14 Backwash batch kinetic experiments summary of transformation capacity utilized

Biofilter Experiment	Backwash Batch Kinetic Experiment	Transformation Capacity Utilized (%)
Mixed Culture Biofilters 1	A1	75
	A2	78
	B	26
Mixed Culture Biofilters 2	A	53
	B	160
	C	165
	D	99

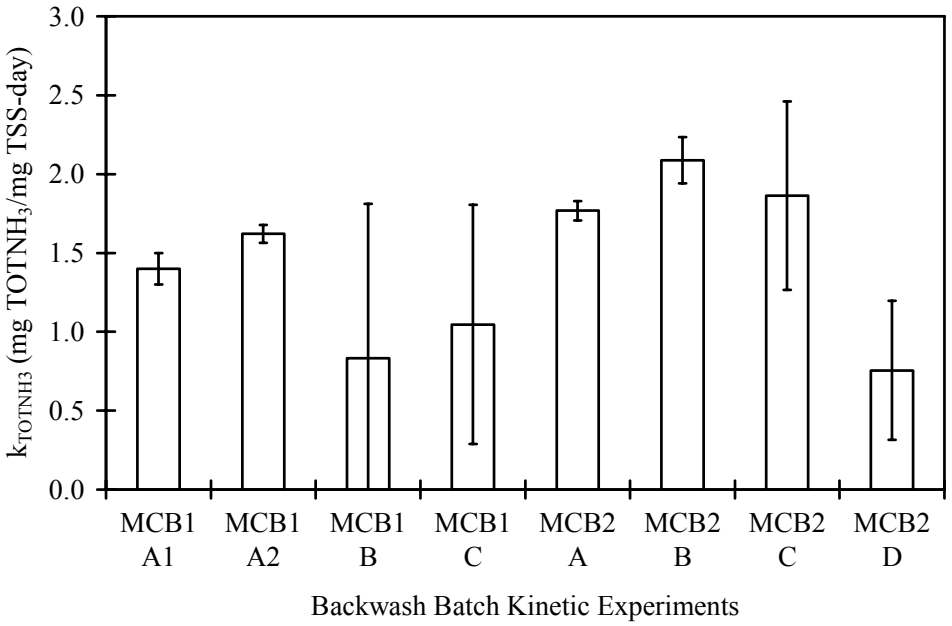

Figure 5.34 Mixed Culture Biofilters 2 backwash batch kinetic tests k_{TOTNH_3} 95% joint CL summary

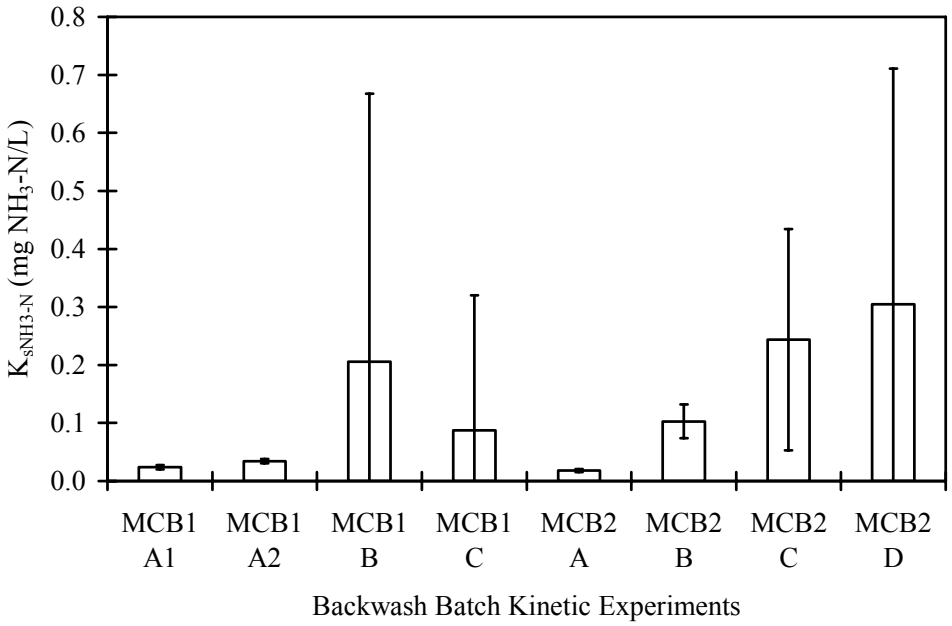

Figure 5.35 Mixed Culture Biofilters 2 backwash batch kinetic tests $K_{s_{NH_3-N}}$ 95% joint CL summary

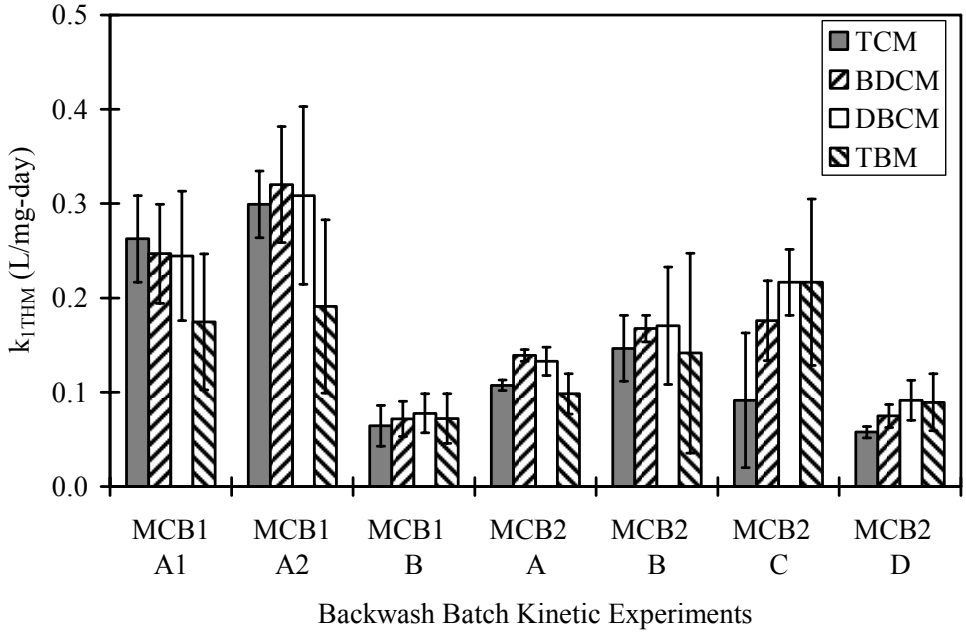

Figure 5.36 Mixed Culture Biofilters 2 backwash batch kinetic tests THM 95% joint CL summary

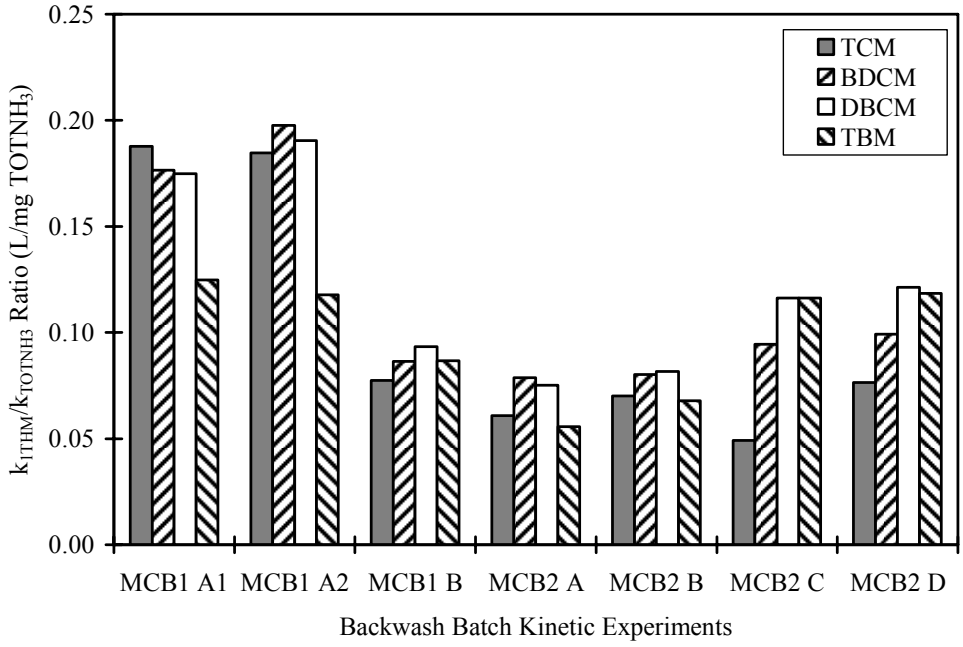

Figure 5.37 Mixed Culture Biofilters 2 backwash batch kinetic experiment coefficient ratio summary

Comparing the $k_{1_{THM}}/k_{TOTNH_3}$ ratios for the backwash batch kinetic tests (Figure 5.37), those conducted on Train A of MCB1 were larger than the other backwash batch kinetic experiments. This was the only biofilter without a measurable $TOTNH_3$ concentration at the time of backwashing. The bacteria in the biofilter's lower regions might not have been selected for less efficient THM degraders, resulting in the larger $k_{1_{THM}}/k_{TOTNH_3}$ ratios for this biofilter.

5.6.5. Molecular Biofilm Investigation

At the end of Run 2, DNA from the biofilters was extracted, quantified, and analyzed. Detailed results of the DNA extraction and verification of intact DNA by gel electrophoresis are shown in Appendix D. From individual total DNA comparisons, no

statistical difference existed between any of the samples for a given biofilter on a total DNA extracted per gram of dry anthracite basis and are presented in Table 5.15 along with their respective standard deviations. Samples designated as 1 are at the influent end of the biofilter with the numbering progressing down the length of the biofilter in equal lengths with 4 being the sample at the effluent end of a given biofilter. Further DNA analysis by real-time PCR was attempted to determine the percentage of the total extracted DNA attributed to ammonia-oxidizing bacteria (AOB). Unfortunately, these attempts were unsuccessful because of poor amplification of the plasmid standards during the analysis with the sample DNA; therefore, no defendable determinations could be made as to the AOB content of the samples.

Overall, the completed DNA analysis indicated that bacteria evenly populate the biofilters along their entire lengths. This even distribution in total DNA for each biofilter section might result from backwashing events in which the media was redistributed within a biofilter or from reattachment of detached bacteria from upper to lower biofilter sections.

Table 5.15 Mixed Culture Biofilters 2 composite sample DNA extraction summary

Train	DNA Density (ng total DNA extracted/g dry anthracite)			
	1 (Influent End)	2	3	4 (Effluent End)
A	1,554±262	2,349±837	2,422±293	2,425±172
B	2,443±634	2,045±95	2,954±304	2,692±514
C	2,273±123	1,702±158	2,002±310	1,673±122
D	1,379±363	2,170±465	2,003±302	2,154±491

5.6.6. Summary

Overall, the Mixed Culture Biofilters 2 degraded the four THMs commonly found in treated drinking water with biofilters seeded with the Lake Austin mixed and *N. oligotropha* enrichment cultures fed nutrient water. Performance of all four biofilter trains was not statistically different for any of the THMs, but this lack of difference might have been a result of the varied performance during this biofilter experiment. Similar trends in $k_{1_{THM}}/k_{TOTNH_3}$ ratios for a given culture were seen when comparing ratios determined from the biofilter performance or the backwash batch kinetic tests. THM removals were similar to those seen with the Lake Austin Biofilters during Runs 3 and 4 on Lake Austin water and at the end of MCB2 for Trains A and B. DNA was distributed equally along the length of the biofilters, indicating a similar bacterial density throughout a biofilter.

The average $k_{1_{THM}}/k_{TOTNH_3}$ ratios were used to predict THM removals (Table 5.16) for the three ICR water types in a similar manner as was done in Chapter 4 based on the batch kinetic experiments. This analysis predicted removals ranging from 6-23% for total THMs, depending on operating conditions, which is similar to those predicted from the batch kinetic experiments (4-23%).

5.7. BIOFILTER OPERATION SUMMARY

Biofilter experiments were conducted with the following seed cultures: (1) pure culture *N. europaea* (ATCC® 19718), (2) *N. oligotropha* enrichment culture isolated from a drinking water distribution system, (3) Lake Austin mixed culture cultured from Lake Austin, Texas, (4) Rio Grande mixed culture cultured from the influent line of a drinking water treatment facility in Laredo, Texas, and (5) GAC from an operating drinking water treatment facility in Laredo, Texas.

Table 5.16 THM cometabolism performance predictions based on MCB2 $k_{1_{THM}}/k_{TOTNH_3}$ ratios

$\Delta TOTNH_3$ (mg N/L)	THM Percent Removal						
	TCM	BDCM	DBCM	TBM	Total THMs for ICR Water Type		
					1	2	3
1	5.2	6.9	6.7	6.0	5.6	6.3	6.4
2	10	13	13	12	11	12	12
4	19	25	24	22	21	23	23

The operating conditions of the mixed culture laboratory-scale biofilters scaled to typical full-scale rapid filtration operating conditions seen in drinking water treatment practice (EBCTs of 2 to 8 minutes and SLRs of 2.5 to 7.0 gpm/ft^2), but the pure culture *N. europaea* laboratory-scale biofilters required an impractical EBCT. Therefore, it is expected that mixed cultures from actual source waters can be established in biofilters at reasonable EBCTs and SLRs without the necessity of seeding with the pure culture *N. europaea*.

Four THMs and $TOTNH_3$ were degraded in all the laboratory-scale nitrifying biofilter experiments. THM degradation increased with increasing bromine substitution, following the trend observed during the batch kinetic studies. Over the THM concentrations studied, competition between THMs did not seem to occur, and influent $TOTNH_3$ concentrations up to 4 mg N/L did not seem to compete with THMs in the biofilters, confirming the results from the batch kinetic experiments. In general, increased $TOTNH_3$ degradation corresponded to increased THM degradation; thus, the

close association between ammonia degradation and THM cometabolism observed in the batch kinetic studies held in the biofilter experiments.

For some biofilter experiments (LAB and MCB1 Train A), it seems that a selection occurred for bacteria less efficient at THM cometabolism, most likely because of THM product toxicity. The LAB and MCB1 were initiated on the secondary setup before being moved to the primary setup, but the MCB2 was started initially on the primary setup. The MCB2 did not show an initial period of higher removals, indicating that startup conditions might have resulted in the initial higher removals. The lower flowrates and greater EBCT associated with the secondary setup might have allowed a greater biomass to populate the biofilters, providing a sink of biomass that required a greater time for selection from THM product toxicity.

THM speciation is important, because each THM exhibits a different product toxicity. The cometabolism stability index (C_{si}) represents a simple and useful tool for judging the likelihood of product toxicity problems in biofilter operation. Because both THM cometabolism rate constants and THM product toxicities increase with increasing THM bromine-substitution, a water's THM speciation will be an important consideration for process implementation. Even though a given water might be kinetically favored based on THM speciation, the resulting THM product toxicity might not allow stable treatment process performance.

Based on total DNA extracted per gram of dry anthracite, no significant difference existed between MCB2 biofilter sections. This analysis indicated that bacteria are distributed equally along a biofilter's length. The similarity in total DNA extracted for each biofilter section might result from backwashing events in which the media was redistributed within a biofilter or from reattachment of detached bacteria from upper to lower biofilter sections.

The backwash batch kinetic tests provided a useful tool to evaluate the biofilm's bacteria. Based on these experiments, the biofilters contained bacteria with similar, yet more efficient, THM kinetics to those seen in the batch kinetic experiments. The biofilm cultures seem to have larger transformation capacities than the batch grown cultures. For biofilters operated with no effluent $TOTNH_3$, backwashing events during normal biofilter operation might have allowed a larger biomass to populate the biofilters through redistribution of bacteria from the biofilter's upper to lower regions. As the biofilter recovered from backwashing events, the lower regions were exposed to substrate initially and not at later times. As a result, the bacteria in the biofilter's lower regions might not have been selected for less efficient THM cometabolism to the extent of the upper regions. Backwash batch kinetic experiments in which the effluent $TOTNH_3$ was zero (MCB1 A1 and A2) had greater $k_{1_{THM}}/k_{TOTNH_3}$ ratios than those conducted with effluent $TOTNH_3$ concentrations at the time of backwashing. For these experiments, the bacteria in the biofilter's lower regions might have skewed the results so that the kinetics seemed greater than they actually were in the active biofilter areas.

Based on the LAB fed Lake Austin water, nutrient limitations might exist when using natural waters. To improve both $TOTNH_3$ and THM degradation, additions of both iron and copper were required with Lake Austin water. Contrasting these results, further experiments seeded with several different source cultures (MCB1 and MCB2) did not show significant effects from the additions of iron, copper, or phosphorus or from nutrient or Lake Austin water feeds. Overall, performance or selection does not seem based specifically on nutrients, source water, or source cultures and most likely results from THM product toxicity

Based on the LAB fed Lake Austin water and various influent monochloramine concentrations, it seems that influent monochloramine concentration of 1 mg/L as Cl_2 (or

less) is a good target for stable operation for a developed biofilm. Because monochloramine addition commenced to a developed biofilm, startup considerations could not be evaluated from these data and require further investigation. The influent monochloramine concentration of 1 mg/L as Cl_2 might be conservative because an increase in influent monochloramine concentration from approximately 1 mg/L to 2.5 mg/L as Cl_2 was made during the experiment. The influent monochloramine concentration of 2.5 mg/L as Cl_2 led to unstable operation, but time did not permit examination of concentrations between 1 mg/L and 2.5 mg/L as Cl_2. As a result, the actual allowable influent monochloramine concentration resides between 1 mg/L to 2.5 mg/L as Cl_2, with the use of 1 mg/L as Cl_2 being conservative.

A simplified THM cometabolism model (Equation 4.1) provided a simple way to compare nitrifiers' THM cometabolism efficiency through calculated $k_{1_{THM}}/k_{TOTNH_3}$ ratios. Table 5.17 summarizes the $k_{1_{THM}}/k_{TOTNH_3}$ ratios determined from batch kinetic experiments, backwash batch kinetic experiments, and biofilter data using Equation 4.1. Overall, the biofilter experiments suggest that for a $\Delta TOTNH_3$ of 2 mg N/L and the ICR water types that total THM removals can initially approach 32-38% (25-31 μg/L total THMs) based on the LAB fed nutrient water. Based on further biofilter experiments (LAB fed Lake Austin water and MCB1 and 2), this initial removal might decline to 11-12% (9-10 μg/L total THMs) over time as bacteria are selected from THM product toxicity. Even if this decreased performance occurs, the 11-12% removal is potentially attractive in drinking water treatment practice. The ability to sustain the initial performance might be enhanced by using GAC as the biofilter media as shown by improving performance of MCB1 Train C for DBCM removal.

Table 5.17 $k_{1_{THM}}/k_{TOTNH_3}$ ratios calculated from batch kinetic, backwash batch kinetic, and biofilter experiments summarized by source culture and experiment type

Source Culture	Experiment	$k_{1_{THM}}/k_{TOTNH_3}$ (L/mg $TOTNH_3$)			
		TCM	BDCM	DBCM	TBM
N. europaea	Batch Kinetic	0.035	0.052	0.070	0.084
	Biofilter	0.14	0.35	0.41	0.48
Lake Austin mixed culture	Batch Kinetic	0.024	0.039	0.049	0.053
	Biofilter LAB Run 1 (Period II)	0.17	0.22	0.26	0.26
	Biofilter LAB Runs 1 and 2	0.13		0.22	
	Biofilter LAB Run 3 (Period X)	0.069			
	Biofilter LAB Run 4 (Period I)	0.072			
	Biofilter MCB2 Train A	0.048	0.063	0.065	0.057
	Biofilter MCB2 Train B	0.050	0.061	0.066	0.054
	Backwash Batch Kinetic MCB2 A	0.061	0.079	0.075	0.056
	Backwash Batch Kinetic MCB2 B	0.070	0.080	0.082	0.068
N. oligotropha enrichment culture	Batch Kinetic	0.039	0.051	0.069	0.089
	Biofilter MCB1 Train B	0.045		0.074	
	Biofilter MCB2 Train C	0.047	0.085	0.070	0.070
	Biofilter MCB2 Train D	0.059	0.076	0.072	0.068
	Backwash Batch Kinetic MCB1 B	0.077	0.086	0.093	0.087
	Backwash Batch Kinetic MCB2 C	0.049	0.094	0.12	0.12
	Backwash Batch Kinetic MCB2 D	0.076	0.10	0.12	0.12
Rio Grande mixed culture	Batch Kinetic	0.037	0.056	0.075	0.087
	Biofilter MCB1 Train A Initial (Final)	0.045		0.38 (0.071)	
	Backwash Batch Kinetic MCB1 A1	0.19	0.18	0.17	0.12
	Backwash Batch Kinetic MCB1 A2	0.18	0.20	0.19	0.12

Chapter 6: Biofilter Modeling

6.1. OVERVIEW

The computer model AQUASIM was used to simulate selected biofilter operating periods. Data from the biofilter experiments and supporting batch kinetic experiments was used in the analyses. In addition, simulations were performed for full-scale biofilters operating under typical conditions for drinking water treatment and at expected THM concentration and speciation to provide a sense of expected process performance in practice.

6.2. TRACER TEST

To better characterize the hydraulic conditions in the experimental biofilters for implementation into the AQUASIM biofilter model, a tracer test was conducted on a biofilter packed with anthracite in an identical way as an experimental biofilter. The test was conducted as described previously with the resulting E-curves shown in Figure 6.1 and Figure 6.2 for the step up and down of the tracer, respectively. The analysis yielded a best fit number of 30- and 25-reactors-in-series for the step up and down data, respectively . Based on this, 28-reactors-in-series was chosen as the number of reactors–in-series to implement into the AQUASIM model as this was the average of the two tracer tests.

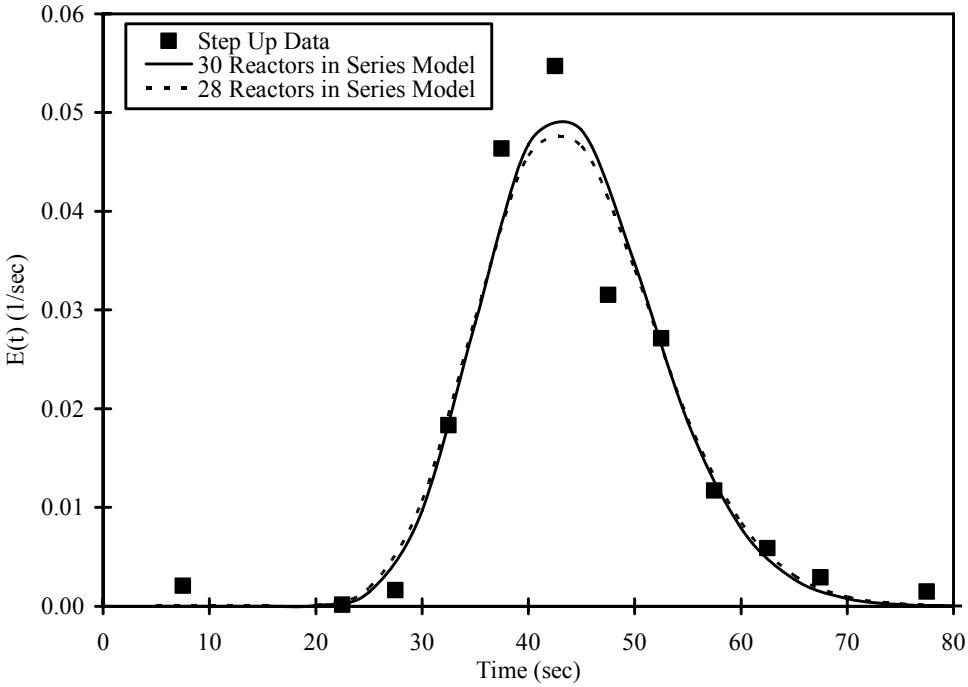

Figure 6.1 Tracer test step up experiment and E-Curves for experimental biofilter

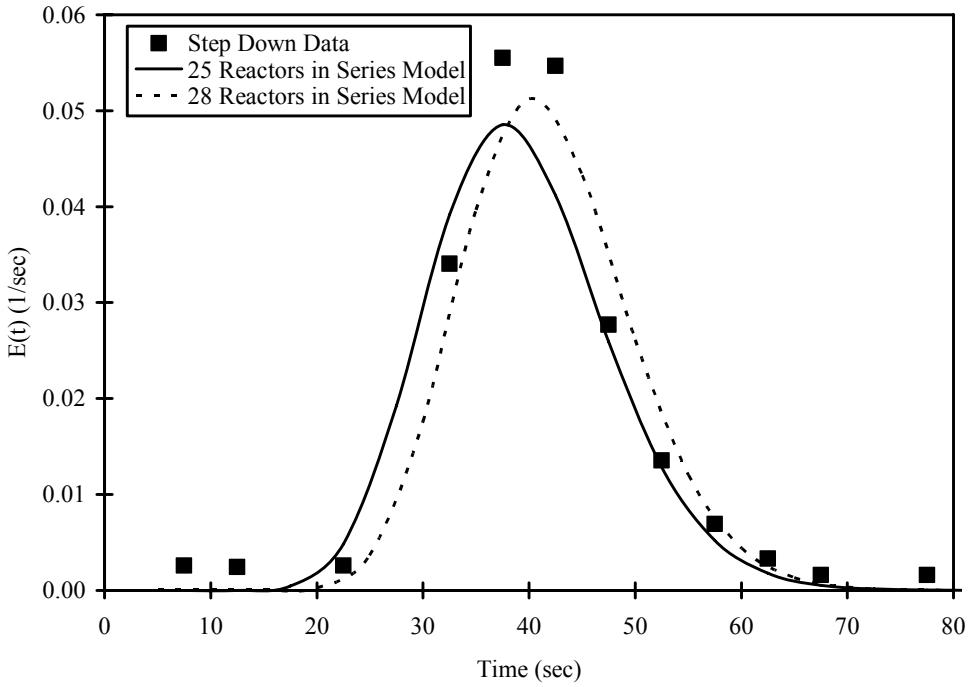

Figure 6.2 Tracer test step down experiment and E-Curves for experimental biofilter

As a check to make certain the AQUASIM model hydraulics corresponded to a reactors-in-series model, an inert tracer was implemented into the AQUASIM model for a 30-reactors-in-series model, simulating the step up tracer test. The modeled effluent concentrations of this step tracer input were used to generate an E-curve from the modeled data. A comparison of the modeled E-curve and the predicted E-curve from the 30-reactors-in-series model is shown as Figure 6.3, detailing the close agreement between the two.

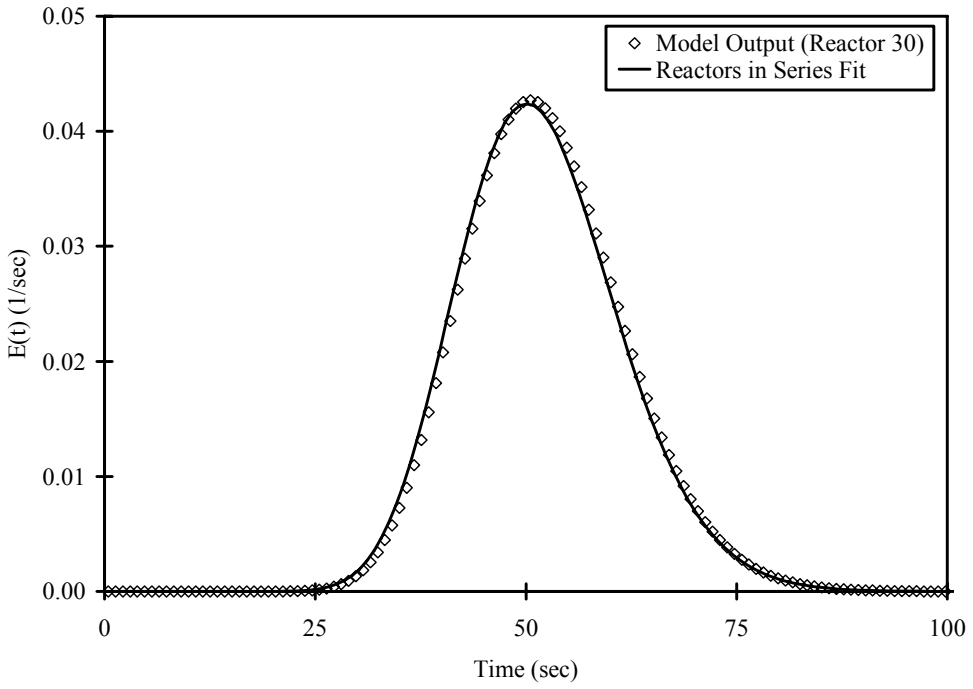

Figure 6.3 Modeled and predicted E-Curve for 30-reactors-in-series implemented into AQUASIM

6.3. KINETIC MODEL

The kinetic model incorporated into AQUASIM was based on a Monod saturation kinetic model for ammonia removal and a reductant model for THM removal that accounted for two limiting reactants, THMs and ammonia-nitrogen (NH_3-N). Because $TOTNH_3$, the sum of the ammonia-nitrogen (NH_3-N) and ammonium-nitrogen (NH_4^+-N) concentrations, is measured analytically, the $TOTNH_3$ concentration was included in the model with a pH correction factor to calculate the NH_3-N concentration. The reductant model (Arcangeli and Arvin 1997) was selected because it was superior to several other models in kinetic studies with *N. europaea* and provided excellent fits to the batch kinetic data collected for the mixed culture nitrifiers (Wahman et al. 2006).

Furthermore, the following assumptions were made: (i) oxygen is not a limiting substrate and was kept at non-limiting levels during the biofilter experiments (in practice, oxygen addition will be required with influent $TOTNH_3$ concentrations greater than 2 mg N/L); (ii) biofilm activity loss from product toxicity is assumed insignificant as the modeled biofilters did not exhibit product toxicity; (iii) the biofilm is homogeneous; (iv) the transport of NH_3-N and THMs from the bulk fluid is governed by external mass-transport resistance through a liquid boundary layer between the bulk fluid and the biofilm (Rittmann and McCarty 2001) and internal mass-transport resistance in the biofilm from molecular diffusion; and (v) the hydraulics of the biofilter can be simulated by a series of completely-mixed reactors.

6.4. MODEL PARAMETERS

To model the inherently nonlinear biofilm system, a software package (AQUASIM) was used (Wanner and Morgenroth 2004). The biofilm model described by Wanner and Reichert (1996) is implemented into AQUASIM as a biofilm reactor compartment (BRC). Based on the tracer studies, experimental biofilters were modeled

as BRCs in series connected by advective links to account for the plug flow conditions of the biofilters. To arrive at apparent steady-state values, the model was run until steady-state conditions were reached (i.e., relaxation of the model), which varied from approximately 70 to 170 days of simulated operation, depending on the modeling conditions.

In AQUASIM, each BRC was selected confined, its biofilm matrix defined as rigid, and its pore volume to contain liquid phase only. Biofilm loss was not controlled by the functionality associated with the BRC but rather through the implementation of a biofilm specific loss rate (b') (Rittmann and McCarty 2001), which uses biofilm thickness, shear stress, and the endogenous decay coefficient to calculate an overall loss rate. The particle radius used for calculation of biofilm area by AQUASIM was the geometric mean of the U.S. standard sieve sizes for the respective filter medias. Other specific required model inputs to characterize transport equations within AQUASIM are summarized in Table 6.1.

During parameter estimation in AQUASIM, the normalized residual sum of squares error between measured and model results were minimized to provide the kinetic parameter estimates. The normalization was achieved by dividing the residual sum of squares by the experimental value squared, resulting in a dimensionless sum of squares error.

Two system configurations were used for modeling purposes based on the computational requirements of the modeling. When possible, the experimental system was modeled as 28-reactors-in-series based on the tracer tests previously described. If this configuration would not work computationally, an alternate arrangement was utilized in which 10-unequal-reactors-in-series were used such that the volume through the first 6-reactors-in-series in both the 28- and 10-reactors-in-series models was similar. The

unequal-reactors-in-series were selected to provide similar changes in liquid phase concentration within in each reactor, providing a better estimation of plug flow reactor performance by using smaller reactor volumes at the influent where reaction rates are greater. Table 6.2 summarizes the reactor volumes for the 10-reactors-in-series model. For the full-scale simulations, the 10-reactors-in-series model was used.

Table 6.1 Model parameters summary

Model parameter	Unit	Value	Source
Ammonia ionization constant	-	$10^{-9.29}$	a
Bicarbonate and carbonic acid equilibrium constant	-	$10^{-6.35}$	a
Diffusivity of TCM in water	m^2/d	8.6×10^{-5}	b
Diffusivity of BDCM in water	m^2/d	8.5×10^{-5}	b
Diffusivity of DBCM in water	m^2/d	8.4×10^{-5}	b
Diffusivity of TBM in water	m^2/d	8.2×10^{-5}	b
Diffusivity of $TOTNH_3$ in water	m^2/d	9.5×10^{-5}	b
Biofilm diffusion to water diffusion coefficients ratio	-	0.80	c
Endogenous decay coefficient	1/d	0.02	This Research
Volatile suspended to total suspended solids ratio	mg VSS/mg TSS	0.80	c
Cell yield coefficient	mg VSS/mg $TOTNH_3$	0.34	c
Maximum bacterial cell density in biofilm	g/m^3	40,000	d

a (Benjamin 2002); b (Montgomery and Welkom 1990); c (Rittmann and McCarty 2001); d (Rittmann 1995)

Table 6.2 Reactor volumes for 10-reactors-in-series model

Reactor number(s)	Percent of total volume in each reactor
1 through 4	2.5
5 and 6	5.0
7	10
8 and 9	20
10	30

6.5. LAKE AUSTIN BIOFILTERS MODELING

Apparent steady-state data from the Lake Austin Biofilters experiment and supporting batch experiments were used to estimate kinetic parameters for TCM, DBCM, and ammonia degradation. Subsequently, the model was verified against other experimental biofilter data. Table 6.3 summarizes the data sets used for parameter estimation (Data Sets 1 through 5) and verification (Data Sets 6 through 11).

In fitting the Lake Austin Biofilters data for estimation of kinetic parameters, the 10-reactors-in-series model was used, because the computational requirements of fitting data with 28-reactors-in-series were excessively long. The verification of the model fits was simulated under both the 10- and 28-reactors-in-series models with no difference in effluent values. In either model, essentially all the degradation was occurring in the first six-reactors-in-series, yielding similar results with either model because of the similar volume through the first six reactors.

Table 6.3 Summary of apparent steady-state performance data for Lake Austin Biofilters

Data Set	Run (Period)	Use	$TOTNH_3$ (mg N/L)		TCM (µg/L)		DBCM (µg/L)		pH		EBCT (min)
			In	Ef[a]	In	Ef	In	Ef	In	Ef	
1	2 (VI)	PE	4.1	0.10	87	50	11	4.5	7.8	6.8	4.0
2	2 (VI)	PE	2.1	-	87	62	12	7.0	7.8	7.0	4.1
3	2 (VII)	PE	2.7	-	87	60	24	14	7.8	6.9	5.2
4	2 (VI)	PE	1.0	-	85	73	11	8.8	7.9	7.4	3.8
5	2 (VII)	PE	1.0	-	91	79	25	20	7.9	7.4	3.9
6	2 (I)	V	4.1	-	52	32	-	-	7.8	6.7	4.1
7	2 (V)	V	4.2	-	-	-	23	8.3	7.8	6.8	4.0
8	2 (I)	V	2.1	-	54	37	-	-	7.8	7.1	4.3
9	2 (V)	V	2.0	-	-	-	23	16	7.8	7.0	3.8
10	2 (I)	V	1.0	-	54	44	-	-	7.9	7.4	4.1
11	2 (V)	V	1.0	-	-	-	23	19	7.9	7.4	3.9

In = Influent

Ef = Effluent

PE = Parameter estimation

V = Verification

EBCT = Empty bed contact time

- = No data

[a]Effluent assumed to be 0.10 mg N/L $TOTNH_3$ based on quantification limit

6.5.1. Kinetic Parameter Estimation

Because the measured effluent total ammonia-nitrogen ($TOTNH_3$) from the biofilter experiments was less than quantification limits (0.10 mg N/L) for all samples, a method to determine appropriate ammonia kinetic parameters (k_{TOTNH_3} and $K_{s_{NH_3\text{-}N}}$) in the modeling was required. $TOTNH_3$ represents the sum of ammonia-nitrogen (NH_3-N) and ammonium-nitrogen (NH_4^+-N). At first, the previously-determined k_{TOTNH_3} (2.9 mg $TOTNH_3$/mg TSS-day) and $K_{s_{NH_3\text{-}N}}$ (0.080 mg/L NH_3-N) parameter values for this mixed culture were used in the modeling (Wahman et al. 2006). Unfortunately, with these kinetic parameter values the model could not simulate the low effluent $TOTNH_3$ concentrations (< 0.10 mg N/L) seen in the biofilter experiments; rather, the modeled effluent $TOTNH_3$ concentrations ranged from 0.51 to 1.8 mg N/L.

For biofilm reactors, the minimum steady-state effluent concentration of the limiting growth substrate is given by S_{min}, as shown in Equation 6.1 (Rittmann and McCarty 2001). S_{min} is dependent on the ammonia maximum specific rate of degradation (k_{TOTNH_3}), cell yield (Y), ammonia half-saturation constant ($K_{s_{NH_3\text{-}N}}$), and the biofilm specific loss rate (b').

$$S_{min,NH_3-N} = K_{S_{NH_3-N}} \frac{b'}{Yk_{TOTNH_3} - b'} \qquad (6.1)$$

The value of $S_{min,\ NH_3\text{-}N}$ was too large to simulate the observed effluent concentration when k_{TOTNH_3} and $K_{s_{NH_3\text{-}N}}$ values from previous batch kinetic experiments were used as model inputs. To compensate for this problem, k_{TOTNH_3} was held at its previously determined value from the batch kinetic experiments, and $K_{s_{NH_3\text{-}N}}$ was estimated by fitting the AQUASIM model for ammonia to Data Set 1 (Table 6.3) and

assuming that the effluent $TOTNH_3$ concentration was 0.10 mg N/L (the quantification limit of $TOTNH_3$ in the biofilter experiments). Data Set 1 was chosen because the effluent pH of this experiment was the lowest of the experiments used in parameter estimation, and as shown by Equation 6.2, the biofilter with the lowest effluent pH would have the greatest effluent $TOTNH_3$ concentration for a given $S_{min,\ NH_3\text{-}N}$.

$$\frac{S_{min,NH_3-N}}{\alpha_1} = S_{min,TOTNH_3} \qquad (6.2)$$

Data Set 1 also had the greatest influent $TOTNH_3$ concentration of any fitted experiment, which in combination with the lowest effluent pH made it the logical choice for estimating $K_{s_{NH_3\text{-}N}}$. The estimated value for $K_{s_{NH_3\text{-}N}}$ and the previously-determined value for k_{TOTNH_3} were then used as model inputs to estimate the THM kinetic parameters. Five sets of apparent steady-state data (Table 6.3) were simultaneously fit in AQUASIM to provide THM kinetic parameter estimates for TCM and DBCM. Kinetic parameters for BDCM and TBM degradation in the biofilters were estimated from the results of previously-conducted batch kinetic tests. The BDCM and TBM rate constants from the batch kinetic tests were multiplied by the ratio of the DBCM rate constants from the biofilter and the batch kinetic tests to adjust the BDCM and TBM kinetic parameters to the conditions of the biofilters.

Table 6.4 Estimated kinetic parameters from Lake Austin Biofilters experiments

Parameter	Unit	Value	Standard Deviation
k_{TOTNH_3}	mg $TOTNH_3$/mg TSS–Day	2.9	0.29[a]
$K_{s_{NH_3\text{-}N}}$	mg/L NH_3-N	0.0027	3.5×10^{-5}
$k_{1_{TCM}}$	L/mg TSS–day	0.50	0.010
$k_{1_{DBCM}}$	L/mg TSS–day	0.87	0.012
$k_{1_{BDCM}}$	L/mg TSS–day	0.69	N/D[b]
$k_{1_{TBM}}$	L/mg TSS–day	0.92	N/D[b]

[a]Assumed as 10% of the value

[b]N/D = Not determined

Estimated values for $TOTNH_3$ and THM kinetic parameters are summarized in Table 6.4 along with their standard deviations calculated by AQUASIM during the estimation procedure. Rittmann and McCarty (2001) report typical ammonia maximum specific degradation rates (k_{TOTNH_3}) of 2.3 and 3.1 mg/mg-d at 20 and 25°C, respectively. The previously determined value of 2.9 mg $TOTNH_3$/mg TSS-day, measured at 23-24°C, compares well with these reported values. Values of K_s in the literature are typically reported as $TOTNH_3$, not NH_3-N, and as such have a much greater value because NH_3-N is a fraction (approximately 0.5 to 33%) of $TOTNH_3$ at typical pH values (7 to 9). In addition, K_s was used as a fitting factor in the biofilter experiments to account for the simplifications inherent in modeling the complex nature of biofilms. The key simplifications in the current model implementation are that it:

1. uses an overall biofilm loss calculation ($b^{'}$) to implement biofilm detachment and decay. It does not account for biomass reattachment in lower biofilter sections after initial detachment (i.e., all detached biomass is assumed lost from the biofilter in the effluent);
2. does not account for the loss and redistribution of biomass during backwash events;
3. is modeled as a homogeneous and not heterogeneous (i.e., multispecies) biofilm. Implementation of heterotrophic bacteria would allow modeling of the spatial distribution of both the nitrifiers and heterotrophs present in the biofilm;
4. uses literature values for yield and biomass density; and
5. assumes batch kinetic parameters determined for suspended growth cultures are representative of the biofilm attached growth biomass.

The THM kinetic parameters were considerably larger (approximately 600%) than those previously determined in batch kinetic studies for mixed-culture nitrifiers grown in suspension (Wahman et al. 2006). A possible explanation for the difference in THM kinetic parameters is the growth conditions of the cultures. In the batch kinetic experiments, the cultures were grown in batch for three days at large initial $TOTNH_3$ concentrations (approximately 700 mg N/L) and then batch kinetic analyses were performed. The experiments modeled herein were biofilms with maximum influent $TOTNH_3$ concentrations of approximately 4 mg N/L and operating for approximately 3,000 hours.

Another explanation is that the value of k_{TOTNH_3} from the batch kinetic experiments was directly implemented in the model and assumed representative of the

biofilm biomass. As seen in the previous batch kinetic experiments and shown by a sensitivity analysis later in this chapter (6.5.2 Sensitivity Analysis), $k_{1_{THM}}$ and k_{TOTNH_3} are inversely correlated. If the actual biofilm k_{TOTNH_3} was significantly different from the implemented k_{TOTNH_3}, a corresponding change in $k_{1_{THM}}$ would also be seen. Therefore, the kinetic ratio $k_{1_{THM}}/k_{TOTNH_3}$ provides a better comparison of AQUASIM modeling to batch kinetic experiment results.

The possibility of a substantially greater kinetic rate ratio under biofilm conditions was confirmed experimentally from biofilm performance data as well as backwash batch kinetic tests performed during the Mixed Culture Biofilters 1 and 2 (Chapter 5, Table 5.17). Comparing the $k_{1_{THM}}/k_{TOTNH_3}$ kinetic ratios, the AQUASIM modeling results provided kinetic ratios of 0.17 and 0.30 L/mg $TOTNH_3$ for TCM and DBCM, respectively. Kinetic ratios from the backwash batch kinetic tests reached 0.20 L/mg $TOTNH_3$ in some instances. In addition, when the LAB data was fit with the simplified model (Equation 4.1) in Chapter 5, the kinetic ratios were 0.13 and 0.22 L/mg $TOTNH_3$ for TCM and DBCM, respectively. It would be expected that the simplified model would underestimate this ratio because the AQUASIM model takes into account diffusion (i.e., for a given $TOTNH_3$ removal and k_{TOTNH_3}, the THM removal rate will need to be greater if diffusion is taken into account). Overall, the backwash batch kinetic experiments produced kinetic rate ratios ranging from values measured previously in batch kinetic studies to those estimated in the current AQUASIM modeling, thereby illustrating that the variability in degradation rates in biofilms can be considerable.

The parameter estimation step was checked by conducting model simulations for Data Sets 1 through 5 with the estimated kinetic parameters as inputs. In each instance, the simulated effluent values showed a very good agreement with the experimental data,

and all the THM experimental values were within the 95% confidence limits (± 3 to 14%) for these effluent values (Figure 6.4), thereby confirming the model calibration.

6.5.2. Sensitivity Analysis

AQUASIM can be used to perform a sensitivity analysis on parameters if their standard deviations are provided; AQUASIM varies the parameters independently to assess how these changes affect the model results. As a representative example of the five fitted data sets, a sensitivity analysis was conducted for Data Set 1 using the kinetic parameters k_{TOTNH_3}, $K_{s_{NH_3\text{-}N}}$, $k_{1_{TCM}}$, and $k_{1_{DBCM}}$. The standard deviations calculated from parameter estimation (Table 6.4) were used for the sensitivity analysis without adjustment. Because k_{TOTNH_3} was not estimated by AQUASIM, a standard deviation for k_{TOTNH_3} of 10% of its value was used because this was representative of the confidence interval seen in the batch kinetic tests (Wahman et al. 2006), and 10% of the value is recommended by Reichert (1998a) when a standard deviation is not estimated by AQUASIM.

AQUASIM provides four sensitivity functions to perform sensitivity analysis. For the analysis presented here, the absolute-relative sensitivity function (Sens AR) was used. The Sens AR represents the absolute change in an arbitrary variable (i.e., effluent steady-state $TOTNH_3$ or THM effluent concentrations) for a 100% change in a model parameter (i.e., k_{TOTNH_3}, $K_{s_{NH_3\text{-}N}}$, $k_{1_{TCM}}$, or $k_{1_{DBCM}}$). The results of the sensitivity analysis are presented in Table 6.5, detailing the effect of the different kinetic parameters on effluent concentrations.

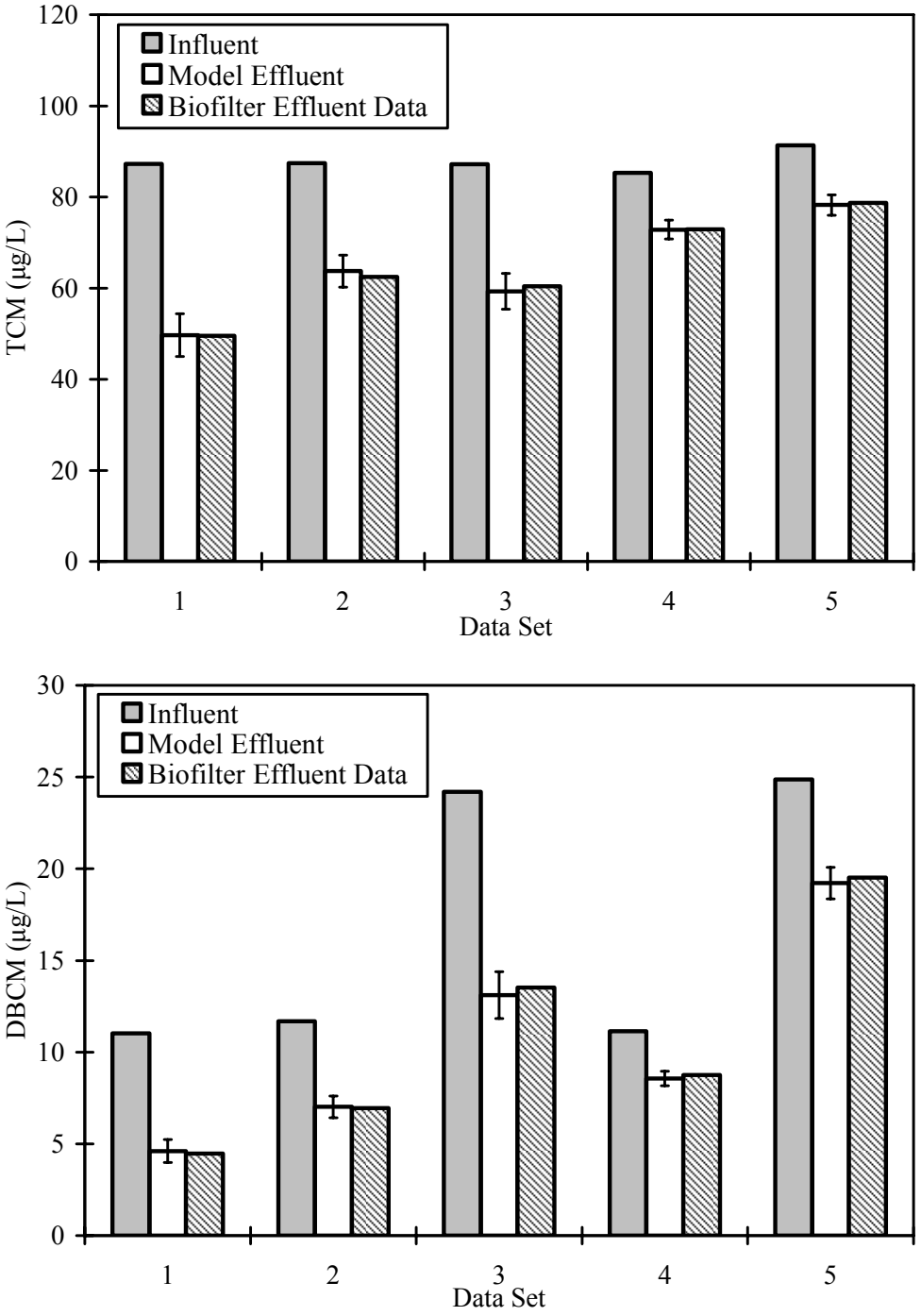

Figure 6.4 Predicted TCM and DBCM concentrations based on fitted parameters for Lake Austin Biofilters

Table 6.5 Absolute-Relative Sensitivity (Sens AR) values for Lake Austin Biofilters Data Set 1

Parameter	Variable Effect (Value)		
	$TOTNH_3$ (mg N/L)	TCM (µg/L)	DBCM (µg/L)
k_{TOTNH_3}	++ (-0.11)	++ (23)	++ (3.1)
$K_{s_{NH_3\text{-}N}}$	++ (0.10)	+ (0.078)	+ (-0.03)
$k_{1_{TCM}}$	-	++ (-23)	-
$k_{1_{DBCM}}$	-	-	++ (-3.0)

-, insignificant effect

+, moderate effect

++, significant effect

As expected and as shown in Table 6.5, the individual THM rate constants and k_{TOTNH_3} are inversely correlated and affect effluent THM concentrations in opposing manners (i.e., an increase in the THM rate constant decreases the concentration while an increase in k_{TOTNH_3} increases the concentration). This effect is expected from the THM rate equation because of its dependence on $TOTNH_3$ concentration. In addition, as expected for effluent $TOTNH_3$ concentration, k_{TOTNH_3} and $K_{s_{NH_3\text{-}N}}$ are inversely correlated. To provide further insight, a qualitative ranking (i.e., insignificant, moderate, or significant) of each kinetic parameter's effect on the predicted effluent concentrations was determined based on the relative values of the Sens AR function in Table 6.5.

The sensitivity of the model to the assumed effluent concentration of 0.10 mg N/L as $TOTNH_3$ was also checked by repeating the parameter estimation step for Data Set 1, assuming an effluent $TOTNH_3$ value of 10% of the quantification level (i.e., 0.01 mg N/L as $TOTNH_3$). As expected based on S_{min} (Equation 6.1), this resulted in an estimated

$K_{s_{NH_3\text{-}N}}$ being only 10% of the originally determined value. No change in the estimated THM rate constants occurred because of this change with determined rate constants of 0.50±0.012 and 0.87±0.014 L/mg-day for TCM and DBCM, respectively, confirming the approach used to estimate the THM parameters.

6.5.3. Model Verification

To verify that the model was accurately representing the biofilter system, the estimated kinetic parameters were used to simulate six other operating conditions (Table 6.3) of the biofilters. The measured and simulated THM effluent concentrations for this verification process are detailed in Figure 6.5 along with the 95% confidence limits for the effluent THM concentrations. As with the effluent THM data presented for parameter estimation, the effluent data in this verification process was not statistically different from the experimentally measured effluent THM values.

6.6. MIXED CULTURE BIOFILTERS 1 AND 2 SIMULATIONS

Similar to the verification of the Lake Austin Biofilter data, apparent steady-state data from the Mixed Culture Biofilters 1 and 2 experiments and supporting kinetic data from the corresponding backwash batch experiments were used to simulate the experimental operating periods summarized in Table 6.6. These simulations were used to evaluate the ability of the model to predict performance using the kinetic parameters determined in the backwash batch kinetic experiments. The simulations were performed using the 28-reactors-in-series model discussed previously.

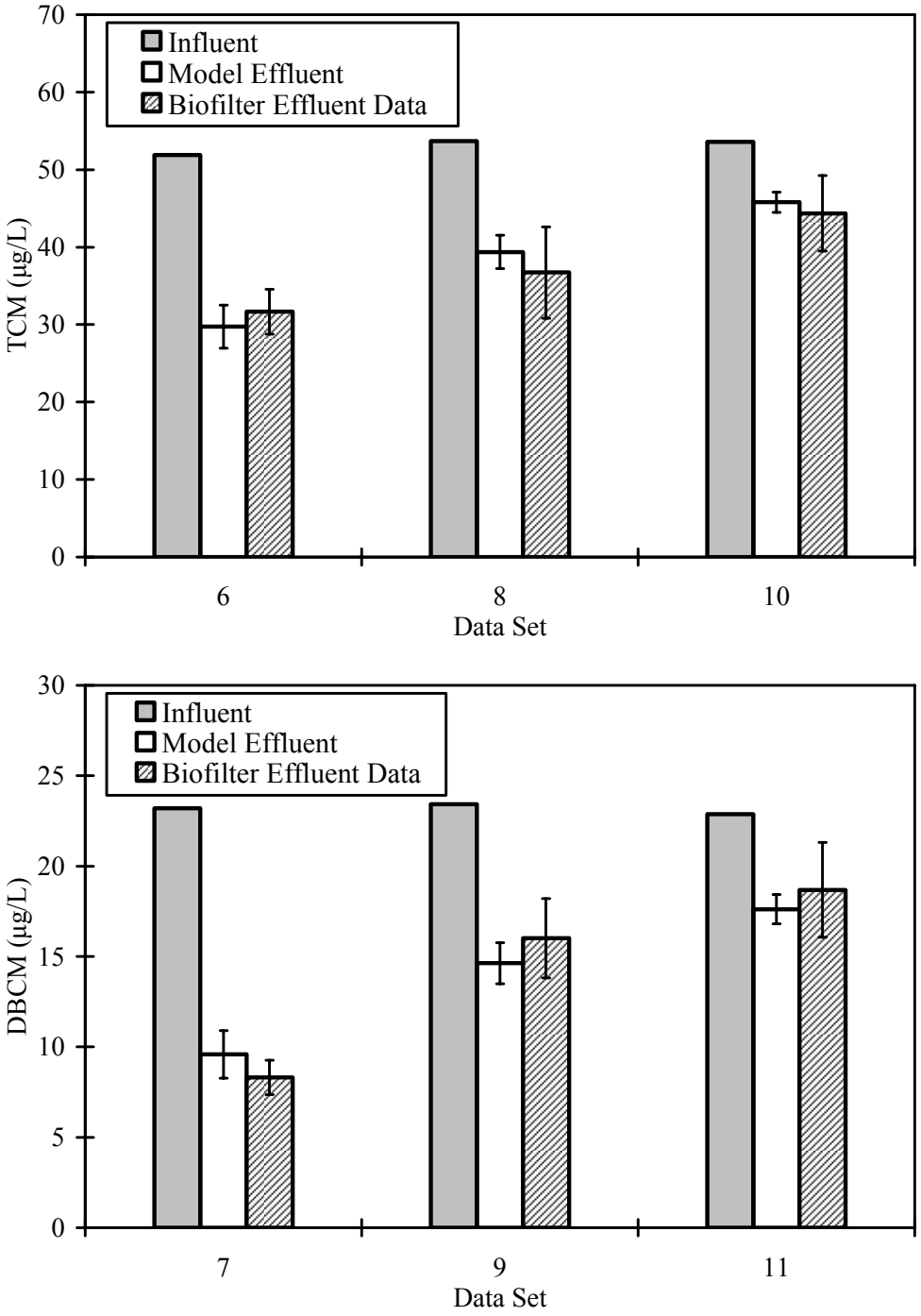

Figure 6.5 Model verification comparison of model and Lake Austin Biofilters THM data

Table 6.6 Summary of apparent steady-state performance data for Mixed Culture Biofilters 1 and 2

Data Set	MCB (Train)	Run (Period)	$TOTNH_3$ (mg N/L)		TCM/BDCM/DBCM/TBM (µg/L)								pH		EBCT (min)
			In	Ef	Influent				Effluent				In	Ef	
12	1 (A)	1(III/IV)	4.2	0.10[a]	104	-	-	-	87	-	-	-	7.9	6.9	4.6
13	1 (A)	2 (I/II)	2.2	0.10[a]	112	-	-	-	99	-	-	-	8.0	7.2	2.4
14	1 (A)	3 (IV)	2.7	0.10[a]	126	-	29	-	109	-	24	-	8.2	7.1	3.1
15	1 (B)	1 (IV)	4.0	0.10[a]	106	-	-	-	88	-	-	-	8.0	6.9	4.4
16	1 (B)	2 (I)	2.1	0.10[a]	111	-	-	-	102	-	-	-	8.0	7.2	2.3
17	1 (B)	3 (IV)	2.1	0.14	119	-	27	-	109	-	23	-	8.2	7.2	2.6
18	2 (B)	1 (I)	4.3	1.8	54	-	27	-	47	-	22	-	8.1	7.2	1.2
19	2 (B)	2 (II)	4.1	1.6	15	15	15	16	13	13	13	14	7.8	7.0	1.1
20	2 (C)	1 (I)	4.1	0.88	54	-	25	-	44	-	20	-	8.1	7.1	1.2
21	2 (C)	2 (II)	4.4	1.6	15	15	15	16	13	12	12	13	7.9	6.9	1.1

In = Influent

Ef = Effluent

EBCT = Empty bed contact time

- = No data

[a]Effluent assumed to be 0.10 mg N/L $TOTNH_3$ based on quantification limit

As with the Lake Austin Biofilters modeling, the effluent $TOTNH_3$ concentrations were overpredicted by the model using the backwash batch kinetic parameters as inputs. To reduce the effluent $TOTNH_3$ to the measured values, the $K_{s_{NH_3\text{-}N}}$ was adjusted until the effluent $TOTNH_3$ matched the biofilter data. The $TOTNH_3$ concentrations for the

adjusted $K_{s_{NH_3\text{-}N}}$ are detailed in Figure 6.6. In addition, the kinetic parameters used in the simulations are summarized in Table 6.7.

After matching the effluent $TOTNH_3$ concentrations, simulations were performed to evaluate the ability of the model to predict the measured effluent THM concentrations. The measured and simulated THM effluent concentrations for these simulations are detailed in Figure 6.7 along with the 95% confidence limits for the effluent THM concentrations. For the majority of the THMs and data sets, the modeled effluent data were not statistically different from the experimentally measured effluent THM values, indicating the model's ability to predict performance with the backwash batch kinetic parameters as inputs. This follows the results obtained when modeling the Lake Austin Biofilters in that if the effluent $TOTNH_3$ concentrations are matched, excellent estimates of the THM effluent concentrations are obtained with the model.

Data Sets 12 through 14 provided the poorest AQUASIM model fits to the experimental data and correspond to data from MCB1 Train A. As explained in Chapter 5, one possible explanation for the lack of agreement between the MCB1 Train A AQUASIM modeling and biofilter data is that Train A was completely removing $TOTNH_3$ at the time of backwashing as opposed to the other trains simulated (Table 6.7). Only a portion of the biofilter would be active in this situation. Therefore, the biomass located in the lower regions of Train A might have only been partly selected for less efficient THM degraders because of THM product toxicity. The Train A backwash kinetic tests might have been conducted with a combination of selected, less efficient and unselected, more efficient THM degrading bacteria located in the biofilter's upper and lower regions, respectively. The net effect is a misrepresentation of the kinetics of the active biomass in the filter.

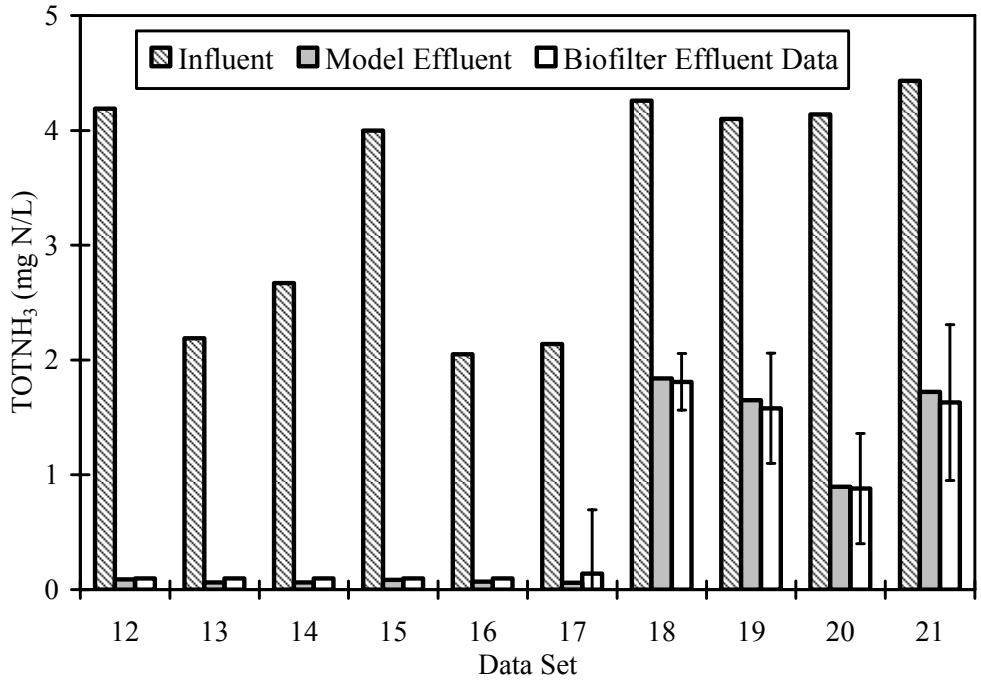

Figure 6.6 Predicted $TOTNH_3$ effluent concentrations based on backwash batch kinetic parameters using adjusted $K_{s_{NH_3\text{-}N}}$ compared to biofilter effluent data

Table 6.7 Kinetic parameter summary for Mixed Culture Biofilters 1 and 2 simulations

Data Set (Exp.)	k_{TOTNH_3} (mg $TOTNH_3$/mg TSS–Day)	$K_{s_{NH_3\text{-}N}}$ (mg NH_3-N/L)		$k_{1_{THM}}$ (L/mg TSS–day)			
		Original	Adjusted	TCM	BDCM	DBCM	TBM
12-14 (MCB1 A)	1.5	0.029	0.0012	0.28	0.28	0.28	0.18
15-17 (MCB1 B)	0.83	0.21	0.00052	0.064	0.072	0.078	0.072
18 (MCB2 B)	2.1	0.10	0.029	0.15	0.17	0.17	0.14
19 (MCB2 B)			0.020				
20 (MCB2 C)	1.9	0.24	0.0074	0.092	0.18	0.22	0.22
21 (MCB2 C)			0.016				

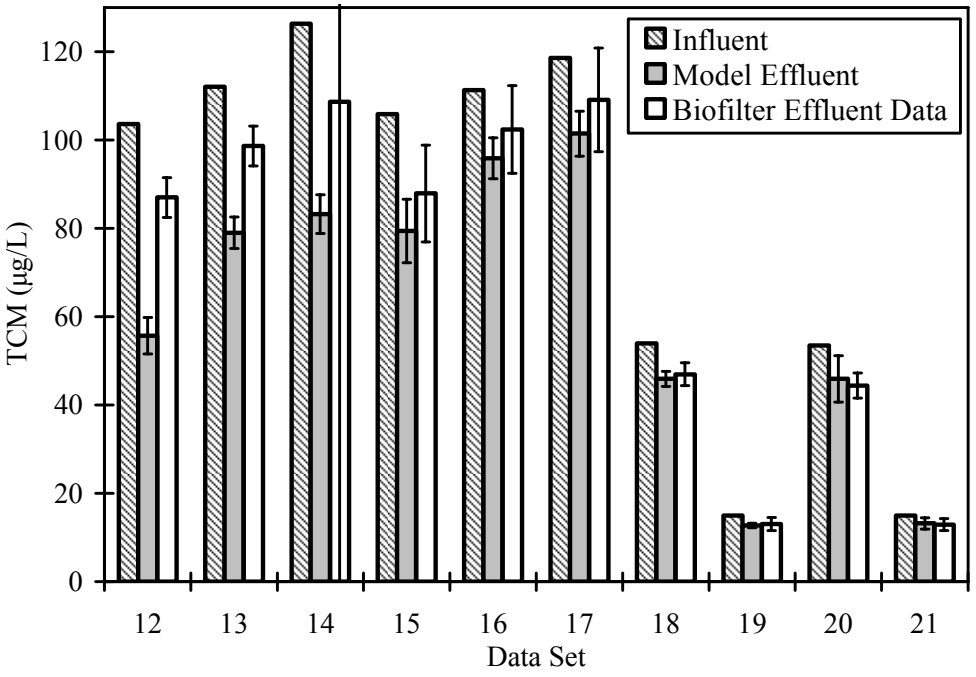
Influent
Model Effluent
Biofilter Effluent Data
TCM (µg/L)
0
20
40
60
80
100
120
12
13
14
15
16
17
18
19
20
21
Data Set

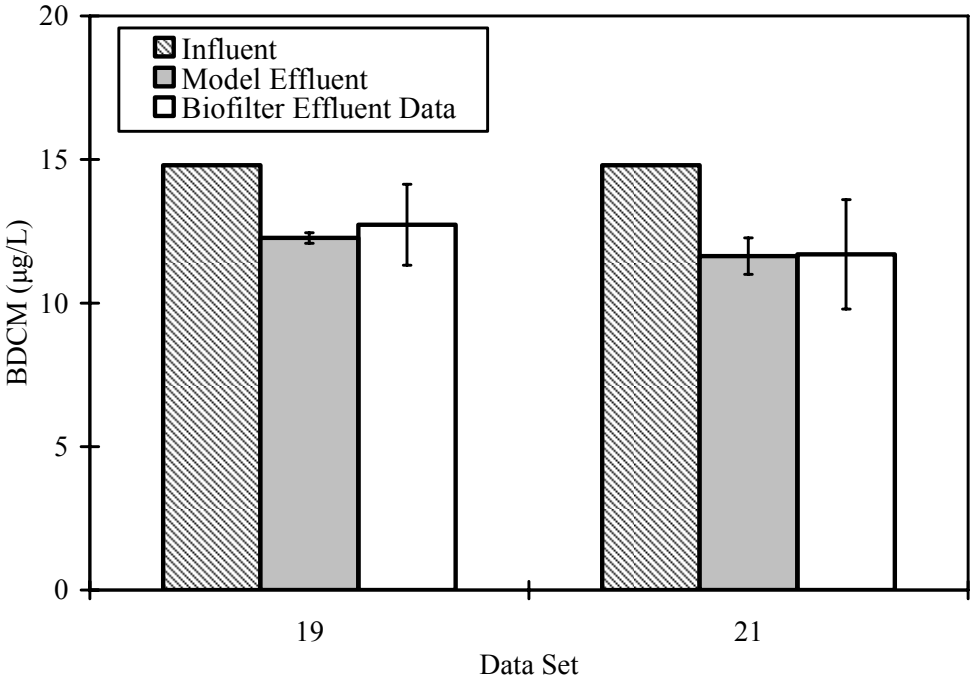
Influent
Model Effluent
Biofilter Effluent Data
BDCM (µg/L)
0
5
10
15
20
19
21
Data Set

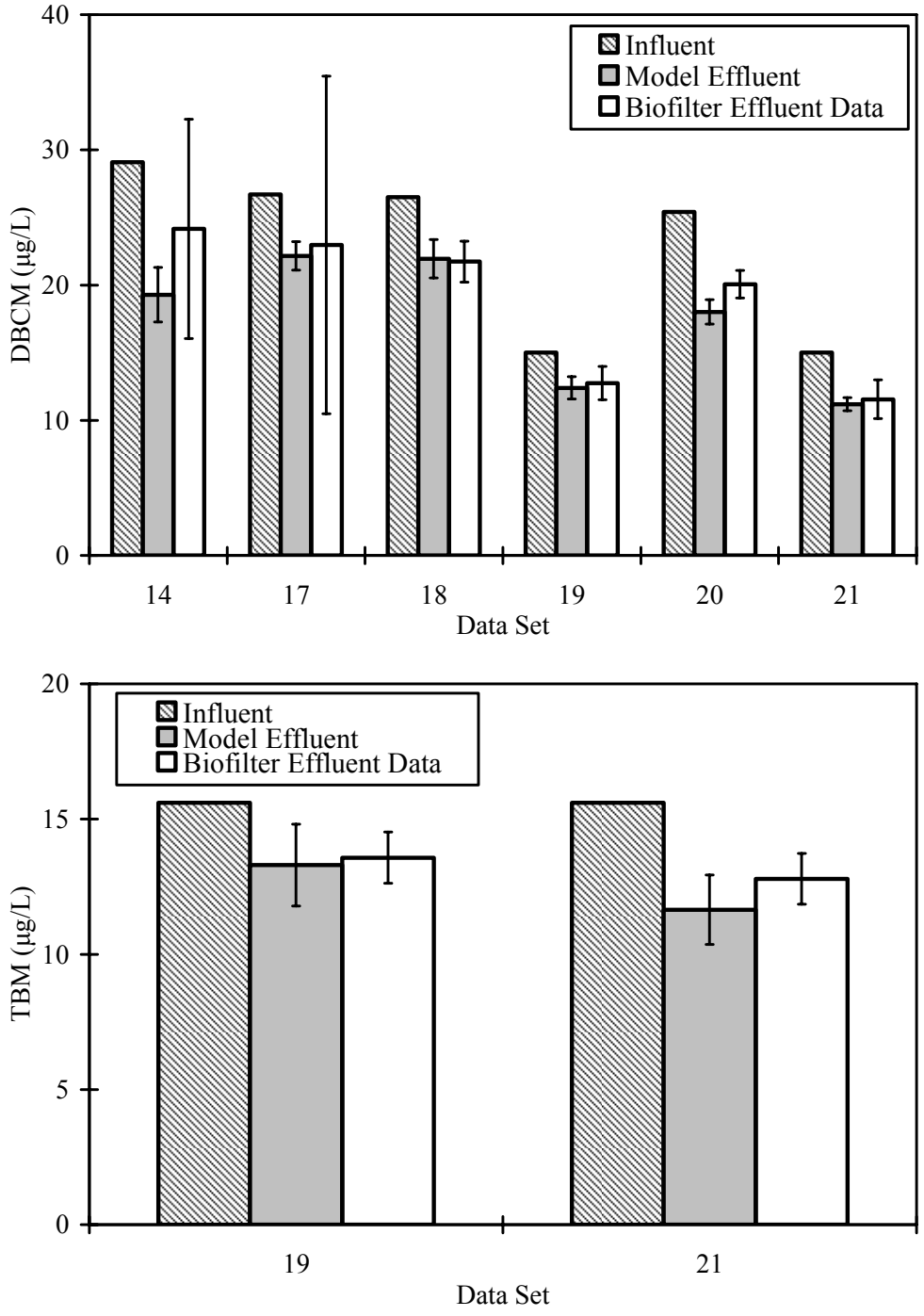

Figure 6.7 Predicted THM effluent concentrations based on backwash batch kinetic parameters and adjusted $K_{s_{NH_3\text{-}N}}$ for Mixed Culture Biofilters 1 and 2 simulations

6.7. MODEL BIOMASS PREDICTIONS

To evaluate the model's ability to predict the biomass profile, the molecular analysis results for the MCB2 were compared with the modeled biomass for Data Sets 19 and 21. The modeled biomass profiles were generated with the adjusted $K_{s_{NH_3\text{-}N}}$ values (Table 6.7) used in the MCB2 simulations for Data Sets 19 and 21. The experimentally determined biomass profiles assume that the AOB present in the biofilm will be a constant percentage of total DNA extracted. Figure 6.8 details a comparison of the measured and modeled biomass profiles along the biofilter's length. To provide a common base of comparison because of the unknown DNA extraction efficiency, each data set was either normalized by the first reactor in series for the model results or the first section for the experimental results.

It is evident that the model did not capture the biofilter's actual biomass profile (Figure 6.8). The model predicted a decrease in the biomass along its length whereas the DNA results did not provide evidence for this decrease. The discrepancy between the model and DNA results is most likely a result of a combination of the model not accounting for backwash events redistributing the media and not allowing for reattachment of detached bacteria. Both of these would allow for a redistribution of biomass over time.

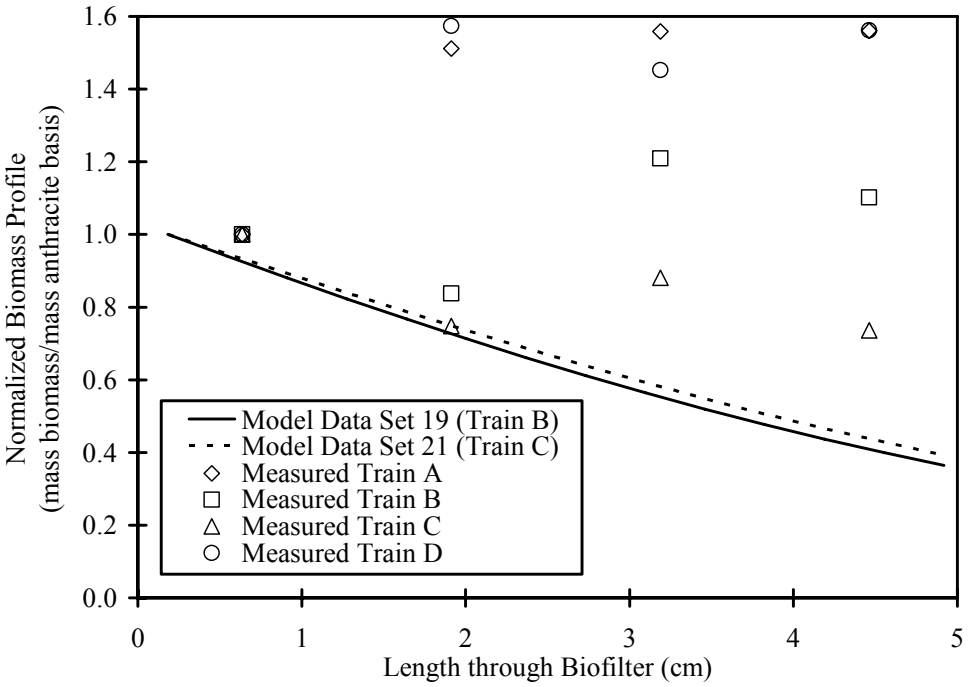

Figure 6.8 Normalized biomass profile comparison for model biomass and total DNA extracted

To predict effluent $TOTNH_3$ concentrations, the modeling required the experimentally determined $K_{s_{NH_3\text{-}N}}$ to be reduced. To evaluate whether modifications to biofilter biomass would allow implementation of the experimentally determined $K_{s_{NH_3\text{-}N}}$, Data Sets 19 and 21 were reanalyzed by adjusting the biofilm profile, the total biofilm mass present (by changing the biofilm density), or both. Models were poised with the desired initial conditions, biomass decay and detachment were disabled, and steady-state simulations were conducted with unadjusted backwash batch kinetic parameters. Figure 6.9 summarizes the results of this analysis for each of these conditions:

1. Influent – influent $TOTNH_3$ for all model simulations;
2. Biofilm Data – experimental effluent $TOTNH_3$ concentrations;
3. Baseline Model – effluent $TOTNH_3$ model predictions with direct implementation of backwash batch kinetic parameters and no biofilm adjustments;
4. Average Biofilm Thickness - effluent $TOTNH_3$ model predictions when the total biomass simulated with the Baseline Model was redistributed to create a constant biofilm thickness in the modeled biofilter;
5. Scaled Biofilm Density - effluent $TOTNH_3$ model predictions when the simulated biomass profile with the Baseline Model was implemented and the biofilm density was scaled to increase total biomass present. The biofilm density was increased in the same proportion as $K_{s_{NH_3\text{-}N}}$ (Table 6.7) was decreased to predict experimental effluent $TOTNH_3$ concentrations; and
6. Average Biofilm Thickness and Scaled Density – effluent model $TOTNH_3$ predictions when both the biofilm thickness and density were adjusted.

Figure 6.9 indicates that simulation of the biofilter with a constant biofilm thickness did not lead to a substantial improvement in predicted effluent $TOTNH_3$ concentrations. Rather, Figure 6.9 indicates that an increase in total biomass present led to a better prediction of effluent $TOTNH_3$ concentrations. Future efforts should focus on correlating total biofilter biomass with modeled biomass. Possible modifications to increase the total biomass present include adjustments to the model for reattachment of detached bacteria, redistribution of biomass through backwashing, and reevaluation of the literature values for yield and biomass density.

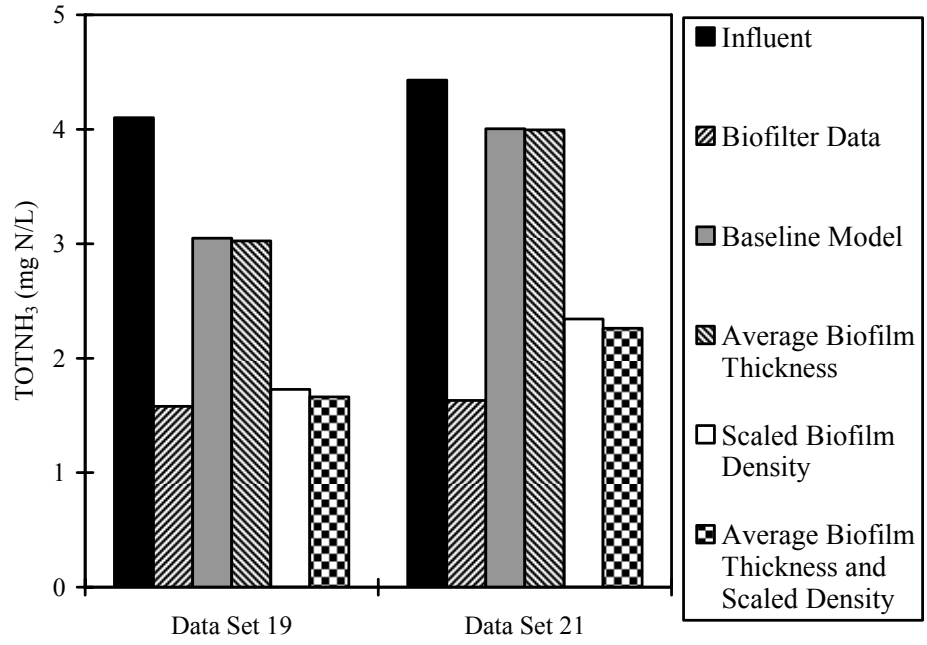

Figure 6.9 Model biofilm biomass adjustments and affect on prediction of effluent $TOTNH_3$ concentrations

6.8. FULL-SCALE MODEL SIMULATIONS

After the kinetic parameter estimations, model verifications, and simulations to verify backwash batch kinetic parameters, a series of model simulations was performed on a full-scale filter. The purpose of the simulations was to estimate the performance of a full-scale operating filter at a drinking water treatment plant under typical conditions. Relevant operational parameters for the simulated full-scale biofilter system are summarized in Table 6.8. The full-scale biofilter simulations were chosen to represent a typical full-scale operating filter in a drinking water treatment plant, operating at average and peak flow conditions. As such, the chosen parameters for the full-scale biofilter fall in the range of typical values reported for rapid filtration where filter depths range from 2-6 feet and surface loading rates (SLRs) range from 2-6 gpm/ft^2 (MWH et al. 2005). In

addition, the selected full-scale filter at peak flow is representative of the experimental biofilters when scaled by the method of Manem and Rittmann (1990) previously summarized in Chapter 5 for the Lake Austin Biofilters.

Two filter-loading conditions were simulated based on average (2 gpm/ft^2) and peak (4 gpm/ft^2) SLRs. In addition, the three typical types of influent THM speciation were modeled (ICR water types 1, 2, and 3) along with three different influent $TOTNH_3$ concentrations (1, 2, and 4 mg N/L). To provide the range of expected THM removals, two different sets of THM kinetic parameters were utilized corresponding to removals seen with the Lake Austin Biofilters and those seen with the Mixed Culture Biofilters 2.

Table 6.8 Simulated full-scale filter parameter summary

Parameter	Unit	Full-scale Filters	
		Average	Peak
Surface loading rate	gpm/ft^2 (m/d)	2.0 (120)	4.0 (240)
Empty bed contact time	minutes	15	7.5
Volume	ft^3 (m^3)	690 (20)	
Depth	feet (m)	4.0 (1.2)	
Porosity	-	0.40	
Influent pH	-	8.0	
Alkalinity	mg/L as $CaCO_3$	200	
Media size (U.S. standard sieve size)	-	12 x 40	
Temperature	ºC	23-24	

Figure 6.10 and Figure 6.11 summarize the total THM removal under these various conditions for the full-scale filter simulations at steady-state. For all THM influent conditions, essentially no difference in total THM removal occurred when the filter SLR was changed from 2 to 4 gpm/ft^2 at steady-state. The nearly identical THM removals occurred because $TOTNH_3$ removal was essentially complete for both conditions, thus supporting the maximum possible THM cometabolism in both instances. Also, an increase in total THM removal was predicted as the THM speciation changed from water type 1 to 3 (Figure 6.10 and Figure 6.11); the more rapid THM degradation kinetics as the degree of bromine substitution increases (Table 6.4 and Table 6.7) account for this result. Compared with water type 1, total THM removals in water types 2 and 3 increased 6-20% and 7-30%, respectively. As the THM speciation becomes more bromine-substituted, product toxicity issues might become a concern and are not accounted for in the current model. An increase in total THM removal also was predicted as the influent $TOTNH_3$ concentration increased, as would be expected from the increased availability of growth substrate and the associated larger biomass in the filter. Because of the nonlinear nature of the kinetics, the increase in THM removal was somewhat less than proportion to the increase in $TOTNH_3$ concentration. Overall, a total THM removal of 9 to 54% was seen in the simulations, which illustrates the potential of THM cometabolism to have a significant impact on treated water quality.

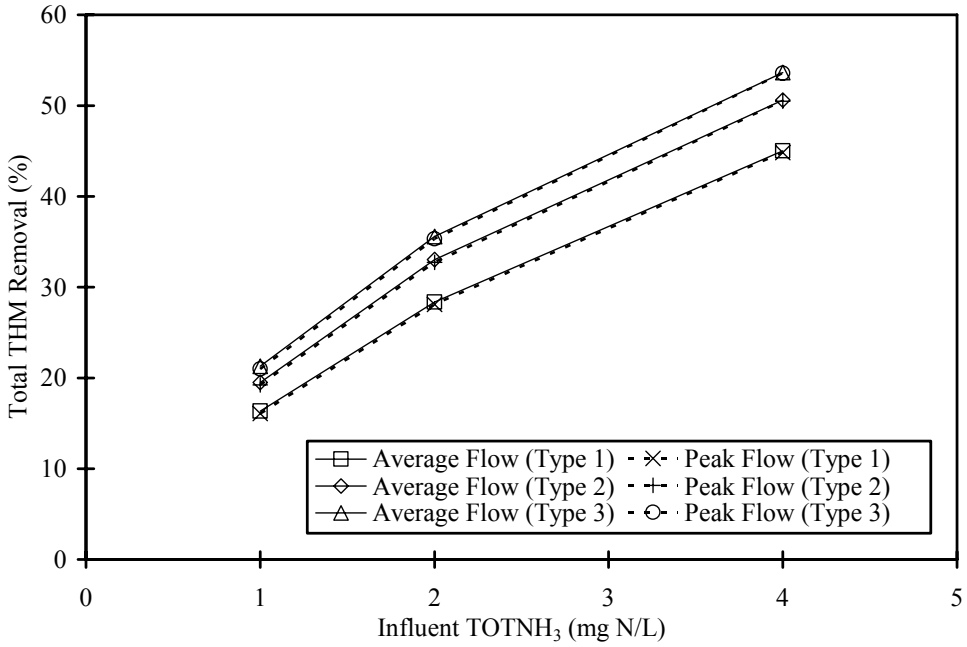

Figure 6.10 Full-scale model simulation total THM percent removal with Lake Austin Biofilters THM kinetics

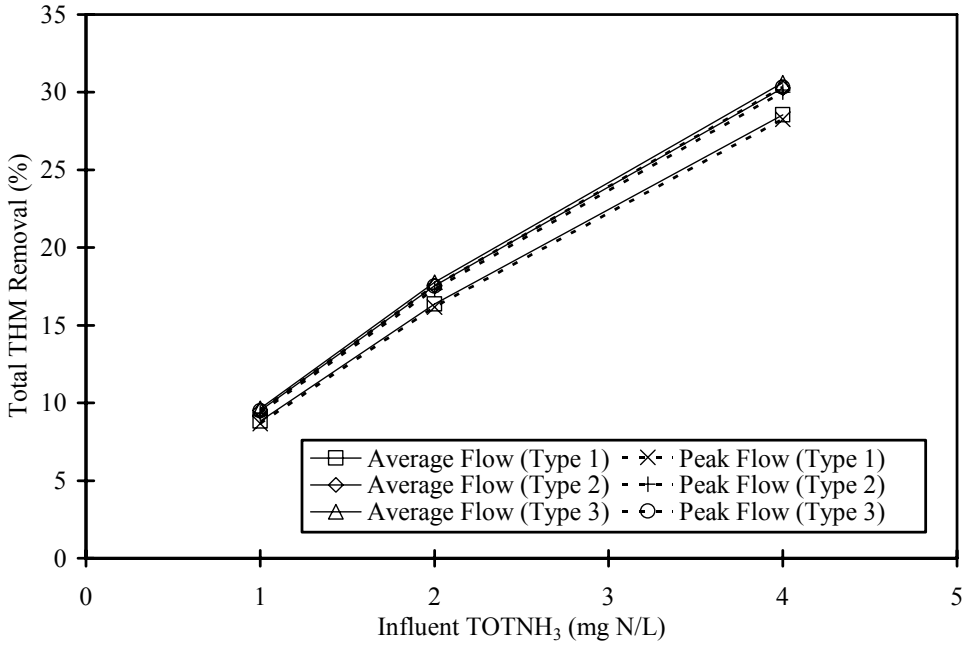

Figure 6.11 Full-scale model simulation total THM percent removal with Mixed Culture Biofilters 2 THM kinetics

To determine how an immediate change in influent flow rate would affect a full-scale system, a simulation was conducted with a full-scale system receiving an influent $TOTNH_3$ of 4 mg/L, having an SLR of 2 gpm/ft^2, treating a type 1 water, and using the Lake Austin Biofilters THM kinetics. After steady state was achieved, the SLR was increased to 4 gpm/ft^2 for twelve hours before being returned to 2 gpm/ft^2. The results of the SLR change for total THM and $TOTNH_3$ effluent concentrations are detailed in Figure 6.12. The effluent $TOTNH_3$ concentration increased from 0.1 to 0.7 mg/L as N, while only a minimal increase (10% or 4 µg/L) in total THM effluent concentration resulted. Based on this simulation, stable THM removal is expected throughout non-steady-state periods of increased flow rate. The greater effluent $TOTNH_3$ concentration associated with such non-steady-state operation promotes greater THM degradation through its effect on the reductant term in the THM rate equation, thereby dampening the impact on THM removal.

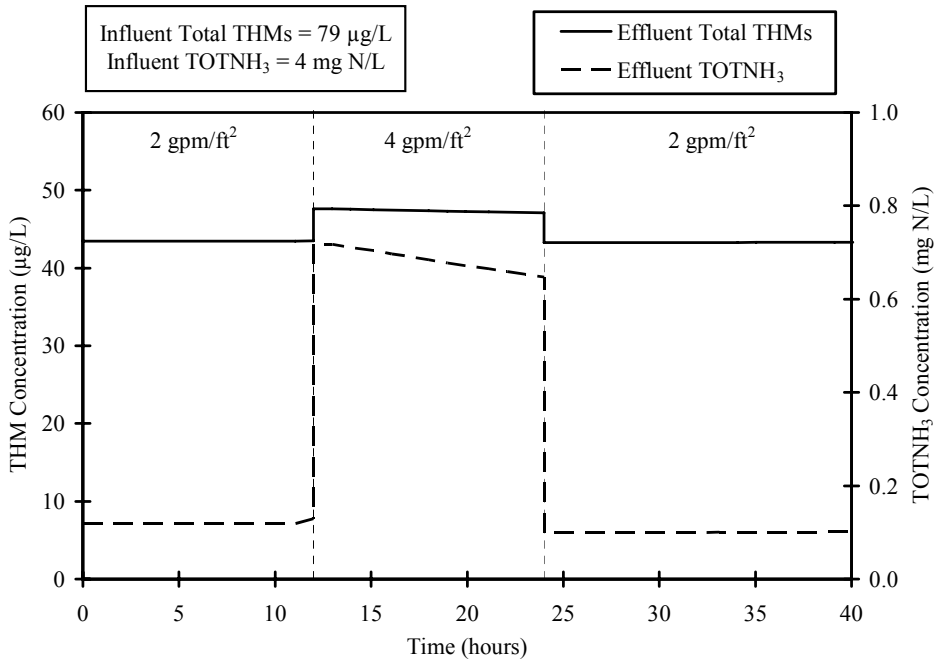

Figure 6.12 Full-scale model simulation with step surface loading rate changes

6.9. SUMMARY

A simple kinetic model for THM cometabolism was incorporated into AQUASIM to describe biofilter performance under conditions in which by-product toxicity is not a concern. The model was used to estimate kinetic parameters for THM cometabolism and subsequently verified with other experimental data. A sensitivity analysis was conducted, indicating that THM effluent concentrations are significantly affected by both the THM and $TOTNH_3$ rate constants.

To explore how the THM removal process might perform in practice, a full-scale filter was simulated under average and peak flow conditions, receiving three different influent THM water types, three different influent $TOTNH_3$ concentrations, and with two different sets of THM kinetic parameters. These simulations demonstrated that influent $TOTNH_3$ concentrations and THM speciation are important in determining expected THM removal in the biofilters. As the influent $TOTNH_3$ concentration increases (greater than 2 mg N/L), supplemental oxygen would be required to maintain aerobic conditions and to satisfy the model assumption that oxygen is not rate-limiting. A further simulation with a step increase in flow rate showed that THM removal was relatively insensitive to changes in flow rate for typical operating conditions.

The empty-bed contact times typically available in practice are long enough for process implementation. In practice, a portion of the EBCT will be required to decrease the monochloramine concentration to less than 1 mg/L as Cl_2 to provide a suitable environment for the biofilm bacteria. Assuming an influent monochloramine concentration of 2 mg/L as Cl_2 and based on modeling conducted by Fairey (2006) for Lake Austin water, a 0.5 to 3 minute EBCT is required for monochloramine removal, depending on the influent pH and GAC used. Based on this, an appropriate GAC can be

chosen to decrease monochloramine to less than 1 mg/L as Cl_2 with minimal use of the available EBCT, depending on design constraints (i.e., GAC cost or available EBCT).

Overall, total THM removal of 9 to 54% was projected in the full-scale simulations, which illustrates the potential of THM cometabolism to have a significant impact on treated water quality for utilities in which their water quality will likely see a benefit from the proposed process. Even though these removals are modest, drinking water treatment plants might only require removals in this range to maintain compliance with existing and future regulations.

Chapter 7: Conclusions

7.1. OVERVIEW

This research provides fundamental information on the feasibility and development of a new biological treatment process for THM destruction based on THM cometabolism by nitrifying bacteria growing on ammonia (NH_3) in multimedia filters under conditions that reflect water treatment plant practice. This research is unique in that almost no work has been done on biological control mechanisms for THMs. By extending findings from aquifer remediation and hazardous waste treatment research to drinking water treatment, a new biological treatment process was evaluated based on THM cometabolism by bacteria growing on ammonia in laboratory-scale biofilters.

Implementation of this process should involve relatively minor retrofitting of existing plants. The cometabolism would occur in granular media filters consisting of an upper layer of granular activated carbon (GAC). Utilities could carry out prechlorination followed by ammonia addition at a relatively low concentration (1 to 4 mg N/L) sometime before the filters. The result will be a mixture of monochloramine and ammonia at typical free chlorine concentrations (e.g., 2 mg/L as Cl_2) in treatment plants. When the water is applied to the upper GAC layer in the filter, monochloramine will be destroyed, releasing ammonia (Fairey et al. 2004; Komorita and Snoeyink 1985). At this point, an appropriate environment for microbial growth is established (i.e., an environment devoid of a disinfectant residual). With respect to THMs, nitrifiers, specifically ammonia oxidizers, can grow on the available ammonia and cometabolize THMs. The filtered water would then be post-disinfected, presumably with chloramines, before distribution.

The overall objective of this research was to study the feasibility of THM cometabolism in laboratory-scale biofilters under conditions that reflected water treatment plant practice. To meet this objective, three main research tasks were undertaken.

Task 1 involved batch kinetic studies to determine cometabolism kinetics for the pure culture organism, *N. europaea*, providing information to the key question as to whether nitrifying bacteria can reliably cometabolize all four THMs at a sufficient rate to make the process attractive to utilities that practice (or want to practice) prechlorination, in particular, utilities practicing a combination of chlorination and chloramination.

Task 2 demonstrated THM cometabolism performance in the envisioned process configuration, continuous-flow biofilters. In addition, operational issues were also studied, including THM product toxicity, nutrient limitations, and monochloramine inhibition of ammonia and THM degradation. Finally, molecular analysis of the developed biofilm was undertaken to provide additional information to interpret process performance.

Task 3 developed a steady-state mathematical model of the process. Apparent steady-state data from the biofilter experiments and supporting batch experiments were used to estimate kinetic parameters. Subsequently, the model was verified against other experimental biofilter data. Finally, the model was used to simulate full-scale filter performance under different filter surface loading rates and THM speciation seen in practice.

7.2. CONCLUSIONS

The major conclusions of this research are grouped according to the stated objectives of this research.

Objective 1. Extend the previous work on TCM cometabolism kinetics to the other three regulated THMs for the pure culture organism Nitrosomonas europaea and compare these findings with those obtained from selected mixed culture nitrifiers.

1. Kinetic coefficients were successfully determined for the pure culture nitrifier, *N. europaea*, with the reductant model providing the best fit to the data for THM degradation kinetics. The reductant model predicts that the degradation rate of each THM increases with increasing THM concentration according to pseudo-first-order kinetics and with increasing ammonia concentration according to Monod kinetics. The reductant model also predicts no THM degradation in the absence of ammonia, which is the electron source for THM cometabolism. Ammonia degradation kinetics were described well by the Monod expression. At concentrations typical of drinking water treatment, no enzyme competition was observed among the THMs or between the THMs and ammonia.
2. The kinetic coefficients determined for mixed-culture nitrifiers compared well to kinetic coefficients determined for the pure culture, *N. europaea*. For all cultures, pseudo-first-order rate constants ranged from 0.037 to 0.16 L/mg TSS-day for TCM, 0.070 to 0.24 L/mg TSS-day for BDCM, 0.10 to 0.34 L/mg TSS-day for DBCM, and 0.11 to 0.43 L/mg TSS-day for TBM. The corresponding Monod half-saturation coefficient for ammonia ranged from 0.022 to 0.29 mg/L NH_3-N, and the maximum specific substrate utilization rate ranged from 1.5 to 4.7 mg $TOTNH_3$/mg TSS-day.
3. Overall, the kinetic coefficients determined for THM cometabolism by all sources of nitrifiers fall above the range of practically feasible kinetic coefficients (0.03 to 0.1 L/mg-day) provided by Segar et. al. (1995) for biofilter cometabolism. Thus, the batch kinetic experiments indicated that THM cometabolism by mixed-culture nitrifying bacteria is fast enough to suggest practical feasibility in a drinking water treatment facility.

4. The effect of temperature on degradation kinetics was examined with *N. europaea* and compared with the results for the *N. oligotropha* enrichment culture. With *N. europaea* at 14°C, the THM pseudo-first-order rate constants ranged from 35% to 50% of their values at 22°C, and the impact of decreased temperature increased with an increasing degree of bromine substitution. The Monod maximum specific substrate utilization rate was affected to an even greater extent than the THM kinetic coefficients and was only 24% of its value at 22°C. Similar results were observed with the *N. oligotropha* enrichment culture. The decreased kinetics at decreased temperatures might be partially mitigated because the THM cometabolism efficiency ($k_{1_{THM}}/k_{TOTNH_3}$) increases with decreasing temperature. Therefore, a lower $TOTNH_3$ removal might not lead to a decreased THM removal at decreased temperatures. Overall, these experiments illustrated the anticipated significant impact of temperature on degradation kinetics.
5. Product toxicity was characterized by measuring the transformation capacity (T_c) of each THM individually with *N. europaea*. TCM had by far the lowest by-product toxicity, with a transformation capacity of 77 nM TCM/mg TSS. The presence of any bromine-substitution caused a substantial increase in product toxicity; transformation capacities ranged from 45 nM/mg for BDCM to 22 nM/mg for TBM. Relative to cometabolism of other halogenated chemicals, TCM is considered to have moderate product toxicity, while the bromine-substituted THMs are considered to have high product toxicity. An additional transformation capacity experiment containing a mixture of all four THMs showed that the overall effect of product toxicity in mixtures could be estimated accurately by summing the effects of the individual THM species. The relative differences in T_c values among the THMs indicates that both the relative speciation of THMs and their individual concentrations will be

important in determining the probable product toxicity associated with their degradation. In particular, significant concentrations of bromine-substituted THMs could be problematic.

6. The kinetic experiments showed that nitrifier communities likely to be seen in drinking water treatment facilities can degrade THMs at a sufficient rate by themselves, without seeding a pure culture. These results also indicated that temperature sensitivity and product toxicity could be concerns if THM cometabolism by nitrifying bacteria was implemented as a treatment option in treatment facilities. In particular, as bromine substitution increases both THM degradation kinetics and product toxicity increase. As a result, utilities will need to balance the attractiveness of faster kinetics with the reality of product toxicity in applying this technology to waters containing significant concentrations of bromine-substituted THMs.

Objective 2. Demonstrate THM cometabolism in continuous-flow biofilters.

A series of biofilter experiments was conducted with the following seed cultures: (1) pure culture *N. europaea* (ATCC® 19718), (2) *N. oligotropha* enrichment culture isolated from a drinking water distribution system, (3) Lake Austin mixed culture cultured from Lake Austin, Texas, (4) Rio Grande mixed culture cultured from the influent line of a drinking water treatment facility in Laredo, Texas, and (5) GAC from an operating drinking water treatment facility in Laredo, Texas.

1. The operating conditions of the mixed culture laboratory-scale biofilters scaled to typical full-scale rapid filtration operating conditions seen in drinking water treatment practice (EBCTs of 2 to 8 minutes and SLRs of 2.5 to 7.0 gpm/ft^2), but the pure culture *N. europaea* laboratory-scale biofilters required an impractically long EBCT. Therefore, it is expected that mixed cultures from actual source waters can be

established in biofilters at reasonable EBCTs and SLRs without the necessity of seeding with the pure culture *N. europaea*.

2. All four THMs and $TOTNH_3$ were degraded in all the laboratory-scale nitrifying biofilter experiments. THM degradation increased with increasing bromine substitution, following the trend observed during the batch kinetic studies. Over the studied THM concentrations, competition between THMs did not seem to occur, and influent $TOTNH_3$ concentrations up to 4 mg N/L did not seem to compete with THMs in the biofilters, confirming the results from the batch kinetic experiments. In general, increased $TOTNH_3$ degradation corresponded to increased THM degradation; thus, the close association between ammonia degradation and THM cometabolism observed in the batch kinetic studies held in the biofilter experiments.
3. For some biofilter experiments (LAB and MCB1 Train A), it seems that a selection occurred, most likely because of THM product toxicity, for bacteria less efficient at THM cometabolism. The LAB and MCB1 were initiated on the secondary setup before being moved to the primary setup, but the MCB2 was started initially on the primary setup. The MCB2 did not show an initial period of higher removals, indicating that startup conditions might have contributed to the initial higher removals.
4. THM speciation is important, because each THM exhibits a different product toxicity. The cometabolism stability index (C_{si}) represents a simple and useful tool for judging the likelihood of product toxicity problems in biofilter operation. Because both THM cometabolism rate constants and THM product toxicities increase with increasing THM bromine-substitution, a water's THM speciation will be an important consideration for process implementation. Even though a given water might be

kinetically favored based on THM speciation, the resulting THM product toxicity might not allow stable treatment process performance.

5. The backwash batch kinetic tests provided a useful tool to evaluate the biofilm's bacteria. Based on these experiments, the biofilters contained bacteria with similar, yet more efficient, THM kinetics to those seen in the batch kinetic experiments. The biofilm cultures seem to have larger transformation capacities than the batch grown cultures.
6. For biofilters operated with no effluent $TOTNH_3$, backwashing events during normal biofilter operation might have allowed a larger biomass to populate the biofilters through redistribution of bacteria from the biofilter's upper to lower regions. As the biofilter recovered from backwashing events, the lower regions were exposed to substrate initially and not at later times. As a result, the bacteria in the biofilter's lower regions might not have been selected for less efficient THM cometabolism to the extent of the upper regions. Backwash batch kinetic experiments in which the effluent $TOTNH_3$ was zero (MCB1 A1 and A2) had greater $k_{1_{THM}}/k_{TOTNH_3}$ ratios than those conducted with effluent $TOTNH_3$ concentrations at the time of backwashing. For these experiments, the bacteria in the biofilter's lower regions might have skewed the results so that the kinetics seemed greater than they actually were in the biofilters.
7. Based on the LAB fed Lake Austin water, nutrient limitations might exist when using natural waters. To improve both $TOTNH_3$ and THM degradation, additions of both iron and copper were required with Lake Austin water. Contrasting these results, further experiments (MCB1 and MCB2) did not show significant effects from nutrients or source water. Overall, performance or selection does not seem based specifically on nutrients, source water, or source cultures.

8. Based on the LAB fed Lake Austin water and various influent monochloramine concentrations, it seems that an influent monochloramine concentration of 1 mg/L as Cl_2 (or less) is a good target for stable operation for a developed biofilm. Because monochloramine addition commenced to a developed biofilm, startup considerations could not be evaluated from these data and require further investigation. The influent monochloramine concentration of 1 mg/L as Cl_2 might be conservative because an increase in influent monochloramine concentration from approximately 1 mg/L to 2.5 mg/L as Cl_2 was made during the experiment. The influent monochloramine concentration of 2.5 mg/L as Cl_2 led to unstable operation, but time did not permit examination of concentrations between 1 mg/L and 2.5 mg/L as Cl_2. As a result, the actual allowable influent monochloramine concentration lies between 1 mg/L to 2.5 mg/L as Cl_2, with the use of 1 mg/L as Cl_2 being conservative.
9. A simplified THM cometabolism model (Equation 4.1) provided a simple way to compare nitrifiers' THM cometabolism efficiency through calculated $k_{1_{THM}}/k_{TOTNH_3}$ ratios. Overall, the biofilter experiments suggest that total THM removals might initially approach 32-38% (25-31 μg/L total THMs) based on the LAB fed nutrient water, a $TOTNH_3$ removal of 2 mg N/L, and typical THM influent concentration and speciation. Further biofilter experiments (LAB fed Lake Austin water and MCB1 and 2) indicate that this initial removal might decline to 11-12% (9-10 μg/L total THMs) over time as bacteria are selected from THM product toxicity. Even if this decreased performance occurs, the 11-12% removal is potentially attractive in drinking water treatment practice. The ability to sustain the initial performance might be enhanced by using GAC as the biofilter media as shown by improving performance of MCB1 Train C for DBCM removal.

Objective 3. Quantify the abundance and spatial distribution of nitrifiers among other microorganisms in the biofilters, thereby improving our ability to interpret process performance data.

1. Based on total DNA present per gram of dry anthracite, no significant differences existed among Mixed Culture Biofilter 2 biofilter sections in a given biofilter. This result indicates that backwashing events or reattachment of bacteria redistribute the bacteria throughout the biofilter's length as opposed to decreasing with length as predicted by the current model.
2. Implementation of a real-time PCR method (Regan et al. 2004) to characterize the AOB present in the biofilter studies was attempted with limited success. Standard curves were generated in initial attempts at method implementation but were unsuccessful when biofilter samples were run; therefore, no determination of the percent AOB of the total DNA extracted, distribution of nitrifiers, or dominant species present in the biofilm could be determined.

Objective 4. Create a steady-state mathematical model of the process and propose a strategy for design and operation based on experimental observations and modeling.

1. A simple kinetic model for THM cometabolism was incorporated into AQUASIM to describe biofilter performance under conditions where by-product toxicity is not a concern. The model was used to estimate kinetic parameters for THM cometabolism and subsequently verified with other experimental data. A sensitivity analysis was conducted, indicating that THM effluent concentrations are significantly affected by both the THM and $TOTNH_3$ rate constants.
2. Kinetic rate constants determined from batch kinetic experiments conducted with biofilter backwash initially were used to simulate biofilter effluent ammonia and THM concentrations. Unfortunately, the effluent ammonia concentrations could not be satisfactorily simulated using the batch kinetic parameters; therefore, the $K_{s_{NH_3\text{-}N}}$

value was adjusted to match the biofilter effluent $TOTNH_3$ concentrations. Using the fitted $K_{s_{NH_3\text{-}N}}$ and the experimentally-determined k_{TOTNH_3}, direct implementation of the experimentally-determined $k_{1_{THM}}$ into the AQUASIM model led to good predictions of the biofilter THM performance for the given biofilter.

3. To explore how the THM removal process might perform in practice, a full-scale filter was simulated under average and peak flow conditions, receiving three different influent THM water types, three different influent $TOTNH_3$ concentrations, and two different sets of THM kinetic parameters. These simulations demonstrated that influent $TOTNH_3$ concentrations and THM speciation are important in determining expected THM removal in the biofilters. As the influent $TOTNH_3$ concentration increases (above 2 mg N/L), supplemental oxygen would be required to maintain aerobic conditions and to satisfy the model assumption that oxygen is not rate-limiting. In addition, the empty-bed contact times typically available in practice are long enough for process implementation. A further simulation with a step increase in flow rate showed that THM removal was relatively insensitive to changes in flow rate for typical operating conditions.
4. Overall, total THM removal of 9 to 54% was projected in the full-scale simulations, which illustrates the potential of THM cometabolism to have a significant impact on treated water quality for utilities where their water quality will likely see a benefit from the proposed process. Even though these removals are modest, drinking water treatment plants might only require removals in this range to maintain compliance with existing and future regulations.
5. Based on the experimental observations and modeling conducted in this research, the design and operation of the proposed process to maximize THM removal should (1) maximize $TOTNH_3$ removal, (2) maximize biofilter run lengths between

backwashing events to limit recovery periods, (3) provide multiple filters in parallel to allow process stability for biofilters recovering from backwashing, (4) minimize the expected monochloramine with a maximum influent concentration of 1 mg/L as Cl_2 through the use of a GAC layer in the biofilter with a 0.5 to 3 minute EBCT in addition to the EBCT provided for THM cometabolism, and (5) anticipate the lower THM removals seen during extended biofilter runs.

7.3. FUTURE WORK

7.3.1. Biofilter Experiments

Future biofilter experiments should be conducted to investigate further the proposed process in laboratory-scale biofilters. The effect of temperature should be evaluated at both a lesser (i.e., 10°C) and greater (i.e., 30°C) temperature to investigate process performance with the possibility that the relative rates of THM and ammonia kinetics will vary at these extremes. In addition, experiments in which backwashing occurs at typical intervals (i.e., 24 hours) seen in practice need to be investigated along with their implications for process performance and stability. In addition and in any future biofilter experiment, the molecular analyses conducted should be expanded to define the biofilter seed cultures, initial cultures established in the biofilter, and cultures present after specific operating periods to investigate apparent selection of cultures during operation.

7.3.2. Model Improvement

The current model implementation uses an overall biofilm loss calculation ($b^{'}$) to implement biofilm shearing and decay. A more robust accounting for biomass needs to be implemented to account for reattachment of biomass and redistribution of biomass during backwash events. AQUASIM provides the ability to model both biofilm surface

attachment and detachment, which might provide a better estimation of the biofilm present as this will allow reattachment to occur at lower biofilter sections, increasing the biomass modeled in a biofilter. In addition, incorporation of a functionality to address backwash effects on the biomass distribution would be beneficial. Ultimately, incorporation of the results of molecular analysis into kinetic equations in lieu of the gross parameter TSS would provide a better description of the process by focusing on the AOB present in the biofilm. Finally, the current model could be expanded in AQUASIM to describe a multi-species (i.e., heterogeneous) biofilm to model the spatial distribution of both the nitrifiers and heterotrophs present.

7.3.3. Drinking Water Distribution System Implications

The current research has applications beyond the envisioned process. The results from this research could be used to provide a better understanding of nitrification episodes in chloraminated distribution systems. It provides a new explanation for the causes and prevention of such episodes and the nitrifiers that might inhabit these systems. Areas that could be investigated include whether THM cometabolism leads to selection of THM tolerant nitrifiers because of THM product toxicity. Along these lines, do fewer nitrification episodes happen at lower temperatures because nitrification kinetics are slower or because the ratio of ($k_{1_{THM}}/k_{TOTNH_3}$) is higher at lower temperatures and THM product toxicity inhibits the episode? Further issues that should be investigated are whether monochloramine is a cometabolite of AOB and whether pipe materials (i.e., iron and copper) provide trace nutrients that enhance nitrification in distribution systems.

Appendix A: Kinetic Model Derivations

NH_3-N FRACTION OF TOTNH_3 - COMMON TO ALL MODELS

Notes:

1. $pK_{a,T}$ determination valid for 0ºC < T < 50ºC.
2. s determination valid for I < 0.5 M.

$$\alpha_1 = \frac{1}{1+10^{(pK_a - pH - s)}} = \frac{[NH_3]}{[TOTNH_3]}$$

$$pK_{a,T} = -\log K_{a,T} = 0.09018 + \frac{2729.92}{T + 273.16}$$

$$pH = -\log\{H^+\}$$

$$s = \log_{10}\gamma_{NH_4^+} = -Az^2\left[\frac{I^{1/2}}{1+I^{1/2}} - 0.2I\right]$$

$$A = 1.82483\times10^6\left[E(T+273.16)\right]^{-1.5}$$

$$E = 87.74 - 0.4008T + 9.398\times10^{-4}T^2 - 1.41\times10^{-6}T^3$$

$$I = \frac{1}{2}\sum c_i z_i^{\,2}$$

AMMONIA DEGRADATION - COMMON TO ALL MODELS

Assumptions:

1. THMs do not compete with ammonia.

$$r_{TOTNH_3} = -\frac{k_{TOTNH_3} XS_{NH_3-N}}{K_{s_{NH_3-N}} + S_{NH_3-N}} = -\frac{k_{TOTNH_3} XS_{TOTNH_3}\alpha_1}{K_{s_{NH_3-N}} + S_{TOTNH_3}\alpha_1}$$

THM DEGRADATION

Competition Model

Assumptions:

1. Ammonia competes with THMs.
2. THMs do not compete with ammonia.
3. Reductant is not a limiting reactant.

$$r_{THM} = -\frac{k_{THM} X S_{THM}}{K_{s_{THM}} + S_{THM} + \frac{K_{s_{THM}}}{K_{s_{NH_3-N}}} S_{NH_3-N}} = -\frac{k_{THM} X S_{THM}}{K_{s_{THM}} + S_{THM} + \frac{K_{s_{THM}}}{K_{s_{NH_3-N}}} S_{TOTNH_3} \alpha_1}$$

Factoring out $K_{s_{THM}}$ from denominator

$$r_{THM} = -\frac{k_{THM} X S_{THM}}{K_{s_{THM}} \left(1 + \frac{S_{THM}}{K_{s_{THM}}} + \frac{S_{TOTNH_3} \alpha_1}{K_{s_{NH_3-N}}}\right)}$$

If $K_{s_{THM}} >> S_{THM}$

$$r_{THM} = -\frac{k_{1THM} X S_{THM}}{1 + \frac{S_{TOTNH_3} \alpha_1}{K_{s_{NH_3-N}}}}$$

Reductant Model

Assumptions:

1. Ammonia does not compete with THMs.
2. THMs do not compete with ammonia.
3. Two limiting reactants (THM and Reductant).

$$r_{THM} = -\frac{k_{THM} XS_{THM}}{K_{s_{THM}} + S_{THM}} \left(\frac{S_{NH_3-N}}{K_{s_{NH_3-N}} + S_{NH_3-N}} \right) = -\frac{k_{THM} XS_{THM}}{K_{s_{THM}} + S_{THM}} \left(\frac{S_{TOTNH_3} \alpha_1}{K_{s_{NH_3-N}} + S_{TOTNH_3} \alpha_1} \right)$$

Divide reductant term by $S_{NH_3\text{-}N}$

$$r_{THM} = -\frac{k_{THM} XS_{THM}}{K_{s_{THM}} + S_{THM}} \left(\frac{1}{\frac{K_{s_{NH_3-N}}}{S_{TOTNH_3} \alpha_1} + 1} \right)$$

If $K_{s_{THM}} >> S_{THM}$ and simplifying

$$r_{THM} = -\frac{k_{1THM} XS_{THM}}{1 + \frac{K_{s_{NH_3-N}}}{S_{TOTNH_3} \alpha_1}}$$

Combined Model

Assumptions:

1. Ammonia competes with THMs.
2. THMs do not compete with ammonia.
3. Two limiting reactants (THM and Reductant).

Starting with competition model and adding reductant term:

$$r_{THM} = -\frac{k_{1THM} XS_{THM}}{1+\frac{S_{NH_3-N}}{K_{s_{NH_3-N}}}}\left(\frac{1}{\frac{K_{s_{NH_3-N}}}{S_{NH_3-N}}+1}\right) == -\frac{k_{1THM} XS_{THM}}{1+\frac{S_{TOTNH_3}\alpha_1}{K_{s_{NH_3-N}}}}\left(\frac{1}{\frac{K_{s_{NH_3-N}}}{S_{TOTNH_3}\alpha_1}+1}\right)$$

Simplifying

$$r_{THM} = -\frac{k_{1THM} XS_{THM}}{\left(1+\frac{S_{TOTNH_3}\alpha_1}{K_{s_{NH_3-N}}}\right)\left(\frac{K_{s_{NH_3-N}}}{S_{TOTNH_3}\alpha_1}+1\right)}$$

First-Order Model

Assumptions:

1. Ammonia does not compete with THMs.
2. THMs do not compete with ammonia.
3. Reductant is not a limiting reactant.

$$r_{THM} = -\frac{k_{THM} XS_{THM}}{K_{s_{THM}} + S_{THM}}$$

If $K_{s_{THM}} >> S_{THM}$ and simplifying

$$r_{THM} = -k_{1THM} XS_{THM}$$

$k_{1_{THM}}/k_{TOTNH_3}$ - BATCH REACTOR DERIVATION

Assumptions:

1. Batch reactor.
2. Ammonia does not compete with THMs.
3. THMs do not compete with ammonia.
4. THMs do not compete with each other.
5. Two limiting reactants (THM and Reductant).

Ammonia Degradation

$$\frac{dS_{TOTNH_3}}{dt} = -\frac{k_{TOTNH_3} XS_{NH_3-N}}{K_{s_{NH_3-N}} + S_{NH_3-N}}$$

THM Degradation

$$\frac{dS_{THM}}{dt} = -k_{1THM} XS_{THM} \left(\frac{S_{NH_3-N}}{K_{s_{NH_3-N}} + S_{NH_3-N}} \right)$$

Divide ammonia degradation by THM degradation and simplify

$$\frac{\frac{dS_{TOTNH_3}}{dt}}{\frac{dS_{THM}}{dt}} = \frac{-\frac{k_{TOTNH_3} XS_{NH_3-N}}{K_{s_{NH_3-N}} + S_{NH_3-N}}}{-k_{1THM} XS_{THM}\left(\frac{S_{NH_3-N}}{K_{s_{NH_3-N}} + S_{NH_3-N}}\right)} = \frac{dS_{TOTNH_3}}{dS_{THM}} = \frac{k_{TOTNH_3}}{k_{1THM} S_{THM}}$$

Separating variables and integrating

$$\int_{S_{TOTNH_3}(0)}^{S_{TOTNH_3}(t)} dS_{TOTNH_3} = \frac{k_{TOTNH_3}}{k_{1THM}} \int_{S_{THM}(0)}^{S_{THM}(t)} \frac{dS_{THM}}{S_{THM}}$$

$$S_{TOTNH_3}(t) - S_{TOTNH_3}(0) = \frac{k_{TOTNH_3}}{k_{1THM}} \left(\ln S_{THM}(t) - \ln S_{THM}(0)\right)$$

Substitute $-\Delta TOTNH_3 = S_{TOTNH_3}(t) - S_{TOTNH_3}(0)$ and rearrange

$$-\Delta TOTNH_3 \frac{k_{1THM}}{k_{TOTNH_3}} = \ln S_{THM}(t) - \ln S_{THM}(0) = \ln \frac{S_{THM}(t)}{S_{THM}(0)}$$

Raise to the e and rearrange to final equation form for a batch reactor at any given time, t. By analogy, this would also represent a plug flow reactor with hydraulic residence time, t.

$$\frac{S_{THM}(t)}{S_{THM}(0)} = e^{-\Delta TOTNH_3 \frac{k_{1THM}}{k_{TOTNH_3}}}$$

Appendix B: 95% Joint Confidence Limit Determination Method

ASSUMPTIONS AND DECISIONS

1. Sum of squares error is normalized at each point by the square of the measured concentration (Robinson 1985).
2. Estimated $K_{s_{NH_3-N}}$ from ammonia kinetics analysis is used as a constant in the THM kinetics analysis.
3. For sensitivity coefficient determinations, the parameters are perturbed by 1% similar to Smith, McCarty, and Kitinidis (1997; 1998).

GENERAL PROCEDURE

1. Determination of Ammonia Kinetics.
   a. Monod kinetic coefficients were estimated by nonlinear regression analysis using the Solver routine in Excel. A fourth-order Runge-Kutta numerical approximation of the Monod equation was fitted to the data by minimizing the weighted residual sum of squares between the predicted and experimental values.
   b. The weighting was achieved by dividing each squared error by the experimentally measured value squared, resulting in a dimensionless squared error.
   c. Three parameters were determined: the initial ammonia concentration (S_0), the half-saturation coefficient ($K_{s_{NH_3-N}}$), and the maximum substrate utilization rate (k_{TOTNH_3}).
2. Determination of THM Kinetics.
   a. The same fitting and weighting method was performed as per the ammonia kinetics, and the previously determined ammonia kinetic parameters were used in THM parameter determination.

b. Two parameters were determined for each THM: the initial THM concentration (S_0) and pseudo-first-order degradation rate ($k_{1_{THM}}$).

3. Determination of Confidence Intervals.

a. $$SSE = \sum_{i=1}^{n} \frac{\left(S_i^{obs} - S_i^{pred}\right)^2}{\left(S_i^{obs}\right)^2}$$

i. SSE = minimized weighted sum of squares error.

ii. S_i^{obs} = observed concentration, mg/L.

iii. S_i^{pred} = predicted concentration, mg/L.

b. $$o^2 = \frac{1}{n-p} SSE$$

i. o^2 = mean square fitting error.

ii. n = number of data points.

iii. p = number of parameters determined (3 for ammonia, 2 for each THM).

c. $$\frac{\partial S_i^{pred}}{\partial X} \approx \frac{S_i^{pred}(X + \Delta X) - S_i^{pred}(X)}{\Delta X}$$

i. $\frac{\partial S_i^{pred}}{\partial X}$ = sensitivity coefficient for parameter X.

ii. $S_i^{pred}(X)$ = predicted concentration for original Runge-Kutta approximation.

iii. $S_i^{pred}(X + \Delta X)$ = predicted concentration for Runge-Kutta approximation when X is perturbed by ΔX.

iv. ΔX = perturbed amount (set at 1% of X).

d. Sensitivity matrix for ammonia (3 parameters).

i. $$A = \begin{bmatrix} \sum_{i=1}^{n} \frac{1}{\left(S_i^{obs}\right)^2}\left(\frac{\partial S_i^{pred}}{\partial K_{s_{NH_3-N}}}\right)^2 & \sum_{i=1}^{n} \frac{1}{\left(S_i^{obs}\right)^2}\left(\frac{\partial S_i^{pred}}{\partial K_{s_{NH_3-N}}}\right)\left(\frac{\partial S_i^{pred}}{\partial k_{TOTNH_3}}\right) & \sum_{i=1}^{n} \frac{1}{\left(S_i^{obs}\right)^2}\left(\frac{\partial S_i^{pred}}{\partial K_{s_{NH_3-N}}}\right)\left(\frac{\partial S_i^{pred}}{\partial S_0}\right) \\ \sum_{i=1}^{n} \frac{1}{\left(S_i^{obs}\right)^2}\left(\frac{\partial S_i^{pred}}{\partial K_{s_{NH_3-N}}}\right)\left(\frac{\partial S_i^{pred}}{\partial k_{TOTNH_3}}\right) & \sum_{i=1}^{n} \frac{1}{\left(S_i^{obs}\right)^2}\left(\frac{\partial S_i^{pred}}{\partial k_{TOTNH_3}}\right)^2 & \sum_{i=1}^{n} \frac{1}{\left(S_i^{obs}\right)^2}\left(\frac{\partial S_i^{pred}}{\partial k_{TOTNH_3}}\right)\left(\frac{\partial S_i^{pred}}{\partial S_0}\right) \\ \sum_{i=1}^{n} \frac{1}{\left(S_i^{obs}\right)^2}\left(\frac{\partial S_i^{pred}}{\partial K_{s_{NH_3-N}}}\right)\left(\frac{\partial S_i^{pred}}{\partial S_0}\right) & \sum_{i=1}^{n} \frac{1}{\left(S_i^{obs}\right)^2}\left(\frac{\partial S_i^{pred}}{\partial k_{TOTNH_3}}\right)\left(\frac{\partial S_i^{pred}}{\partial S_0}\right) & \sum_{i=1}^{n} \frac{1}{\left(S_i^{obs}\right)^2}\left(\frac{\partial S_i^{pred}}{\partial S_0}\right)^2 \end{bmatrix}$$

e. Sensitivity matrix for each THM (2 parameters).

i. $$A = \begin{bmatrix} \sum_{i=1}^{n} \frac{1}{\left(S_i^{obs}\right)^2}\left(\frac{\partial S_i^{pred}}{\partial S_0}\right)^2 & \sum_{i=1}^{n} \frac{1}{\left(S_i^{obs}\right)^2}\left(\frac{\partial S_i^{pred}}{\partial S_0}\right)\left(\frac{\partial S_i^{pred}}{\partial k_{1_{THM}}}\right) \\ \sum_{i=1}^{n} \frac{1}{\left(S_i^{obs}\right)^2}\left(\frac{\partial S_i^{pred}}{\partial S_0}\right)\left(\frac{\partial S_i^{pred}}{\partial k_{1_{THM}}}\right) & \sum_{i=1}^{n} \frac{1}{\left(S_i^{obs}\right)^2}\left(\frac{\partial S_i^{pred}}{\partial k_{1_{THM}}}\right)^2 \end{bmatrix}$$

f. $\mathbf{V} = \sigma^2 \mathbf{A}^{-1}$

i. $\mathbf{V}$ = mean square error (MSE) matrix.

ii. $\mathbf{A}^{-1}$ = inverse of A.

g. The standard error (analogous to standard deviation) of a single parameter can be calculated as the square root of a diagonal in the V matrix.

i. Ammonia.

1. $\sqrt{V_{11}} = \sigma_{K_{s_{NH_3-N}}}$
2. $\sqrt{V_{22}} = \sigma_{k_{TOTNH_3}}$
3. $\sqrt{V_{33}} = \sigma_{S0}$

ii. THMs.

1. $\sqrt{V_{11}} = \sigma_{S0}$
2. $\sqrt{V_{22}} = \sigma_{k_{1_{THM}}}$

h. Correlation coefficients between two parameters can also be calculated from cells in the V matrix. The closer the coefficient is to 1 or -1, the more interdependent the variables. Values close to zero indicate greater independence of the variables.

i. Ammonia.

1. $K_{s_{NH_3-N}} \& k_{TOTNH_3} = \frac{V_{12}}{\sqrt{V_{11}V_{22}}}$
2. $K_{s_{NH_3-N}} \& S_0 = \frac{V_{13}}{\sqrt{V_{11}V_{33}}}$
3. $k_{TOTNH_3} \& S_0 = \frac{V_{23}}{\sqrt{V_{22}V_{33}}}$

ii. THMs.

1. $S_0 \& k_{1THM} = \frac{V_{12}}{\sqrt{V_{11}V_{22}}}$

i. Ammonia joint confidence interval.

i. It is a three-dimensional ellipsoid that satisfies the following inequality:

1. $$\frac{1}{\sigma^2}\left[\begin{array}{l} A_{11}\left(K_{s_{NH_3-N}} - \hat{K}_{s_{NH_3-N}}\right)^2 + A_{22}\left(k_{TOTNH_3} - \hat{k}_{TOTNH_3}\right)^2 + A_{33}\left(S_0 - \hat{S}_0\right)^2 + \\ 2A_{12}\left(K_{s_{NH_3-N}} - \hat{K}_{s_{NH_3-N}}\right)\left(k_{TOTNH_3} - \hat{k}_{TOTNH_3}\right) + \\ 2A_{13}\left(K_{s_{NH_3-N}} - \hat{K}_{s_{NH_3-N}}\right)\left(S_0 - \hat{S}_0\right) + \\ 2A_{23}\left(k_{TOTNH_3} - \hat{k}_{TOTNH_3}\right)\left(S_0 - \hat{S}_0\right) \end{array}\right] \le Z$$

2. $Z = p * F(p, n-p, 1-\alpha)$
3. $\hat{K}_{s_{NH_3-N}}, \hat{k}_{TOTNH_3}, \hat{S}_0$ = determined kinetics parameters.
4. $K_{s_{NH_3-N}}, k_{TOTNH_3}, S_0$ = variables to satisfy inequality.
5. $F(p, n-p, 1-\alpha)$ = value from F-distribution table for given number of parameters, degrees of freedom, and desired confidence interval.

ii. Boundary points can be determined by setting equal to Z instead of less than or equal to Z.

iii. To create plots, S_0 was assumed a constant and set at either the value determined from the kinetics analysis or this value ± 2 single parameter standard deviations (i.e. $\hat{S}_0$ or $\hat{S}_0 \pm 2\sigma$).

iv. Once this substitution is made into the above inequality, the equation can be rearranged into a quadratic equation that can be used to develop the joint confidence interval. To do this in Excel, values are assumed for $K_{s_{NH3-N}}$ and the quadratic equation is solved for both roots with $x = k_{TOTNH_3} - \hat{k}_{TOTNH_3}$. The equation takes the form:

1. $$A_{22}x^2 + \left[2A_{12}\left(K_{s_{NH_3-N}} - \hat{K}_{s_{NH_3-N}}\right) + 2A_{23}\left(S_0 - \hat{S}_0\right)\right]x +$$
$$A_{11}\left(K_{s_{NH_3-N}} - \hat{K}_{s_{NH_3-N}}\right)^2 + A_{33}\left(S_0 - \hat{S}_0\right)^2 +$$
$$2A_{13}\left(K_{s_{NH_3-N}} - \hat{K}_{s_{NH_3-N}}\right)\left(S_0 - \hat{S}_0\right) - z\sigma^2$$

2. For use in the quadratic equation $x = \dfrac{-b \pm \sqrt{b^2 - 4ac}}{2a}$, the following are defined:

   a. $a = A_{22}$

   b. $b = 2A_{12}\left(K_{s_{NH_3-N}} - \hat{K}_{s_{NH_3-N}}\right) + 2A_{23}\left(S_0 - \hat{S}_0\right)$

   c. $$c = A_{11}\left(K_{s_{NH_3-N}} - \hat{K}_{s_{NH_3-N}}\right)^2 + A_{33}\left(S_0 - \hat{S}_0\right)^2 +$$
   $$2A_{13}\left(K_{s_{NH_3-N}} - \hat{K}_{s_{NH_3-N}}\right)\left(S_0 - \hat{S}_0\right) - z\sigma^2$$

3. The spreadsheet requires solver to find the upper and lower values of $K_{s_{NH_3-N}}$ by solving the two points where $b^2 - 4ac = 0$.

v. Once the range of $K_{s_{NH_3-N}}$ values is defined, the spreadsheet generates the two values of k_{TOTNH_3} that correspond to each assumed value of $K_{s_{NH_3-N}}$ for all the valid $K_{s_{NH_3-N}}$ values. These are then plotted and define the joint confidence interval.

j. For each THM joint confidence interval.

i. It is a two-dimensional ellipsoid that satisfies the following inequality:

1. $$\frac{1}{\sigma^2}\begin{bmatrix} A_{11}\left(S_0-\hat{S}_0\right)^2+A_{22}\left(k_{1_{THM}}-\hat{k}_{1_{THM}}\right)^2+ \\ 2A_{12}\left(S_0-\hat{S}_0\right)\left(k_{1_{THM}}-\hat{k}_{1_{THM}}\right)\end{bmatrix}\le Z$$

2. $Z = p * F(p, n-p, 1-\alpha)$

3. $\hat{k}_{1_{THM}}, \hat{S}_0$ = determined kinetics parameters.

4. $k_{1_{THM}}, S_0$ = variables to satisfy inequality.

5. $F(p, n-p, 1-\alpha)$= value from F-distribution table for given number.

ii. Boundary points can be determined by setting equal to Z instead of less than or equal to Z.

iii. Once this substitution is made into the above inequality, the equation can be rearranged into a quadratic equation that can be used to develop the joint confidence interval. To do this in excel, values are assumed for S_0 and the quadratic equation is solved for both roots with $x = k_{1_{THM}} - \hat{k}_{1_{THM}}$. The equation takes the form:

1. $$A_{22}x^2+\left[2A_{12}\left(S_0-\hat{S}_0\right)\right]x+A_{11}\left(S_0-\hat{S}_0\right)^2-z\sigma^2$$

2. For use in the quadratic equation $x=\frac{-b\pm\sqrt{b^2-4ac}}{2a}$, the following are defined:

a. $a = A_{22}$

b. $b = 2A_{12}\left(S_0-\hat{S}_0\right)$

c. $c = A_{11}\left(S_0-\hat{S}_0\right)^2-z\sigma^2$

3. The spreadsheet requires solver to find the upper and lower values of S_0 by solving the two points where $b^2-4ac=0$.

iv. Once the range of S_0 values is defined, the spreadsheet generates the two values of $k_{1_{THM}}$ that correspond to each assumed value of S_0 for all the valid S_0 values. These are then plotted and define the joint confidence interval.

Appendix C: Typical AQUASIM Biofilm Model Implementation

VARIABLES

Alpha1_Ammonia

Description: Fraction of $TOTNH_3$ that is Ammonia-Nitrogen (Based on 23.5°C)
Type: Formula Variable
Unit:
Expression: if Alpha_Calculation=0 then 1/(S_H_Plus/Ammonia_Ka+1) else Alpha_Calculation endif

---

Alpha_Calculation

Description: Determines whether to calculate alpha (Enter 0) or use given value (Enter desired alpha value)
Type: Formula Variable
Unit:
Expression: 0

Ammonia_Ka

Description: K_a for ammonia acid-base equilibrium equation at 23.5°C
Type: Formula Variable
Unit:
Expression: 5.10505e-010

Area_Biofilm

Description: Biofilm area in a reactor (Per User Manual, Page 50)
Type: Formula Variable
Unit: m^2
Expression: 4*pi*n_p*(r_p+Z)^2

Biofilm_Water_Fraction

Description: Water fraction of the biofilm matrix (This is porosity if pore volume does not contain solids)
Type: Program Variable
Unit:
Reference to: Water Fraction

Calcnum

Description: Calculation number counter
Type: Program Variable
Unit:
Reference to: Calculation Number

Carbonate_K_1

Description: Equilibrium constant for H_2CO_3 and HCO_3^- equation

Type: Formula Variable
Unit:
Expression: 4.46684e-007

Column_Area
Description: Cross-sectional column area per lab setup
Type: Formula Variable
Unit: m^2
Expression: pi/4*(Column_Diameter)^2

Column_Diameter
Description: Column diameter per lab setup
Type: Formula Variable
Unit: m
Expression: 1.5/100

Column_Length
Description: Length of column per lab setup
Type: Formula Variable
Unit: m
Expression: 10.2/100

Column_Volume
Description: Column volume per lab setup
Type: Formula Variable
Unit: m^3
Expression: Column_Area*Column_Length

D_BDCM
Description: Diffusivity of BDCM in water at 20°C (Groundwater Chemicals Desk Reference, Page 137)
Type: Formula Variable
Unit: m^2/d
Expression: 8.5e-005

D_DBCM
Description: Diffusivity of DBCM in water at 20°C (Groundwater Chemicals Desk Reference, Page 314)
Type: Formula Variable
Unit: m^2/d
Expression: 8.4e-005

D_NH3
Description: Diffusivity of NH_3 in Water at 20°C (Groundwater Chemicals Desk Reference, Page 50)
Type: Formula Variable

Unit: m^2/d
Expression: 9.5e-005

D_TBM
Description: Diffusivity of TBM in water at 20°C (Groundwater Chemicals Desk Reference, Page 139)
Type: Formula Variable
Unit: m^2/d
Expression: 8.2e-005

D_TCM
Description: Diffusivity of TCM in water at 20°C (Groundwater Chemicals Desk Reference, Page 233)
Type: Formula Variable
Unit: m^2/d
Expression: 8.6e-005

D_X
Description: Biomass Diffusivity (Per AquaSIM Tutorial, Page 120)
Type: Formula Variable
Unit: m^2/d
Expression: 1e-007

---

k1_BDCM
Description: Pseudo-first-order BDCM degradation rate (Per kinetics studies)
Type: Constant Variable
Unit: m^3/gX-d
Value: 0.15
Standard Deviation: 0.015
Minimum: 0.01
Maximum: 1
Sensitivity Analysis: inactive
Parameter Estimation: inactive

---

k1_DBCM
Description: Pseudo-first-order DBCM degradation rate (Per kinetics studies)
Type: Constant Variable
Unit: m^3/gX-d
Value: 0.20
Standard Deviation: 0.020
Minimum: 0.01
Maximum: 1
Sensitivity Analysis: inactive
Parameter Estimation: inactive

---

k1_TBM

Description: Pseudo-first-order TBM degradation rate (Per kinetics studies)
Type: Constant Variable
Unit: m^3/gX-d
Value: 0.23
Standard Deviation: 0.023
Minimum: 0.01
Maximum: 1
Sensitivity Analysis: inactive
Parameter Estimation: inactive

---

k1_TCM

Description: Pseudo-first-order TCM degradation rate (Per kinetics studies)
Type: Constant Variable
Unit: m^3/gX-d
Value: 0.1
Standard Deviation: 0.01
Minimum: 0.01
Maximum: 1
Sensitivity Analysis: inactive
Parameter Estimation: inactive

---

kd

Description: Endogenous decay coefficient (Per kinetics studies)+Specific biofilm-detachment loss coefficient (Per Rittmann & McCarty, Equations 4.32, 4.33, & 4.35)
Type: Formula Variable
Unit: 1/d
Expression: if LF<3e-005 then (0.02+0.0842*Sigma^0.58) else (0.02+0.0842*(Sigma/(1+433.2*((LF*100)-0.003)))^0.58) endif

---

kd_Calculation

Description: Determines whether to calculate kd (Enter 0) or use given value (Enter desired kd value)
Type: Formula Variable
Unit:
Expression: 0

Ks_NH3

Description: Half-saturation constant for NH_3-N (Per kinetics studies or 0.57 from Rittmann & McCarty Table 9.4)
Type: Constant Variable
Unit: gN/m^3
Value: 0.16
Standard Deviation: 0.016
Minimum: 0.0001

Maximum: 1
Sensitivity Analysis: inactive
Parameter Estimation: inactive

---

k_TRIN

Description: Maximum specific substrate utilization rate for $TOTNH_3$ (Per kinetics studies)
Type: Contstant Variable
Unit: 1/d
Value: 2.9
Standard Deviation: 0.29
Minimum: 0.1
Maximum: 10
Sensitivity Analysis: inactive
Parameter Estimation: inactive

LF

Description: Biofilm thickness (Calculated by AquaSIM)
Type: Program Variable
Unit: m
Reference to: Biofilm Thickness

LF_Initial

Description: Assumed initial condition for biofilm thickness
Type: Formula Variable
Unit: m
Expression: 1e-008

LL_BDCM

Description: Liquid boundary layer thickness for BDCM (Per Rittmann & McCarty, Equation 4.30)
Type: Formula Variable
Unit: m
Expression: D_BDCM*Re_m^0.75*Sc_BDCM^0.67/(5.7*Vel_Water_Superficial)

LL_DBCM

Description: Liquid boundary layer thickness for DBCM (Per Rittmann & McCarty, Equation 4.30)
Type: Formula Variable
Unit: m
Expression: D_DBCM*Re_m^0.75*Sc_DBCM^0.67/(5.7*Vel_Water_Superficial)

LL_NH3

Description: Liquid boundary layer thickness for NH_3 (Per Rittmann & McCarty, Equation 4.30)
Type: Formula Variable

Unit: m
Expression: D_NH3*Re_m^0.75*Sc_NH3^0.67/(5.7*Vel_Water_Superficial)

LL_TBM
Description: Liquid boundary layer thickness for TBM (Per Rittmann & McCarty, Equation 4.30)
Type: Formula Variable
Unit: m
Expression: D_TBM*Re_m^0.75*Sc_TBM^0.67/(5.7*Vel_Water_Superficial)

LL_TCM
Description: Liquid boundary lLayer thickness for TCM (Per Rittmann & McCarty, Equation 4.30)
Type: Formula Variable
Unit: m
Expression: D_TCM*Re_m^0.75*Sc_TCM^0.67/(5.7*Vel_Water_Superficial)

---

mu
Description: Absolute viscosity of water at 20°C (Per Metcalf & Eddy, Table C-2)
Type: Formula Variable
Unit: g/cm-d
Expression: 864

Number_Reactors
Description: Number of reactors in series to model column hydrodynamics
Type: Formula Variable
Unit:
Expression: 30

---

n_p
Description: Number of particles in each reactor (Calculated based on 30x40 particles)
Type: Formula Variable
Unit:
Expression: (Column_Volume*(1-Porosity_Column_Initial))/(Number_Reactors*4/3*pi*r_p^3)

---

pH
Description: Bulk water pH
Type: Formula Variable
Unit:
Expression: -log10(S_H_Plus)

---

pH_Initial
Description: Feed water pH (Per typical column influent)
Type: Formula Variable
Unit:

Expression: -log10(Sin_H_Plus)

Porosity_Column_Actual

Description: Actual porosity of column during a simulation
Type: Formula Variable
Unit:
Expression: Porosity_Column_Initial*Vol_BulkWater/Vol_Reactor

---

Porosity_Column_Initial

Description: Assumed initial porosity of a reactor (Must reenter Reactor Volume if this is changed)
Type: Formula Variable
Unit:
Expression: 0.4

Q_Influent

Description: Influent flow to reactors (Based on 4 minute EBCT)
Type: Real List Variable
Unit: m^3/d
Argument: calcnum
Standard Deviations: global
Rel. Stand. Deviat.: 0
Abs. Stand. Deviat.: 1
Minimum: 0
Maximum: 1e+009
Interpolation Method: Linear Interpolation
Sensitivity Analysis: inactive
Real Data Pairs (2 pairs):

0	0.006480
1	0.006336

Ratio_FilmD_WaterD

Description: Ratio of film diffusion coefficient to water diffusion coefficient (Per Rittmann & McCarty, Page 221)
Type: Formula Variable
Unit:
Expression: 0.8

Re_m

Description: Modified Reynolds number (Per Rittmann & McCarty, Equation 4.30)
Type: Formula Variable
Unit:
Expression: 2*rho_water*(r_p*2*100)*(Vel_Water_Superficial*100)/((1-Porosity_Column_Actual)*mu)

---

rho_water

Description: Density of water at 20°C
Type: Formula Variable
Unit: g/cm^3
Expression: 1

---

rho_X
Description: Maximum Bacterial cell density in biofilm (Per Rittmann & McCary, Table 9.4)
Type: Formula Variable
Unit: g/m^3
Expression: 40000

---

r_p
Description: Radius of anthracite particles calculated by geometric mean (Based on 30x40 mesh size)
Type: Formula Variable
Unit: m
Expression: (sqrt(594*420)/2)*1e-006

Sc_BDCM
Description: BDCM Schmidt number (Per Rittmann & McCarty, Equation 4.30)
Type: Formula Variable
Unit:
Expression: mu/(rho_water*D_BDCM*100^2)

Sc_DBCM
Description: DBCM Schmidt number (Per Rittmann & McCarty, Equation 4.30)
Type: Formula Variable
Unit:
Expression: mu/(rho_water*D_DBCM*100^2)

Sc_NH3
Description: NH_3 Schmidt number (Per Rittmann & McCarty, Equation 4.30)
Type: Formula Variable
Unit:
Expression: mu/(rho_water*D_NH3*100^2)

Sc_TBM
Description: TBM Schmidt number (Per Rittmann & McCarty, Equation 4.30)
Type: Formula Variable
Unit:
Expression: mu/(rho_water*D_TBM*100^2)

Sc_TCM
Description: TCM Schmidt number (Per Rittmann & McCarty, Equation 4.30)
Type: Formula Variable

Unit:
Expression: mu/(rho_water*D_TCM*100^2)

Sigma
Description: Shear stress for use in detachment rate (Per Rittmann & McCarty, Equation 4.33)
Type: Formula Variable
Unit: g/cm-s^2
Expression: 200*mu*(Vel_Water_Superficial*100)*(1-Porosity_Column_Actual)^2/((r_p*2*100)^2* Porosity_Column_Actual^3*(SSA/100)*7.46e+009)

Sin_Alkalinity
Description: Feed water alkalinity concentration (Per typical Lake Austin water)
Type: Formula Variable
Unit: mg/L as CaCO3
Expression: 150

Sin_BDCM
Description: Influent BDCM concentration (Per experiment design)
Type: Formula Variable
Unit: gBDCM/m^3
Expression: 0

Sin_Carbonate
Description: Calculated initial total carbonate based on initial alkalinity and initial pH
Type: Formula Variable
Unit: mg/L as CaCO3
Expression: Sin_Alkalinity*(Sin_H_Plus/Carbonate_K_1+1)

Sin_DBCM
Description: Influent DBCM concentration (Per experiment design)
Type: Formula Variable
Unit: gDBCM/m^3
Expression: 0.025

Sin_H_Plus
Description: Feed water hydrogen ion concentration (Per experiment design)
Type: Formula Variable
Unit: M
Expression: 1e-008

Sin_TBM
Description: Influent TBM concentration (Per experiment design)
Type: Formula Variable
Unit: gTBM/m^3
Expression: 0

Sin_TCM

Description: Influent TCM concentration (Per experiment design)
Type: Formula Variable
Unit: gTCM/m^3
Expression: 0.1

Sin_TRIN

Description: Influent $TOTNH_3$ concentration
Type: Formula Variable
Unit: g $TOTNH_3$/m^3
Expression: 4

SSA

Description: Specific surface area of anthracite particle
Type: Formula Variable
Unit: 1/m
Expression: 3/r_p

S_Alkalinity

Description: Alkalinity bulk water concentration
Type: Formula Variable
Unit: mg/L as CaCO3
Expression: Sin_Alkalinity-7.1*(Sin_TRIN-S_TRIN)

S_BDCM

Description: BDCM bulk liquid concentration
Type: Dyn. Volume State Var.
Unit: gBDCM/m^3
Relative Accuracy: 1e-006
Absolute Accuracy: 1e-006

S_Carbonate

Description: Calculated carbonate based on $TOTNH_3$ degradation
Type: Formula Variable
Unit: mg/L as CaCO3
Expression: Sin_Carbonate-0.35*(Sin_TRIN-S_TRIN)

S_DBCM

Description: DBCM bulk liquid concentration
Type: Dyn. Volume State Var.
Unit: gDBCM/m^3
Relative Accuracy: 1e-006
Absolute Accuracy: 1e-006

S_H_Plus

Description: Bulk water hydrogen ion concentration
Type: Formula Variable
Unit: M
Expression: Carbonate_K_1*(S_Carbonate/S_Alkalinity-1)

S_TBM
Description: TBM bulk liquid concentration
Type: Dyn. Volume State Var.
Unit: gTBM/m^3
Relative Accuracy: 1e-006
Absolute Accuracy: 1e-006

S_TCM
Description: TCM bulk liquid concentration
Type: Dyn. Volume State Var.
Unit: gTCM/m^3
Relative Accuracy: 1e-006
Absolute Accuracy: 1e-006

S_TRIN
Description: $TOTNH_3$ bulk liquid concentration
Type: Dyn. Volume State Var.
Unit: gN/m^3
Relative Accuracy: 1e-006
Absolute Accuracy: 1e-006

S_TRIN_Min
Description: Minimum substrate concentration for the biofilm
Type: Formula Variable
Unit: g/m^3
Expression: (Ks_NH3/Alpha1_Ammonia)*kd/(Yield*k_TRIN-kd)

Tc_BDCM
Description: BDCM transformation capacity (Per experiments)
Type: Formula Variable
Unit: gBDCM/gX
Expression: 0.0073

Tc_DBCM
Description: DBCM transformation capacity (Per experiments)
Type: Formula Variable
Unit: gDBCM/gX
Expression: 0.0065

Tc_TBM
Description: TBM transformation capacity (Per experiments)

Type: Formula Variable
Unit: gTBM/gX
Expression: 0.0056

Tc_TCM
Description: TCM transformation capacity (Per experiments)
Type: Formula Variable
Unit: gTCM/gX
Expression: 0.0092

Vel_Water_Actual
Description: Actual water velocity in the column
Type: Formula Variable
Unit: m/d
Expression: Vel_Water_Superficial/Porosity_Column_Actual

Vel_Water_Superficial
Description: Superficial column water velocity
Type: Formula Variable
Unit: m/d
Expression: Q_Influent/Column_Area

Vol_BulkWater
Description: Bulk water volume
Type: Program Variable
Unit: m^3
Reference to: Bulk Volume

Vol_Reactor
Description: Volume of the reactor
Type: Program Variable
Unit: m^3
Reference to: Reactor Volume

X
Description: Biofilm biomass concentration
Type: Dyn. Volume State Var.
Unit: gX/m^3
Relative Accuracy: 1e-006
Absolute Accuracy: 1e-006

X_Fraction
Description: Biomass fraction of biofilm
Type: Formula Variable
Unit:
Expression: 1.0

Yield

Description: Yield coefficient for nitrifier (Per Rittmann & McCarty, Table 3.1)
Assumes VSS/TSS ratio of 0.8
Type: Formula Variable
Unit:
Expression: 0.34/0.8

Z

Description: Biofilm distance from substratum
Type: Program Variable
Unit: m
Reference to: Space Coordinate Z

PROCESSES

Decay_X

Description: Nitrifiers Endogenous Decay
Type: Dynamic Process
Rate: kd*X
Stoichiometry: Variable : Stoichiometric Coefficient
X : -1

Deg_BDCM

Description: Bromodichloromethane Degradation Rate
Type: Dynamic Process
Rate: k1_BDCM*X*S_BDCM*Alpha1_Ammonia*S_TRIN/(Ks_NH3+ Alpha1_Ammonia*S_TRIN)
Stoichiometry: Variable : Stoichiometric Coefficient
X : -1/Tc_BDCM
S_BDCM : -1

Deg_DBCM

Description: Dibromchloromethane Degradation Rate
Type: Dynamic Process
Rate: k1_DBCM*X*S_DBCM*Alpha1_Ammonia*S_TRIN/(Ks_NH3+ Alpha1_Ammonia*S_TRIN)
Stoichiometry: Variable : Stoichiometric Coefficient
X : -1/Tc_DBCM
S_DBCM : -1

Deg_TBM

Description: Tribromomethane Degradation Rate
Type: Dynamic Process
Rate: k1_TBM*X*S_TBM*Alpha1_Ammonia*S_TRIN/(Ks_NH3+ Alpha1_Ammonia*S_TRIN)
Stoichiometry: Variable : Stoichiometric Coefficient
X : -1/Tc_TBM
S_TBM : -1

Deg_TCM

Description: Trichloromethane Degradation
Type: Dynamic Process
Rate: k1_TCM*X*S_TCM*Alpha1_Ammonia*S_TRIN/(Ks_NH3+ Alpha1_Ammonia*S_TRIN) Stoichiometry: Variable :
Stoichiometry: Variable : Stoichiometric Coefficient
X : -1/Tc_TCM
S_TCM : -1

Growth_X

Description:	Nitrifiers Growth Rate
Type:	Dynamic Process
Rate:	Yield*k_TRIN*X*S_TRIN*Alpha1_Ammonia/(Ks_NH3+ Alpha1_Ammonia*S_TRIN)
Stoichiometry:	Variable : Stoichiometric Coefficient X : 1 S_TRIN : -1/Yield

---

COMPARTMENTS

Reactor_1

Description: Biofilm Reactor Compartment (1st in series)
Type: Biofilm Reactor Compartment
Compartment Index: 0
Active Variables: S_TRIN, S_TCM, S_BDCM, S_DBCM, S_TBM, X
Active Processes: Growth_X, Decay_X, Deg_TCM, Deg_BDCM, Deg_DBCM, Deg_TBM
Initial Conditions: Variable(Zone) : Initial Condition
LF(Biofilm Matrix) : LF_Initial
X(Biofilm Matrix) : rho_X*X_Fraction
Inflow: Q_Influent
Loadings: Variable : Loading
S_BDCM : Q_Influent*Sin_BDCM
S_TRIN : Q_Influent*Sin_TRIN
S_DBCM : Q_Influent*Sin_DBCM
S_TBM : Q_Influent*Sin_TBM
S_TCM : Q_Influent*Sin_TCM

Particulate Variables:

X:

- Density: rho_X
- Surf. Att. Coeff.: 0
- Surf. Det. Coeff.: 0
- Vol. Att. Coeff.: 0
- Vol. Det. Coeff.: 0
- Layer Resist.: 0
- Pore Diffusivity: 0
- Matrix Diffusivity: 0

Dissolved Variables:

S_TRIN:

- Layer Resist.: LL_NH3/D_NH3
- Pore Diffusivity: D_NH3*Ratio_FilmD_WaterD

S_BDCM:

- Layer Resist.: LL_BDCM/D_BDCM
- Pore Diffusivity: D_BDCM*Ratio_FilmD_WaterD

S_DBCM:

- Layer Resist.: LL_DBCM/D_DBCM
- Pore Diffusivity: D_DBCM*Ratio_FilmD_WaterD

S_TBM:

- Layer Resist.: LL_TBM/D_TBM
- Pore Diffusivity: D_TBM*Ratio_FilmD_WaterD

S_TCM:

- Layer Resist.: LL_TCM/D_TCM
- Pore Diffusivity: D_TCM*Ratio_FilmD_WaterD

Reactor Type: confined
Reactor Volume: 2.4e-007
Pore Volume: liquid phase only
Biofilm Matrix: rigid
Detach. Velocity: 0
Film Surface: Area_Biofilm
Rate of epsFl: 0
Num. of Grid Pts: 22 (low resolution)
Accuracies:
- Rel. Acc. Q: 0.001
- Abs. Acc. Q: 0.001
- Rel. Acc. V: 0.001
- Abs. Acc. V: 1e-010
- Rel. Acc. Z: 0.001
- Abs. Acc. Z: 1e-010
- Rel. Acc. EPS: 0.001
- Abs. Acc. EPS: 0.001

Reactor_2 ****Note: Typical of Reactors 2 through n in series***
Description: Biofilm Reactor Compartment (2nd in series)
Type: Biofilm Reactor Compartment
Compartment Index: 0
Active Variables: S_TRIN, S_TCM, S_BDCM, S_DBCM, S_TBM, X
Active Processes: Growth_X, Decay_X, Deg_TCM, Deg_BDCM, Deg_DBCM, Deg_TBM
Initial Conditions: Variable(Zone) : Initial Condition
LF(Biofilm Matrix) : LF_Initial
X(Biofilm Matrix) : rho_X*X_Fraction
Inflow: 0
Loadings:
Particulate Variables:
- X:
  - Density: rho_X
  - Surf. Att. Coeff.: 0
  - Surf. Det. Coeff.: 0
  - Vol. Att. Coeff.: 0
  - Vol. Det. Coeff.: 0
  - Layer Resist.: 0
  - Pore Diffusivity: 0
  - Matrix Diffusivity: 0

Dissolved Variables:
- S_TRIN:
  - Layer Resist.: LL_NH3/D_NH3
  - Pore Diffusivity: D_NH3*Ratio_FilmD_WaterD
- S_BDCM:

Layer Resist.: LL_BDCM/D_BDCM
Pore Diffusivity: D_BDCM*Ratio_FilmD_WaterD
S_DBCM:
Layer Resist.: LL_DBCM/D_DBCM
Pore Diffusivity: D_DBCM*Ratio_FilmD_WaterD
S_TBM:
Layer Resist.: LL_TBM/D_TBM
Pore Diffusivity: D_TBM*Ratio_FilmD_WaterD
S_TCM:
Layer Resist.: LL_TCM/D_TCM
Pore Diffusivity: D_TCM*Ratio_FilmD_WaterD
Reactor Type: confined
Reactor Volume: 2.4e-007
Pore Volume: liquid phase only
Biofilm Matrix: rigid
Detach. Velocity: 0
Film Surface: Area_Biofilm
Rate of epsFl: 0
Num. of Grid Pts: 22 (low resolution)
Accuracies:
Rel. Acc. Q: 0.001
Abs. Acc. Q: 0.001
Rel. Acc. V: 0.001
Abs. Acc. V: 1e-010
Rel. Acc. Z: 0.001
Abs. Acc. Z: 1e-010
Rel. Acc. EPS: 0.001
Abs. Acc. EPS: 0.001

LINKS

Link_12	****Note: Typical of Links between All Reactors in Series***
Description:	Effluent Reactor 1 is Influent to Reactor 2
Type:	Advective Link
Link Index:	0
Compartment In:	Reactor_1
Connection In:	Outflow
Compartment Out:	Reactor_2
Connection Out:	Inflow
Bifurcations:	

Appendix D: Supplemental Experimental Data

D.1. Batch Kinetic Experiments Method Verification

D.1.1. Abiotic Syringe Experiments

To verify that THMs would not volatilize from the gas-tight syringes during the batch kinetic experiments, two abiotic experiments were conducted. Figure D.1 and Figure D.2 detail the results from these experiments. As can be seen in these figures, individual THM levels remained essentially constant during the experiment with the deviation of any given THM of ±4% from the average individual THM values for the length of the experiment.

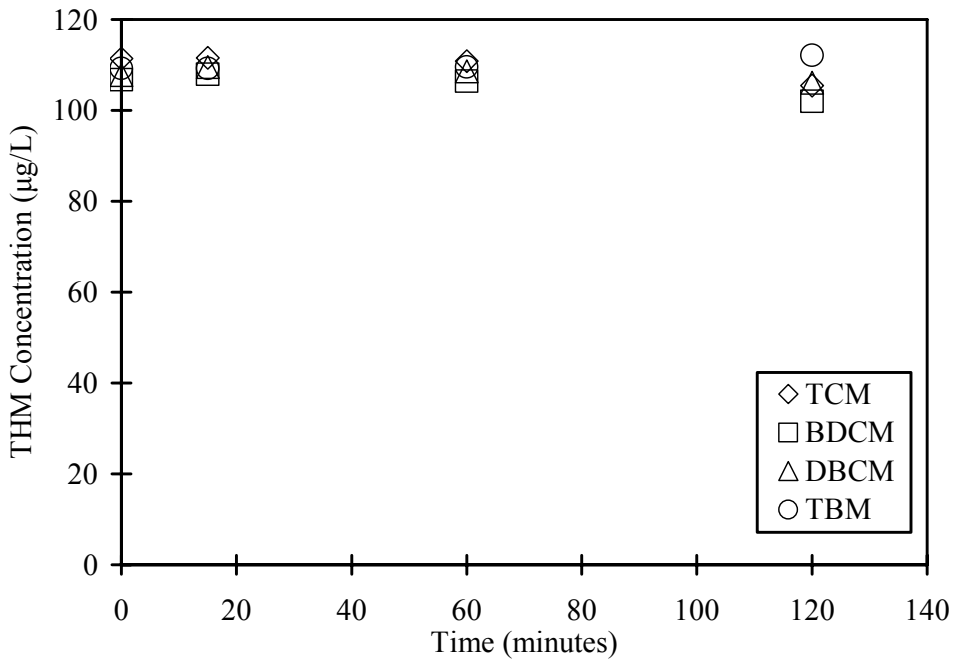

Figure D.1 Abiotic Syringe Experiment 1 THM concentrations conducted to verify no THM volatilization from gas-tight syringe

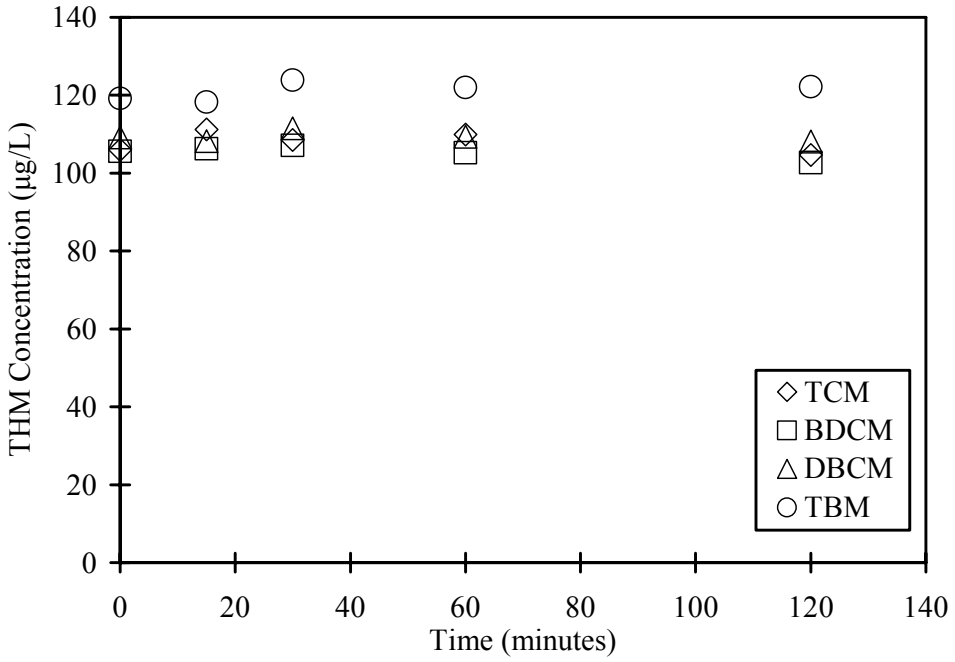

Figure D.2 Abiotic Syringe Experiment 2 THM concentrations conducted to verify no THM volatilization from gas-tight syringe

D.1.2. Experimental Conditions Determination

Initially, several experiments were performed with *N. europaea* under a variety of conditions to determine the experimental conditions that would result in THM cometabolism. These initial experiments were conducted as previously described in Chapter 3 except that buffer water was not aerated with pure oxygen as these experiments did not anticipate this requirement. In addition, 250-mL gas-tight syringes were used in lieu of 500-mL syringes along with glass beakers to allow for oxygen transfer during ammonia only degradation experiments. Table D.1 details the nominal conditions for these experiments.

Table D.1 Nominal conditions summary for Initial Experiments conducted to determine experimental conditions for batch kinetic experiments

Initial Exp.#	Test Unit[a]	TSS (mg/L)	$TOTNH_3$ (mg N/L)	TCM (µg/L)	BDCM (µg/L)	DBCM (µg/L)	TBM (µg/L)	HYD[b] (µM)	HAM[c] (µM)
1	A	28	0	100	100	100	100	0	0
2	A	107	0	100	100	100	100	0	0
2	C	88	0	100	100	100	100	0	0
3	C	58	1	100	0	0	0	0	0
3	BK	64	10	0	0	0	0	0	0
4	A	185	0	100	100	100	100	600	0
4	C	182	0	100	0	0	0	600	0
4	BK	192	20	0	0	0	0	0	0
5	A	269	0	100	100	100	100	600	0
5	B	267	0	100	100	100	100	600	0
5	C	262	0	100	100	100	100	0	90
6	BK	227	10	0	0	0	0	0	0
7	BK1	230	11	0	0	0	0	0	0
7	BK2	230	11	0	0	0	0	0	0
8	BK	141	11	0	0	0	0	0	0
8	CF	96	Constant Feed	0	0	0	0	0	0

[a]BK = beaker; A, B, C = gas-tight syringe A, B, or C; and

CF = ammonia constant feed experimental setup per Ely (1996)

[b]Hydrazine

[c]Hydroxlyamine

The "test unit" column in Table D.1 refers to either one of three 250-mL gas-tight syringes (A, B, or C) or a beaker (BK) that was used in experiments containing ammonia without THM addition. In Initial Experiment (IE) 1 and IE 2, no ammonia was present in the syringe. These experiments resulted in varied and minimal (2 to 15%) THM degradation during the entire length of the experiments (120 to 140 minutes).

IE 1 and IE 2 suggested that ammonia was required for THM cometabolism. IE 3BK was conducted in a beaker to verify ammonia degradation by the bacteria, and IE 3C was conducted with ammonia and TCM present to test the hypothesis that ammonia was required for THM cometabolism. Results of IE 3BK verified ammonia degradation and are shown as Figure D.3, but results of IE 3C, as shown in Figure D.4, were inconclusive as to whether the addition of ammonia to the experiment led to any TCM cometabolism.

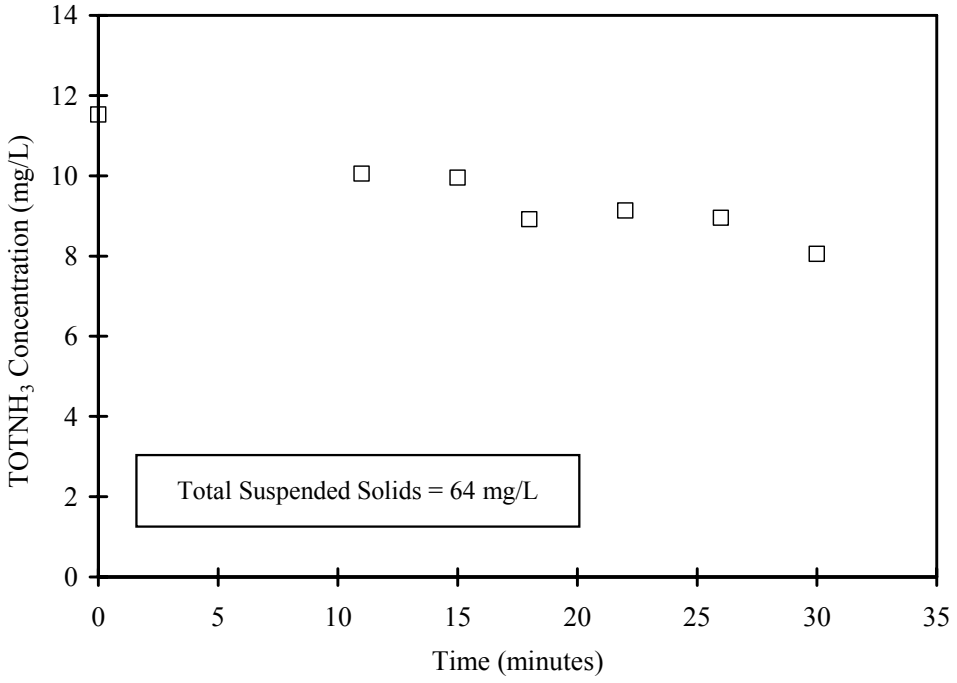

Figure D.3 $TOTNH_3$ concentrations for Initial Experiment 3BK conducted to verify ammonia degradation by *N. europaea*

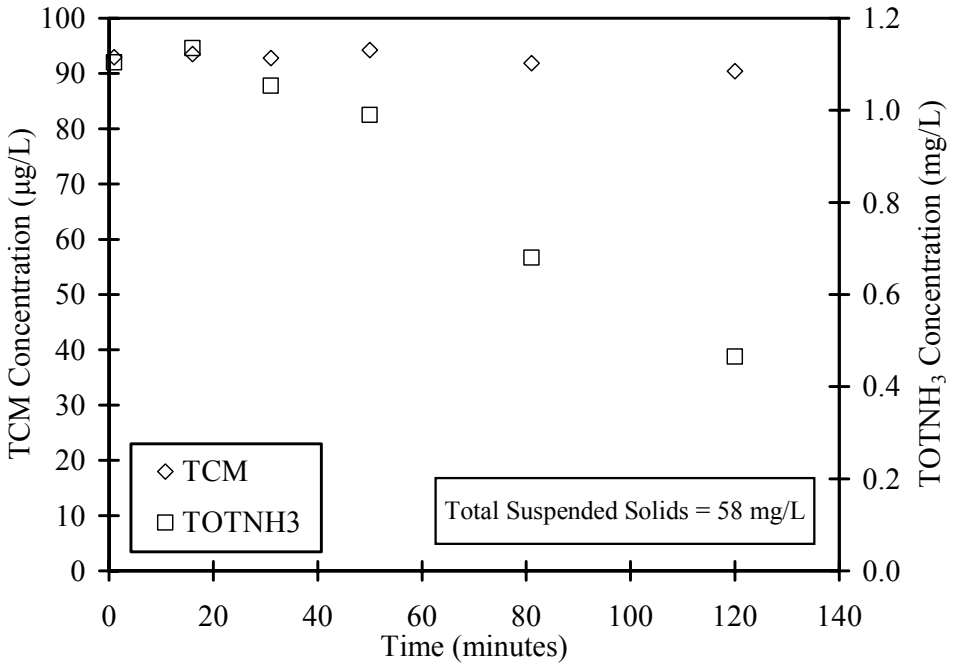

Figure D.4 $TOTNH_3$ and TCM concentrations for Initial Experiment 3C conducted to evaluate the requirement of $TOTNH_3$ for THM cometabolism

As a result, it was proposed that insufficient ammonia was present to provide the reducing power required for TCM to be degraded in IE 3C. Based on this hypothesis, IE 4 and IE 5 were conducted by adding hydrazine (HYD) or hydroxylamine (HAM) for reducing power as was previously done by Hyman et al. (1985). For IE 4A and IE 4C, excess reducing power was provided by adding hydrazine with the results shown in Figure D.5 and Figure D.6. IE 4BK was run in parallel to verify ammonia degradation. As a comparison, hydroxylamine was added in IE 5C with hydrazine added for IE 5A and IE 5B.

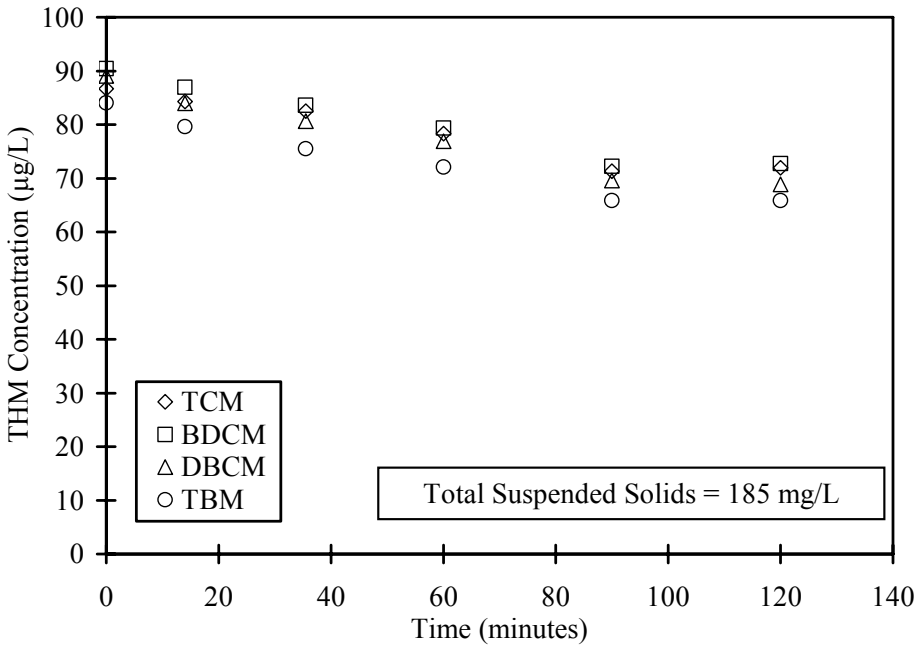

Figure D.5 THM concentrations for Initial Experiment 4A conducted to evaluate THM cometabolism with hydrazine as a reductant source

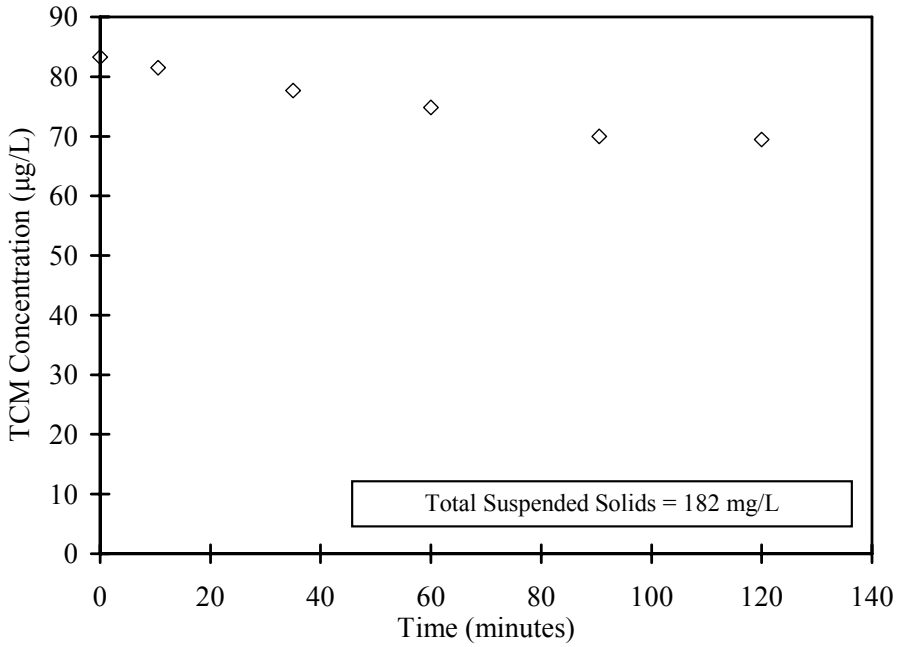

Figure D.6 TCM concentrations for Initial Experiment 4C conducted to evaluate TCM cometabolism with hydrazine as a reductant source

At the end of each of the experiments with hydrazine (IE 4A, IE 4C, IE 5A, and IE 5B), dissolved oxygen was likely limiting as these values reached levels less than 2 mg/L as is illustrated by the last data points in Figure D.5 and Figure D.6 where removal appeared to have stopped. Stoichiometric calculations also indicated that dissolved oxygen would be depleted before hydrazine. Overall, these experiments provided evidence that a reductant source was required for *N. europaea* to cometabolize the four THMs and that $TOTNH_3$ was not provided in a sufficient concentration in IE 3C.

To arrive at initial kinetic parameters for THM cometabolism, first order degradation kinetics were assumed for IE 4A and IE 4C, and the corresponding first-order kinetic parameters were determined and are shown in Table D.2 with their 95% confidence limits (CLs). These values were obtained by excluding the last data point in each experiment because of apparent oxygen limitation.

Table D.2 Initial Experiment first-order kinetic comparison, $k_{1_{THM}}$ (L/mg-d) ± 95% CL

Initial Exp. #	TCM	BDCM	DBCM	TBM
4A	0.016 ± 0.003	0.019 ± 0.002	0.020 ± 0.002	0.020 ± 0.002
4C	0.015 ± 0.001			

Table D.2 shows no significant difference in the degradation rate of TCM with and without the presence of the other THMs, implying that there was no competition between TCM and the other THMs. The degradation rate for each THM was similar in IE 4A.

Because ammonia degradation would lead to consumption of dissolved oxygen, experiments conducted with saturation based on air could lead to oxygen limiting

conditions during the batch kinetic studies conducted in gas-tight syringes. To address this issue, the buffer media was oxygenated with pure oxygen prior to batch kinetic experiments to non-limiting levels based on starting $TOTNH_3$ concentrations. To confirm that the high level of oxygen would not adversely affect the nitrifiers, baseline experiments were conducted and kinetic parameters determined for experiments conducted with ambient dissolved oxygen concentrations (IE 7BK1, IE 7BK2, and IE 8BK). A summary of the results for these experiments is shown as Table D.3. These 95% joint CLs overlap several of the batch kinetic experiments conducted for *N. europaea* presented in Chapter 4, indicating no apparent effect from elevated dissolved oxygen levels during the batch kinetic experiments.

Table D.3 Ammonia kinetic parameter comparison and 95% joint CLs for Initial Experiments conducted with ambient dissolved oxygen concentrations

Initial Exp. #	k_{TOTNH_3} (mg $TOTNH_3$/mg TSS-d)	$K_{s_{NH_3\text{-}N}}$ (mg NH_3-N/L)
7BK1	6.4 ± 4.9	0.47 ± 0.46
7BK2	4.3 ± 0.95	0.12 ± 0.04
8BK	6.8 ± 6.3	0.91 ± 1.13

One further initial experiment was conducted to verify ammonia degradation under Ely's (1996) experimental conditions. For this experiment, a beaker was provided an initial ammonia concentration (approximately 19 mg/L $TOTNH_3$) and then fed a continuous ammonia feed with $TOTNH_3$ and nitrite-nitrogen concentrations measured over time and shown as Figure D.7 and Figure D.8, respectively. During this experiment, the rate of nitrite production would correspond to the rate of ammonia degradation.

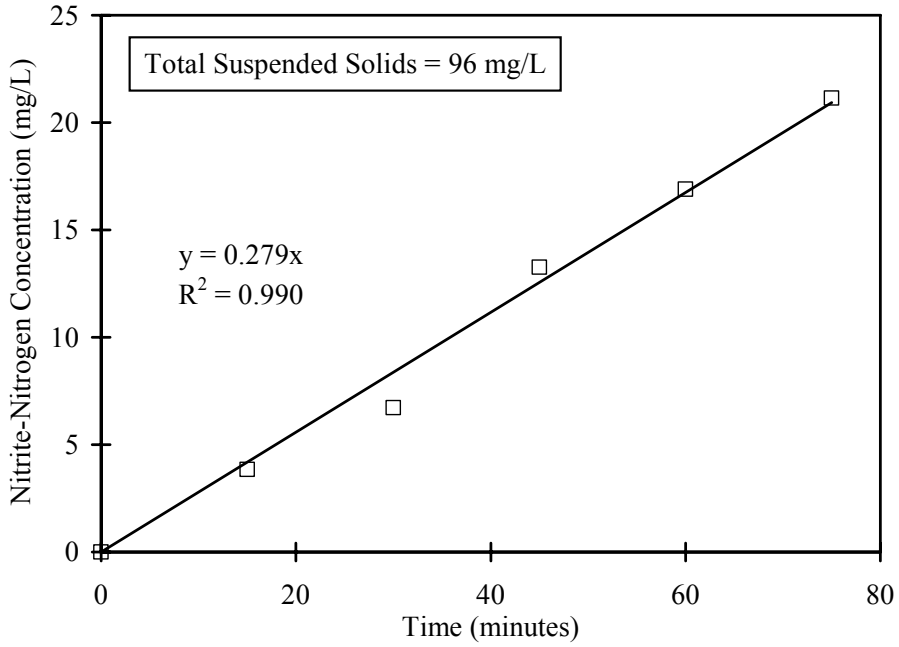

Figure D.7 Nitrite-nitrogen production during Initial Experiment 8CF

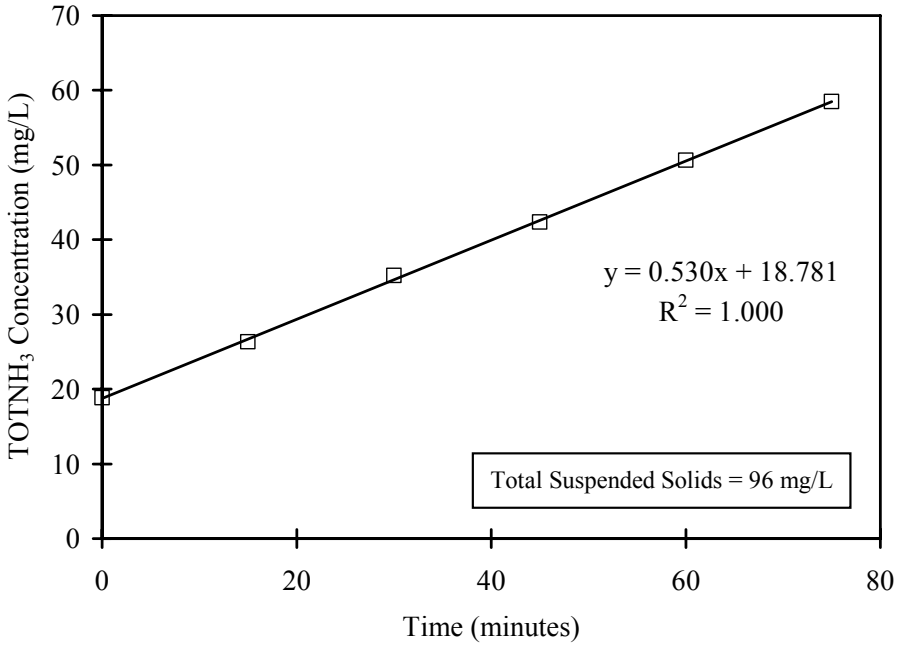

Figure D.8 $TOTNH_3$ concentrations during Initial Experiment 8CF

Because the minimum NH_3-N concentration during the experiment (0.90 mg/L) was much larger than the expected $K_{s_{NH_3\text{-}N}}$ based on comparison with IE 7 BK2, the rate of nitrite-nitrogen production corresponds with k_{TOTNH_3}. From the slope of the nitrite-nitrogen production and measured TSS in the reactor, a value of k_{TOTNH_3} and its corresponding 95% CL was determined as 4.2 ± 0.29 mg $TOTNH_3$/mg TSS-d and is not significantly different than that determined from the values presented in Table D.3.

Because of these initial experiments, the test method for the batch kinetic experiments was slightly modified from the initial experiments to the final form previously described in Chapter 3 as follows:

- 500-mL, glass, gas-tight syringes were used for the reactor in lieu of 250-mL syringes to provide sufficient volume so that both ammonia and THM samples could be taken simultaneously.
- Buffered water used in the kinetics tests was preaerated with pure oxygen to a dissolved oxygen content that would not be limiting based on the known ammonia addition.
- Ammonia was provided in an amount to be present throughout experiments and to degrade to such levels as to allow determination of both the maximum specific rate of degradation, k_{TOTNH_3}, and half-saturation constant, $K_{s_{NH_3\text{-}N}}$.
- Ammonia and THM kinetics were simultaneously determined from a single gas-tight syringe experiment.
- pH was measured with each ammonia sample, and temperature was measured for each experiment to allow conversion from $TOTNH_3$ to NH_3-N.
- Initial and final dissolved oxygen concentrations were measured to verify non-limiting oxygen conditions.

D.2. ABIOTIC SYRINGE EXPERIMENTS DATA

Table D.4 Abiotic Syringe Experiment 1 experimental data

Time (minutes)	THM Concentrations (µg/L)			
	TCM	BDCM	DBCM	TBM
0	111	107	108	109
15	112	108	110	109
60	111	106	109	110
120	106	102	106	112

Table D.5 Abiotic Syringe Experiment 2 experimental data

Time (minutes)	THM Concentrations (µg/L)			
	TCM	BDCM	DBCM	TBM
0	106	106	109	119
15	111	106	108	118
30	108	107	112	124
60	110	105	109	122
120	105	103	108	122

D.3. INITIAL BATCH KINETIC EXPERIMENTS DATA AND 95% JOINT CONFIDENCE INTERVALS

Table D.6 Initial Experiment 1A experimental data

Time (minutes)	THM Concentrations (µg/L)			
	TCM	BDCM	DBCM	TBM
0.00	95	94	89	88
11.00	97	94	90	89
22.50	93	90	86	85
37.00	92	89	84	84
56.00	93	91	87	87
80.00	92	90	86	86
120.00	81	85	84	86

Table D.7 Initial Experiment 2A experimental data

Time (minutes)	THM Concentrations (µg/L)			
	TCM	BDCM	DBCM	TBM
0.00	88	93	92	94
9.75	82	86	85	87
19.00	82	85	83	84
35.00	87	92	92	94
60.00	83	86	84	86
90.00	83	85	83	85
120.00	74	82	83	86

Table D.8 Initial Experiment 2C experimental data

Time (minutes)	THM Concentrations (µg/L)			
	TCM	BDCM	DBCM	TBM
0.00	86	92	90	92
26.00	82	88	85	90
50.00	81	86	81	87
75.00	75	80	76	81
100.00	80	85	80	86
120.00	80	87	83	88
135.00	77	82	78	83

Table D.9 Initial Experiment 3C experimental data

Time (minutes)	$TOTNH_3$ (mg/L)	TCM (µg/L)
1.00	1.1	93
16.00	1.1	94
31.00	1.1	93
50.00	0.99	94
81.00	0.68	92
120.00	0.47	90

Table D.10 Initial Experiment 3BK experimental data

Time (minutes)	$TOTNH_3$ (mg/L)
0.00	12
11.00	10
15.00	10
18.00	8.9
22.00	9.1
26.00	9.0
30.00	8.0

Table D.11 Initial Experiment 4A experimental data

Time (minutes)	THM Concentrations (µg/L)			
	TCM	BDCM	DBCM	TBM
0.00	87	90	89	84
14.00	84	87	84	80
35.50	83	84	81	76
60.00	78	79	77	72
90.00	71	72	70	66
120.00	72	73	69	66

Table D.12 Initial Experiment 4C experimental data

Time (minutes)	TCM (μg/L)
0.00	83
10.50	81
35.00	78
60.00	75
90.50	70
120.00	70

Table D.13 Initial Experiment 4BK experimental data

Time (minutes)	pH	$TOTNH_3$ (mg/L)
0.00	8.2	23
12.00	8.2	19
24.50	8.3	16
34.50	8.4	12
54.50	8.5	5.0
74.50	8.7	2.2

Table D.14 Initial Experiment 5A experimental data

Time (minutes)	THM Concentrations (µg/L)			
	TCM	BDCM	DBCM	TBM
0.00	93	98	99	93
20.00	91	95	95	90
40.00	89	94	94	89
60.00	87	91	91	86
80.00	84	89	89	85
120.00	85	89	88	84

Table D.15 Initial Experiment 5B experimental data

Time (minutes)	THM Concentrations (µg/L)			
	TCM	BDCM	DBCM	TBM
0.00	91	95	95	90
20.00	89	94	94	90
40.00	88	92	91	87
60.00	86	90	89	85
80.00	87	89	88	84
120.00	86	89	86	84

Table D.16 Initial Experiment 5C experimental data

Time (minutes)	THM Concentrations (µg/L)			
	TCM	BDCM	DBCM	TBM
0.00	94	98	97	101
20.00	94	96	95	99
40.00	94	96	94	98
60.00	93	95	92	96
80.00	94	95	93	97
120.00	90	93	91	95

Table D.17 Initial Experiment 7BK1 experimental data

Time (minutes)	$TOTNH_3$ (mg/L)
0.00	11
8.00	7.7
16.00	3.4
24.00	1.3
32.00	0.33
38.00	0.11

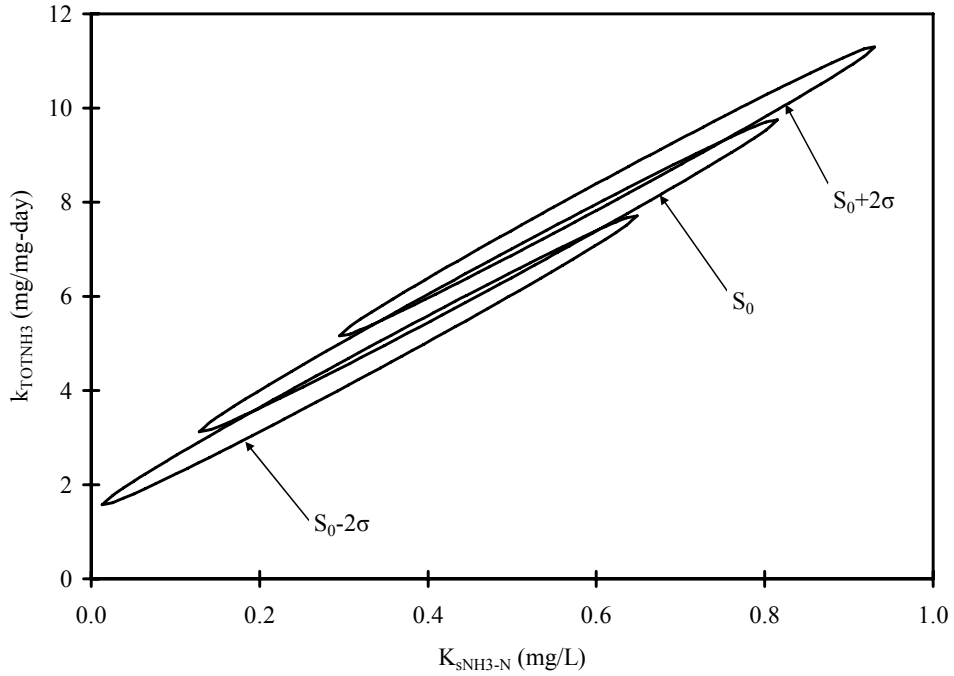

Figure D.9 Initial Experiment 7BK1 95% joint confidence intervals for $TOTNH_3$

Table D.18 Initial Experiment 7BK2 experimental data

Time (minutes)	$TOTNH_3$ (mg/L)
0.00	11
8.00	6.6
16.00	3.3
24.00	1.3
32.00	0.40
38.00	0.14

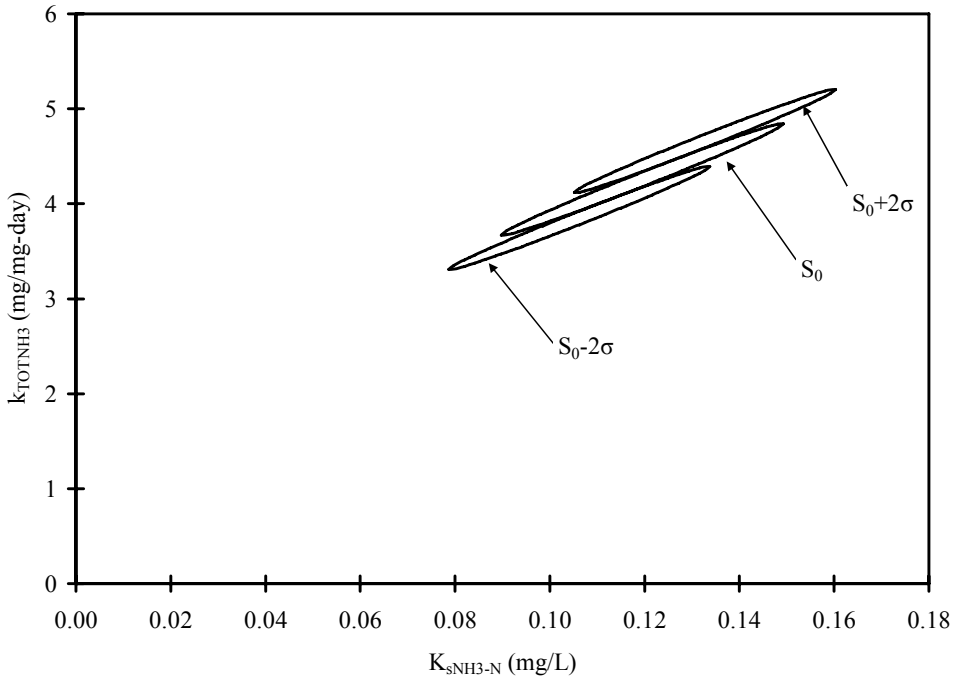

Figure D.10 Initial Experiment 7BK2 95% joint confidence intervals for $TOTNH_3$

Table D.19 Initial Experiment 8BK experimental data

Time (minutes)	$TOTNH_3$ (mg/L)
0.00	11
15.00	7.7
23.00	5.7
30.00	4.0
38.00	2.1
46.00	0.96
54.00	0.40
62.00	0.27

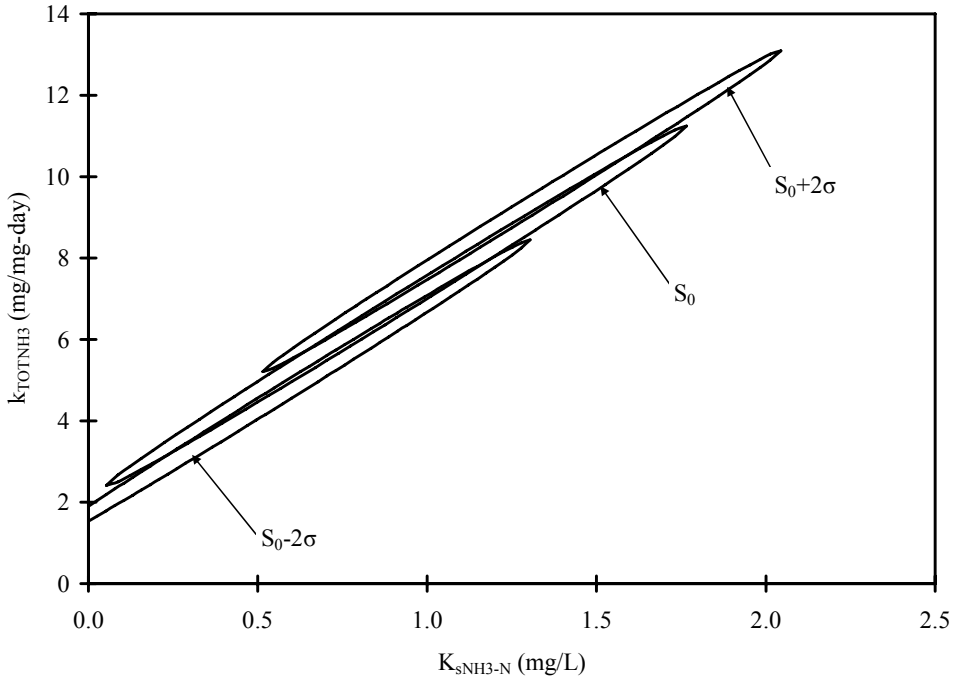

Figure D.11 Initial Experiment 8BK 95% joint confidence intervals for $TOTNH_3$

Table D.20 Initial Experiment 8CF experimental data

Time (minutes)	Nitrite-Nitrogen (mg/L)	$TOTNH_3$ (mg/L)
0.00	0.0	19
15.00	3.8	26
30.00	6.7	35
45.00	13	42
60.00	17	51
75.00	21	58

D.4. BATCH KINETIC EXPERIMENTS DATA AND 95% JOINT CONFIDENCE INTERVALS

Table D.21 Experiment 1 experimental data

$TOTNH_3$ Time (minutes)	pH	$TOTNH_3$ (mg/L)	THM Time (minutes)	THM Concentrations (μg/L)			
				TCM	BDCM	DBCM	TBM
0.00	8.6	7.8	1.50	92	94	91	92
10.00	8.4	6.5	11.25	86	88	85	85
20.00	8.3	5.5	21.50	84	84	80	79
29.50	8.2	4.5	31.50	80	79	73	72
43.25	8.1	3.4	44.75	78	76	69	67
60.00	7.9	2.6	61.25	76	72	65	62

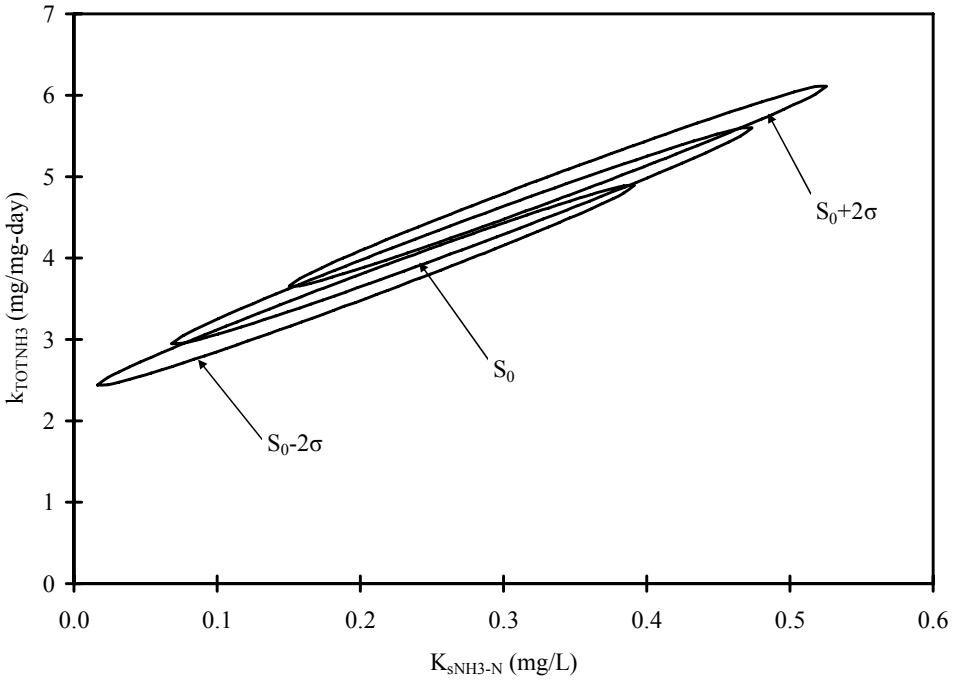

Figure D.12 Experiment 1 95% joint confidence intervals for $TOTNH_3$

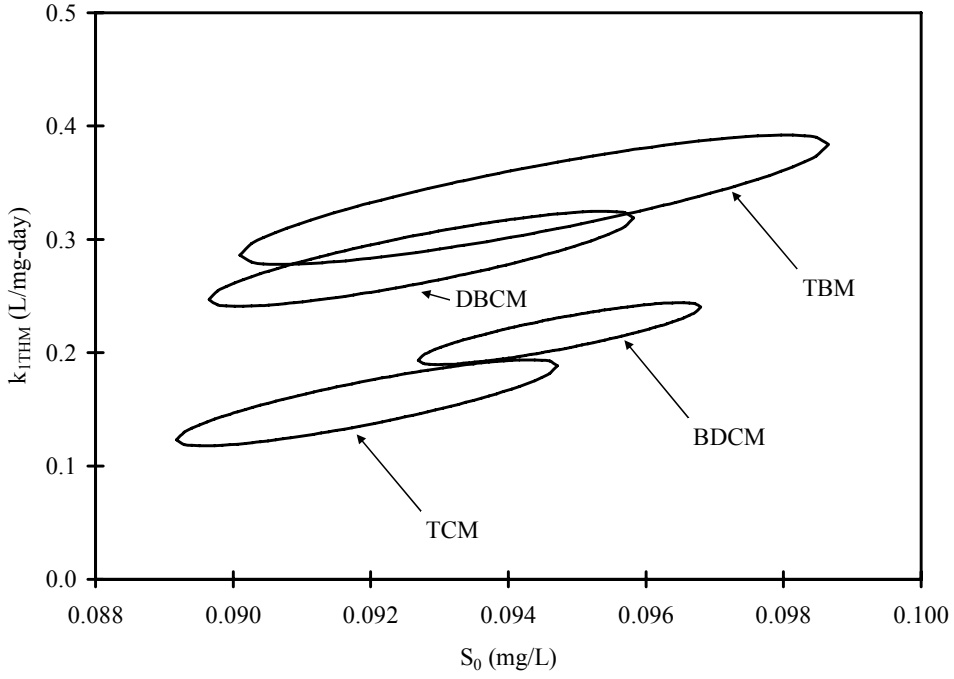

Figure D.13 Experiment 1 95% joint confidence intervals for THMs

Table D.22 Tukey's paired comparison for $k_{1_{THM}}$ for Experiment 1

Experiment	Observations	σ	σ^2
TCM	6	0.019	0.00036
BDCM	6	0.014	0.00019
DBCM	6	0.021	0.00044
TBM	6	0.029	0.00081
Total Observations =	24	Pooled σ^2 =	0.00045
Degrees of Freedom (v) =	20	Pooled σ =	0.021
Treatments (k) =	4		
$q_{k,v,0.025}$ =	4.426		
Allowable $y_{bar,i}$-$y_{bar,j}$ = ±	0.038		

Absolute value of $y_{bar,i}$-$y_{bar,j}$

	TCM	BDCM	DBCM	TBM
TCM				
BDCM	0.061			
DBCM	0.13	0.066		
TBM	0.18	0.12	0.052	

Table D.23 Experiment 2 experimental data

$TOTNH_3$ Time (minutes)	pH	$TOTNH_3$ (mg/L)	THM Time (minutes)	THM Concentrations (µg/L)			
				TCM	BDCM	DBCM	TBM
0.00	8.9	7.4	1.50	95	96	96	98
10.25	8.8	6.1	11.50	93	92	91	92
20.00	8.7	5.3	21.50	88	87	83	83
30.25	8.7	4.1	31.75	86	83	78	77
40.00	8.6	3.1	41.50	83	78	72	71
50.50	8.5	2.1	52.00	79	74	67	65
60.25	8.4	1.4	62.00	76	71	63	60
80.25	8.3	0.41	81.50	75	66	58	54

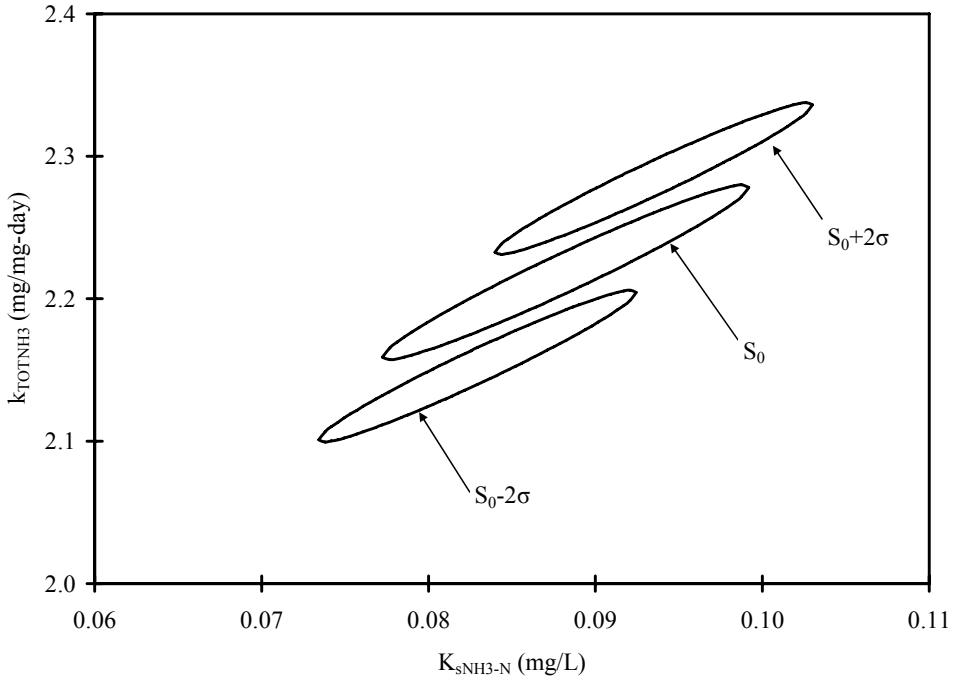

Figure D.14 Experiment 2 95% joint confidence intervals for $TOTNH_3$

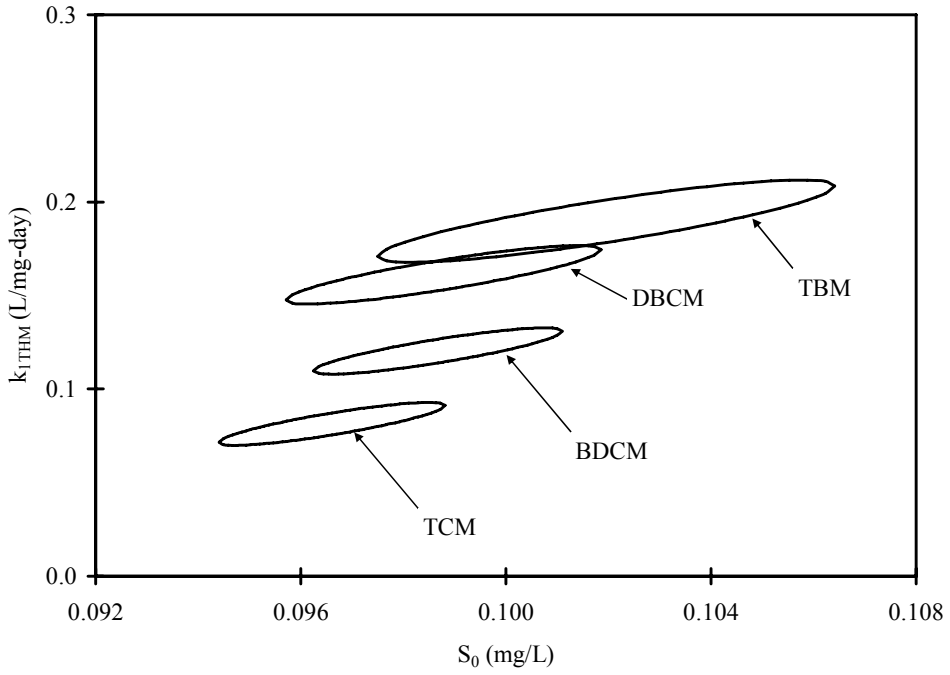

Figure D.15 Experiment 2 95% joint confidence intervals for THMs

Table D.24 Tukey's paired comparison for $k_{1_{THM}}$ for Experiment 2

Experiment	Observations	σ	σ^2
TCM	8	0.0057	0.000033
BDCM	8	0.0062	0.000038
DBCM	8	0.0078	0.000061
TBM	8	0.011	0.00012
Total Observations =	32	Pooled σ^2 =	0.000063
Degrees of Freedom (v) =	28	Pooled σ =	0.0079
Treatments (k) =	4		
$q_{k,v,0.025}$ =	4.296		
Allowable $y_{bar,i}$-$y_{bar,j}$ = ±	0.012		

Absolute value of $y_{bar,i}$-$y_{bar,j}$

	TCM	BDCM	DBCM	TBM
TCM				
BDCM	0.039			
DBCM	0.080	0.041		
TBM	0.11	0.069	0.029	

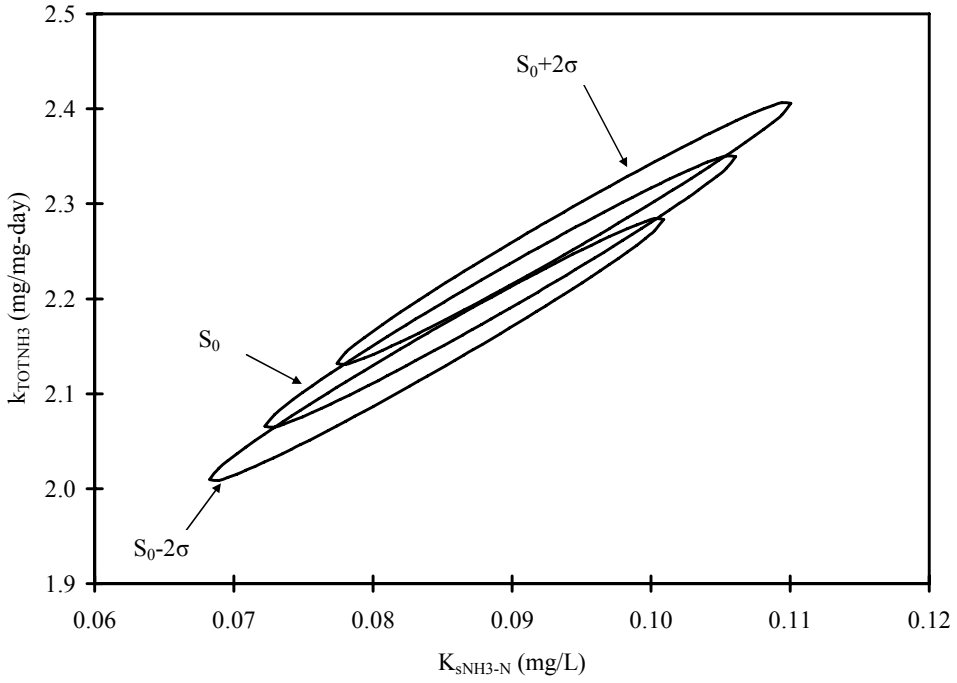

Figure D.16 Experiment 2 (4 mg/L start) 95% joint confidence intervals for $TOTNH_3$

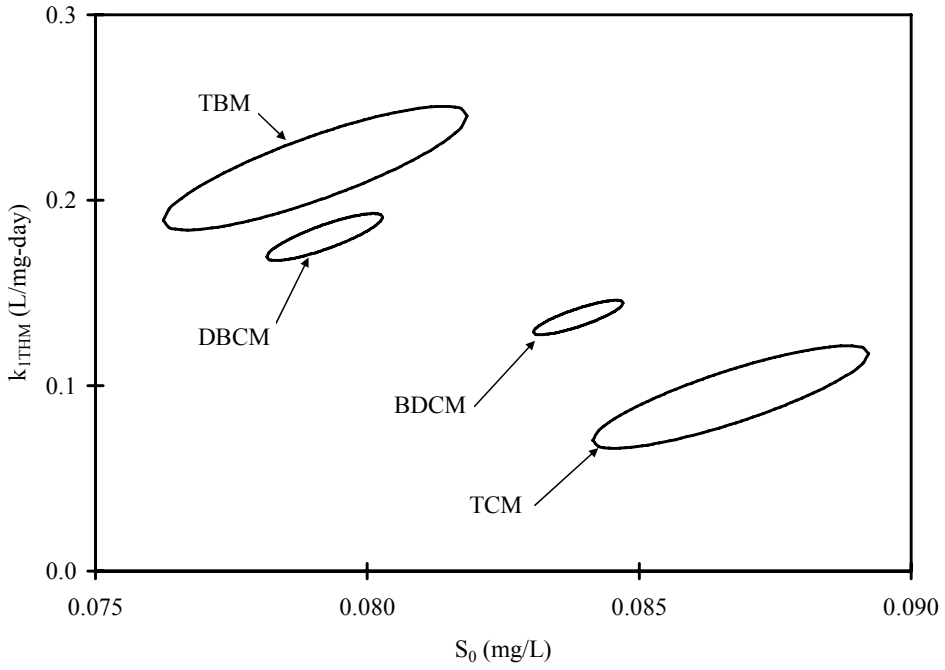

Figure D.17 Experiment 2 (4 mg/L start) 95% joint confidence intervals for THMs

Table D.25 Experiment 3 experimental data

$TOTNH_3$ Time (minutes)	pH	$TOTNH_3$ (mg/L)	THM Time (minutes)	THM Concentrations (µg/L)			
				TCM	BDCM	DBCM	TBM
0.00	8.6	3.9	1.50	101	101	101	104
8.25	8.6	2.9	9.50	97	97	97	99
16.25	8.5	2.2	17.50	94	93	91	91
24.50	8.4	1.5	25.50	92	89	84	82
32.75	8.3	0.90	34.00	91	86	81	79
40.25	8.3	0.54	41.50	88	85	80	78
48.25	8.3	0.31	49.75	88	84	78	75
56.25	8.3	0.15	57.50	87	82	75	71

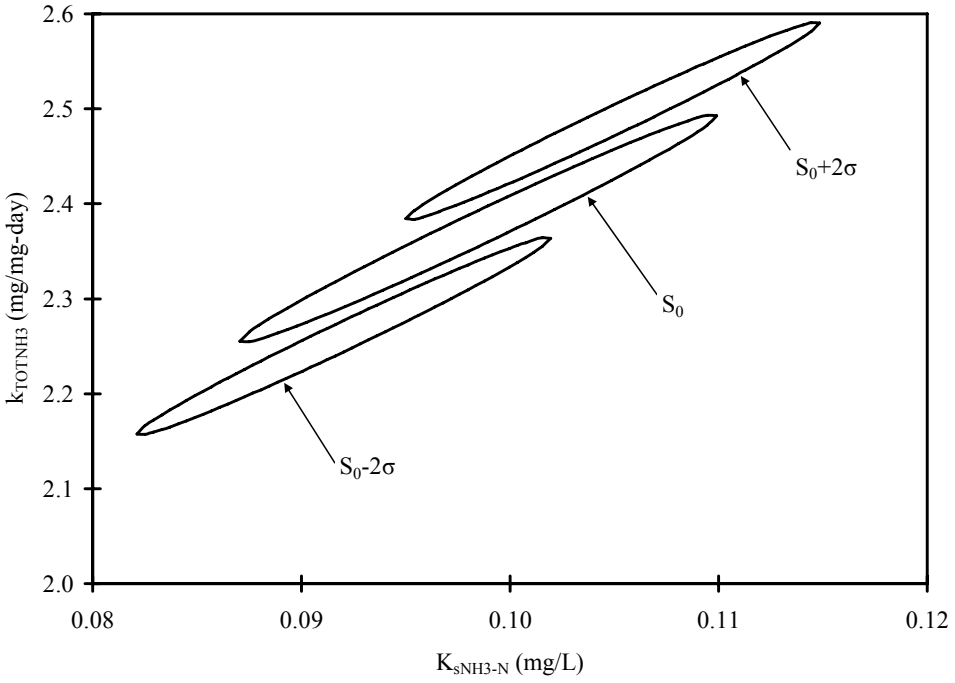

Figure D.18 Experiment 3 95% joint confidence intervals for $TOTNH_3$

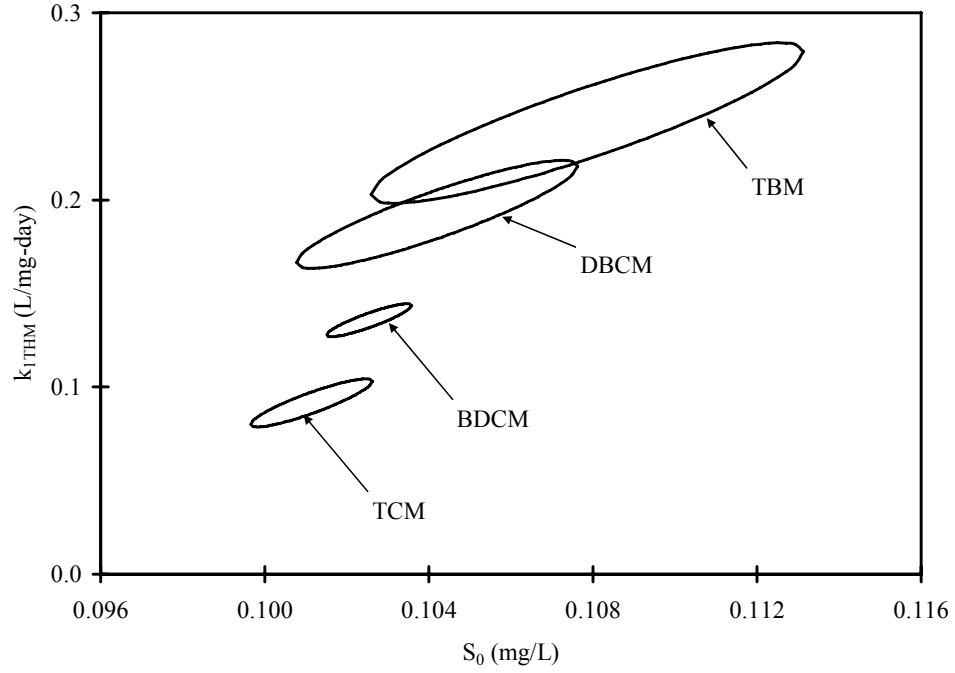

Figure D.19 Experiment 3 95% joint confidence intervals for THMs

Table D.26 Tukey's paired comparison for $k_{1_{THM}}$ for Experiment 3

Experiment	Observations	σ	σ^2
TCM	8	0.0064	0.000041
BDCM	8	0.0044	0.000019
DBCM	8	0.014	0.00021
TBM	8	0.021	0.00046
Total Observations =	32	Pooled σ^2 =	0.00018
Degrees of Freedom (v) =	28	Pooled σ =	0.013
Treatments (k) =	4		
$q_{k,v,0.025}$ =	4.296		
Allowable $y_{bar,i}$-$y_{bar,j}$ = ±	0.020		

Absolute value of $y_{bar,i}$-$y_{bar,j}$

	TCM	BDCM	DBCM	TBM
TCM				
BDCM	0.044			
DBCM	0.10	0.057		
TBM	0.15	0.11	0.049	

Table D.27 Experiment 4 experimental data

$TOTNH_3$ Time (minutes)	pH	$TOTNH_3$ (mg/L)	THM Time (minutes)	THM Concentrations (µg/L)			
				TCM	BDCM	DBCM	TBM
0.00	8.7	7.8	1.50	91	93	93	
10.00	8.6	6.1	11.25	87	87	84	
20.00	8.5	4.5	21.25	82	79	76	
30.25	8.4	2.9	31.50	77	72	66	
40.00	8.3	1.7	41.25	74	67	61	
50.00	8.3	0.98	51.25	72	65	58	
60.00	8.2	0.57	61.25	70	62	55	
71.25	8.2	0.33	72.50	71	63	56	

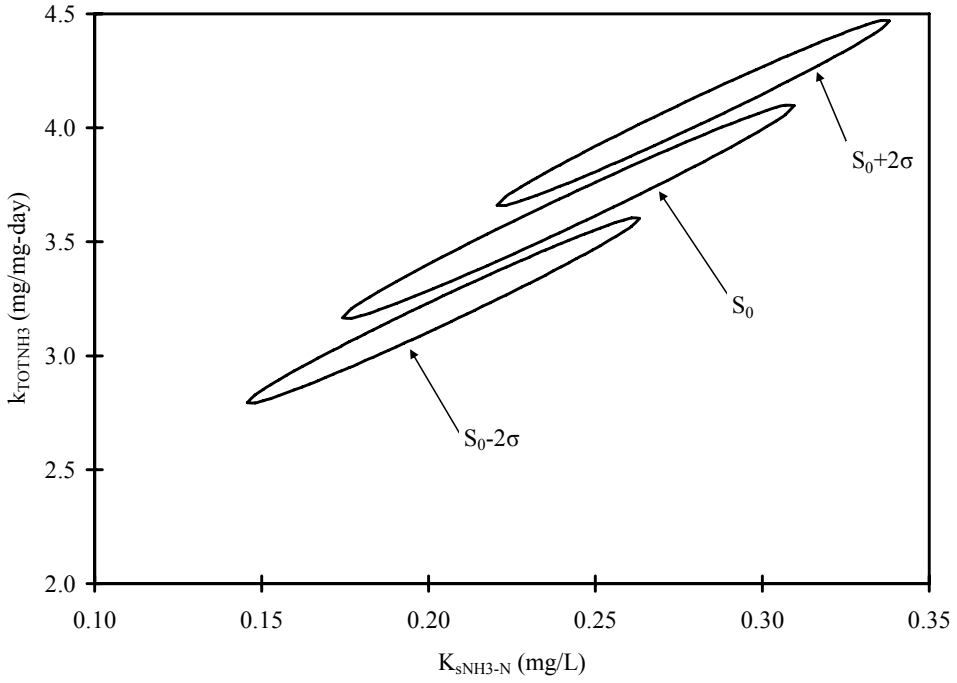

Figure D.20 Experiment 4 95% joint confidence intervals for $TOTNH_3$

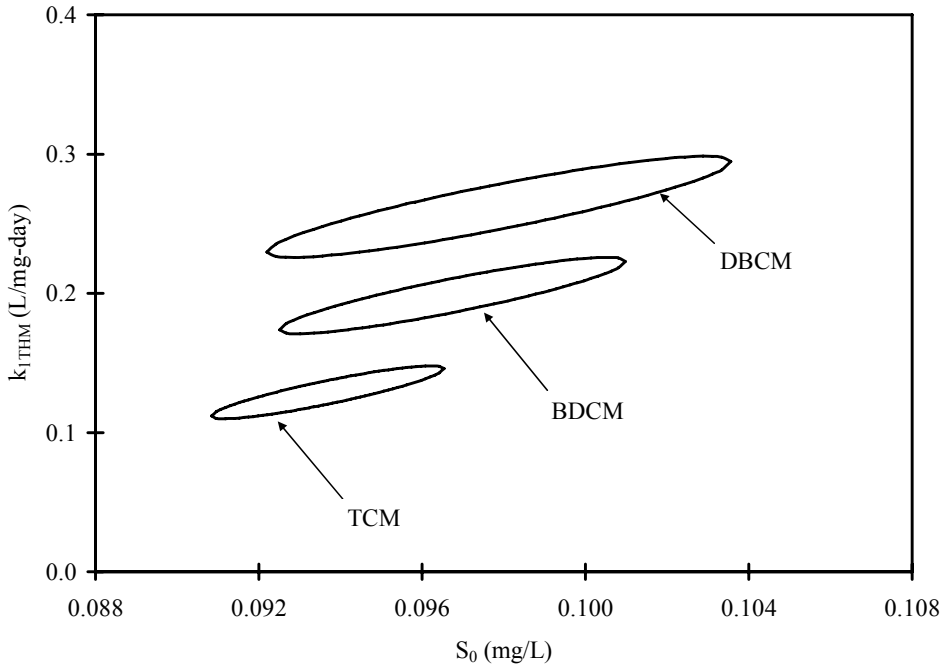

Figure D.21 Experiment 4 95% joint confidence intervals for THMs

Table D.28 Tukey's paired comparison for $k_{1_{THM}}$ for Experiment 4

Experiment	Observations	σ	σ^2
TCM	8	0.010	0.000090
BDCM	8	0.014	0.00019
DBCM	8	0.018	0.00033
TBM			
Total Observations =	24	Pooled σ^2 =	0.00020
Degrees of Freedom (v) =	21	Pooled σ =	0.014
Treatments (k) =	3		
$q_{k,v,0.025}$ =	4.031		
Allowable $y_{bar,i}$-$y_{bar,j}$ = ±	0.020		

Absolute value of $y_{bar,i}$-$y_{bar,j}$

	TCM	BDCM	DBCM	TBM
TCM				
BDCM	0.069			
DBCM	0.13	0.064		
TBM				

Table D.29 Experiment 5 (22°C Temperature Experiment) experimental data

$TOTNH_3$ Time (minutes)	pH	$TOTNH_3$ (mg/L)	THM Time (minutes)	THM Concentrations (µg/L)			
				TCM	BDCM	DBCM	TBM
0.00	8.6	5.7	1.75	82	79	74	71
20.75	8.4	3.2	11.25	80	76	71	69
30.50	8.3	2.3	22.25	77	72	66	63
39.75	8.3	1.4	32.00	76	69	62	58
50.25	8.2	0.75	41.25	72	65	57	53
			52.00	73	65	56	51

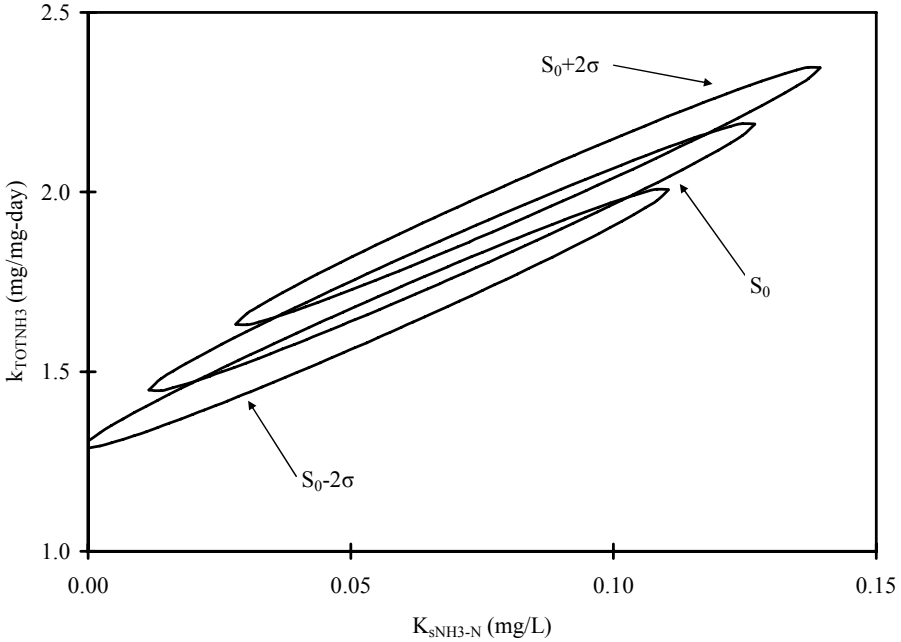

Figure D.22 Experiment 5 (22°C Temperature Experiment) 95% joint confidence intervals for $TOTNH_3$

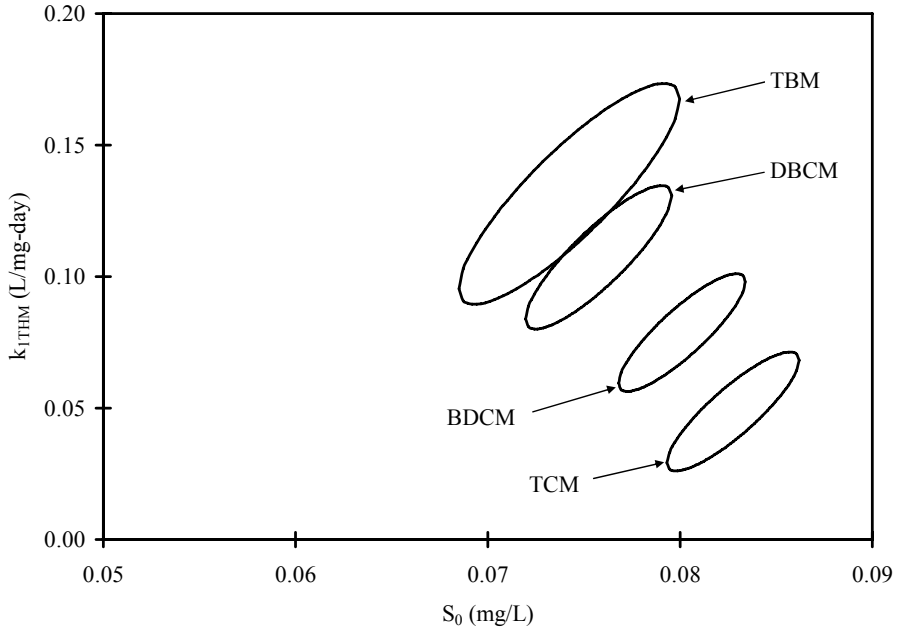

Figure D.23 Experiment 5 (22°C Temperature Experiment) 95% joint confidence intervals for THMs

Table D.30 Tukey's paired comparison for $k_{1_{THM}}$ for Experiment 5

Experiment	Observations	σ	σ^2
TCM	6	0.011	0.00013
BDCM	6	0.011	0.00013
DBCM	6	0.014	0.00019
TBM	6	0.021	0.00044
Total Observations =	24	Pooled σ^2 =	0.00022
Degrees of Freedom (v) =	20	Pooled σ =	0.015
Treatments (k) =	4		
$q_{k,v,0.025}$ =	4.426		
Allowable $y_{bar,i}$-$y_{bar,j}$ = ±	0.027		

Absolute value of $y_{bar,i}$-$y_{bar,j}$

	TCM	BDCM	DBCM	TBM
TCM				
BDCM	0.030			
DBCM	0.059	0.029		
TBM	0.083	0.053	0.024	

Table D.31 14°C Temperature Experiment experimental data

$TOTNH_3$ Time (minutes)	pH	$TOTNH_3$ (mg/L)	THM Time (minutes)	THM Concentrations (µg/L)			
				TCM	BDCM	DBCM	TBM
0.00	8.6	6.1	1.00	83	80	78	78
40.75	8.6	5.1	21.25	81	78	76	75
60.25	8.5	4.7	41.75	79	74	71	70
81.25	8.5	4.2	61.50	76	72	68	67
101.25	8.4	3.6	82.00	75	71	66	64
			101.50	71	67	61	59

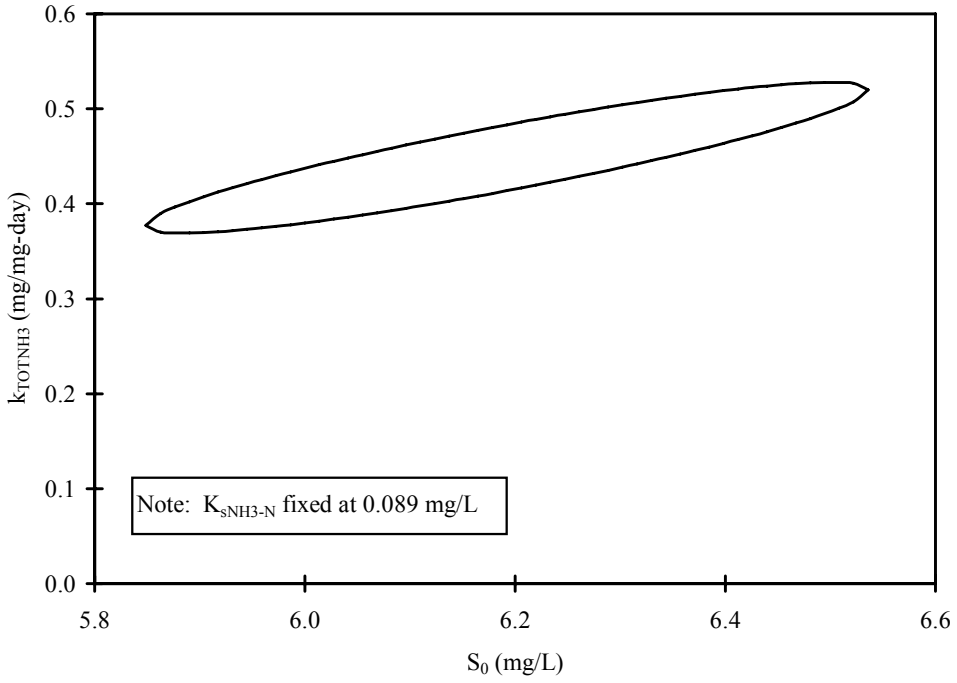

Figure D.24 14°C Temperature Experiment 95% joint confidence intervals for $TOTNH_3$

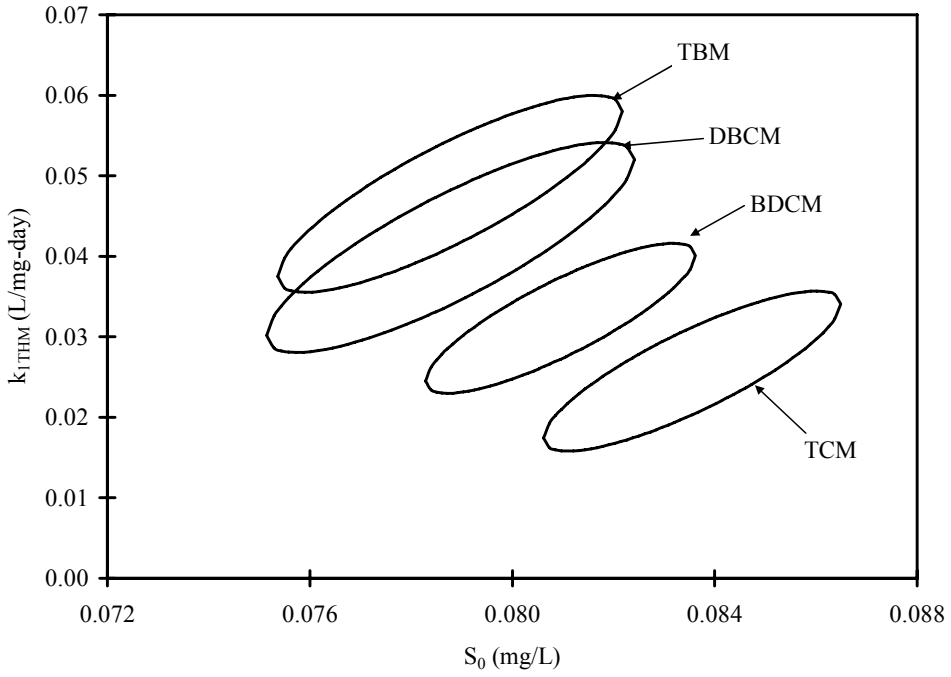

Figure D.25 14°C Temperature Experiment 95% joint confidence intervals for THMs

Table D.32 Tukey's paired comparison for $k_{1_{THM}}$ for 14°C Temperature Experiment

Experiment	Observations	σ	σ^2
TCM	6	0.0050	0.000025
BDCM	6	0.0047	0.000022
DBCM	6	0.0065	0.000043
TBM	6	0.0061	0.000032
Total Observations =	24	Pooled σ^2 =	0.000032
Degrees of Freedom (v) =	20	Pooled σ =	0.0056
Treatments (k) =	4		
$q_{k,v,0.025}$ =	4.426		
Allowable $y_{bar,i}$-$y_{bar,j}$ = ±	0.010		

Absolute value of $y_{bar,i}$-$y_{bar,j}$

	TCM	BDCM	DBCM	TBM
TCM				
BDCM	0.0066			
DBCM	0.015	0.0088		
TBM	0.022	0.015	0.0067	

D.5. ^{14}C-RADIOLABELED CHLOROFORM EXPERIMENT DATA

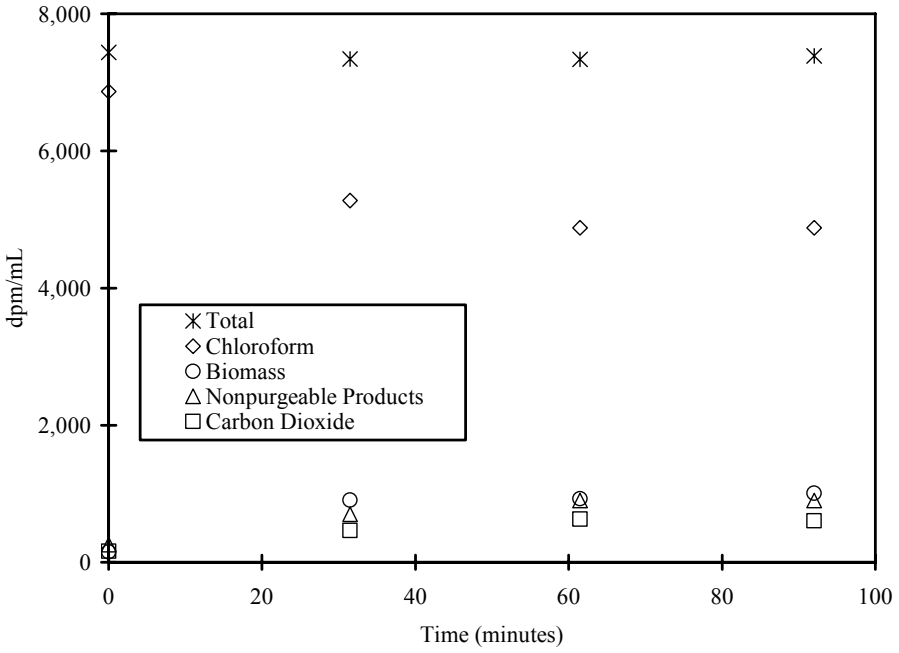

Figure D.26 ^{14}C-Radiolabeled Chloroform Experiment experimental data

D.6. ENDOGENOUS DECAY EXPERIMENT DATA

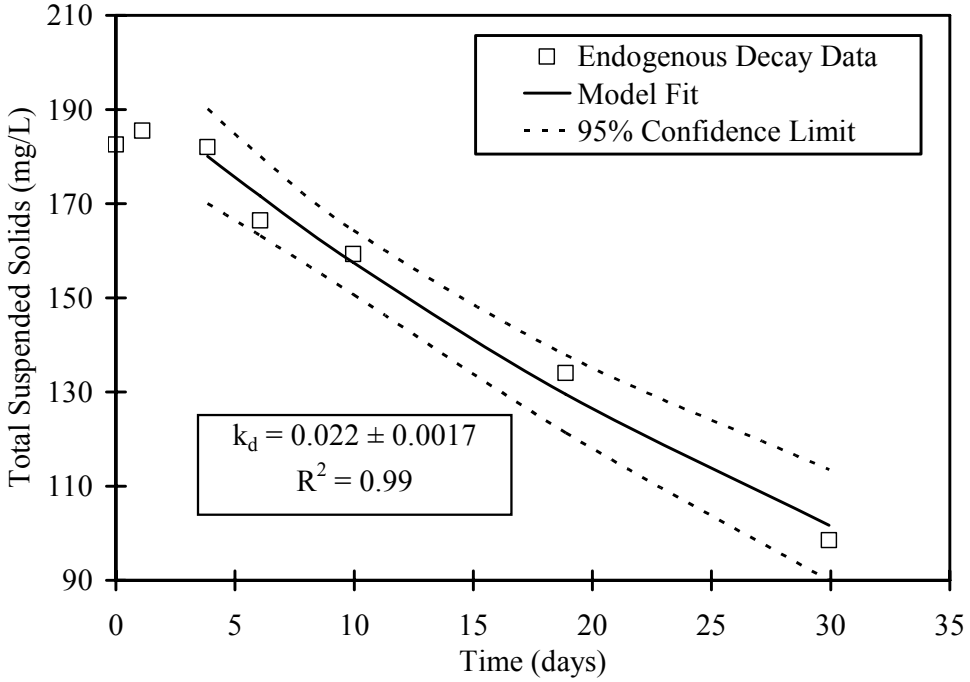

Figure D.27 Endogenous Decay Experiment TSS concentrations and model fit

D.7. *NITROSOMONAS EUROPAEA* BIOFILTERS EXPERIMENT DATA

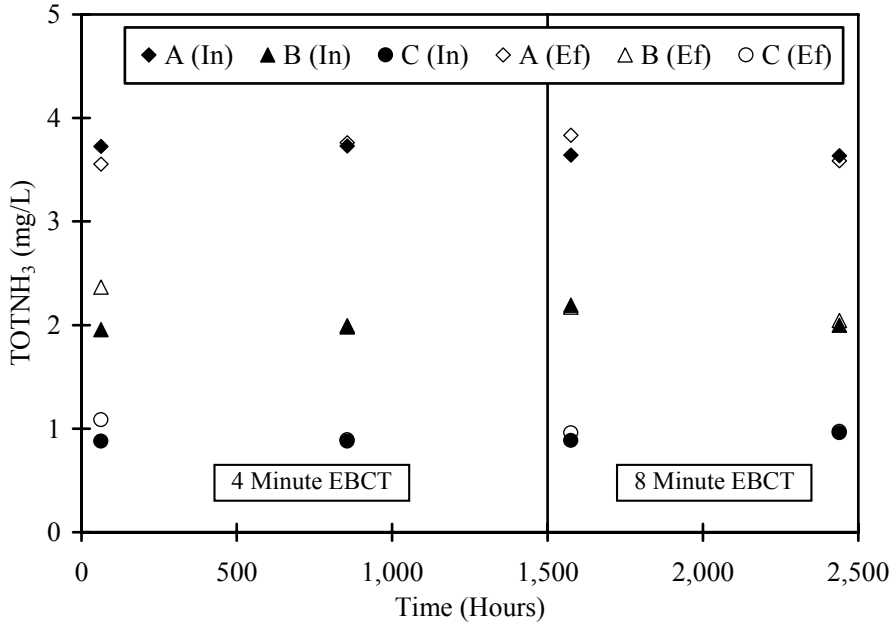

Figure D.28 *N. europaea* Biofilters primary column setup $TOTNH_3$ performance

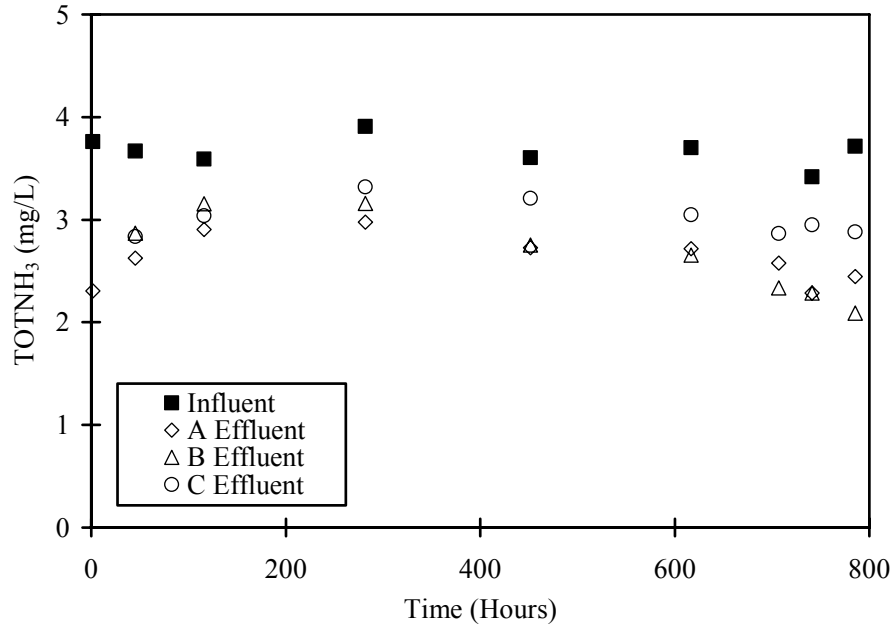

Figure D.29 *N. europaea* Biofilters secondary column setup $TOTNH_3$ performance

D.8. LAKE AUSTIN BIOFILTERS EXPERIMENT DATA

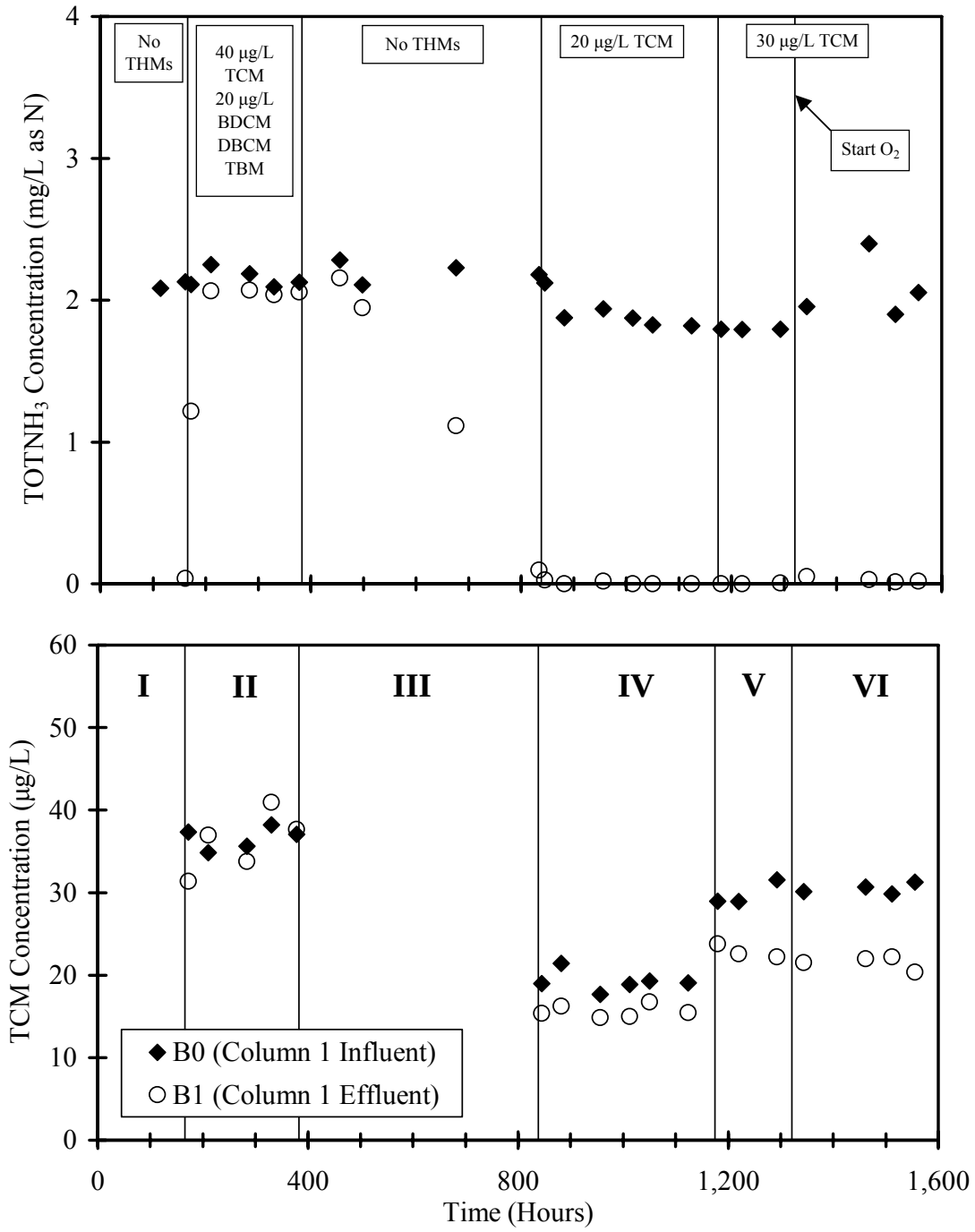

Figure D.30 Lake Austin Biofilters Run 1 Train B $TOTNH_3$ and TCM concentrations fed nutrient water

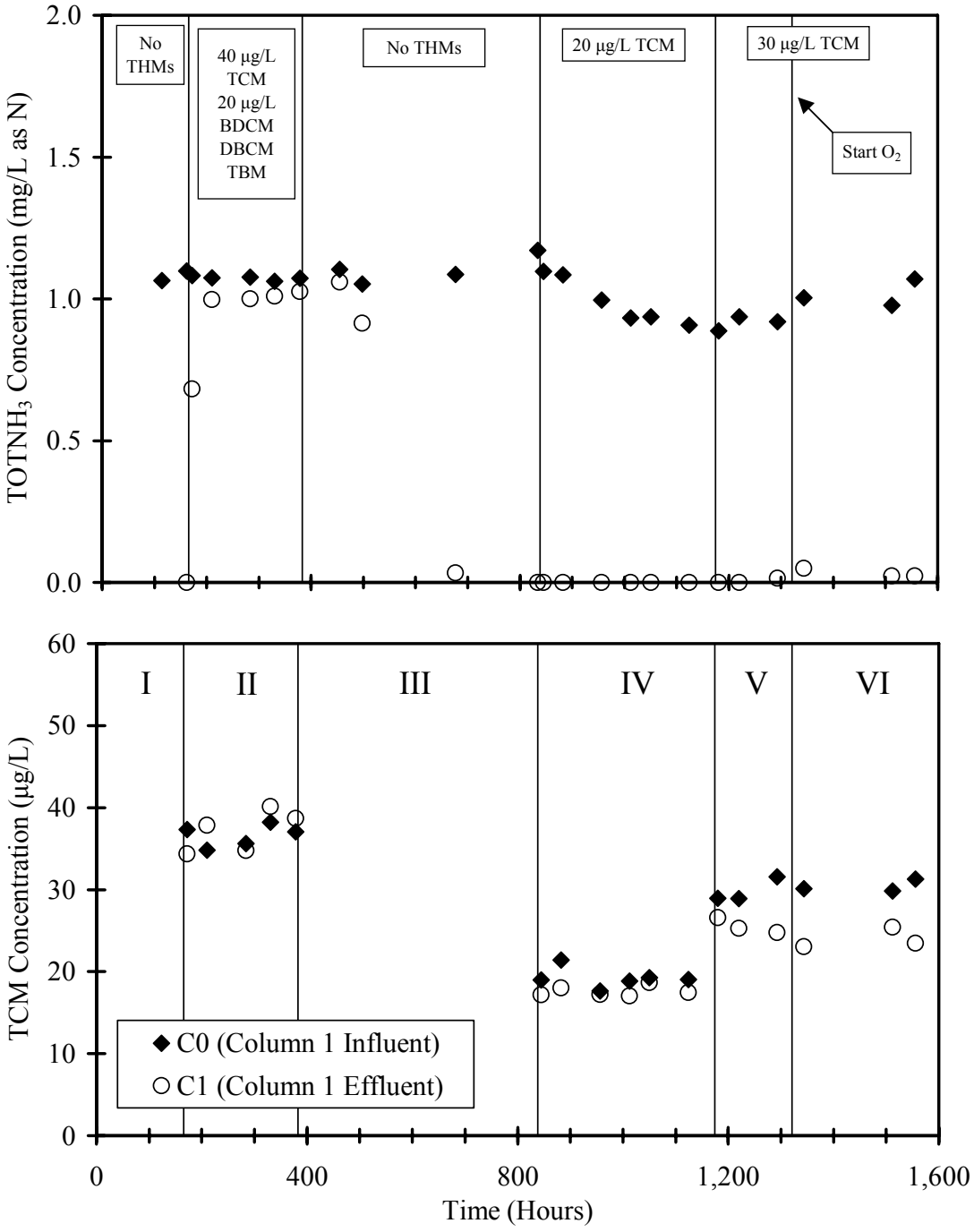

Figure D.31 Lake Austin Biofilters Run 1 Train C $TOTNH_3$ and TCM concentrations fed nutrient water

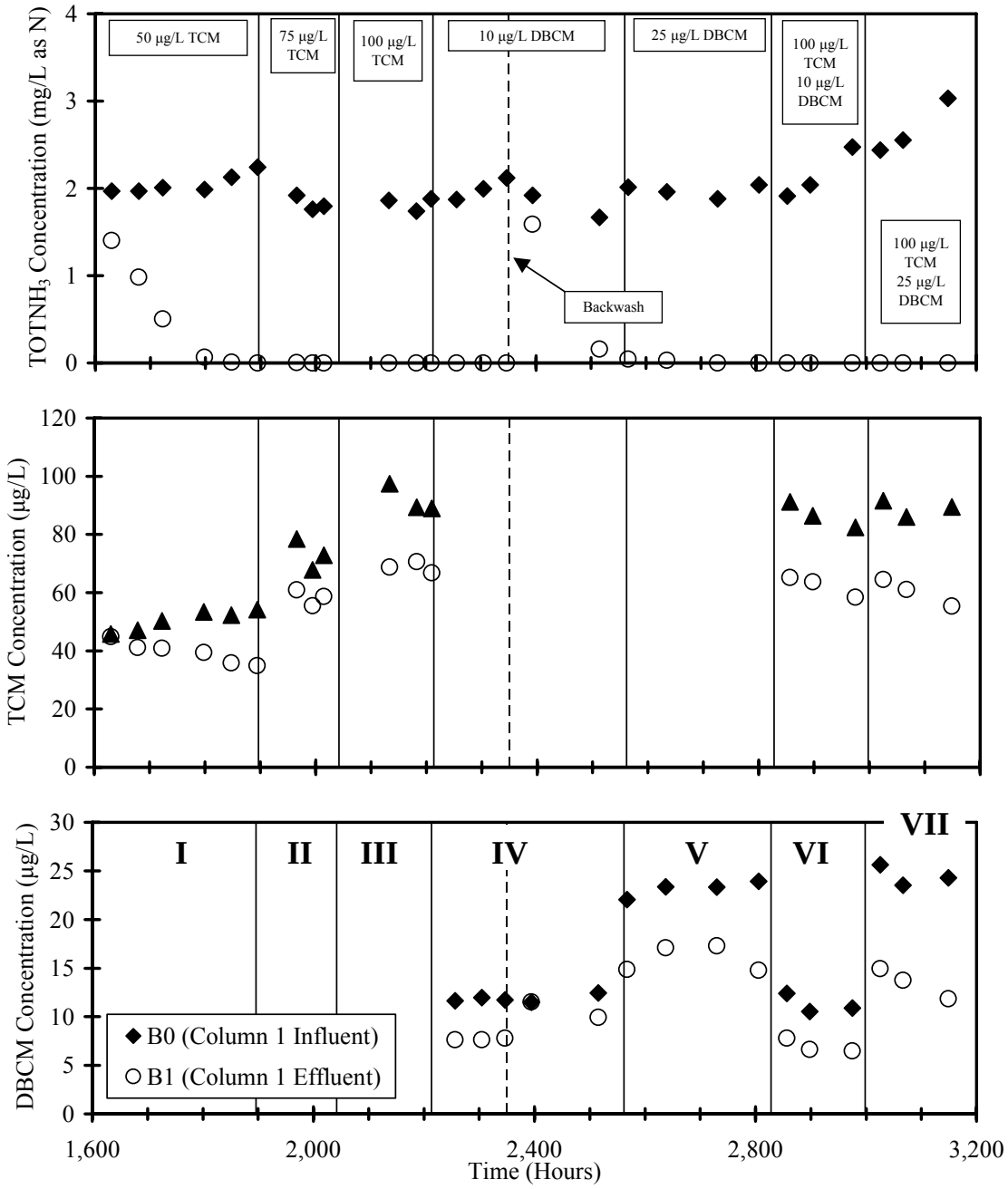

Figure D.32 Lake Austin Biofilters Run 2 Train B $TOTNH_3$, TCM, and DBCM concentrations fed nutrient water

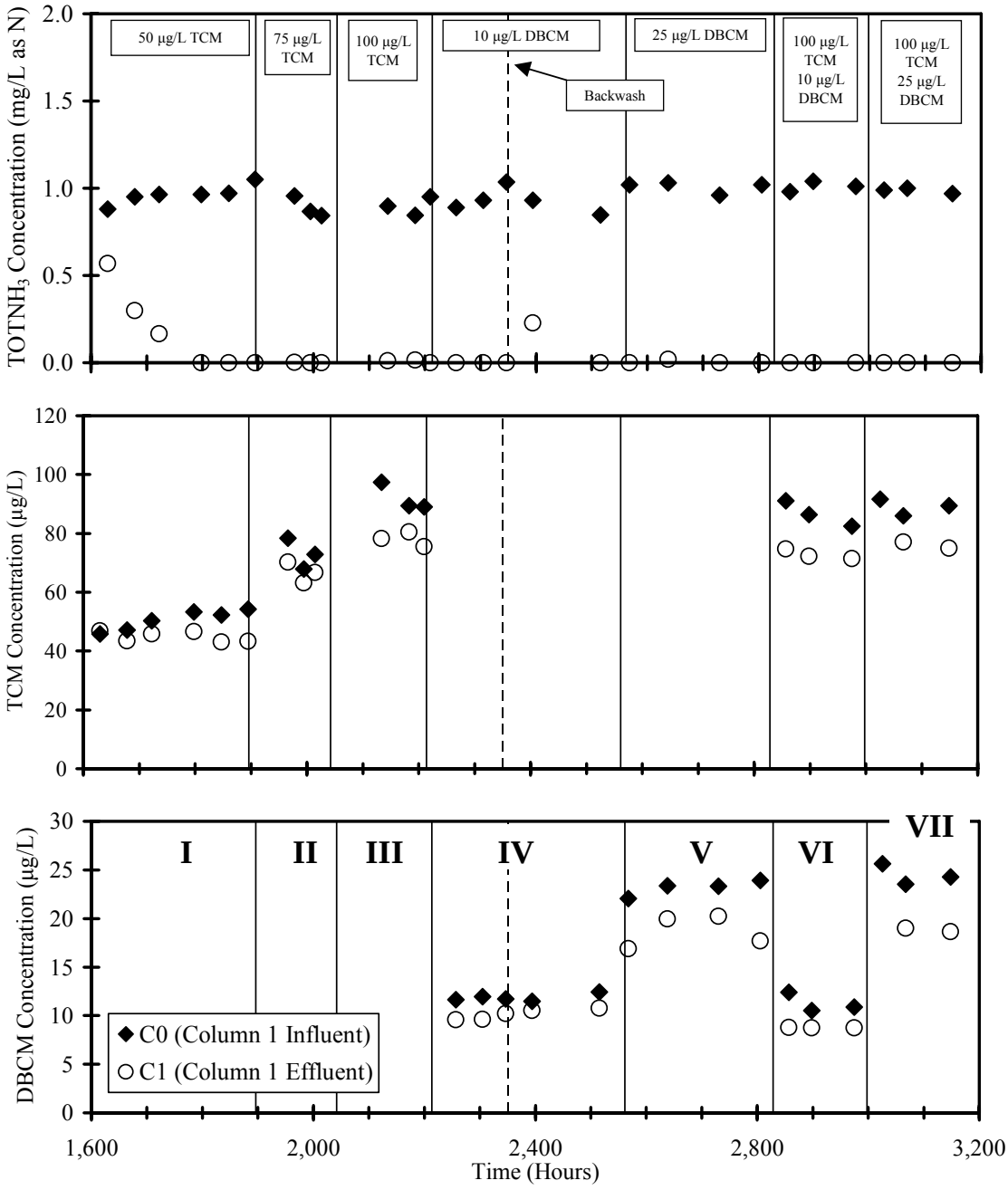

Figure D.33 Lake Austin Biofilters Run 2 Train C $TOTNH_3$, TCM, and DBCM concentrations fed nutrient water

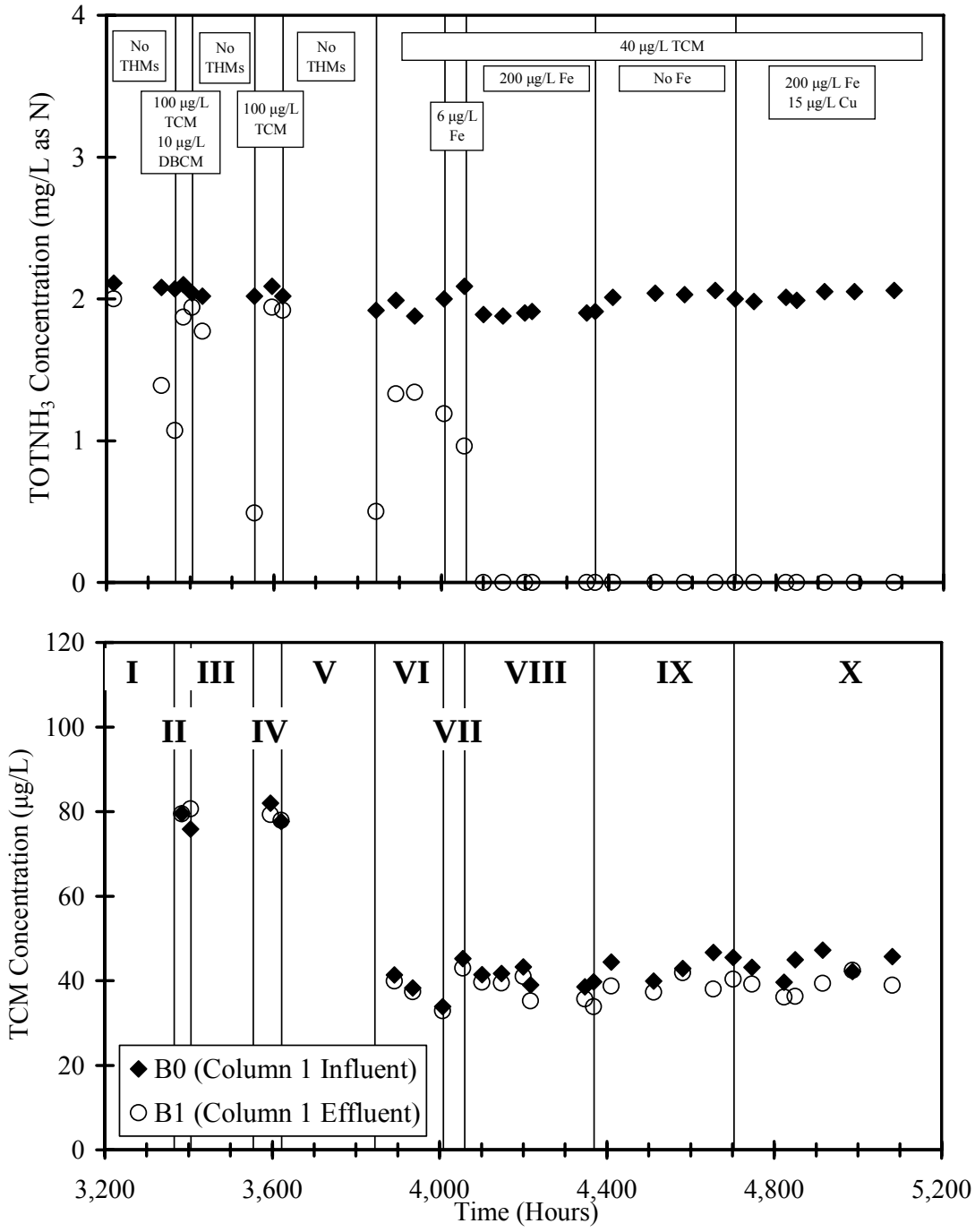

Figure D.34 Lake Austin Biofilters Run 3 Train B $TOTNH_3$ and TCM concentrations fed Lake Austin water

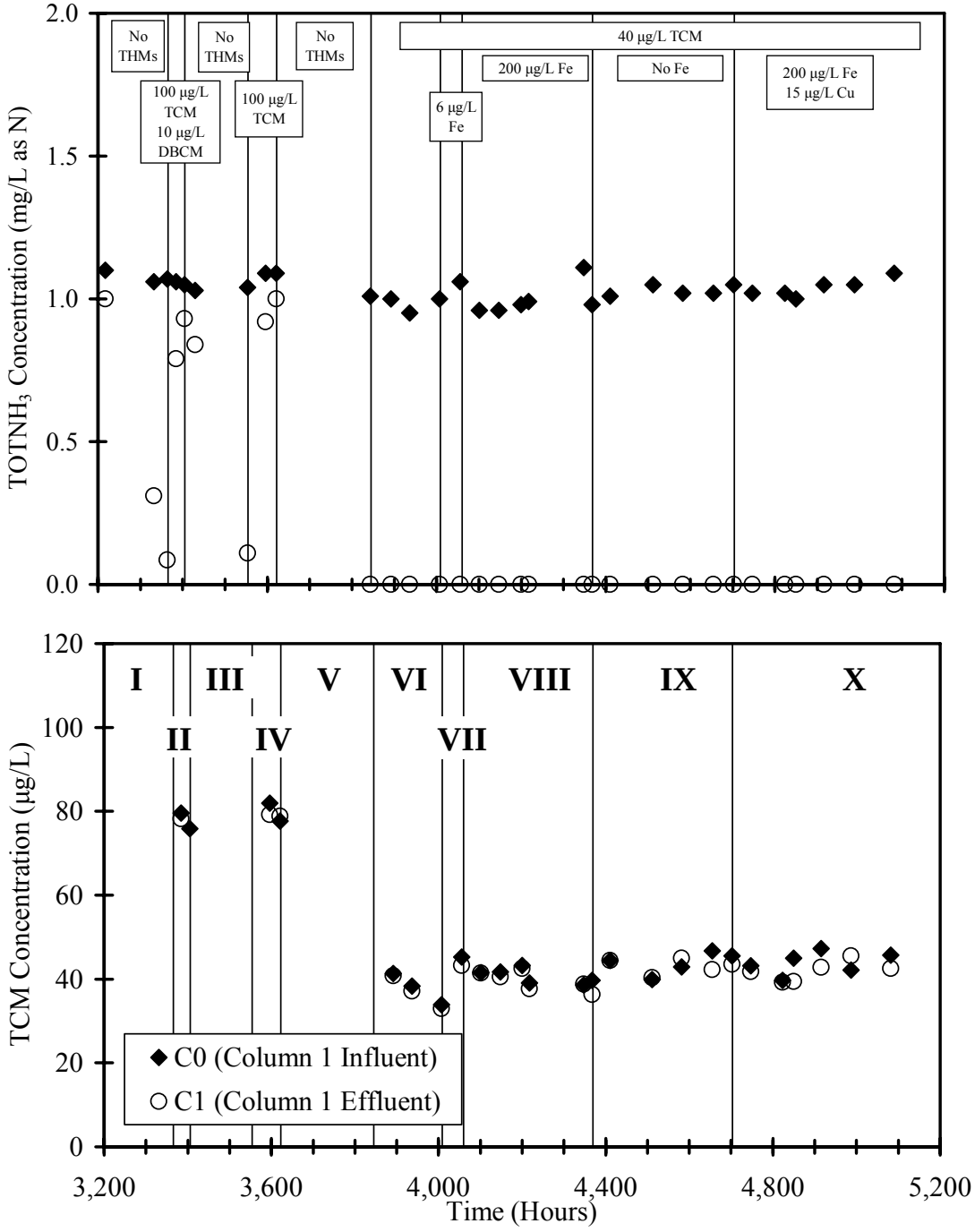

Figure D.35 Lake Austin Biofilters Run 3 Train C $TOTNH_3$ and TCM concentrations fed Lake Austin water

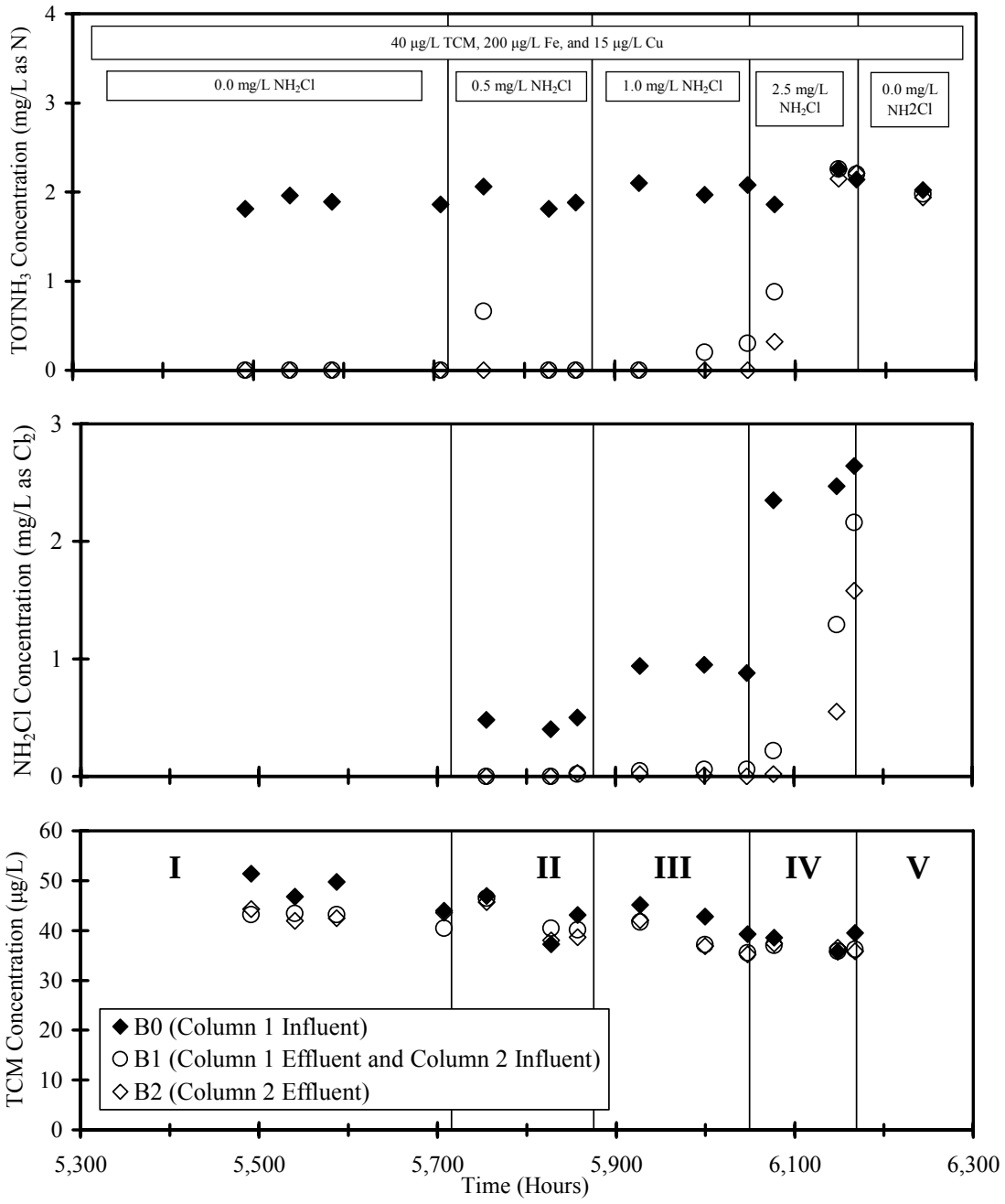

Figure D.36 Lake Austin Biofilters Run 3 Train B $TOTNH_3$, NH_2Cl, and TCM concentrations fed Lake Austin water

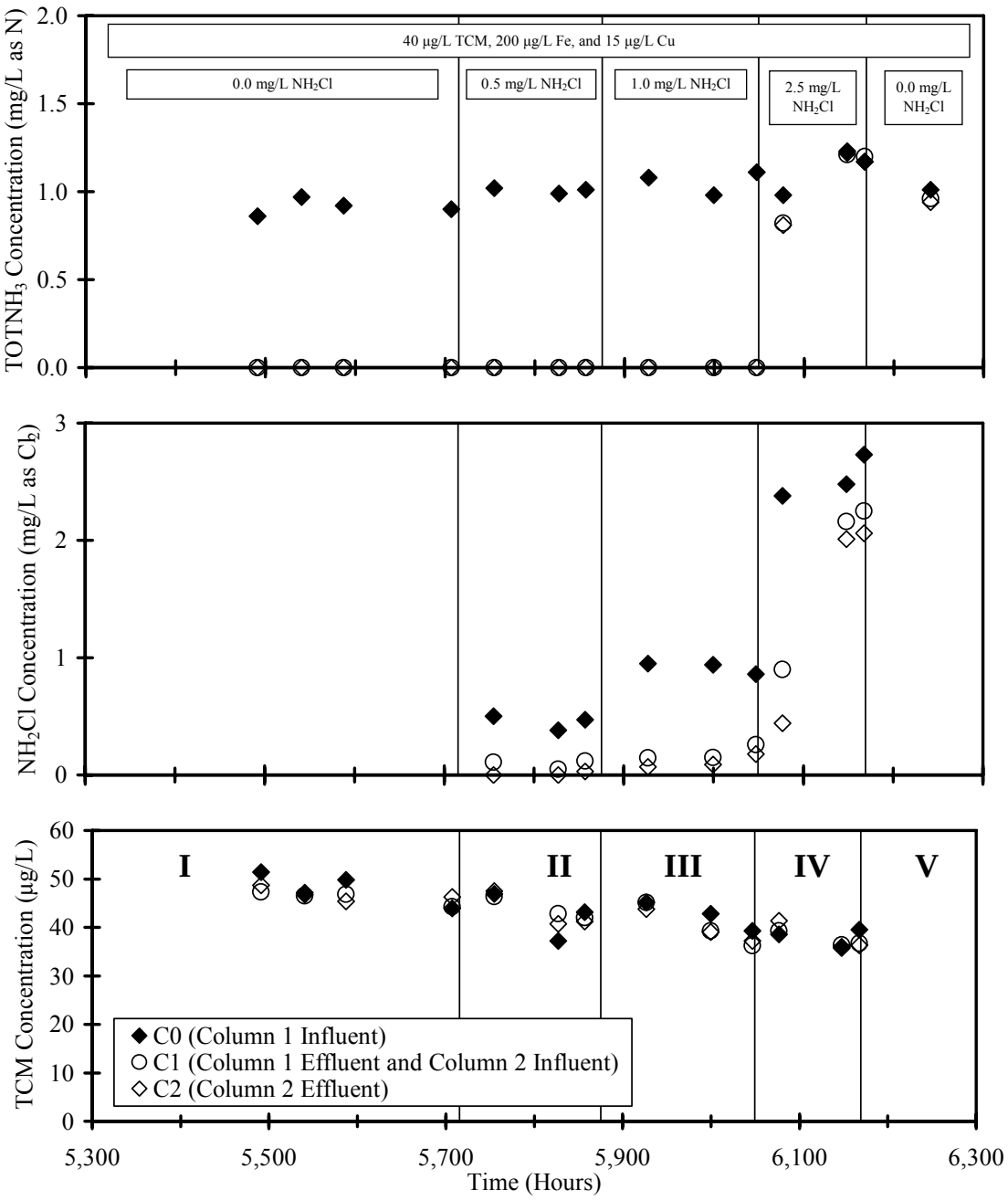

Figure D.37 Lake Austin Biofilters Run 3 Train C $TOTNH_3$, NH_2Cl, and TCM concentrations fed Lake Austin water

D.9. MIXED CULTURE BIOFILTERS 1 BACKWASH BATCH KINETIC EXPERIMENTS DATA AND 95% CONFIDENCE INTERVALS

Table D.33 Backwash Batch Kinetic Experiment MCB1 A1 experimental data

$TOTNH_3$ Time (minutes)	pH	$TOTNH_3$ (mg/L)	THM Time (minutes)	THM Concentrations (µg/L)			
				TCM	BDCM	DBCM	TBM
1.00	9.0	6.8	3.50	81	85	87	89
16.75	8.9	6.2	38.50	67	73	76	81
45.00	8.8	5.1	87.75	48	52	56	67
90.25	8.5	3.2	129.50	34	39	42	55
133.00	8.3	1.5	179.00	25	28	30	42
167.00	8.2	0.51	202.00	23	26	27	37
183.00	8.2	0.23					
194.00	8.2	0.10					
205.50	8.1	0.05					

Total Suspended Solids = 44 mg/L

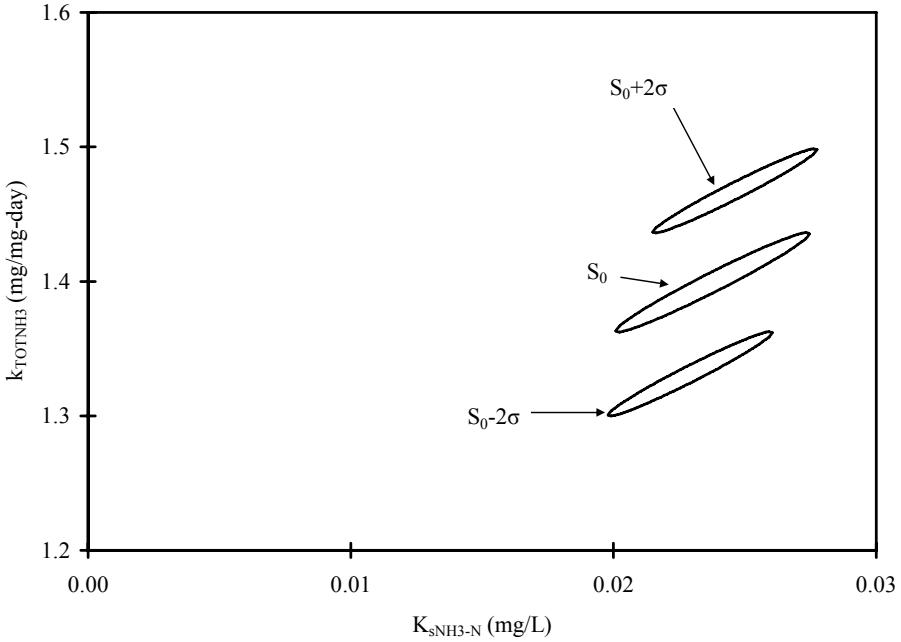

Figure D.38 Backwash Batch Kinetic Experiment MCB1 A1 95% joint confidence intervals for $TOTNH_3$

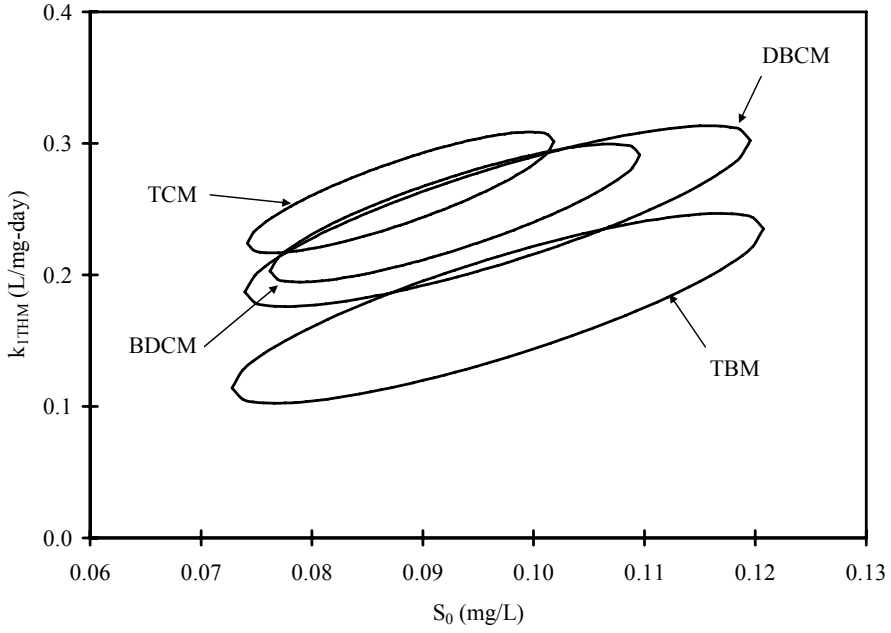

Figure D.39 Backwash Batch Kinetic Experiment MCB1 A1 95% joint confidence intervals for THMs

Table D.34 Tukey's paired comparison for $k_{1_{THM}}$ for MCB1 A1

Experiment	Observations	σ	σ^2
TCM	6	0.0023	0.00053
BDCM	6	0.0026	0.00069
DBCM	6	0.0034	0.0012
TBM	6	0.036	0.0013
Total Observations =	24	Pooled σ^2 =	0.00093
Degrees of Freedom (v) =	20	Pooled σ =	0.030
Treatments (k) =	4		
$q_{k,v,0.025}$ =	4.426		
Allowable $y_{bar,i}$-$y_{bar,j}$ = ±	0.055		

Absolute value of $y_{bar,i}$-$y_{bar,j}$

	TCM	BDCM	DBCM	TBM
TCM				
BDCM	0.016			
DBCM	0.018	0.0023		
TBM	0.088	0.072	0.070	

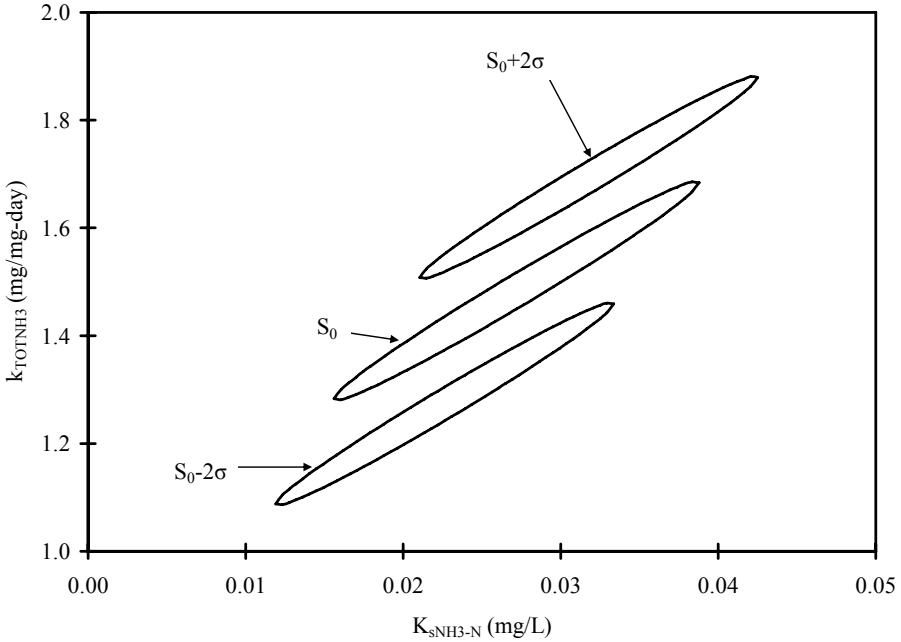

Figure D.40 Backwash Batch Kinetic Experiment MCB1 A1 (3.5 mg/L start) 95% joint confidence intervals for $TOTNH_3$

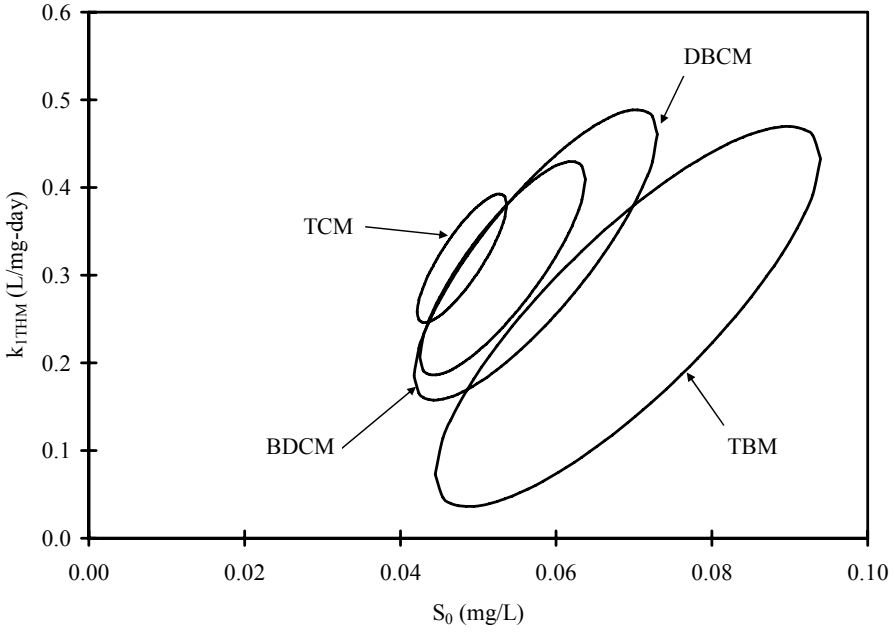

Figure D.41 Backwash Batch Kinetic Experiment MCB1 A1 (3.5 mg/L start) 95% joint confidence intervals for THMs

Table D.35 Tukey's paired comparison for $k_{1_{THM}}$ for MCB1 A1 (3.5 mg/L start)

Experiment	Observations	σ	σ^2
TCM	4	0.037	0.0013
BDCM	4	0.061	0.0037
DBCM	4	0.083	0.0069
TBM	4	0.11	0.012
Total Observations =	16	Pooled σ^2 =	0.0059
Degrees of Freedom (v) =	12	Pooled σ =	0.077
Treatments (k) =	4		
$q_{k,v,0.025}$ =	4.762		
Allowable $y_{bar,i}$-$y_{bar,j}$ = ±	0.18		

Absolute value of $y_{bar,i}$-$y_{bar,j}$

	TCM	BDCM	DBCM	TBM
TCM				
BDCM	0.011			
DBCM	0.0039	0.015		
TBM	0.066	0.055	0.070	

Table D.36 Backwash Batch Kinetic Experiment MCB1 A2 experimental data

$TOTNH_3$ Time (minutes)	pH	$TOTNH_3$ (mg/L)	THM Time (minutes)	THM Concentrations (µg/L)			
				TCM	BDCM	DBCM	TBM
1.75	8.7	4.3	3.50	83	88	91	93
16.00	8.7	3.7	30.00	73	79	85	91
32.00	8.6	3.2	76.75	55	57	63	76
51.00	8.6	2.6	102.25	47	50	55	70
79.00	8.5	1.7	117.00	44	45	49	65
104.50	8.4	0.96	145.50	40	40	42	57
119.00	8.3	0.63					
135.25	8.3	0.33					
150.25	8.2	0.17					

Total Suspended Solids = 33 mg/L

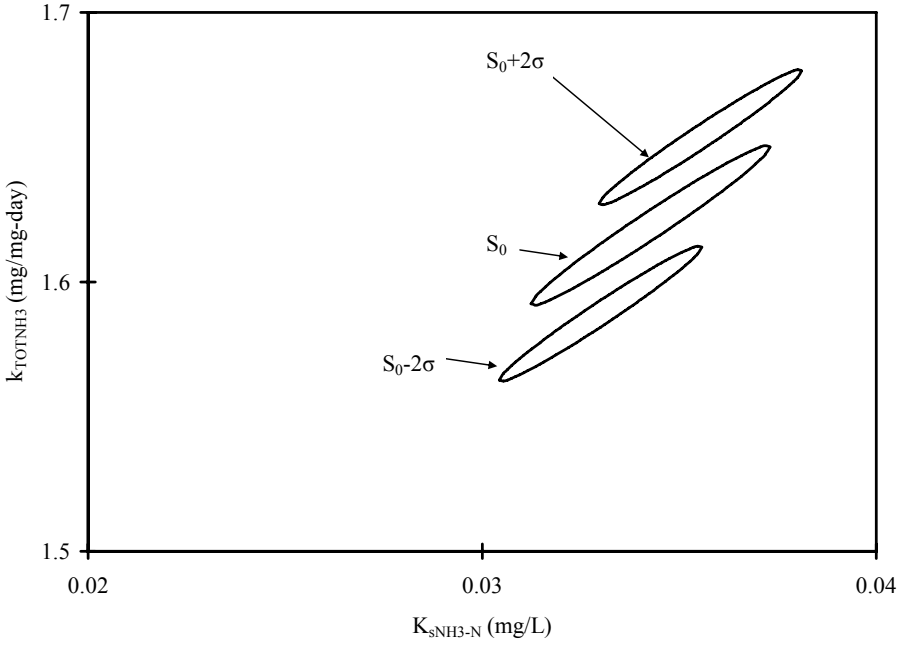

Figure D.42 Backwash Batch Kinetic Experiment MCB1 A2 95% joint confidence intervals for $TOTNH_3$

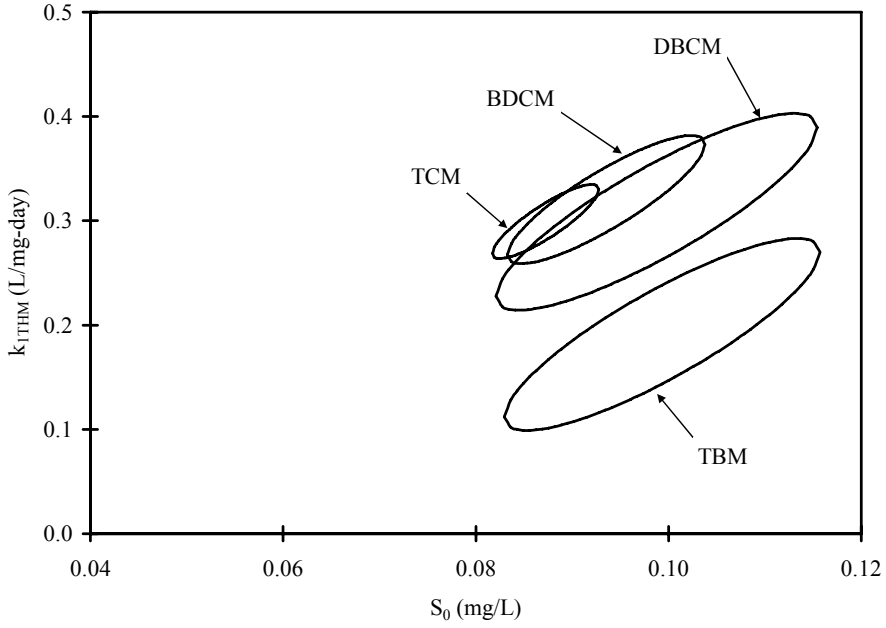

Figure D.43 Backwash Batch Kinetic Experiment MCB1 A2 95% joint confidence intervals for THMs

Table D.37 Tukey's paired comparison for $k_{1_{THM}}$ for MCB1 A2

Experiment	Observations	σ	σ^2
TCM	6	0.018	0.00031
BDCM	6	0.031	0.00094
DBCM	6	0.047	0.0022
TBM	6	0.046	0.0021
Total Observations =	24	Pooled σ^2 =	0.0014
Degrees of Freedom (v) =	20	Pooled σ =	0.037
Treatments (k) =	4		
$q_{k,v,0.025}$ =	4.426		
Allowable $y_{bar,i}$-$y_{bar,j}$ = ±	0.068		

Absolute value of $y_{bar,i}$-$y_{bar,j}$

	TCM	BDCM	DBCM	TBM
TCM				
BDCM	0.021			
DBCM	0.009	0.012		
TBM	0.108	0.129	0.118	

Table D.38 Backwash Batch Kinetic Experiment MCB1 B experimental data

$TOTNH_3$ Time (minutes)	pH	$TOTNH_3$ (mg/L)	THM Time (minutes)	THM Concentrations (µg/L)			
				TCM	BDCM	DBCM	TBM
1.50	8.7	4.2	2.75	90	98	103	105
16.50	8.7	3.8	46.50	85	91	95	99
48.50	8.6	3.3	119.25	77	80	83	87
90.50	8.5	2.4	150.25	73	77	79	82
121.50	8.4	1.8	179.50	70	72	74	76
152.25	8.4	1.1	322.00	65	69	72	76
182.00	8.2	0.82					
225.75	8.2	0.66					

Total Suspended Solids = 65 mg/L

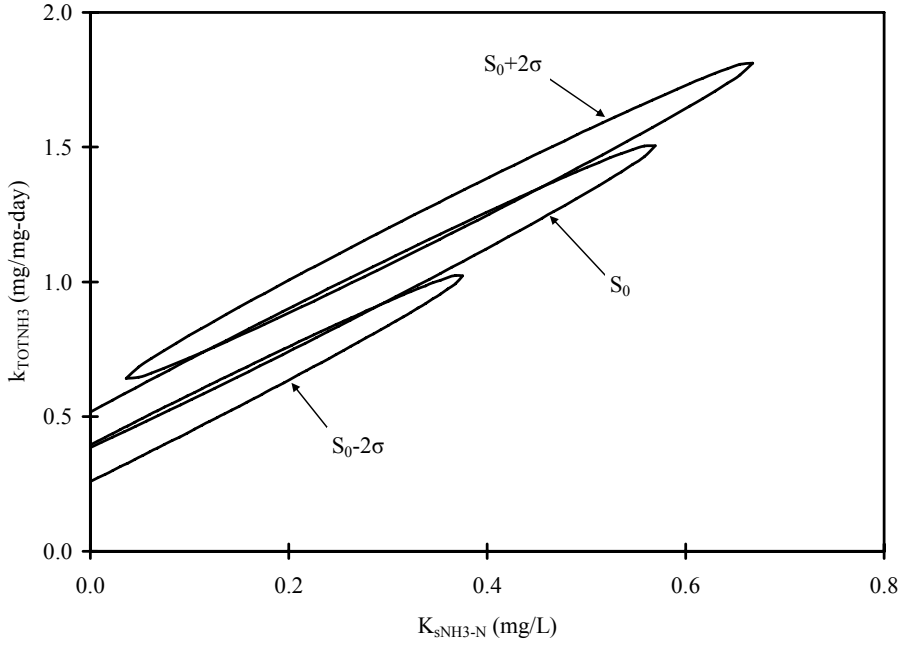

Figure D.44 Backwash Batch Kinetic Experiment MCB1 B 95% joint confidence intervals for $TOTNH_3$

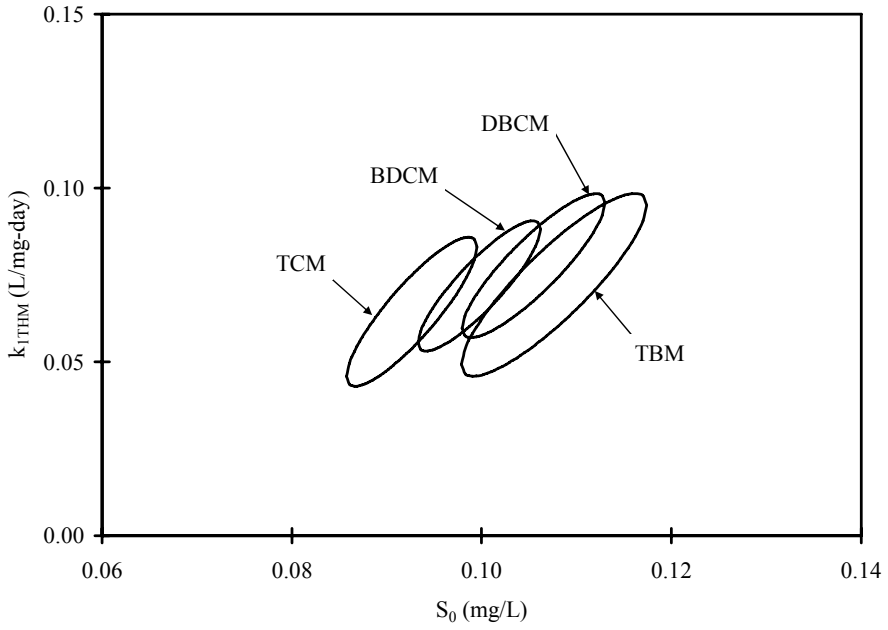

Figure D.45 Backwash Batch Kinetic Experiment MCB1 B 95% joint confidence intervals for THMs

Table D.39 Tukey's paired comparison for $k_{1_{THM}}$ for MCB1 B

Experiment	Observations	σ	σ^2
TCM	6	0.011	0.00011
BDCM	6	0.0094	0.000088
DBCM	6	0.010	0.00011
TBM	6	0.013	0.00017
Total Observations =	24	Pooled σ^2 =	0.00012
Degrees of Freedom (v) =	20	Pooled σ =	0.01097
Treatments (k) =	4		
$q_{k,v,0.025}$ =	4.426		
Allowable $y_{bar,i}$-$y_{bar,j}$ = ±	0.020		

Absolute value of $y_{bar,i}$-$y_{bar,j}$

	TCM	BDCM	DBCM	TBM
TCM				
BDCM	0.007			
DBCM	0.013	0.006		
TBM	0.008	0.00033	0.0055	

Table D.40 Backwash Batch Kinetic Experiment MCB1 C experimental data

Time (minutes)	pH	$TOTNH_3$ (mg/L)
1.25	8.9	8.0
11.50	8.9	7.8
63.75	8.8	7.2
135.00	8.7	6.5
349.25	8.3	3.4
544.00	8.1	1.1
601.00	8.1	1.0

Total Suspended Solids = 23 mg/L

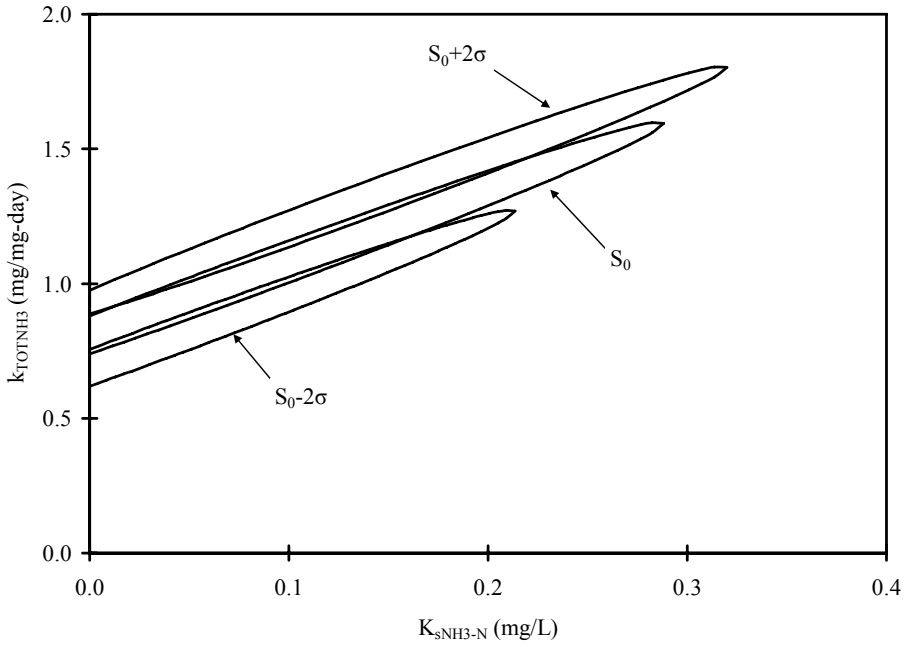

Figure D.46 Backwash Batch Kinetic Experiment MCB1 C 95% joint confidence intervals for $TOTNH_3$

D.10. MIXED CULTURE BIOFILTERS 2 BACKWASH BATCH KINETIC EXPERIMENTS DATA AND 95% CONFIDENCE INTERVALS

Table D.41 Backwash Batch Kinetic Experiment MCB2 A experimental data

$TOTNH_3$ Time (minutes)	pH	$TOTNH_3$ (mg/L)	THM Time (minutes)	THM Concentrations (µg/L)			
				TCM	BDCM	DBCM	TBM
2.50	8.7	5.0	5.25	78	82	85	94
15.00	8.6	4.6	51.50	71	73	75	86
56.00	8.4	3.4	107.00	64	64	67	80
93.00	8.3	2.2	157.00	59	58	60	73
120.50	8.2	1.4	201.00	58	56	59	73
150.50	8.1	0.62	239.00	57	55	58	70
179.00	8.0	0.18					

Total Suspended Solids = 27 mg/L

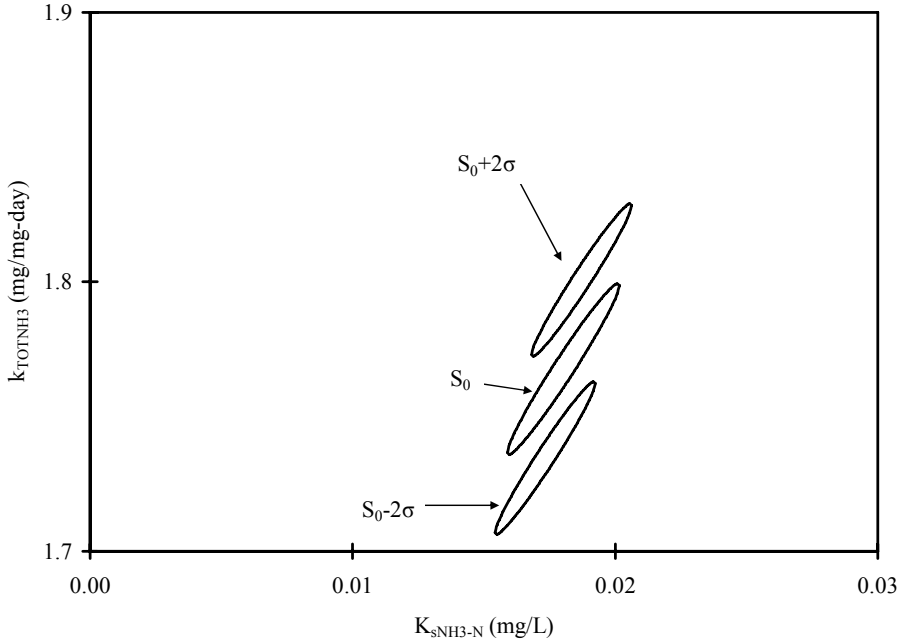

Figure D.47 Backwash Batch Kinetic Experiment MCB2 A 95% joint confidence intervals for $TOTNH_3$

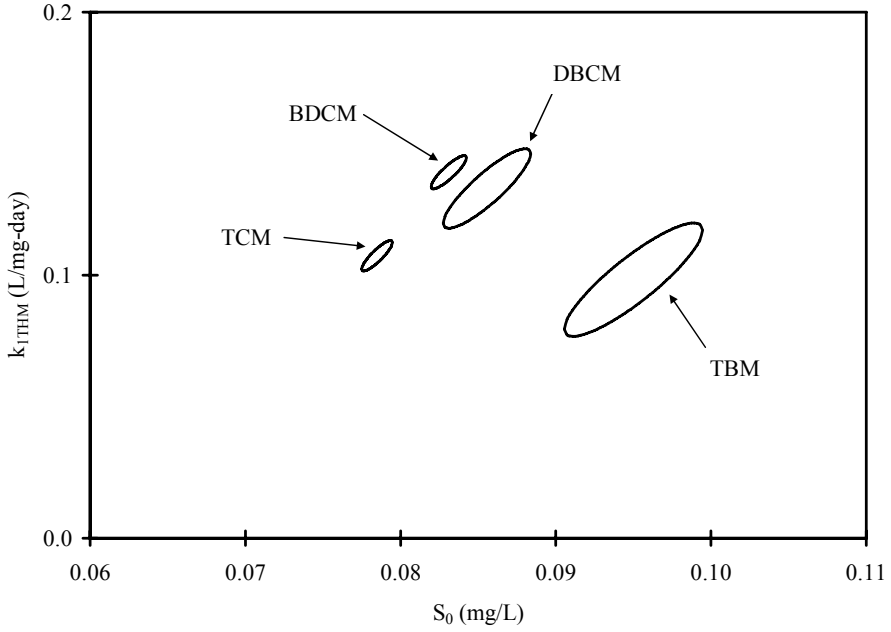

Figure D.48 Backwash Batch Kinetic Experiment MCB2 A 95% joint confidence intervals for THMs

Table D.42 Tukey's paired comparison for $k_{1_{THM}}$ for MCB2 A

Experiment	Observations	σ	σ^2
TCM	6	0.0029	0.0000084
BDCM	6	0.0032	0.000010
DBCM	6	0.0076	0.000057
TBM	6	0.011	0.00012
Total Observations =	24	Pooled σ^2 =	0.000048
Degrees of Freedom (v) =	20	Pooled σ =	0.0069
Treatments (k) =	4		
$q_{k,v,0.025}$ =	4.426		
Allowable $y_{bar,i}$-$y_{bar,j}$ = ±	0.012		

Absolute value of $y_{bar,i}$-$y_{bar,j}$

	TCM	BDCM	DBCM	TBM
TCM				
BDCM	0.032			
DBCM	0.026	0.0062		
TBM	0.0091	0.041	0.035	

Table D.43 Backwash Batch Kinetic Experiment MCB2 B experimental data

$TOTNH_3$ Time (minutes)	pH	$TOTNH_3$ (mg/L)	THM Time (minutes)	THM Concentrations (µg/L)			
				TCM	BDCM	DBCM	TBM
2.00	8.7	4.9	6.50	78	86	93	110
15.25	8.6	4.8	61.00	75	83	91	110
55.25	8.6	4.4	181.00	70	76	81	96
133.00	8.5	3.6	301.00	67	70	73	87
192.00	8.5	3.1	367.50	62	68	75	94
266.50	8.4	2.5	425.00	62	65	70	87
305.00	8.4	2.2					
361.50	8.3	1.8					
428.00	8.3	1.4					

Total Suspended Solids = 7.5 mg/L

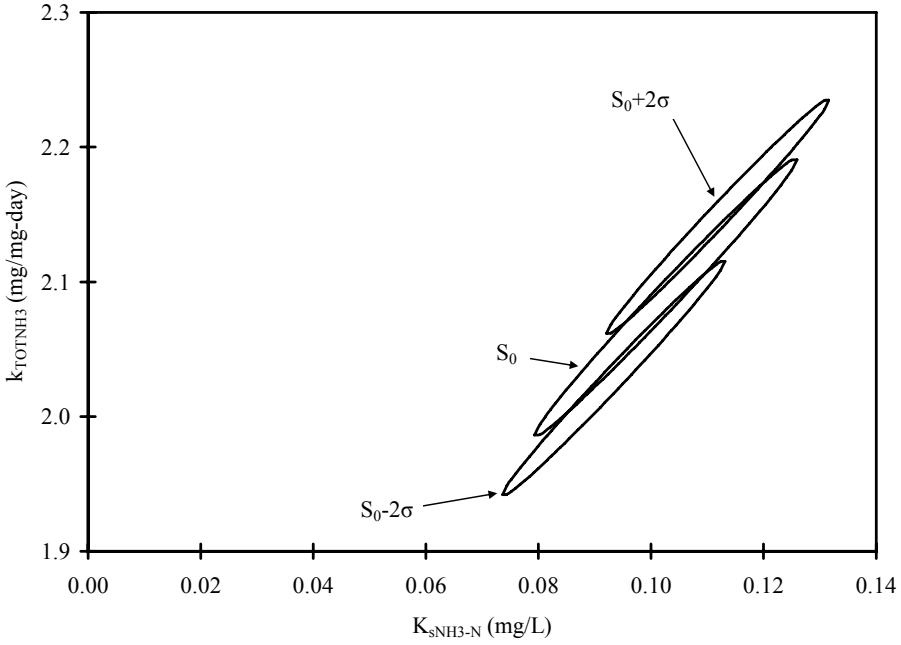

Figure D.49 Backwash Batch Kinetic Experiment MCB2 B 95% joint confidence intervals for $TOTNH_3$

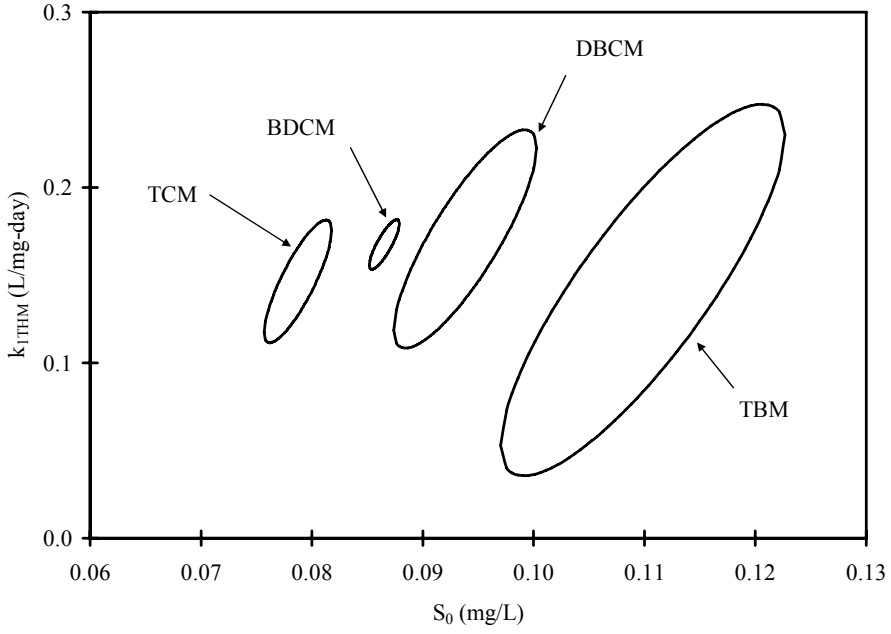

Figure D.50 Backwash Batch Kinetic Experiment MCB2 B 95% joint confidence intervals for THMs

Table D.44 Tukey's paired comparison for $k_{1_{THM}}$ for MCB2 B

Experiment	Observations	σ	σ^2
TCM	6	0.017	0.00031
BDCM	6	0.0071	0.000050
DBCM	6	0.031	0.00097
TBM	6	0.053	0.0028
Total Observations =	24	Pooled σ^2 =	0.0010
Degrees of Freedom (v) =	20	Pooled σ =	0.032
Treatments (k) =	4		
$q_{k,v,0.025}$ =	4.426		
Allowable $y_{bar,i}$-$y_{bar,j}$ = ±	0.058		

Absolute value of $y_{bar,i}$-$y_{bar,j}$

	TCM	BDCM	DBCM	TBM
TCM				
BDCM	0.021			
DBCM	0.024	0.0031		
TBM	0.0050	0.026	0.029	

Table D.45 Backwash Batch Kinetic Experiment MCB2 C experimental data

$TOTNH_3$ Time (minutes)	pH	$TOTNH_3$ (mg/L)	THM Time (minutes)	THM Concentrations (µg/L)			
				TCM	BDCM	DBCM	TBM
15.00	8.7	4.9	59.00	70	82	94	120
61.25	8.7	4.4	232.00	67	75	84	100
118.00	8.7	4.0	488.00	64	65	70	85
236.00	8.6	3.2	582.00	62	63	67	82
419.50	8.6	2.2	653.00	59	60	66	83
538.50	8.4	1.7					
600.25	8.4	1.4					
655.00	8.4	1.3					

Total Suspended Solids = 7.3 mg/L

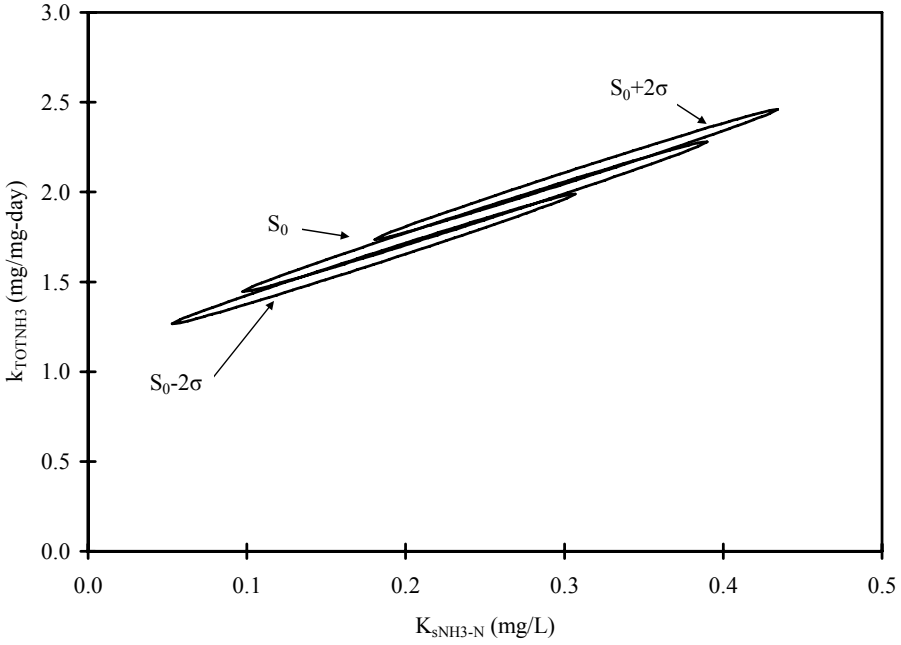

Figure D.51 Backwash Batch Kinetic Experiment MCB2 C 95% joint confidence intervals for $TOTNH_3$

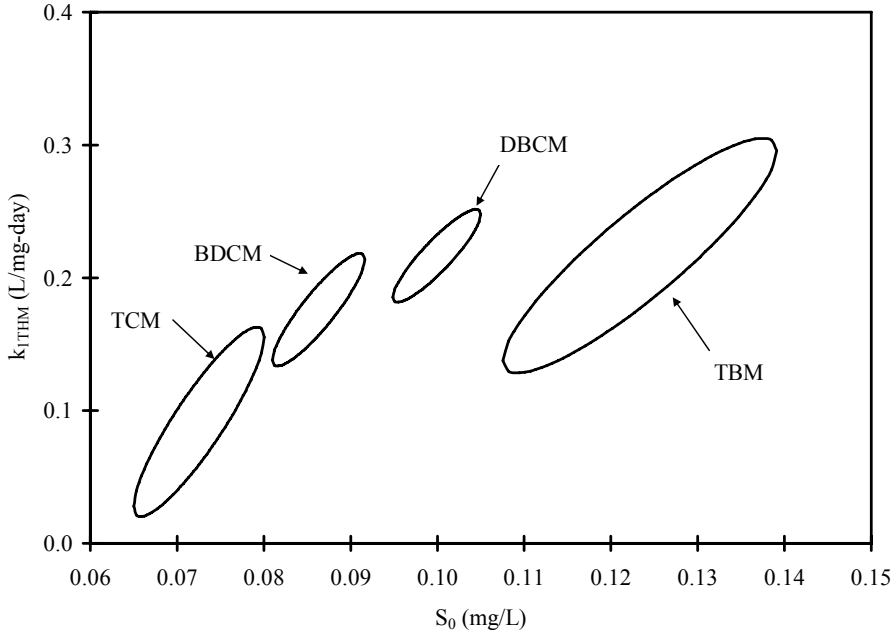

Figure D.52 Backwash Batch Kinetic Experiment MCB2 C 95% joint confidence intervals for THMs

Table D.46 Tukey's paired comparison for $k_{1_{THM}}$ for MCB2 C

Experiment	Observations	σ	σ^2
TCM	5	0.036	0.0013
BDCM	5	0.021	0.00045
DBCM	5	0.017	0.00031
TBM	5	0.044	0.0019
Total Observations =	20	Pooled σ^2 =	0.00099
Degrees of Freedom (v) =	16	Pooled σ =	0.032
Treatments (k) =	4		
$q_{k,v,0.025}$ =	4.548		
Allowable $y_{bar,i}$-$y_{bar,j}$ = ±	0.064		

Absolute value of $y_{bar,i}$-$y_{bar,j}$

	TCM	BDCM	DBCM	TBM
TCM				
BDCM	0.084			
DBCM	0.125	0.041		
TBM	0.125	0.041	0.000086	

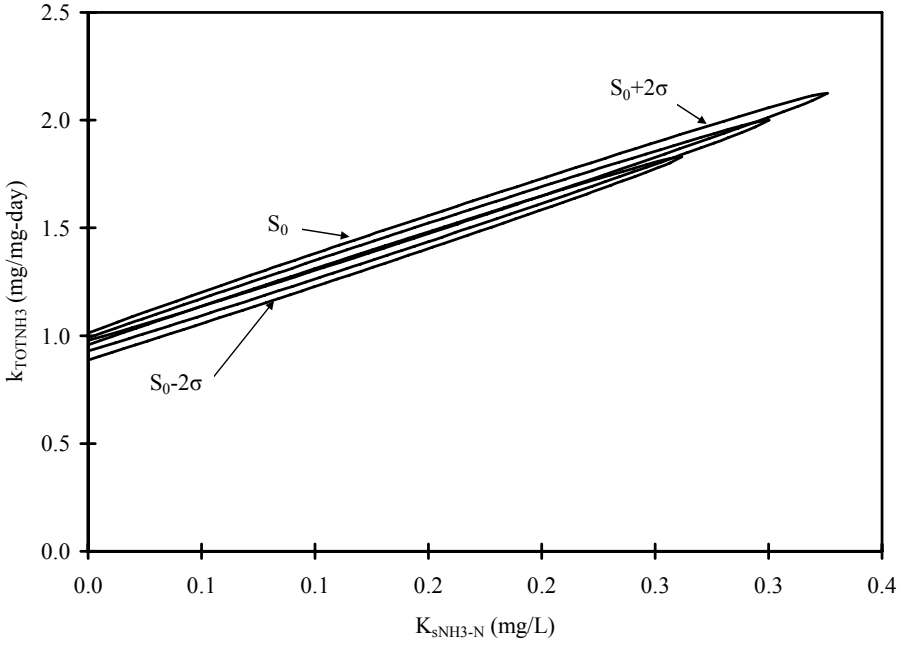

Figure D.53 Backwash Batch Kinetic Experiment MCB2 C (3 mg/L start) 95% joint confidence intervals for $TOTNH_3$

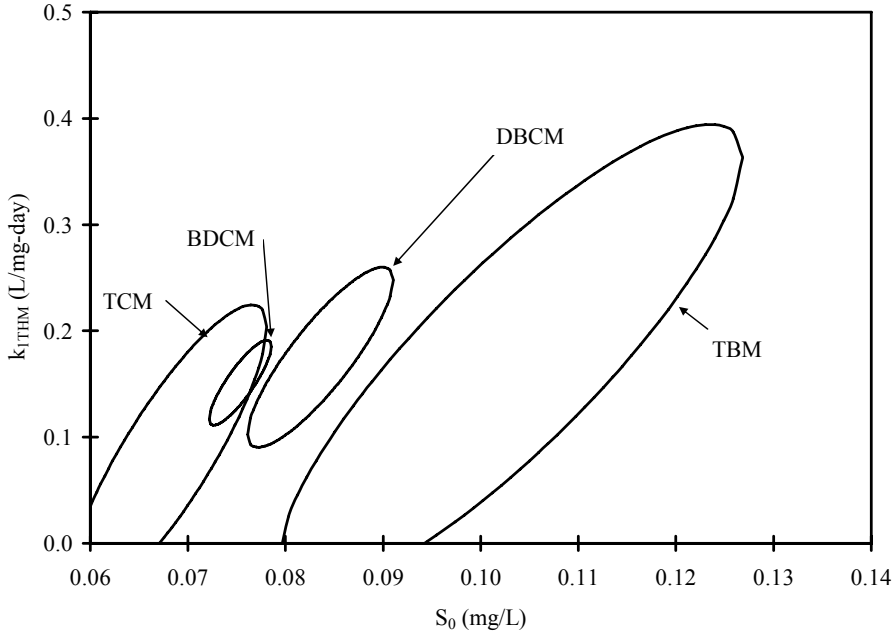

Figure D.54 Backwash Batch Kinetic Experiment MCB2 C (3 mg/L start) 95% joint confidence intervals for THMs

Table D.47 Tukey's paired comparison for $k_{1_{THM}}$ for MCB2 C (3 mg/L start)

Experiment	Observations	σ	σ^2
TCM	4	0.070	0.0050
BDCM	4	0.020	0.00040
DBCM	4	0.042	0.0018
TBM	4	0.11	0.012
Total Observations =	16	Pooled σ^2 =	0.0048
Degrees of Freedom (v) =	12	Pooled σ =	0.069
Treatments (k) =	4		
$q_{k,v,0.025}$ =	4.762		
Allowable $y_{bar,i}$-$y_{bar,j}$ = ±	0.16		

Absolute value of $y_{bar,i}$-$y_{bar,j}$

	TCM	BDCM	DBCM	TBM
TCM				
BDCM	0.067			
DBCM	0.091	0.024		
TBM	0.091	0.024	0.00034	

Table D.48 Backwash Batch Kinetic Experiment MCB2 D experimental data

$TOTNH_3$ Time (minutes)	pH	$TOTNH_3$ (mg/L)	THM Time (minutes)	THM Concentrations (µg/L)			
				TCM	BDCM	DBCM	TBM
1.50	8.7	4.8	4.00	75	84	95	120
16.25	8.7	4.7	59.50	73	79	89	110
61.50	8.7	4.3	233.45	68	71	75	91
119.00	8.7	3.9	491.50	62	64	68	84
236.00	8.6	3.2	578.00	60	62	65	79
425.00	8.6	2.4	645.00	59	61	64	78
548.00	8.4	1.9					
597.00	8.4	1.7					
648.00	8.4	1.5					

Total Suspended Solids = 17 mg/L

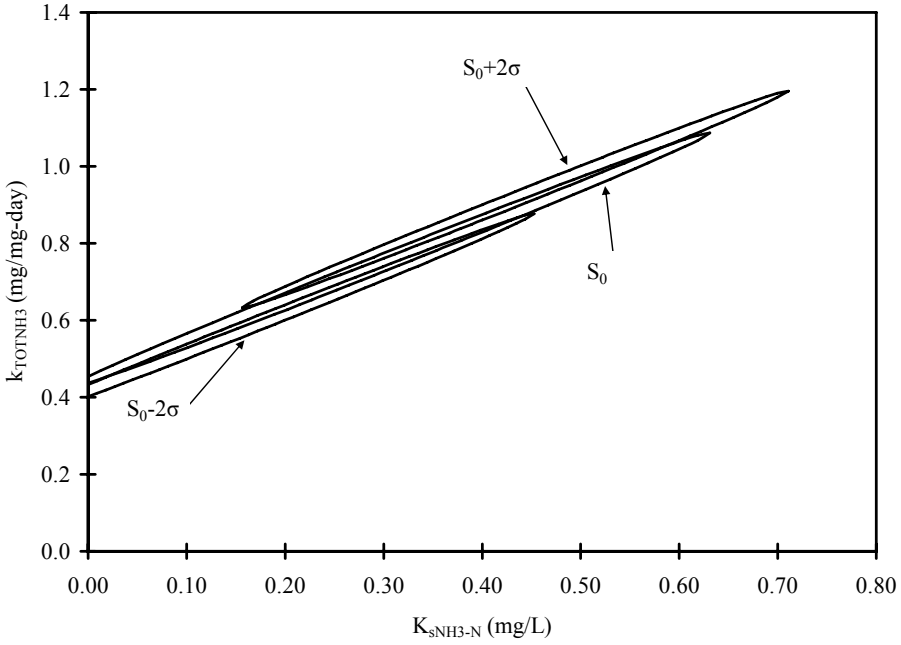

Figure D.55 Backwash Batch Kinetic Experiment MCB2 D 95% joint confidence intervals for $TOTNH_3$

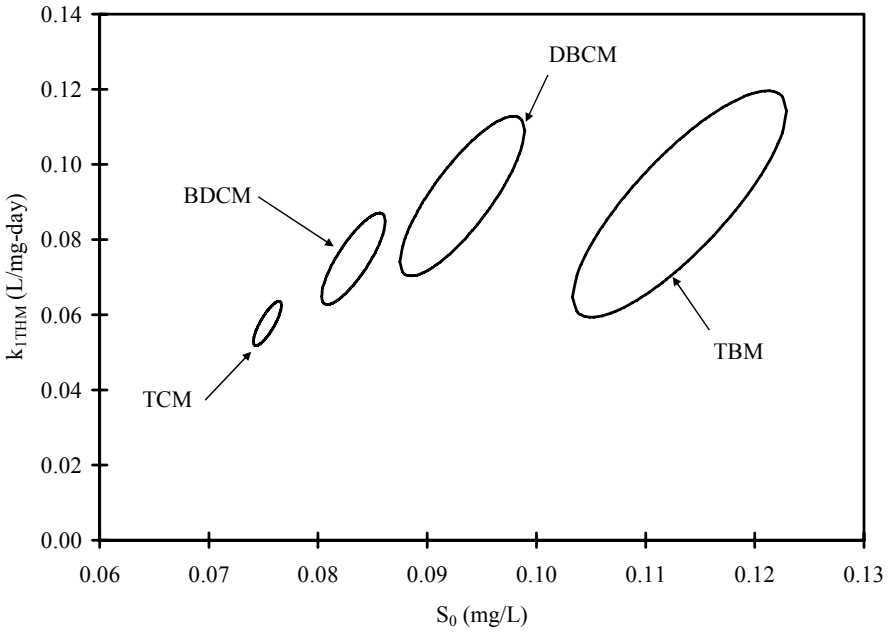

Figure D.56 Backwash Batch Kinetic Experiment MCB2 D 95% joint confidence intervals for THMs

Table D.49 Tukey's paired comparison for $k_{1_{THM}}$ for MCB2 D

Experiment	Observations	σ	σ^2
TCM	6	0.0030	0.0000087
BDCM	6	0.0061	0.000037
DBCM	6	0.011	0.00011
TBM	6	0.015	0.00023
Total Observations =	24	Pooled σ^2 =	0.00010
Degrees of Freedom (v) =	20	Pooled σ =	0.0098
Treatments (k) =	4		
$q_{k,v,0.025}$ =	4.426		
Allowable $y_{bar,i}$-$y_{bar,j}$ = ±	0.018		

Absolute value of $y_{bar,i}$-$y_{bar,j}$

	TCM	BDCM	DBCM	TBM
TCM				
BDCM	0.017			
DBCM	0.034	0.017		
TBM	0.032	0.015	0.0021	

D.11. MOLECULAR BIOFILM INVESTIGATION DATA

Table D.50 Biofilter moisture content determination

Sample	Weights (mg)					Moisture Content (%)
	Pan	Pan + Wet Anthracite	Pan + Dry Anthracite	Wet Anthracite	Dry Anthracite	
1	949.86	2,998.68	2,358.90	2,048.82	1,409.04	31
2	946.94	3,198.44	2,465.88	2,251.50	1,518.94	33
3	946.97	2,895.78	2,270.76	1,948.81	1,323.79	32
4	947.31	3,254.63	2,504.45	2,307.32	1,557.14	33
5	948.02	2,979.30	2,313.24	2,031.28	1,365.22	33
6	947.10	2,808.17	2,198.74	1,861.07	1,251.64	33
7	945.95	3,146.70	2,445.62	2,200.75	1,499.67	32
8	950.80	2,973.90	2,344.20	2,023.10	1,393.40	31
9	951.52	3,210.50	2,507.13	2,258.98	1,555.61	31
10	950.53	2,755.00	2,196.82	1,804.47	1,246.29	31
					Average	32
					Std. Dev.	0.74

Table D.51 MCB2 Train A (Lake Austin mixed culture) DNA extraction summary

Sample	Weights (g)				DNA (ng/μL)	A_{260}	A_{280}	$\frac{A_{260}}{A_{280}}$	Extracted DNA (ng/g)[a]
	Initial	Final	Wet Weight	Dry Weight					
1-1	3.0112	3.8887	0.8775	0.5974	21.43	0.429	0.265	1.62	1,793
1-2	2.9520	3.9464	0.9944	0.6770	17.26	0.345	0.197	1.76	1,275
1-3	2.9036	3.7598	0.8562	0.5829	18.59	0.372	0.228	1.63	1,595
2-1	2.9908	3.6897	0.6989	0.4758	30.15	0.603	0.345	1.75	3,168
2-2	2.9921	3.7240	0.7319	0.4983	14.91	0.298	0.181	1.65	1,496
2-3	2.9579	3.8088	0.8509	0.5793	27.61	0.552	0.326	1.70	2,383
3-1	2.9930	3.9122	0.9192	0.6258	28.18	0.564	0.318	1.77	2,251
3-2	2.9276	3.7030	0.7754	0.5279	23.81	0.476	0.284	1.68	2,255
3-3	2.9446	3.7935	0.8489	0.5780	31.91	0.638	0.370	1.72	2,761
4-1	2.9676	3.7260	0.7584	0.5164	27.09	0.542	0.287	1.89	2,623
4-2	3.0185	3.8333	0.8148	0.5548	26.02	0.520	0.289	1.80	2,345
4-3	2.9415	3.8466	0.9051	0.6162	28.44	0.569	0.307	1.85	2,308

[a](ng/g) = ng DNA/g dry anthracite

Table D.52 MCB2 Train B (Lake Austin mixed culture) DNA extraction summary

Sample	Weights (g)				DNA (ng/μL)	A_{260}	A_{280}	$\frac{A_{260}}{A_{280}}$	Extracted DNA (ng/g)[a]
	Initial	Final	Wet Weight	Dry Weight					
1-1	2.9704	3.8548	0.8844	0.6021	27.74	0.555	0.306	1.81	2,303
1-2	2.8906	3.8934	1.0028	0.6827	42.81	0.856	0.468	1.83	3,135
1-3	2.9025	3.8112	0.9087	0.6187	23.38	0.468	0.261	1.79	1,890
2-1	2.9151	4.0025	1.0874	0.7403	31.91	0.638	0.375	1.70	2,155
2-2	2.8734	3.8096	0.9362	0.6374	25.46	0.509	0.302	1.68	1,997
2-3	3.0127	4.1191	1.1064	0.7533	29.89	0.598	0.322	1.86	1,984
3-1	2.8968	3.6966	0.7998	0.5445	30.37	0.607	0.320	1.90	2,789
3-2	2.9893	3.8472	0.8579	0.5841	38.61	0.772	0.405	1.91	3,305
3-3	2.9998	3.9117	0.9119	0.6209	34.38	0.688	0.359	1.92	2,769
4-1	2.9728	3.7509	0.7781	0.5298	23.88	0.478	0.268	1.78	2,254
4-2	2.9993	3.8588	0.8595	0.5852	30.01	0.600	0.329	1.82	2,564
4-3	2.9456	3.7859	0.8403	0.5721	37.28	0.746	0.407	1.83	3,258

[a](ng/g) = ng DNA/g dry anthracite

Table D.53 MCB2 Train C (*N. oligotropha* enrichment culture) DNA extraction summary

Sample	Weights (g)				DNA (ng/μL)	A_{260}	A_{280}	$\frac{A_{260}}{A_{280}}$	Extracted DNA (ng/g)[a]
	Initial	Final	Wet Weight	Dry Weight					
1-1	2.9898	3.7982	0.8084	0.5504	26.55	0.531	0.290	1.83	2,412
1-2	2.9009	3.7395	0.8386	0.5710	24.86	0.497	0.281	1.77	2,177
1-3	2.8436	3.6045	0.7609	0.5181	23.11	0.462	0.249	1.86	2,230
2-1	2.9395	3.7939	0.8544	0.5817	21.84	0.437	0.245	1.78	1,877
2-2	2.9572	3.8412	0.8840	0.6019	19.94	0.399	0.198	2.01	1,657
2-3	3.0064	3.9926	0.9862	0.6714	21.11	0.422	0.231	1.83	1,572
3-1	2.9521	3.8154	0.8633	0.5878	19.33	0.387	0.199	1.94	1,644
3-2	2.9496	4.0189	1.0693	0.7280	31.45	0.629	0.359	1.75	2,160
3-3	2.9973	3.8873	0.8900	0.6060	26.67	0.533	0.313	1.71	2,201
4-1	2.9444	3.8038	0.8594	0.5851	19.01	0.380	0.201	1.89	1,624
4-2	2.9889	3.8383	0.8494	0.5783	20.96	0.419	0.237	1.77	1,812
4-3	2.9019	3.8082	0.9063	0.6170	19.54	0.391	0.214	1.82	1,583

[a](ng/g) = ng DNA/g dry anthracite

Table D.54 MCB2 Train D (*N. oligotropha* enrichment culture) DNA extraction summary

Sample	Weights (g)				DNA (ng/μL)	A_{260}	A_{280}	$\frac{A_{260}}{A_{280}}$	Extracted DNA (ng/g)[a]
	Initial	Final	Wet Weight	Dry Weight					
1-1	2.9672	3.7609	0.7937	0.5404	19.16	0.383	0.198	1.93	1,773
1-2	2.9811	3.8161	0.8350	0.5685	12.01	0.240	0.129	1.87	1,056
1-3	3.0049	3.8249	0.8200	0.5583	14.61	0.292	0.167	1.75	1,308
2-1	3.0113	3.8456	0.8343	0.5680	25.25	0.505	0.268	1.88	2,223
2-2	2.9677	3.7905	0.8228	0.5602	29.21	0.584	0.301	1.94	2,607
2-3	2.9755	3.8333	0.8578	0.5840	19.63	0.393	0.208	1.89	1,681
3-1	2.9560	3.8461	0.8901	0.6060	26.23	0.525	0.293	1.79	2,164
3-2	2.9904	4.0459	1.0555	0.7186	23.78	0.476	0.284	1.67	1,655
3-3	2.9348	3.8489	0.9141	0.6224	27.28	0.546	0.291	1.87	2,192
4-1	2.9113	3.8159	0.9046	0.6159	19.95	0.399	0.204	1.96	1,620
4-2	2.9763	3.7728	0.7965	0.5423	24.50	0.490	0.255	1.92	2,259
4-3	2.9518	3.8364	0.8846	0.6023	31.13	0.623	0.297	2.10	2,584

[a](ng/g) = ng DNA/g dry anthracite

Table D.55 Tukey's paired comparison for MCB2 total DNA extractions

Experiment	Samples	Average DNA extracted (ng DNA/g dry anthracite)	σ	σ^2
A1	3	1,554	262	68,506
A2	3	2,349	837	699,770
A3	3	2,422	293	85,790
A4	3	2,425	172	29,723
B1	3	2,443	634	402,430
B2	3	2,045	95	9,063
B3	3	2,954	304	92,479
B4	3	2,692	514	264,403
C1	3	2,273	123	15,155
C2	3	1,702	158	24,838
C3	3	2,002	310	96,169
C4	3	1,673	122	14,883
D1	3	1,379	363	132,105
D2	3	2,170	465	216,688
D3	3	2,003	302	91,490
D4	3	2,154	491	240,904
Total Observations =	48		Pooled σ^2 =	155,275
Degrees of Freedom (v) =	32		Pooled σ =	394
Treatments (k) =	16			
$q_{k,v,0.025}$ =	5.656			
Allowable $y_{bar,i}$-$y_{bar,j}$ = ±	1,287			

Absolute value of $y_{bar,i}$-$y_{bar,j}$																
	A1	A2	A3	A4	B1	B2	B3	B4	C1	C2	C3	C4	D1	D2	D3	D4
A1																
A2	795															
A3	868	73														
A4	871	76	3													
B1	888	94	20	17												
B2	491	304	377	380	397											
B3	1,400	605	532	529	511	909										
B4	1,138	343	270	267	249	647	262									
C1	719	76	149	152	170	228	681	419								
C2	148	647	720	723	741	343	1,252	990	571							
C3	447	347	421	424	441	44	952	690	271	300						
C4	119	676	749	752	769	372	1,281	1,019	600	29	328					
D1	175	970	1,043	1,046	1,064	666	1,575	1,313	894	323	622	294				
D2	616	179	252	255	273	125	784	522	103	468	168	497	791			
D3	449	346	419	422	439	42	951	689	270	302	2	330	624	167		
D4	600	195	268	271	288	109	800	538	119	452	153	481	775	16	151	

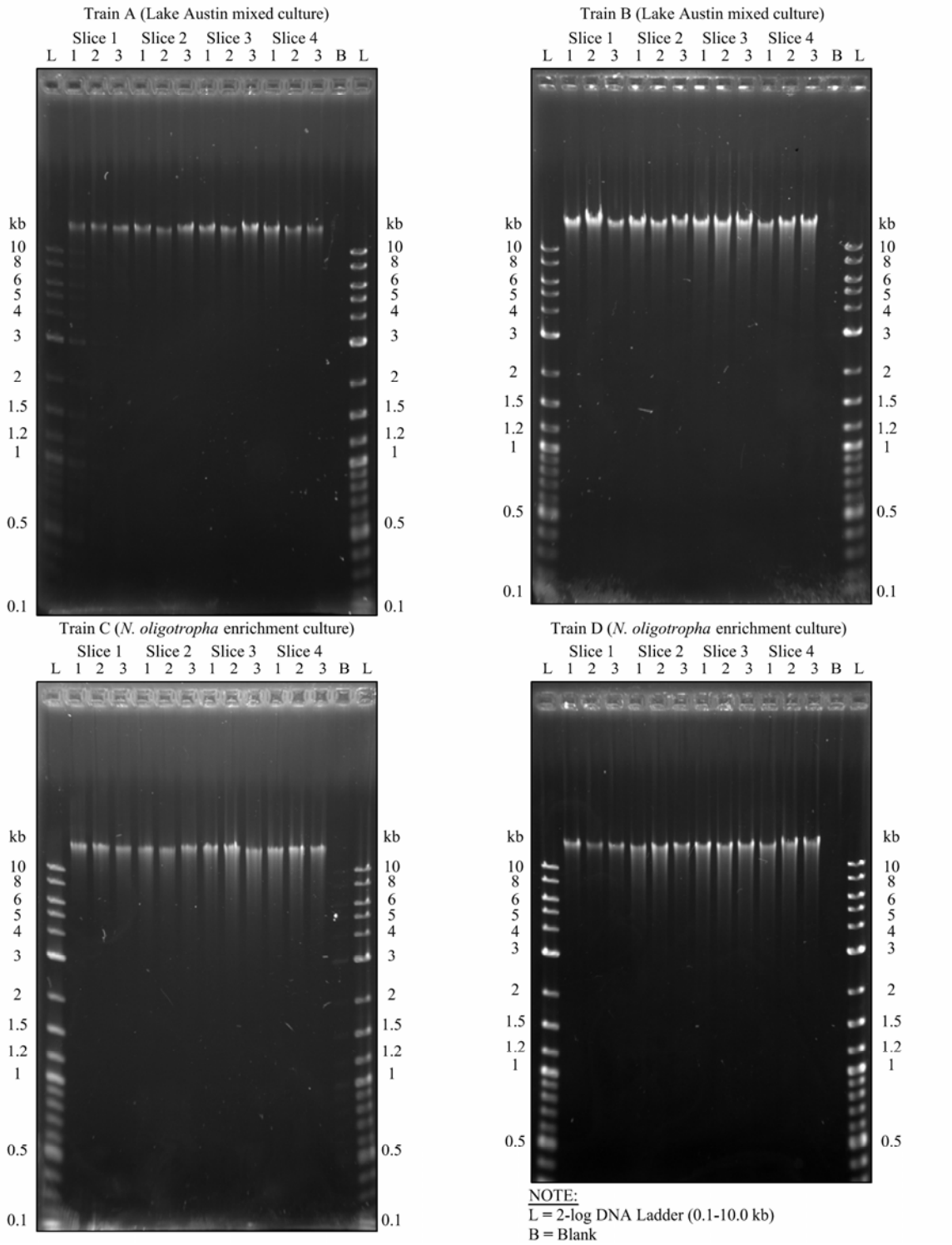

Figure D.57 Mixed Culture Biofilters 2 DNA extraction gel electrophoresis results

Appendix E: Example Standard Curves

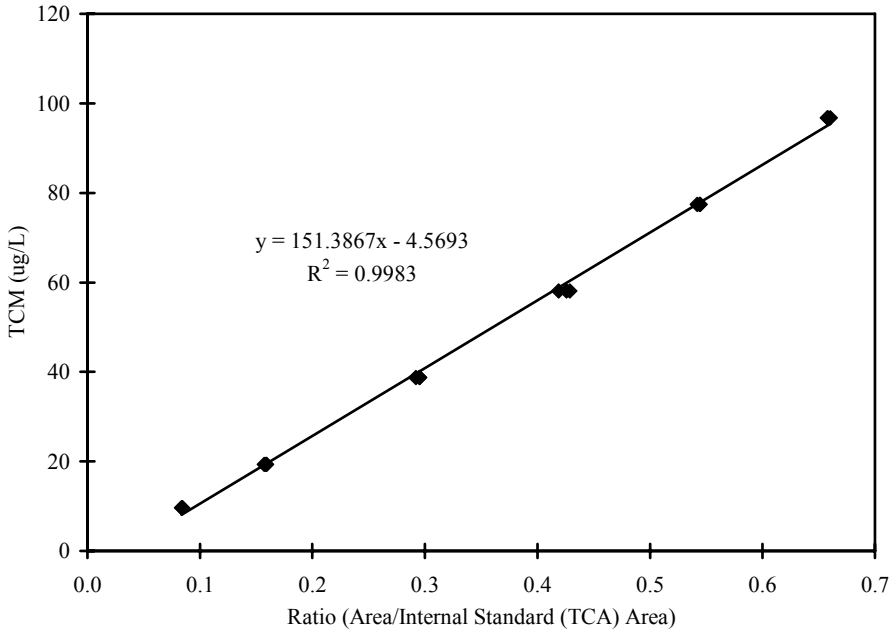

Figure E.1 Example TCM standard curve

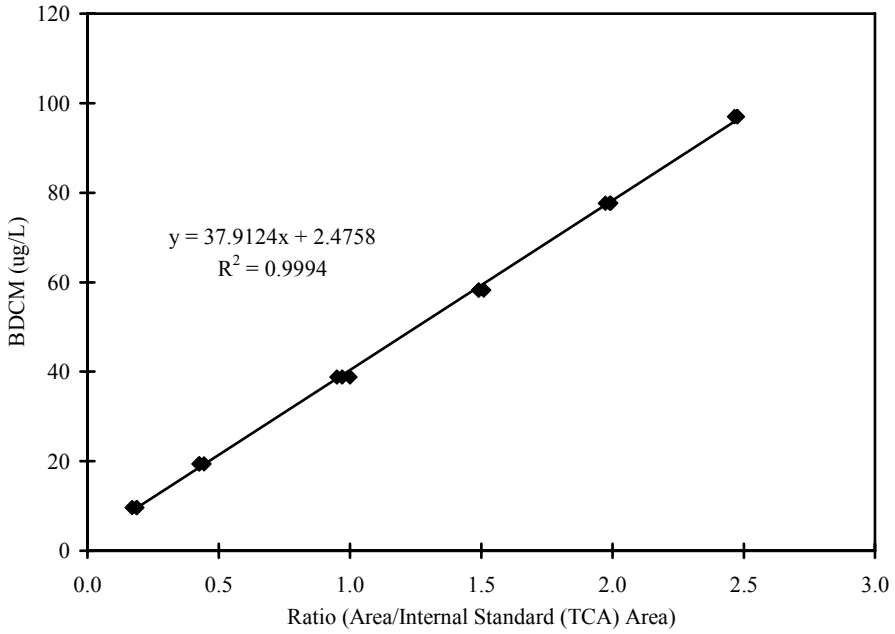

Figure E.2 Example BDCM standard curve

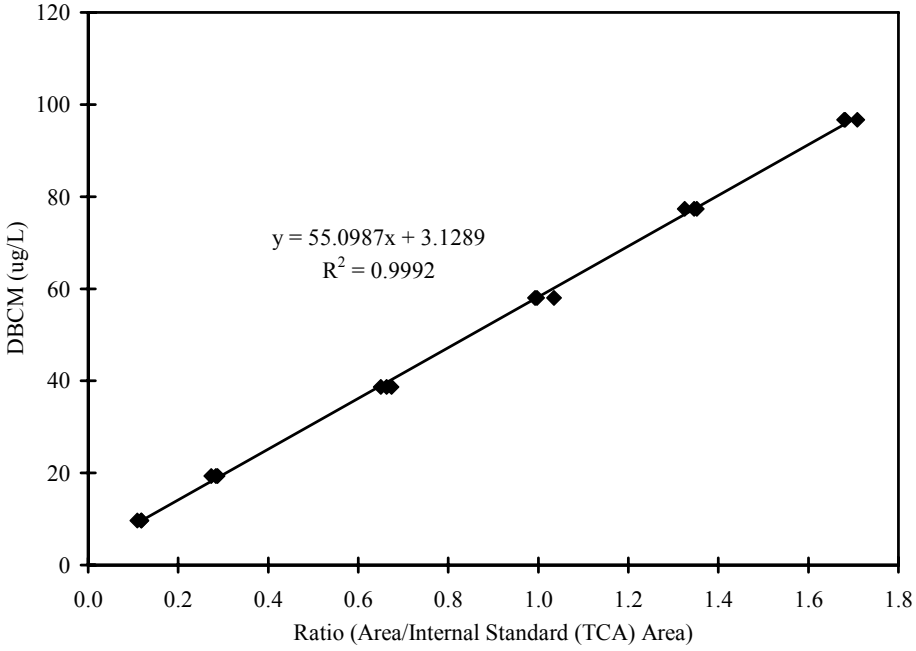

Figure E.3 Example DBCM standard curve

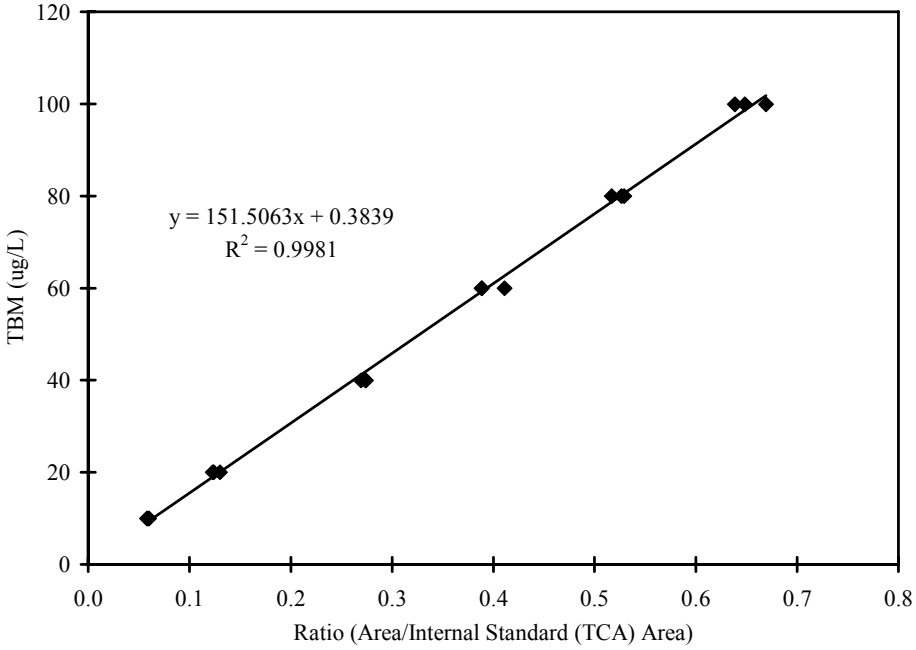

Figure E.4 Example TBM standard curve

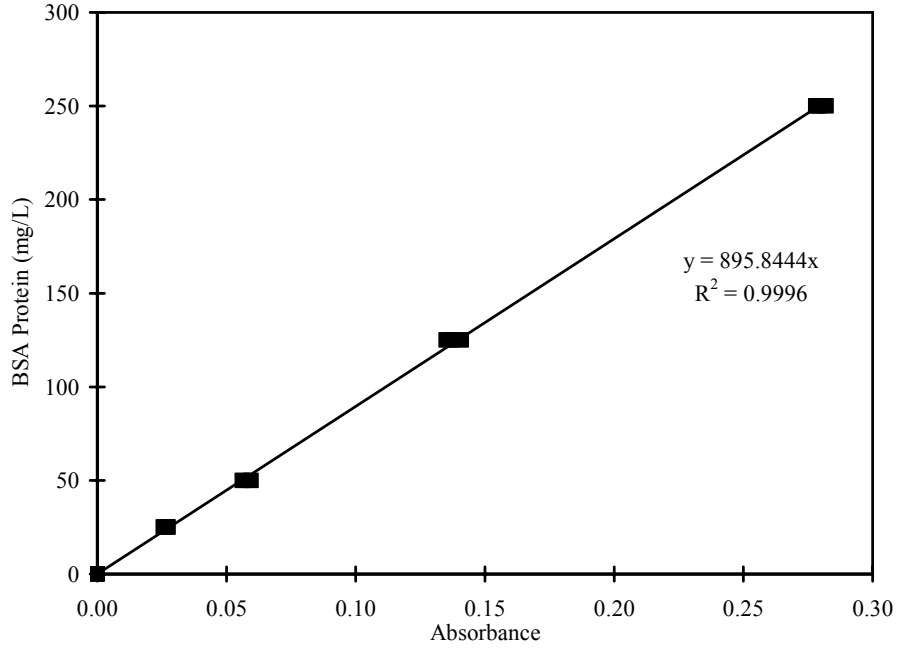

Figure E.5 Example BCA protein assay standard curve

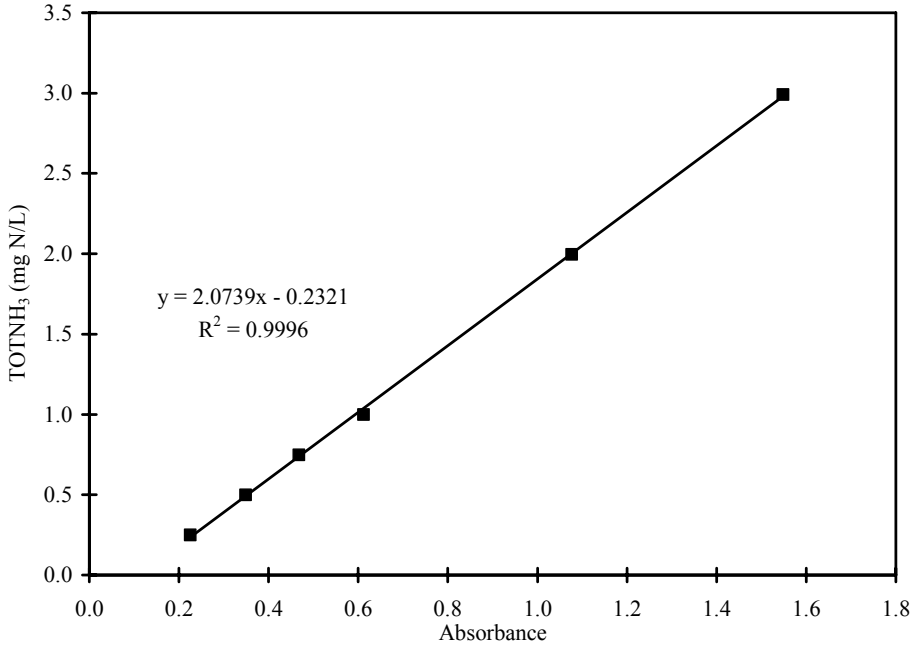

Figure E.6 Example $TOTNH_3$ standard curve (LR)

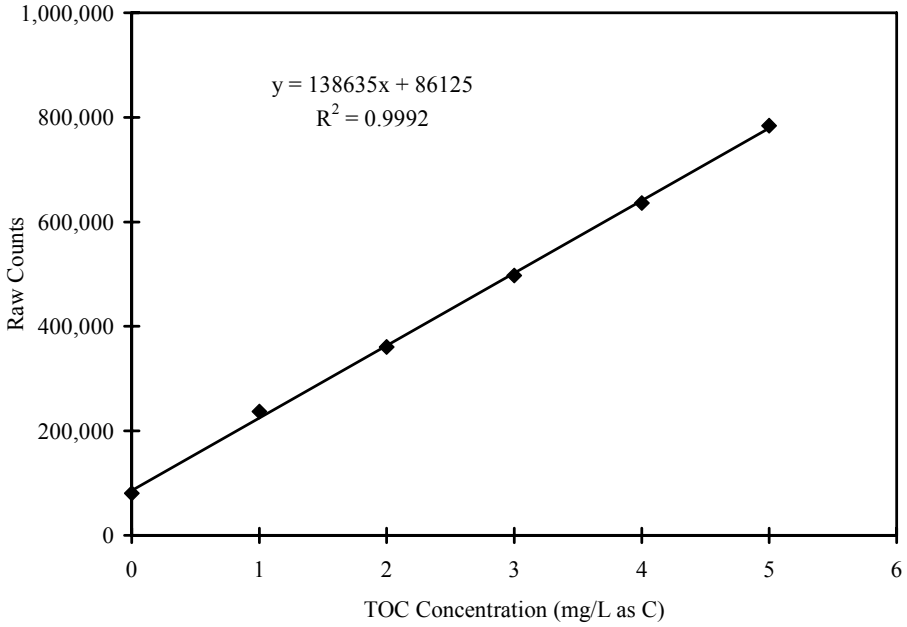

Figure E.7 Example TOC standard curve

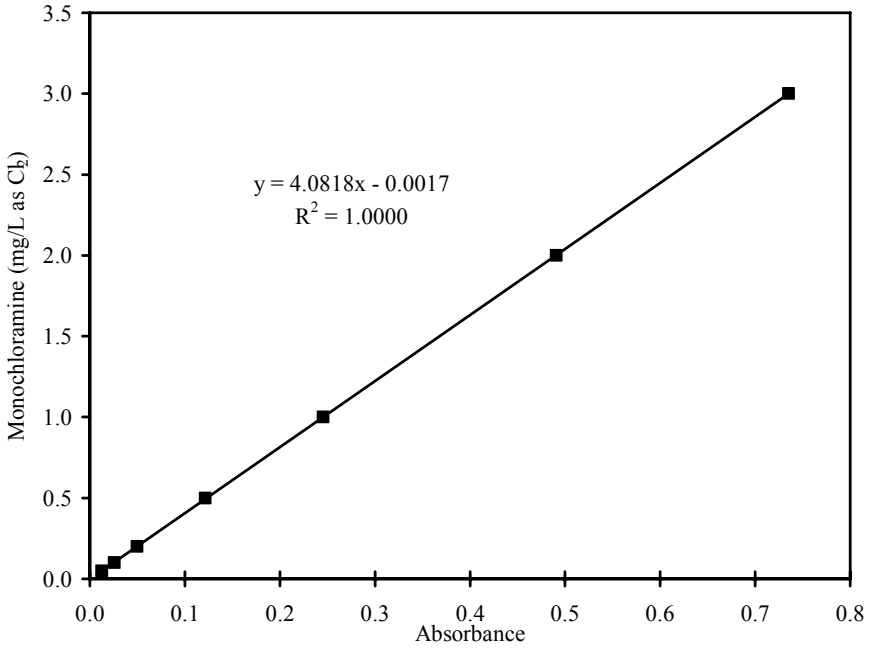

Figure E.8 Example monochloramine standard curve

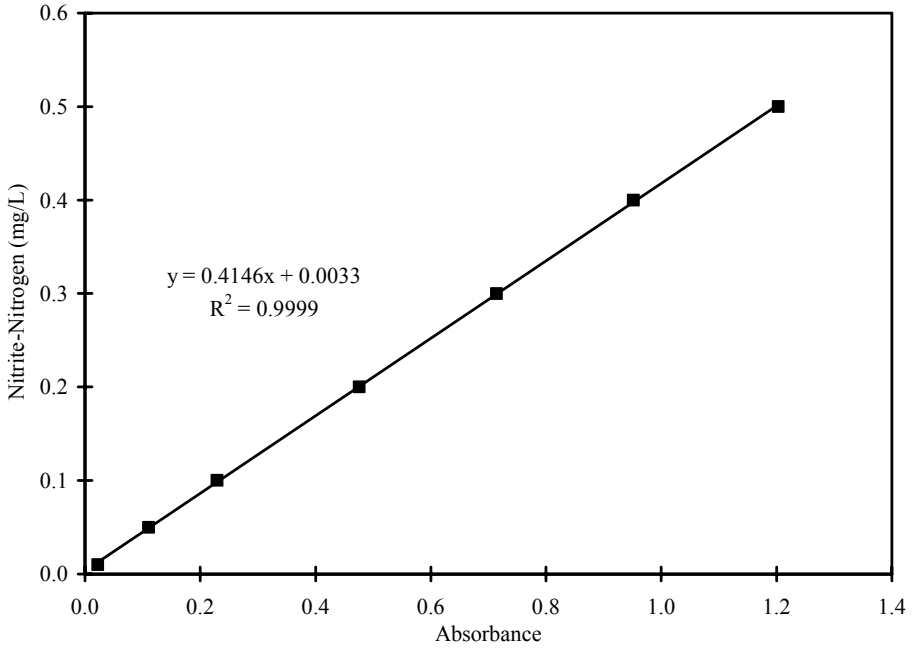

Figure E.9 Example nitrite-nitrogen standard curve (LR)

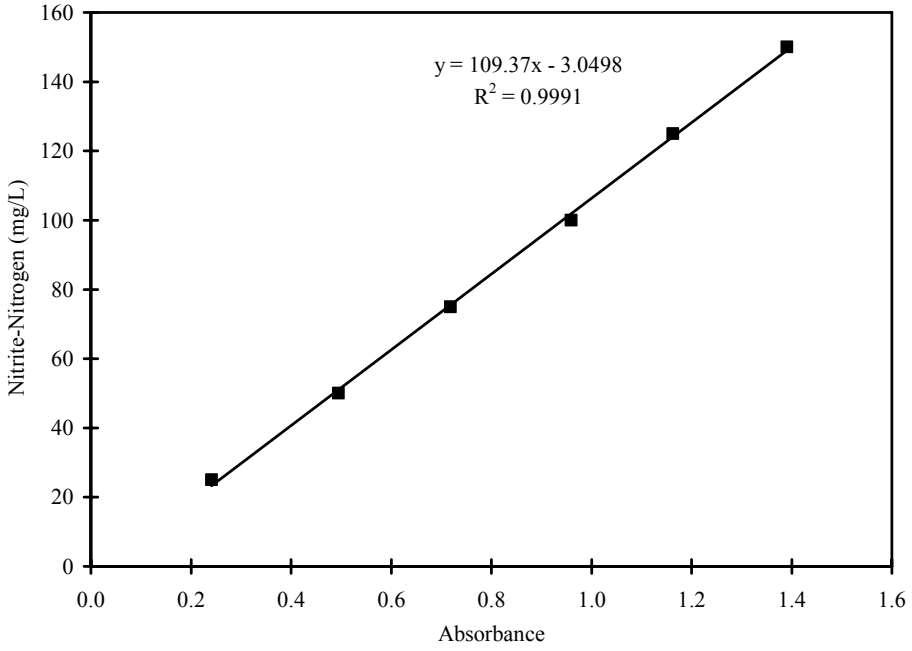

Figure E.10 Example nitrite-nitrogen standard curve (HR)

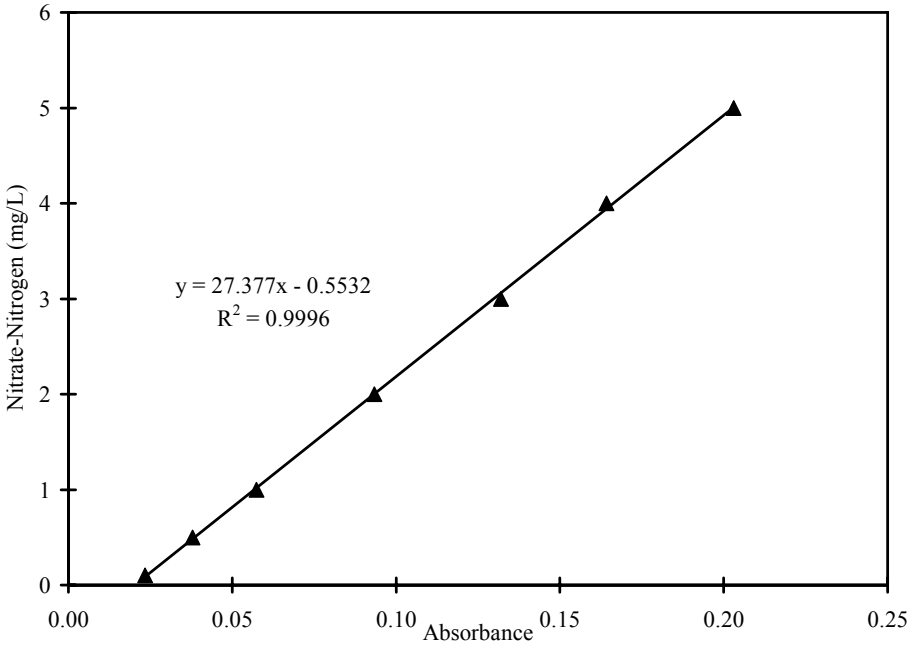

Figure E.11 Example nitrate-nitrogen standard curve

Glossary

The following symbols and abbreviations are used in this dissertation:

A	coefficient based on dielectric constant at temperature T
Å	angstrom
ACS	American Chemical Society
AMO	ammonia monooxygenase
AOB	ammonia oxidizing bacteria
APHA	American Public Health Association
ATCC®	American Type Culture Collection
ATP	adenosine triphosphate
α_1	NH_3-N fraction of $TOTNH_3$
BDCM	bromodichloromethane
BKE	batch kinetic experiment
B.S.	Bachelor of Science
BW	back washed
°C	degrees Celsius
C_1	one carbon containing compounds
C_2	two carbon containing compounds
c_i	concentration of species i
CL	confidence limit
Cl_2:N	chlorine to nitrogen mass ratio
cm	centimeter
cm^3/g	cubic centimeters per gram
C_{si}	cometabolism stability index
DBCM	dibromochloromethane
DBP	disinfection by-product
1,2-DCA	1,2-dichloroethane
1,1-DCE	1,1-dichloroethene
DDI	distilled-deionized
DO	dissolved oxygen
DOM	dissolved organic matter
Dr.	doctor
$\Delta_{0\text{-}1}$	change in concentration across the first column in series
$\Delta_{1\text{-}2}$	change in concentration across the second column in series
ΔDBCM	change in DBCM concentration
ΔTCM	change in TCM concentration

ΔTHM	change in THM concentration
Δ_{Total}	total change in concentration across both columns in series
$\Delta TOTNH_3$	change in $TOTNH_3$ concentration
e^-	electron
E	dielectric constant of water
EBCT	empty bed contact time
EDTA	ethylenediaminetetraacetic acid
EWRE	Environmental and Water Resources Engineering
F400	Filtrasorb 400
g	gram
g/L	grams per liter
g/mL	grams per milliliter
g/mole	grams per mole
GAC	granular activated carbon
GC	gas chromatograph
gpm/ft^2	gallons per minute per square foot
$\gamma_{NH_4^+}$	activity coefficient for ammonium ion
HAA	haloacetic acid
HAO	hydroxylamine oxidoreductase
HDPE	high-density polyethylene
hr	hour
I	ionic strength
ICR	Information Collection Rule
IE	Initial experiment
ISE	ion selective electrode
Jr.	junior
K	degrees Kelvin
k	maximum specific rate of degradation
k_1	pseudo-first-order rate constant
K_a	ammonia/ammonium equilibrium constant
$K_{a,T}$	ammonia/ammonium temperature corrected equilibrium constant
$k_{1_{BDCM}}$	BDCM pseudo-first-order rate constant
k_d	endogenous decay coefficient
$k_{1_{DBCM}}$	DBCM pseudo-first-order rate constant
K_s	half-saturation constant
$K_{s_{NH_3\text{-}N}}$	ammonia half-saturation constant

$K_{s_{THM}}$	THM half-saturation constant
$k_{1_{TBM}}$	TBM pseudo-first-order rate constant
$k_{1_{TCM}}$	TCM pseudo-first-order rate constant
k_{THM}	THM maximum specific rate of degradation
$k_{1_{THM}}$	THM pseudo-first-order rate constant
k_{TOTNH_3}	ammonia maximum specific rate of degradation
L	liter
LAB	Lake Austin Biofilters experiment
LAW	Lake Austin water
LDPE	low-density polyethylene
L/mg-day	liters per milligram per day
M	molar
MCB	mixed culture biofilters
MCL	maximum contaminant level
MIB	2-methylisoborneol
min	minute
mg	milligram
m^2/g	square meters per gram
m/h	meter per hour
mg/L	milligram per liter
mg/L-C	milligram per liter as carbon
mg/L-Cl_2	milligram per liter as chlorine
mg/mg-day	mg per mg per day
mL	milliliter
mL/min	milliliter per minute
mm Hg	millimeters of mercury
M.S.E.	Masters of Science in Engineering
M. trichosporium	*Methylosinus trichosporium*
MW	molecular weight
µg	microgram
µg/L	microgram per liter
µL	microliter
µm	micrometer
µM	micromolar
µmol	micromole
N	normality
NAD^+	nicotinamide adenine dinucleotide, oxidized form
NADH	nicotinamide adenine dinucleotide, reduced form
N/D	not determined
NH_3-N	ammonia-nitrogen
NH_4^+-N	ammonium-nitrogen

N. europaea	*Nitrosomonas europaea*
nM	nanomolar
nm	nanometer
nmole	nanomole
No.	number
NOB	nitrite oxidizing bacteria
N. oligotropha	*Nitrosomonas oligotropha*
NOM	natural organic matter
NO_2^--N	nitrite-nitrogen
NO_3^--N	nitrate-nitrogen
NW	nutrient water
η	bromine incorporation factor
Ph.D.	Doctor of Philosophy
P.O.	Post Office
PQQ	electron carrier, oxidized form
PQQH2	electron carrier, reduced form
r_g'	net rate of bacterial cell growth
r_i	rate of THM bacterial inactivation
rpm	revolutions per minute
r_{THM}	rate of THM degradation
r_{TOTNH_3}	rate of $TOTNH_3$ degradation
s	activity correction term (valid for I < 0.5 M)
S_0	influent concentration
S_{BDCM}	BDCM concentration
S_{DBCM}	DBCM concentration
$S_{F_{THM}}$	final THM concentration
$S_{I_{THM}}$	initial THM concentration
$S_{NH_3\text{-}N}$	ammonia-nitrogen concentration
SSA	specific surface area
S_{TBM}	TBM concentration
S_{TCM}	TCM concentration
S_{THM}	THM concentration
STP	standard temperature and pressure
S_{TOTNH_3}	$TOTNH_3$ concentration
σ	standard deviation
t	time
T	temperature
TBM	tribromomethane (bromoform)

T_c	transformation capacity
TCA	1,1,1-trichloroethane
$T_{c_{BDCM}}$	BDCM transformation capacity
$T_{c_{DBCM}}$	DBCM transformation capacity
TCE	trichloroethylene
TCM	trichloromethane (chloroform)
$T_{c_{TBM}}$	TBM transformation capacity
$T_{c_{TCM}}$	TCM transformation capacity
$T_{c_{THM}}$	THM transformation capacity
TDS	total dissolved solids
THM	trihalomethane
TOC	total organic carbon
$TOTNH_3$	total ammonia-nitrogen
TSS	total suspended solids
TTHM	total THM
U.S.	United States
USEPA	United States Environmental Protection Agency
UT	The University of Texas at Austin
w/v	weight per volume
X	biomass concentration
Y	bacterial cell yield
Y	electron carrier, oxidized form
YH2	electron carrier, reduced form
Z	ionic charge of NH_4^+
z_i	ionic charge of species i

References

Alvarez-Cohen, L., and McCarty, P. L. (1991a). "A Cometabolic Biotransformation Model for Halogenated Aliphatic-Compounds Exhibiting Product Toxicity." *Environmental Science & Technology*, 25(8), 1381-1387.

Alvarez-Cohen, L., and McCarty, P. L. (1991b). "Product Toxicity and Cometabolic Competitive-Inhibition Modeling of Chloroform and Trichloroethylene Transformation by Methanotrophic Resting Cells." *Applied and Environmental Microbiology*, 57(4), 1031-1037.

Alvarez-Cohen, L., and Speitel , G. E. (2001). "Kinetics of Aerobic Cometabolism of Chlorinated Solvents." *Biodegradation*, 12(2), 105-126.

Anthony, C. (1982). *The Biochemistry of Methylotrophs*, Academic Press, London ; New York.

APHA, AWWA, and WEF. (1998). "Standard Methods for the Examination of Water and Wastewater." American Public Health Association : American Water Works Association : Water Environment Federation, Washington, D.C.

Applied Biosystems. (2004). "7900 HT Sequence Detection Systems." Applied Biosystems, Foster City, California.

Arcangeli, J. P., and Arvin, E. (1997). "Modeling of the Cometabolic Biodegradation of Trichloroethylene by Toluene Oxidizing Bacteria in a Biofilm System." *Environmental Science & Technology*, 31(11), 3044-3052.

Arciero, D., Vannelli, t., Logan, M., and Hooper, A. B. (1989). "Degradation of Trichloroethylene by the Ammonia-Oxidizing Bacterium *Nitrosomonas europaea*." *Biochemical and Biophysical Research Communications*, 159(2), 640-3.

Arp, D. J., Sayavedra-Soto, L. A., and Hommes, N. G. (2002). "Molecular Biology and Biochemistry of Ammonia oxidation by *Nitrosomonas europaea*." *Archives of Microbiology*, 178(4), 250-255.

Arp, D. J., and Stein, L. Y. (2003). "Metabolism of Inorganic N Compounds by Ammonia-Oxidizing Bacteria." *Critical Reviews in Biochemistry and Molecular Biology*, 38, 471-495.

Arp, D. J., Yeager, C. M., and Hyman, M. R. (2001). "Molecular and Cellular Fundamentals of Aerobic Cometabolism of Trichloroethylene." *Biodegradation*, 12(2), 81-103.

Aziz, C. E., Georgiou, G., and Speitel, G. E. (1999). "Cometabolism of Chlorinated Solvents and Binary Chlorinated Solvent Mixtures Using *M. trichosporium* OB3b PP358." *Biotechnology and Bioengineering*, 65(1), 100-107.

Baribeau, H., Kinner, C. A., Stephen, J. R., De Leon, R., Rochelle, P. A., and Clark, D. L. (2000). "Microbial Population Characterization of Suspended and Fixed Biomass in Drinking Water Reservoirs." *Proceedings - Water Quality Technology Conference*, 890-901.

Bauer, R. C., and Snoeyink, V. L. (1973). "Reactions of Chloramines With Active Carbon." *Journal WPCF*, 45(11), 2290.

Benjamin, M. M. (2002). *Water Chemistry*, McGraw-Hill, New York, NY.

Berthouex, P. M., and Brown, L. C. (2002). *Statistics for Environmental Engineers*, CRC Press LLC, Boca Raton, Florida.

Chain, P., Lamerdin, J., Larimer, F., Regala, W., Lao, V., Land, M., Hauser, L., Hooper, A., Klotz, M., Norton, J., Sayavedra-Soto, L., Arciero, D., Hommes, N., Whittaker, M., and Arp, D. (2003). "Complete Genome Sequence of the Ammonia-oxidizing Bacterium and Obligate Chemolithoautotroph *Nitrosomonas europaea*." *Journal of Bacteriology*, 185(9), 2759-2773.

Chang, H.-L., and Alvarez-Cohen, L. (1996). "Biodegradation of Individual and Multiple Chlorinated Aliphatic Hydrocarbons by Methane-oxidizing Cultures." *Applied and Environmental Microbiology*, 62(9), 3371-3377.

Chang, S. W., Hyman, M. R., and Williamson, K. J. (2002). "Cooxidation of Naphthalene and Other Polycyclic Aromatic Hydrocarbons by the Nitrifying Bacterium, *Nitrosomonas europaea*." *Biodegradation*, 13(6), 373-81.

City of Austin Water Utility. (n.d.). "Water Quality Reports Archive." http://www.ci.austin.tx.us/water/waterreports.htm, Accessed October 19, 2006.

Clark, R. M., Boutin, B. K., and National Risk Management Research Laboratory (U.S.). Office of Research and Development. (2001). *Controlling Disinfection By-products and Microbial Contaminants in Drinking Water*, National Risk

Management Research Laboratory, Office of Research and Development, U.S. Environmental Protection Agency, Cincinnati, Ohio.

Connell, G. F., Routt, J. C., Macler, B., Andrews, R. C., Chen, J. M., Chowdhury, Z. K., Crozes, G. F., Finch, G. B., Hoehn, R. C., Jacangelo, J. G., Penkal, A., Schaeffer, G. R., Schulz, C. R., and Uza, M. P. (2000a). "Committee Report: Disinfection at Large and Medium-size Systems." *Journal American Water Works Association*, 92(5), 32-43.

Connell, G. F., Routt, J. C., Macler, B., Andrews, R. C., Chen, J. M., Chowdhury, Z. K., Crozes, G. F., Finch, G. B., Hoehn, R. C., Jacangelo, J. G., Penkal, A., Schaeffer, G. R., Schulz, C. R., and Uza, M. P. (2000b). "Committee Report: Disinfection at Small Systems." *Journal American Water Works Association*, 92(5), 24-31.

Criddle, C. S. (1993). "The Kinetics of Cometabolism." *Biotechnology and Bioengineering*, 41(11), 1048-1056.

Cunliffe, D. A. (1991). "Bacterial Nitrification in Chloraminated Water Supplies." *Applied and Environmental Microbiology*, 57(11), 3399-3402.

Dalton, H., and Stirling, D. I. (1982). "Co-metabolism." *Philosophical Transactions of the Royal Society of London. Series B, Biological Sciences*, 297,, 481-496.

Davidson, I. W. F., Sumner, D. D., and Parker, J. C. (1982). "Chloroform - A Review of Its Metabolism, Teratogenic, Mutagenic, and Carcinogenic Potential." *Drug and Chemical Toxicology*, 5(1), 1-87.

Ely, R. L. (1996). "Effects of Substrate Interactions, Toxicity, and Bacterial Response During Cometabolism of Chlorinated Solvents by Nitrifying Bacteria," Dissertation, Oregon State University.

Ely, R. L., Williamson, K. J., Hyman, M. R., and Arp, D. J. (1997). "Cometabolism of Chlorinated Solvents by Nitrifying Bacteria: Kinetics, Substrate Interactions, Toxicity Effects, and Bacterial Response." *Biotechnology and Bioengineering*, 54(6), 520-534.

Emerson, K., Russo, R. C., Lund, R. E., and Thurston, R. V. (1975). "Aqueous Ammonia Equilibrium Calculations - Effect of Ph and Temperature." *Journal of the Fisheries Research Board of Canada*, 32(12), 2379-2383.

Fairey, J. L. (2006). "Elucidation of Physiochemical Properties of Granular Activated Carbon for Monochloramine Destruction in Natural Waters," Dissertation, The University of Texas at Austin, Austin, Texas.

Fairey, J. L., Katz, L. E., and Speitel, G. E., Jr. (2004). "Monochloramine Destruction in GAC Beds." *Proceedings - Water Quality Technology Conference*.

Fairey, J. L., Speitel, G. E., Jr., and Katz, L. E. (2006). "Impact of Natural Organic Matter on Monochloramine Reduction by Granular Activated Carbon: The Role of Porosity and Electrostatic Surface Properties." *Environmental Science & Technology*, 40(13), 4268-4273.

Fairey, J. L., Speitel, G. E., Jr., and Katz, L. E. (Submitted for Review). "Monochloramine Destruction with Granular Activated Carbon in Drinking Water Filters." *Journal American Water Works Association*.

Gerwe, C. E. (2003). "Natural Organic Matter (NOM) Adsorption onto and Coprecipitation with Solids Formed during Softening," Dissertation, The University of Texas at Austin.

Ginestet, P., Audic, J. M., and Block, J. C. (2001). "Chlorinated Solvents Cometabolism by an Enriched Nitrifying Bacterial Consortium." *Water Science & Technology: Water Supply*, 1(4), 95-102.

Henry, A. E. (2004). "Cometabolism of Trihalomethanes by Mixed Culture Nitrifiers under Drinking Water Treatment Conditions," Thesis, The University of Texas at Austin, Austin, Texas.

Hokanson, D. R., Hand, D. W., Crittenden, J. C., and Oman, E. J. (1998). "Adsorption Design Software (AdDesignS)." Center for Clean Industrial and Treatment Technologies (CenCITT) Michigan Technological University, Houghton, Michigan.

Hommes, N. G., Sayavedra-Soto, L. A., and Arp, D. J. (2003). "Chemolithoorganotrophic Growth of *Nitrosomonas europaea* on Fructose." *Journal of Bacteriology*, 185(23), 6809-6814.

Hooper, A. B., and Terry, K. R. (1974). "Photoinactivation of Ammonia Oxidation in *Nitrosomonas*." *Journal of Bacteriology*, 119(3), 899-906.

Hooper, A. B., Vannelli, T., Bergmann, D. J., and Arciero, D. M. (1997). "Enzymology of the Oxidation of Ammonia to Nitrite by Bacteria." *Antonie Van Leeuwenhoek International Journal of General and Molecular Microbiology*, 71(1-2), 59-67.

Hyman, M. R., Murton, I. B., and Arp, D. J. (1988). "Interaction of Ammonia Monooxygenase from *Nitrosomonas-Europaea* with Alkanes, Alkenes, and Alkynes." *Applied and Environmental Microbiology*, 54(12), 3187-3190.

Hyman, M. R., Page, C. L., and Arp, D. J. (1994). "Oxidation of Methyl Fluoride and Dimethyl Ether by Ammonia Monoxygenase in *Nitrosomonas europaea*." *Applied and Environmental Microbiology*, 60(8), 3033-5.

Hyman, M. R., Sansome-Smith, A. W., Shears, J. H., and Wood, P. M. (1985). "A Kinetic Study of Benzene Oxidation to Phenol by Whole Cells of *Nitrosomonas europaea* and Evidence for the Further Oxidation of Phenol to Hydroquinone." *Archives of Microbiology*, 143(3), 302-6.

Hyman, M. R., and Wood, P. M. (1983). "Methane Oxidation by *Nitrosomonas europaea*." *Biochemical Journal*, 212(1), 31-37.

Hyman, M. R., and Wood, P. M. (1984a). "Bromocarbon Oxidations by *Nitrosomonas europaea*." *Microb. Growth C1 Compd., Proc. Int. Symp.*, 49-52.

Hyman, M. R., and Wood, P. M. (1984b). "Ethylene Oxidation by *Nitrosomonas europaea*." *Archives of Microbiology*, 137(2), 155-158.

Jafvert, C. T., and Valentine, R. L. (1992). "Reaction Scheme for the Chlorination of Ammoniacal Water." *Environmental Science and Technology*, 26(3), 577.

Janssen, D. B., Scheper, A., Dijkhuizen, L., and Witholt, B. (1985). "Degradation of Halogenated Aliphatic-Compounds by *Xanthobacter-Autotrophicus Gj10*." *Applied and Environmental Microbiology*, 49(3), 673-677.

Jones, R. D., and Morita, R. Y. (1983a). "Carbon Monoxide Oxidation by Chemolithotrophic Ammonium Oxidizers." *Canadian Journal of Microbiology*, 29(11), 1545-1551.

Jones, R. D., and Morita, R. Y. (1983b). "Methane Oxidation by *Nitrosococcus oceanus* and *Nitrosomonas europaea*." *Applied and Environmental Microbiology*, 45(2), 401-410.

Juliette, L. Y., Hyman, M. R., and Arp, D. J. (1993). "Inhibition of Ammonia Oxidation in *Nitrosomonas europaea* by Sulfur Compounds: Thioethers are Oxidized to Sulfoxides by Ammonia Monooxygenase." *Applied and Environmental Microbiology*, 59(11), 3718-27.

Keener, W. K., and Arp, D. J. (1993). "Kinetic Studies of Ammonia Monooxygenase Inhibition in *Nitrosomonas europaea* by Hydrocarbons and Halogenated Hydrocarbons in an Optimized Whole-cell Assay." *Applied and Environmental Microbiology*, 59(8), 2501-10.

Keener, W. K., and Arp, D. J. (1994). "Transformations of Aromatic Compounds by *Nitrosomonas europaea*." *Applied and Environmental Microbiology*, 60(6), 1914-20.

Keener, W. K., Russell, S. A., and Arp, D. J. (1998). "Kinetic Characterization of the Inactivation of Ammonia Monooxygenase in *Nitrosomonas europaea* by Alkyne, Aniline and Cyclopropane Derivatives." *Biochimica et Biophysica Acta*, 1388(2), 373-385.

Knowles, C. J. (1980). *The Diversity of Bacterial Respiratory Systems*, CRC Press, Boca Raton, Fla.

Komorita, J. D., and Snoeyink, V. L. (1985). "Monochloramine Removal from Water by Activated Carbon." *Journal American Water Works Association*, 77(1), 62-64.

Krasner, S. W. (1999). "Chemistry of Disinfection By-Product Formation." Formation and control of disinfection by-products in drinking water, P. C. Singer, ed., American Water Works Association, Denver, CO, 27-52.

Large, P. J. (1983). *Methylotrophy and Methanogenesis*, American Society for Microbiology, Washington, D. C.

Lawler, D. F., and Benjamin, M. E. (forthcoming). *Physical/Chemical Treatment Processes for Water and Wastewater*, The McGraw-Hill Companies, n.p.

Letterman, R. D., and American Water Works Association. (1999). *Water Quality and Treatment : A Handbook of Community Water Supplies*, McGraw-Hill, New York.

Lieberman, R. L., and Rosenzweig, A. C. (2005a). "Crystal Structure of a Membrane-Bound Metalloenzyme that Catalyses the Biological Oxidation of Methane." *Nature*, 434, 177-182.

Lieberman, R. L., and Rosenzweig, A. C. (2005b). "The Quest for the Particulate Methane Monooxygenase Active Site." *Dalton Transactions*(21), 3390-3396.

Mackay, I. M. (2004). "Real-Time PCR in the Microbiology Laboratory." *Clinical Microbiology and Infection*, 10(3), 190-211.

Madigan, M. T., Martinko, J. M., and Parker, J. (2000). *Brock Biology of Microorganisms Ninth Edition*, Prentice-Hall, Inc., Upper Saddle River, New Jersey.

Manem, J. A., and Rittmann, B. E. (1990). "Scaling Procedure for Biofilm Processes." *Water Science and Technology*, 22(1/2), 329-346.

McRae, B. M., LaPara, T. M., and Hozalski, R. M. (2004). "Biodegradation of Haloacetic Acids by Bacterial Enrichment Cultures." *Chemosphere*, 55(6), 915-925.

Melin, E. S., Puhakka, J. A., Strand, S. E., Rockne, K. J., and Ferguson, J. F. (1996). "Fluidized-bed Enrichment of Marine Ammonia-to-nitrite Oxidizers and Their Ability to Degrade Chloroaliphatics." *International Biodeterioration & Biodegradation*, 38(1), 9-18.

Messer, J. J., Ho, J., and Grenney, W. J. (1984). "Ionic Strength Correction for Extent of Ammonia Ionization in Freshwater." *Canadian Journal of Fisheries and Aquatic Sciences*, 41(5), 811-15.

Montgomery, J. H., and Welkom, L. M. (1990). *Groundwater Chemicals Desk Reference*, Lewis Publishers, Chelsea, Mich.

Motosugi, K., and Soda, K. (1983). "Microbial Degradation of Synthetic Organochlorine Compounds." *Experientia*, 39(11), 1214-1220.

MWH, Crittenden, J. C., Trussell, R. R., Hand, D. W., Howe, K. J., and Tchobanoglous, G. (2005). *Water Treatment: Principles and Design*, John Wiley & Sons, Inc., Hoboken, New Jersey.

Okano, Y., Hristova, K. R., Leutenegger, C. M., Jackson, L. E., Denison, R. F., Gebreyesus, B., Lebauer, D., and Scow, K. M. (2004). "Application of Real-Time

PCR to Study Effects of Ammonium on Population Size of Ammonia-Oxidizing Bacteria in Soil." *Applied and Environmental Microbiology*, 70(2), 1008-1016.

Owen, D. M. (1999). "Treatment Costs for Disinfection By-Product Control." Formation and control of disinfection by-products in drinking water, P. C. Singer, ed., American Water Works Association, Denver, CO, 371-391.

Pohl, L. R., Bhooshan, B., Whittaker, N. F., and Krishna, G. (1977). "Phosgene: A Metabolite of Chloroform." *Biochemical and Biophysical Research Communications*, 79(3), 684-91.

Pontius, F. W. (2003). "Update on USEPA's Drinking Water Regulations." *Journal American Water Works Association*, 95(3), 57-68.

Pressley, T. A., Bishop, D. F., and Roan, S. G. (1972). "Ammonia-nitrogen Removal by Breakpoint Chlorination." *Environmental Science and Technology*, 6(7), 622.

Prosser, J. I. (1986). *Nitrification*, Published for the Society for General Microbiology by IRL Press, Oxford ; Washington, DC.

Prosser, J. I. (1989). "Autotrophic Nitrification in Bacteria." *Advances in Microbial Physiology*, 30, 125-181.

Randtke, S. J. (1999). "Disinfection By-product Precursor Removal by Coagulation and Precipitative Softening." Formation and control of disinfection by-products in drinking water, P. C. Singer, ed., American Water Works Association, Denver, CO, 237-258.

Rasche, M. E., Hicks, R. E., Hyman, M. R., and Arp, D. J. (1990a). "Oxidation of Monohalogenated Ethanes and N-Chlorinated Alkanes by Whole Cells of *Nitrosomonas-Europaea*." *Journal of Bacteriology*, 172(9), 5368-5373.

Rasche, M. E., Hyman, M. R., and Arp, D. J. (1990b). "Biodegradation of Halogenated Hydrocarbon Fumigants by Nitrifying Bacteria." *Applied and Environmental Microbiology*, 56(8), 2568-2571.

Rasche, M. E., Hyman, M. R., and Arp, D. J. (1991). "Factors Limiting Aliphatic Chlorocarbon Degradation by *Nitrosomonas europaea* - Cometabolic Inactivation of Ammonia Monooxygenase and Substrate Specificity." *Applied and Environmental Microbiology*, 57(10), 2986-2994.

Regan, J. M., Cho, A.-Y., Kim, S., and Smith, C. D. (2004). "Monitoring Nitrification in Chloraminated Systems using Molecular Detection Strategies." *Proceedings - Water Quality Technology Conference and Exhibition*.

Reichert, P. (1994). "AQUASIM - A Tool for Simulation and Data Analysis of Aquatic Systems." *Water Science and Technology*, 30(2), 21-30.

Reichert, P. (1998a). *AQUASIM 2.0 - Tutorial*, Swiss Federal Institute for Environmental Science and Technology (EAWAG), Dubendorf, Switzerland.

Reichert, P. (1998b). *AQUASIM 2.0 - User Manual*, Swiss Federal Institute for Environmental Science and Technology (EAWAG), Dubendorf, Switzerland.

Reichert, P., and Wanner, O. (1997). "Movement of Solids in Biofilms: Significance of Liquid Phase Transport." *Water Science and Technology*, 36(1, Biofilm Systems III), 321-328.

Rittmann, B. E. (1995). "Fundamentals and Application of Biofilm Processes in Drinking Water Treatment." *Handbook of Environmental Chemistry*, 5(Pt. B), 61-87.

Rittmann, B. E. (2002). "The Role of Molecular Methods in Evaluating Biological Treatment Processes." *Water Environment Research*, 74(5), 421-+.

Rittmann, B. E., and McCarty, P. L. (2001). *Environmental Biotechnology: Principles and Applications*, McGraw-Hill, Boston.

Roalson, S. R., Jihyang, K., Lawler, D. F., and Speitel , G. E. (2003). "Enhanced Softening: Effects of Lime Dose and Chemical Additions." *Journal American Water Works Association*, 95(11), 97-109.

Robinson, J. A. (1985). "Determining Microbial Kinetic Parameters Using Nonlinear Regression Analysis." *Advances in Microbial Ecology*, 8, 61-114.

Schwarzenbach, R. P., Gschwend, P. M., and Imboden, D. M. (2003). *Environmental Organic Chemistry*, Wiley, Hoboken, N.J.

Science Applications International Corporation. (2001). "Information Collection Rule Query Tool, Version 1.0." USEPA, ed., USEPA.

Segar, R. L., Dewys, S. L., and Speitel Jr., G. E. (1995). "Sustained Trichloroethylene Cometabolism by Phenol-Degrading Bacteria in Sequencing Biofilm Reactors." *Water Environment Research*, 67(5), 764-774.

Segar, R. L., Jr. (1994). "Endogenous Cometabolism of Chlorinated Ethenes by Biofilms Grown on Phenol."

Shears, J. H., and Wood, P. M. (1985). "Spectroscopic Evidence for a Photosensitive Oxygenated State of Ammonia Monooxygenase." *Biochemical Journal*, 226(2), 499-507.

Singer, P. C. (1999). *Formation and control of disinfection by-products in drinking water*, American Water Works Association, Denver, CO.

Singer, P. C., Arora, H., Dundore, E., Brophy, K., and Weinberg, H. S. (1999a). "Control of Haloacetic Acid Concentrations by Biofiltration. A Case Study." *Proceedings - Water Quality Technology Conference*, 1771-1779.

Singer, P. C., Harrington, G. W., Cowman, G. A., Smith, M. E., Schecter, D. S., and Harrington, L. J. (1999b). *Impacts of Ozonation on the Formation of Chlorination and Chloramination By-Products, Report No. 90766*, American Water Works Association Research Foundation, Denver, CO.

Smith, L. H., Kitanidis, P. K., and McCarty, P. L. (1997). "Numerical Modeling and Uncertainties in Rate Coefficients for Methane Utilization and TCE Cometabolism by a Methane-oxidizing Mixed Culture." *Biotechnology and Bioengineering*, 53(3), 320-331.

Smith, L. H., McCarty, P. L., and Kitanidis, P. K. (1998). "Spreadsheet Method for Evaluation of Biochemical Reaction Rate Coefficients and Their Uncertainties by Weighted Nonlinear Least-squares Analysis of the Integrated Monod Equation." *Applied and Environmental Microbiology*, 64(6), 2044-2050.

Soderberg, R. W., and Meade, J. W. (1991). "The Effects of Ionic-strength on Un-ionized Ammonia Concentration." *Progressive Fish-Culturist*, 53(2), 118-120.

Speitel, G. E., Thompson, R. C., and Weissman, D. (1993). "Biodegradation Kinetics of *Methylosinus-Trichosporium Ob3b* at Low Concentrations of Chloroform in the Presence and Absence of Enzyme Competition by Methane." *Water Research*, 27(1), 15-24.

Stein, L. Y. (1998). "Effects of Ammonia, pH, and Nitrite on the Physiology of *Nitrosomonas europaea*, an Obligate Ammonia-oxidizing Bacterium."

Suzuki, I., Dular, U., and Kwok, S. C. (1974). "Ammonia or Ammonium Ion as Substrate for Oxidation by *Nitrosomonas europaea* Cells and Extracts." *Journal of Bacteriology*, 120(1), 556-8.

Suzuki, I., Kwok, S.-C., and Dular, U. (1976). "Competitive Inhibition of Ammonia Oxidation in *Nitrosomonas europaea* by Methane, Carbon Monoxide or Methanol." *FEBS Letters*, 72(1), 117-20.

Symons, J. M., AWWA, and US EPA. (1982). *Treatment Techniques for Controlling Trihalomethanes in Drinking Water*, AWWA, Denver.

Tsang, D. C. Y., and Suzuki, I. (1982). "Cytochrome C554 as a Possible Electron Donor in the Hydroxylation of Ammonia and Carbon Monoxide in *Nitrosomonas europaea*." *Canadian Journal of Biochemistry*, 60(11), 1018-1024.

Uemoto, H., Ando, A., and Saiki, H. (2000). "Effect of Oxygen Concentration on Nitrogen Removal by *Nitrosomonas europaea* and *Paracoccus denitrificans* Immobilized within Tubular Polymeric Gel." *Journal of Bioscience and Bioengineering*, 90(6), 654-660.

USEPA. (1995). "Method 551.1 Determination of Chlorination Disinfection Byproducts, Chlorinated Solvents, and Halogenated Pesticides/Herbicides in Drinking Water by Liquid-Liquid Extraction and Gas Chromatography with Electron-Capture Detection (Revision 1.0)." Methods for the Determination of Organic Compounds in Drinking Water: Supplement III, Cincinnati, Ohio.

USEPA. (1998). "National Primary Drinking Water Regulations: Disinfectants and Disinfection Byproducts Rule; Final Rule." *Federal Register*, 63(241), 69390-69476.

USEPA. (1999). "EPA Guidance Manual - Alternative Disinfectants and Oxidants."

USEPA. (2006). "National Primary Drinking Water Regulations: Stage 2 Disinfectants and Disinfection Byproducts Rule." *Federal Register*, 71(2), 387-493.

Valentine, R. L., and Jafvert, C. T. (1988). "General Acid Catalysis of Monochloramine Disproportionation." *Environmental Science and Technology*, 22(6), 691.

Vannelli, T., and Hooper, A. B. (1992). "Oxidation of Nitrapyrin to 6-Chloropicolinic Acid by the Ammonia-oxidizing Bacterium *Nitrosomonas europaea*." *Applied and Environmental Microbiology*, 58(7), 2321-2325.

Vannelli, T., and Hooper, A. B. (1993). "Reductive Dehalogenation of the Trichloromethyl Group of Nitrapyrin by the Ammonia-oxidizing Bacterium *Nitrosomonas europaea*." *Applied and Environmental Microbiology*, 59(11), 3597-601.

Vannelli, T., and Hooper, A. B. (1995). "NIH Shift in the Hydroxylation of Aromatic Compounds by the Ammonia-oxidizing Bacterium *Nitrosomonas europaea*. Evidence Against an Arene Oxide Intermediate." *Biochemistry*, 34(37), 11743-9.

Vannelli, T., Logan, M., Arciero, D. M., and Hooper, A. B. (1990). "Degradation of Halogenated Aliphatic Compounds by the Ammonia-oxidizing Bacterium *Nitrosomonas europaea*." *Applied and Environmental Microbiology*, 56(4), 1169-1171.

Vannelli, T. M. (1994). "Oxidation of Halogenated Alkanes, Alkenes, and Aromatics by the Ammonia-oxidizing Bacterium *Nitrosomonas europaea*."

Vikesland, P. J., Ozekin, K., and Valentine, R. L. (1998). "Effect of Natural Organic Matter on Monochloramine Decomposition: Pathway Elucidation Through the Use of Mass and Redox Balances." *Environmental Science and Technology*, 32(10), 1409.

Vikesland, P. J., Ozekin, K., and Valentine, R. L. (2001). "Monochloramine Decay in Model and Distribution System Waters." *Water Research*, 35(7), 1766.

Vikesland, P. J., and Valentine, R. L. (2002a). "Iron Oxide Surface-catalyzed Oxidation of Ferrous Iron by Monochloramine: Implications of Oxide Type and Carbonate on Reactivity." *Environmental Science and Technology*, 36, 512.

Vikesland, P. J., and Valentine, R. L. (2002b). "Modeling the Kinetics of Ferrous Iron Oxidation by Monochloramine." *Environmental Science and Technology*, 36, 662.

Vlieg, J. E. T. V., deKoning, W., and Janssen, D. B. (1997). "Effect of Chlorinated Ethene Conversion on Viability and Activity of *Methylosinus trichosporium OB3b*." *Applied and Environmental Microbiology*, 63(12), 4961-4964.

Voysey, P. A., and Wood, P. M. (1987). "Methanol and Formaldehyde Oxidation by an Autotrophic Nitrifying Bacterium." *Journal of General Microbiology*, 133, 283-290.

Wahman, D. G., Henry, A. E., Katz, L. E., and Speitel, G. E., Jr. (2006). "Cometabolism of Trihalomethanes by Mixed Culture Nitrifiers." *Water Research*, 40(18), 3349-3358.

Wanner, O., and Morgenroth, E. (2004). "Biofilm modeling with AQUASIM." *Water Science and Technology*, 49(11-12), 137-144.

Wanner, O., and Reichert, P. (1996). "Mathematical Modeling of Mixed-culture Biofilms." *Biotechnology and Bioengineering*, 49(2), 172-84.

Whittaker, M., Bergmann, D., Arciero, D., and Hooper, A. B. (2000). "Electron Transfer During the Oxidation of Ammonia by the Chemolithotrophic Bacterium *Nitrosomonas europaea*." *Biochimica Et Biophysica Acta-Bioenergetics*, 1459(2-3), 346-355.

Williams, S. L., Williams, R. L., and Gordon, A. S. (1997). "The Impact of Bacterial Degradation of Haloacetic Acids (HAA) in the Distribution System." *Proceedings - Water Quality Technology Conference*, 461-465.

Williams, S. L., Williams, R. L., and Yuan, J. (1998). "Bacterial Degradation of Haloacetic Acids in the Distribution System." *Proceedings - Water Quality Technology Conference*, 632-637.

Wolfe, R. L., Ward, R., and Olson, B. H. (1984). "Inorganic Chloramines as Drinking Water Disinfectants: A Review." *Journal American Water Works Association*, 76(5), 74.

Wong-Chong, G. M., and Loehr, R. C. (1975). "The Kinetics of Microbial Nitrification." *Water Research*, 9, 1099-1106.

Woolschlager, J., Rittmann, B., Piriou, L., Kiene, L., and Schwartz, B. (2001). "Using a Comprehensive Water Model to Identify the Major Mechanisms of Chloramine Decay in Distribution Systems." *Water Science & Technology: Water Supply*, 1(4), 103-110.

Woolschlager, J. E. (2000). "A Comprehensive Disinfection and Water Quality Model for Drinking Water Distribution Systems," Dissertation, Northwestern University, Evanston.

Xie, Y., and Zhou, H. (2000). "Biologically Active Carbon for Haloacetic Acid Control." *Proceedings - Water Quality Technology Conference*, 1437-1443.

Xie, Y. F. F., and Zhou, H. J. (2002). "Use of BAC for HAA removal - Part 2, Column Study." *Journal American Water Works Association*, 94(5), 126-134.

Zahn, J. A., Arciero, D. M., Hooper, A. B., and DiSpirito, A. A. (1996). "Evidence for an Iron Center in the Ammonia Monooxygenase from *Nitrosomonas europaea*." *FEBS Letters*, 397(1), 35-38.

Zavaleta, J. O., Hauchman, F. S., and Cox, M. W. (1999). "Epidemiology and Toxicology of Disinfection By-Products." Formation and control of disinfection by-products in drinking water, P. C. Singer, ed., American Water Works Association, Denver, CO, 95-117.

Vita

David Gerard Wahman was born to David R. and Laverne A. Wahman on November 7, 1973 in Batesville, Indiana. He was raised in Oldenburg, Indiana with his two sisters, Mary and Melissa. He attended Batesville High School and subsequently went to Rose-Hulman Institute of Technology in Terre Haute, Indiana, graduating s*umma cum laude* with a B.S. in Civil Engineering in May 1996. Upon graduation, David began work in Batesville, Indiana for Chaffee & Associates, Inc., as a project engineer, designing water and wastewater treatment systems. David obtained his Professional Engineering license in 2001. In January 2002, David began graduate school in the Environmental and Water Resources Engineering (EWRE) Department at The University of Texas at Austin (UT). He received a M.S.E in EWRE in December 2003 and continued research at UT to pursue his doctorate degree in Civil Engineering.

Permanent address: P.O. Box 176, Oldenburg, IN 47036

This dissertation was typed by the author.